

LIPID TRAFFICKING AND LIPID BREAKDOWN
IN CHLAMYDOMONAS

By

Jaruswan Warakanont

A DISSERTATION

Submitted to
Michigan State University
in partial fulfillment of the requirements
for the degree of

Plant Biology—Doctor of Philosophy

2015

ABSTRACT

LIPID TRAFFICKING AND LIPID BREAKDOWN IN CHLAMYDOMONAS

By

Jaruswan Warakanont

With their high photosynthetic efficiency and the ability to synthesize triacylglycerol (TAG), unicellular microalgae have an important ecological role, as well as value for production of triacylglycerol lipids that can be converted to biodiesel. The recent state of knowledge about microalgal lipid metabolism had been deduced from that of a model seed plant, *Arabidopsis*. However, recent studies have revealed that aspects of lipid metabolism differ between microalgae and *Arabidopsis*. Investigating these differences was a cornerstone of this study, using *Chlamydomonas*, a representative of microalgae, and *Arabidopsis*. Two major approaches were undertaken: forward and reverse genetics.

The forward genetic screening used insertional mutagenesis of *Chlamydomonas* and focused on a knockout mutation of a gene, which proved to be an orthologue of the *Arabidopsis* *TRIGALACTOSYLDIACYLGLYCEROL 2 (TGD2)*. The *tgd2* mutant exhibits increases in cellular concentrations of phosphatidic acid (PtdOH) and triacylglycerol (TAG); the latter contains signature fatty acids of monogalactosyldiacylglycerol (MGDG), pointing to its likely origin of synthesis. The mutant also experiences low viability in extended culture. Similar to AtTGD2, CrTGD2 is located in the chloroplast inner envelope membrane and binds PtdOH *in vitro*. Radioactive labeling experiments suggest that CrTGD2 functions in transferring a lipid precursor, presumably PtdOH, from the outer chloroplast envelope into the chloroplast. This study shows that, in contrast to prevailing assumptions, *Chlamydomonas* is able to import lipids

from the endoplasmic reticulum (ER) to the chloroplast, and utilizes the eukaryotic pathway to synthesize galactoglycerolipids.

The reverse genetics investigation focused on CrLIP4, a putative TAG lipase. *CrLIP4* is an orthologue of a major Arabidopsis TAG lipase. Reverse transcription PCR revealed that the *CrLIP4* transcript is reduced in abundance during N deprivation when TAG accumulates. Down-regulation of this gene through an artificial microRNA construct resulted in delayed TAG degradation. Expression of CrLIP4 in *Escherichia coli* alters the pattern of neutral lipids. Recombinant CrLIP4 exhibited TAG lipase activity. These results show that CrLIP4 has TAG lipase activity both in *in vitro* and *in vivo*.

In summary, two Arabidopsis orthologues in Chlamydomonas were characterized through forward and reverse genetic approaches. The results elaborate and refine our understanding of Chlamydomonas lipid metabolism, and are likely relevant for other unicellular microalgae.

Copyright by
JARUSWAN WARAKANONT
2015

ACKNOWLEDGEMENTS

In the Fall 2009, I was accepted to a PhD program in the Department of Crop and Soil Science at Michigan State University by Prof. Mariam B. Sticklen. However, after a year had passed my classmate Paula Marquardt made me realized that I would be happier switching my research to different directions. I began looking for a new lab and Benning lab was one of them. Through help and support from my Plant Biochemistry classmates, Cheng Peng, Benshen Liu and Chia-Hong Tsai, I had a chance to talk to Prof. Christoph Benning.

In December 2010, through a series of talking and discussion, I transferred to the Plant Biology program and to the Benning lab with help from the director of graduate studies Prof. Alan Prather, my advisor at the time Prof. Mariam B. Sticklen, my current committee member Prof. Barbara B. Sears, my former advisor in Thailand Dr. Yindee Chanviwattana, and my former Sticklen's labmates Sang Hyuck Park and Thang Xuan Nguyen. The most important person is Prof. Christoph Benning who was kind enough to accept me into his lab without knowing me from a rotation system and with the fact that I had only a little experience in molecular biology; zero in biochemistry.

In the new lab, I have earned valuable experience, learned many techniques, and encountered many challenges including comprehensive exams and difficult experiments. I would not have gone through this unforgettable time without help, guidance and support from the following individuals to whom I express my profound gratitude.

First and foremost, I would like to express my deepest appreciation to my advisor Prof. Christoph Benning for his endless support in many aspects. At the beginning of my research in his lab, I spent many months cloning a gene (*CrLIP4*). At the same time, I also tried to identify a

mutation in the mutant (*tgd2*) with two molecular biology techniques without a successful result. Christoph was very patient with me during that difficult time. At the end, he accepted my idea to sequence the genome of the *tgd2* mutant, which then became a successful story in my thesis research. In general, he has allowed me to think, tackle problems, and conduct research freely with my own pace. However, this does not stop him from giving me directions and advices when needed. He is a great scientist and advisor at the same time. Throughout his guidance and nurturing, he helps me develop skill for being independent scientist in the future.

Beside my advisor, I am immensely grateful to the rest of my committee, who always provide me knowledge and advice for my research. I sincerely appreciate Prof. Barbara B. Sears for her tremendous help on my writing and genetic analysis of the *Chlamydomonas* mutant. I appreciate Prof. John B. Ohlrogge for his advice on radioactive labeling experiments and for hooding me in the graduation ceremony. I would like to thank Prof. Min-Hao Kuo for his suggestions and comments on yeast experiments and for having his graduate student Witawas Handee helped me in the yeast project. All of them are supportive and helpful. Their comments and questions always help me improve my work.

I would like to thank all of my labmates from the past and present. I am very grateful to Rebecca Roston, Simone Säuner, and Yang Yang who spent hours discussing the results, giving me suggestions and knowledge. I am thankful to Astrid Vieler, Blair Bullard, Que Kong, Xiabo Li, and Bensheng Liu, who always willing to share their knowledge and exchanging nice conversation with me. My gratitude also goes to Elena J. S. Michel, an undergraduate who worked with me. Due to her talent and dedication, she helped me complete the CrTGD2 project. I would like to thank other lab members: Chia-Hong Tsai, Agnieszka Zienkiewicz, Krzysztof Zienkiewicz, Wei Ma, Zheng Wang, Anna Hurlock, Kun Wang, Patric Horn, Zhi-Yan Du, Linda

Danhof, Rachel Miller, Sanjay, Bagya Muthan, Eric Poliner, Tomomi Takeuchi, Anastasiya Lavell, all the undergrad students and visiting scholars, for their encouragement, support, and being great friends throughout my time here.

I am thankful for financial support from a Royal Thai Government scholarship for the first five years and for the research assistantship through my advisor throughout my study.

I am greatly indebted to my former advisors, Dr. Yindee Chanviwattana and Assoc. Prof. Jarunya Narangajavana, as well as Dr. Oranuch Leelapon who encourage me to continue my graduate study abroad. Without them I would never have a great academic and cultural experiences in the United States. In addition, I would like to thank all of my former teachers who educated me throughout my study from a kindergarten through a graduate school.

I am grateful to my parents and my grandmother for their unconditional love, patience, and supportiveness. I fully appreciate my siblings who are always on my side and take care of our parents while I am away. All of my family members have shaped the way I am; no word can describe how important they are.

I would like to thank my boyfriend Pawin Ittisamai warmly for helping me with everything, being with me here in the United States, and being so supportive and thoughtful. He always has a positive way of thinking. He is the only person who understands me in every aspect. He is a technical guy for me. He can help fixing and finding answers for computer, camera, telephone, television, bicycle, outdoor gears, etc. He helps me relieve the stress of graduate school by entertaining me through different activities including watching movies, and traveling to several places in Europe and the US. Besides, he helped me taking photos and finish all of my experimental dishes; some of which I hesitated to try.

Another person who plays an important role in my life is Lisa Luchita. She is my first Italian friend. I knew her from Prof. Michael Morris class in Summer 2009. Lisa introduced me a different perspective of life. She emphasized how importance of travel toward the understanding of the differences among people in different regions and backgrounds. She also inspired me about cooking which then became my passion through the GialloZafferano website. It is my pleasure to know her. I consider knowing her as a turning point in my life.

I am thankful to my dearest friend Teeda Sasipreeyajan for being such a good friend since my first grade at the Chulalongkorn University Demonstration School or Satit Chula in short. She and her husband who is also my friend from Satit Chula moved to Ann Arbor in the fall of 2014. Since their arrival, we took turns visiting each other. We traveled to many places together. We exchanged stories through many delicious meals. All of these activities keep me happy during the final stage of my PhD study.

Last but not least, my living in the US would not be completed without learning the American culture from the locals. I am thankful to Alan and Carol Prais who inviting Pawin and I to their house in the Pre-academic program in 2009. They continued inviting us to the American celebrations of Thanksgivings and Christmas. Finally, I deeply appreciate Pooh Stevenson and Richard Bowie from the Owosso Organics. They not only supplied me organic vegetables and eggs for five years but they are also ones of the greatest persons I have ever met. Their way of thinking reflects how good and sustainable their farm is.

I find that studying PhD in the US is not only giving me academic experience but also broadening my perspective toward many aspects. I hope my learning could help contribute improving our human society in the future.

TABLE OF CONTENTS

LIST OF TABLES	xiv
LIST OF FIGURES	xv
CHAPTER 1: Lipid metabolism in <i>Chlamydomonas reinhardtii</i>	1
WHY STUDY LIPID METABOLISM IN CHLAMYDOMONAS?	2
LIPID METABOLISM IN CHLAMYDOMONAS VS. ARABIDOPSIS.....	4
Fatty acid composition	4
Lipid species	5
Genes involved in lipid metabolism	6
LIPOLYSIS AND LIPASES	7
Lipases are interfacial enzymes	7
Many TAG lipases contain a patatin domain.....	7
Patatin-domain containing enzymes are unique lipases.....	8
MUTANT SCREENING AND IDENTIFICATION OF A RESPONSIBLE GENE	9
Forward genetic screening	9
Map-based cloning.....	10
PCR-based methods	10
Whole genome resequencing	12
Forward genetic screening in <i>Chlamydomonas</i>	13
AIM OF THE THESIS RESEARCH	14
REFERENCES	20
CHAPTER 2: Chloroplast lipid transfer processes in <i>Chlamydomonas reinhardtii</i> involving a <i>TRIGALACTOSYLDIACYLGLYCEROL 2 (TGD2)</i> orthologue	32
ABSTRACT.....	33
SIGNIFICANT STATEMENT.....	33
INTRODUCTION	34
RESULTS	37
The <i>tgd2</i> mutant accumulates triacylglycerol enriched in MGDG acyl groups	37
Cultures of <i>tgd2</i> show early senescence	38
Changes in the ultrastructure of <i>tgd2</i> cells.....	38
Molecular and genetic analysis of the <i>tgd2</i> mutant locus.....	39
<i>CrTGD2</i> is a presumed orthologue of <i>AtTGD2</i>	40
Altered galactoglycerolipid labeling and impaired ER-to-plastid lipid trafficking in <i>tgd2</i>	40
Altered labeling of non-galactoglycerolipids in <i>tgd2</i>	42
Biosynthesis of MGDG is increased in the <i>tgd2</i> mutant.....	42
<i>CrTGD2</i> is present in the chloroplast inner envelope membrane.....	43
<i>CrTGD2</i> binds PtdOH <i>in vitro</i>	44
DISCUSSION.....	45
Galactoglycerolipid metabolism is altered in <i>tgd2</i>	46

What happens to MGDG as it is metabolized in the <i>tgd2</i> mutant?.....	47
Does CrTGD2 play a role in the transfer of lipids from the ER to the chloroplast?.....	48
MATERIALS AND METHODS.....	50
Algal strains and growth conditions	50
Generation of <i>tgd2</i> mutant and genetic analyses	50
DNA isolation and Southern blot analysis.....	50
Whole genome resequencing	50
Lipid analysis	50
Viability assay.....	51
Transmission electron microscopy	51
Phylogenetic analysis.....	53
Heterologous complementation analysis	52
[¹⁴ C]-Acetate pulse-chase labeling	52
<i>DsRED-CrTGD2</i> pLW01, <i>DsRED-AtTGD2</i> pLW01 and <i>DsRED</i> pLW01 constructs, recombinant protein expression and purification	52
CrTGD2 antibody	52
Immunoblotting.....	52
Subcellular fractionation.....	53
Protease protection assay	54
MGDG synthase assay	54
Lipid binding assay	54
ACCESSION NUMBERS	55
ACKNOWLEDGEMENTS.....	56
APPENDICES	66
APPENDIX A. SUPPORTING FIGURES	67
APPENDIX B. SUPPORTING TABLES	82
APPENDIX C. SUPPORTING DATA	85
APPENDIX D. SUPPORTING METHODS	87
REFERENCES	91
CHAPTER 3: Characterization of Chlamydomonas LIP4, a putative triacylglycerol lipase	100
ABSTRACT.....	101
INTRODUCTION	102
RESULTS	104
<i>CrLIP4</i> is down-regulated during N-deprivation.....	104
CrLIP4 contains DUF3336, transmembrane, and patatin domains and a large IDR at its C terminus	104
Phylogenetic analysis of CrLIP4	105
Down-regulation of <i>CrLIP4</i> transcript resulted in slower TAG degradation	106
<i>CrLIP4</i> coding sequence cloned from Chlamydomonas dw15.1 contains four amino acid changes and a five amino acid insertion compared to the gene model.....	106
CrLIP4 was not able to rescue yeast <i>tgl3Δ</i> , <i>tgl4Δ</i> , or <i>tgl3Δtgl4Δ</i> mutants	107
CrLIP4 could not complement Arabidopsis <i>sdp1</i> mutants	108
Recombinant CrLIP4 and SDP1 protein expression in <i>Escherichia coli</i>	109

Recombinant CrLIP4 showed TAG lipase activity <i>in vitro</i>	109
DISCUSSION.....	110
MATERIALS AND METHODS.....	112
Algal strain and growth condition.....	112
Artificial microRNA (amiRNA) knockdown.....	112
RNA isolation and cDNA synthesis.....	113
Quantitative reverse transcription PCR (qRT-PCR).....	113
Bioinformatic analysis.....	113
Phylogenetic reconstructions.....	114
Lipid analysis.....	114
Cloning of <i>CrLIP4</i> coding sequence.....	114
Expression of CrLIP4 in yeast <i>tgl3Δtgl4Δ</i> double, <i>tgl3Δ</i> , and <i>tgl4Δ</i> single mutants.....	115
Western blot analysis.....	115
Analysis of CrLIP4 overexpression in yeast <i>tgl3Δtgl4Δ</i> double, and <i>tgl3Δ</i> and <i>tgl4Δ</i> single mutants.....	116
Plant materials and growth conditions.....	116
Genomic DNA isolation from Arabidopsis leaves.....	116
Genotyping of <i>sdp1</i> T-DNA insertion lines.....	116
Construction of pMDC32- <i>CrLIP4</i> plasmid.....	117
Preparation of Agrobacterium competent cells.....	117
Agrobacterium transformation.....	117
Arabidopsis transformation.....	117
Construction of pET28- <i>AtSDP1</i> and pET28- <i>CrLIP4</i> plasmids.....	118
Recombinant AtSDP1 and CrLIP4 protein production.....	118
Recombinant protein purification.....	118
Lipase assay.....	119
ACCESSION NUMBERS.....	119
REFERENCES.....	141
CHAPTER 4: Conclusion and Perspective.....	148
SUMMARY OF PHYSIOLOGICAL, GENETIC, AND BIOCHEMICAL FEATURES OF CHLAMYDOMONAS TGD2.....	149
Phenotype of the <i>tgd2</i> mutant.....	149
Identification of the mutation in <i>tgd2</i>	149
Characterization of changes in lipid trafficking in the <i>tgd2</i> mutant.....	150
Synthesis of galactoglycerolipid in <i>tgd2</i> is affected.....	150
Localization and lipid binding property of CrTGD2.....	150
Function of CrTGD2 and consequence of its absence.....	150
New insights from this study.....	151
Remaining questions and future directions.....	152
MGDG and DGDG syntheses.....	152
<i>Feedback inhibition of DGDG synthesis</i>	152
<i>Inaccuracy in the measurement of DGDG synthesis</i>	153
<i>PtdOH inhibits DGDG synthase</i>	153
<i>Labeling of other lipids</i>	153

<i>Metabolic flux analysis</i>	153
Does CrTGD2 form a complex with CrTGD1 and CrTGD3?.....	153
The absence of <i>TGD4</i> and <i>TGD5</i> in the <i>Chlamydomonas</i> genome.....	154
<i>TGD4 and TGD5 may be present in Chlamydomonas but</i> <i>may not be detectable</i>	154
Other potential function(s) of CrTGD2	154
Which galactolipase and/or lipoxygenase is responsible for degradation of MGDG?	155
Localization of MGDG and DGDG synthases	155
CrLIP4, A PUTATIVE TAG LIPASE	155
Conclusion	155
Future directions	156
Heterologous expression in yeast and Arabidopsis experiments.....	156
<i>Heterologous expression of CrLIP4 in yeast double mutant</i>	156
<i>Heterologous expression of CrLIP4 in single mutants of yeast</i>	156
<i>Heterologous expression of CrLIP4 in Arabidopsis mutant</i>	156
Substrate specificity and kinetics study of CrLIP4.....	157
Inhibitors of lipases.....	157
The function of the intrinsic disordered region (IDR) of CrLIP4.....	157
Target mutation to obtain a <i>CrLIP4</i> loss-of-function mutant.....	158
<i>Targeting Induced Local Lesions in Genomes (TILLING)</i>	158
<i>Homologous recombination</i>	158
<i>Zinc-finger nucleases</i>	158
<i>Transcription activator-like effector nucleases</i>	159
<i>CRISPR-Cas9</i>	159
SUMMARY	160
REFERENCES	161

SUPPORTING CHAPTER: Critical Role of <i>Chlamydomonas reinhardtii</i> Ferredoxin-5 in Maintaining Membrane Structure and Dark Metabolism.....	167
ABSTRACT.....	168
SIGNIFICANT STATEMENT.....	168
INTRODUCTION	168
RESULTS	170
<i>fdx5</i> is a null mutant.....	170
FDX5 localizes to chloroplasts	170
Disruption of FDX5 causes a dark growth deficiency.....	170
Photosynthesis and respiration decrease in dark-maintained <i>fdx5</i>	171
Photosynthetic electron flow is altered in dark-maintained <i>fdx5</i>	171
Photosynthetic polypeptides are not altered in <i>fdx5</i>	172
Dark-maintained <i>fdx5</i> has altered membrane ultrastructure	172
Membrane lipids are altered in dark-maintained <i>fdx5</i>	173
FDX5 interacts with Cr Δ 4FAD and CrFAD6 desaturases	174
Increased TAG in <i>fdx5</i> mutant in the dark.....	174
DISCUSSION.....	175
MATERIALS AND METHODS.....	178

Strains, mutant isolation and growth conditions.....	178
Complementation and transformation.....	178
Phenotyping and growth rates.....	179
Photosynthetic O ₂ evolution and respiratory O ₂ consumption	179
Transmission electron microscopy (TEM)	179
Analysis of total and membrane lipids.....	179
TAG analysis and staining of lipid droplets	179
Mating-Based Split Ubiquitin assay	180
ACKNOWLEDGEMENTS	180
APPENDICES	185
APPENDIX A. SUPPORTING FIGURES	186
APPENDIX B. SUPPORTING TABLES	206
APPENDIX C. SUPPORTING DATA	216
APPENDIX D. SUPPORTING METHODS.....	218
REFERENCES	220

LIST OF TABLES

Table 2.S1.	Bacterial Artificial Chromosomes (BACs) used in the <i>tgd2</i> complementation analysis.....	82
Table 2.S2.	Sequences of primers for probing the deletion in chromosome 16 of the <i>tgd2</i> mutant	83
Table 2.S3.	Sequences of primers used for constructing plasmids as indicated	84
Table 3.1.	Protein domains identified in CrLIP4 homologues	136
Table 3.2.	Target and primer sequences for artificial microRNA of CrLIP4	138
Table 3.3.	Sequences of Primers used for various purposes as indicated.....	139
Table A.S1.	Genes encoding ferredoxins in the Chlamydomonas genome	207
Table A.S2.	Primers used in this study	208
Table A.S3.	Strains used in this study	210
Table A.S4.	Constructs used in this study	211
Table A.S5.	Pull down assay using FDX5 to establish interacting proteins.....	212

LIST OF FIGURES

Figure 1.1.	Chemical structures of fatty acids and lipids	15
Figure 1.2.	Lipolysis of neutral lipids	16
Figure 1.3.	Screening of Chlamydomonas mutants	17
Figure 1.4.	Identification of the insertion locus in the Chlamydomonas <i>tgd2</i> mutant using whole-genome resequencing.....	18
Figure 2.1.	Lipid phenotypes of Chlamydomonas <i>tgd2</i> mutant.....	56
Figure 2.2.	Viability assay for the PL (dw15.1), <i>tgd2</i> and complemented line <i>TGD2 tgd2</i> grown in N-replete medium.....	58
Figure 2.3.	Ultrastructural changes in the <i>tgd2</i> mutant.....	59
Figure 2.4.	[¹⁴ C]-Acetate pulse-chase labeling of PL (dw15.1), <i>tgd2</i> mutant, and <i>TGD2 tgd2</i> complemented line.....	60
Figure 2.5.	Galactoglycerolipid synthesis of PL (15.1) and <i>tgd2</i> chloroplasts	61
Figure 2.6.	Localization of CrTGD2.....	62
Figure 2.7.	Lipid binding assay.....	63
Figure 2.8.	Proposed model of CrTGD2 function.....	64
Figure 2.S1.	Separation of Phosphatidic acid (PtdOH) and oligogalactoglycerolipids by thin layer chromatography (TLC).....	67
Figure 2.S2.	Cell viability and acyl group composition of TAGs during extended culturing time	68
Figure 2.S3.	Ultrastructure of chloroplast membranes.....	69
Figure 2.S4.	Southern blot analysis of the <i>tgd2</i> mutant and the PL (dw15.1).....	70

Figure 2.S5.	Analysis of progeny from crosses between <i>tgd2</i> and CC-198	71
Figure 2.S6.	Mutant locus in the <i>tgd2</i> genome and complementation	73
Figure 2.S7.	Amino acid sequence alignment of AtTGD2 and CrTGD2.....	75
Figure 2.S8.	Phylogenetic analysis of CrTGD2 homologues.....	76
Figure 2.S9.	Lack of Arabidopsis TGD2 complementation in Chlamydomonas <i>tgd2</i> mutant ..	78
Figure 2.S10.	Lack of Chlamydomonas TGD2 complementation in Arabidopsis <i>tgd2</i> mutant ..	79
Figure 2.S11.	Pulse chase [¹⁴ C]-acetate labeling of MGDG in the PL (dw15.1).....	81
Figure 3.1.	Relative expression of <i>CrLIP4</i> transcript compared to TAG concentration during N deprivation and N resupply.....	120
Figure 3.2.	Amino acid sequence analysis of CrLIP4.....	121
Figure 3.3.	Prediction of transmembrane helices (TMD) and alignment of intrinsic disorder regions (IDRs) of CrLIP4 homologues.....	122
Figure 3.4.	Phylogenetic analysis of CrLIP4 homologues.....	124
Figure 3.5.	Down regulation of <i>CrLIP4</i> transcript with artificial microRNA (amiRNA)	126
Figure 3.6.	Sequence alignment of the <i>CrLIP4</i>	127
Figure 3.7.	Heterologous expression of <i>CrLIP4</i> in the yeast <i>tgl3Δtgl4Δ</i> double mutant	128
Figure 3.8.	Heterologous expression of <i>CrLIP4</i> in yeast <i>tgl3Δ</i> and <i>tgl4Δ</i> mutants	129
Figure 3.9.	Heterologous expression of CrLIP4 in Arabidopsis <i>sdp1</i> mutants.....	130
Figure 3.10.	CrLIP4 recombinant protein expression in <i>E. coli</i>	132
Figure 3.11.	<i>In vitro</i> lipase assay.....	134

Figure A.1.	The <i>fdx5</i> mutant is unable to grow and has attenuated respiration and photosynthesis rates in the dark	182
Figure A.2.	Altered membrane morphologies and lipid compositions in dark-maintained <i>fdx5</i>	183
Figure A.3.	C16:4 ^{Δ4,7,10,13} fatty acid is decreased in dark-grown <i>fdx5</i> and FDX5 interacts with fatty acid desaturases	184
Figure A.4.	PGD1-mediated TAG accumulation in <i>fdx5</i> in the dark.....	185
Figure A.S1.	Ferredoxin-mediated electron transfer reactions	187
Figure A.S2.	Generation and molecular analyses of <i>fdx5</i> mutant	188
Figure A.S3.	Localization of FDX5	190
Figure A.S4.	<i>fdx5</i> growth at different light intensities	192
Figure A.S5.	The <i>fdx5</i> dark growth deficiency is linked to paromomycin resistance.....	193
Figure A.S6.	Elevated light-induced O ₂ consumption occurs in <i>fdx5</i> maintained in the dark ..	194
Figure A.S7.	Fluorescence and spectroscopic analyses show impairment of photosynthetic electron transport	195
Figure A.S8.	Immunoblot of representative photosynthetic proteins.....	197
Figure A.S9.	Profiles of fatty acids in MGDG after growth in the light and dark	198
Figure A.S10.	Profiles of fatty acids in DGDG after growth in the light and dark.....	199
Figure A.S11.	Localization of CrΔ4FAD and CrFAD6.....	200
Figure A.S12.	Separation of neutral lipids in different cell types under different light conditions	201
Figure A.S13.	Genotyping of the <i>fdx5pgd1</i> double mutants	203

Figure A.S14. Fatty acid profiles in <i>fdx5</i> and the <i>fdx5#13</i> strains in the dark at 48 h.	203
Figure A.S15. Model for FDX5-mediated regulation of thylakoid membrane structure in the dark	204
Figure A.S16. The impact of PGD1 on lipid production in the various strains in the dark	205

CHAPTER 1

Lipid metabolism in *Chlamydomonas reinhardtii*

Photosynthetic organisms play an important role in utilizing solar energy to produce chemical energy in the form of carbon-based molecules. This energy makes life on earth possible. In today's world, microalgae contribute to almost half of the total carbon assimilation on earth (Moroney & Ynalvez, 2001). Microalgae serve as primary producers in different ecological systems. They synthesize energy-rich compounds such as starch, triacylglycerol (TAG), and hydrogen. Many species of microalgae can produce polyunsaturated fatty acids (PUFAs) that are valuable for nutrition and provide the basis of healthy "fish oils" (Riediger *et al.*, 2009). Due to their short life cycle, minimal space requirements, and the ability of many species to grow in salt or wastewater, microalgae are a good option for the production of biofuels and bio-products (Demirbas & Fatih Demirbas, 2011; Dismukes *et al.*, 2008; Koller *et al.*, 2014; Spolaore *et al.*, 2006). Both biodiesel and PUFAs are derived from the metabolism of lipids. Most of what we know about lipid metabolism of microalgae has been deduced by analogy to either plants or fungi. However, microalgae appear to have some unique characteristics indicating that their metabolic processes may differ from those of plants. In this chapter, I will emphasize (i) the importance of studying lipid metabolism in a model algal species, *Chlamydomonas reinhardtii*, (ii) comparison of lipid metabolism between *Arabidopsis* and *C. reinhardtii*, (iii) the action of triacylglycerol (TAG) lipases for lipolysis, and (iv) mutant screening and identification.

WHY STUDY LIPID METABOLISM IN CHLAMYDOMONAS?

Chlamydomonas sp. is a unicellular eukaryotic microalga in the division Chlorophyta of the kingdom Viridiplantae. Early research on various species of genus *Chlamydomonas* focused on genetic mechanisms, flagella, and photosynthesis (Goodenough, 2015) for many reasons. First, *Chlamydomonas* sp. harbors a haploid genome that allows genetic analysis to be carried out easily (Harris, 1989). Second, mutants occur spontaneously or can be induced through the application of chemicals, irradiation or procedures for gene disruption (Harris, 2001). These two reasons make *Chlamydomonas* a good model organism for studying gene function since mutants can be selected that immediately show a phenotype. Third, *C. reinhardtii* in particular can grow under heterotrophic conditions, which allows photosynthesis-deficient mutants to survive in the presence of acetate. Finally, the *C. reinhardtii* genome has been sequenced (Merchant *et al.*, 2007). For these reasons, much research has been focused on *C. reinhardtii*, which I will refer to as *Chlamydomonas* in this dissertation.

Chlamydomonas was not considered to be an oleaginous alga and was reported to be unable to synthesize very long chain PUFA according to the US Department of Energy's survey (Sheehan *et al.*, 1998). However, recent research has shown that the alga can accumulate TAG under stress conditions especially in starchless mutants (James *et al.*, 2011; Y. Li *et al.*, 2010; Wang *et al.*, 2009; Work *et al.*, 2010). The attempt to find alternative renewable energy to replace fossil fuels has stimulated research on algal lipid metabolism using *Chlamydomonas* as a model organism. This is due to the fact that its genetics and physiology are well-characterized, and molecular genetics and genomics tools are more developed than for other algae (Day & Goldschmidt-Clermont, 2011; Michelet *et al.*, 2011; Rochaix, 2002). Moreover, as mentioned previously, its genome has been sequenced (Merchant *et al.*, 2007). Therefore, using *Chlamydomonas* as a model organism to study lipid metabolism in microalga has advantages over other microalgae that accumulate more oil but are not as well characterized.

Initial research on lipid metabolism of *Chlamydomonas* focused on identification of the specific lipid molecules, sites of lipid biosynthesis and fatty acid composition (Li-Beisson *et al.*, 2015). These biochemical analyses revealed differences in lipid metabolism of *Chlamydomonas* and plants, as I will discuss in the following section. More than 10 mutants defective in lipid metabolism have been identified and characterized since 1989 as reviewed by Li-Beisson *et al.* (2015). Among these mutants, novel genes were identified that are involved in biosynthesis and degradation of different lipid species; i.e. fatty acid desaturases, TAG and polar lipid synthases, and a lipase. These investigations have illustrated the value of mutant screening for identifying new genes involved in the metabolism of lipids.

Although 48 orthologues of plant and yeast lipid proteins were annotated in the *Chlamydomonas* genome (Riekhof *et al.*, 2005), many of the proteins have not been characterized. One example of these is a TAG lipase as I will discuss later in this Chapter and in Chapter 3. Conceivably, gene orthologues present in the genome of the alga have a different role than they do in plant metabolism. This issue will be addressed in Chapter 2.

LIPID METABOLISM IN CHLAMYDOMONAS VS. ARABIDOPSIS

Our current knowledge of algal lipid metabolism is based on studies in Arabidopsis. Regarding *in silico* analysis of lipid genes in Chlamydomonas, the overall picture of lipid metabolism in this alga is similar to and simpler than that of Arabidopsis (Riekhof *et al.*, 2005). In general, we believe that major pathways for fatty acid synthesis, diacylglycerol (DAG) assembly and glycerolipid biosynthesis are conserved between Chlamydomonas and Arabidopsis. This assumption is based on the presence of homologues of genes encoding enzymes involved in the lipid common pathways (Li-Beisson *et al.*, 2015). In most cases, Chlamydomonas lipid genes are present in fewer copies than those in Arabidopsis. However, analyses of Chlamydomonas fatty acid components, lipid species, and lipid biosynthesis enzymes have revealed that evolutionary divergence of microalgae and seed plants has resulted in differences in synthetic pathways. These differences will be addressed in the following three subsections.

Fatty acid composition. Chlamydomonas fatty acid composition is similar to that of Arabidopsis in that glycerolipids contain fatty acids with 16 or 18 carbons (C16 or C18). As described in more detail in Chapter 2, in plants, the presence of C16 or C18 acyl groups in the *sn*-2 position of the glycerol backbone is reflective of the synthetic pathway of the corresponding lipid. Lipids containing C16 acyl groups at their *sn*-2 position are derived from prokaryotic pathway and are synthesized within the chloroplast, while those with C18 are derived from the endoplasmic reticulum-based eukaryotic pathway (Heinz & Roughan, 1983; Roughan & Slack, 1982). The discrimination between these two pathways is based on substrate preferences of acyltransferases located either in the chloroplast or the endoplasmic reticulum (ER) (Frentzen *et al.*, 1983; Kim *et al.*, 2005; Kunst *et al.*, 1988; Roughan & Slack, 1982). Positional analysis by Giroud *et al.* (1988) concluded that the plastidic and extraplastidic lipids of Chlamydomonas are almost exclusively synthesized through the prokaryotic and eukaryotic pathways, respectively. However, substrate preferences of acyltransferases in Chlamydomonas still remain to be tested.

One difference from Arabidopsis is that Chlamydomonas synthesizes unique fatty acids containing front-end $\Delta 4$ or $\Delta 5$ double bonds (Figure 1.1A). The $\Delta 4$ double bond is present in 16:4 ^{$\Delta 4,7,10,13$} (number of carbons : number of double bonds with ^{Δ Number} indicating the position of the double bond counted from the carboxyl end) of monogalatosyldiacylglycerol (MGDG) (Giroud *et al.*, 1988; Zäuner *et al.*, 2012), while the $\Delta 5$ double bond can be found in 18:3 ^{$\Delta 5,9,12$}

and 18:4^{Δ5,9,12,15} of diacylglyceryl-*N,N,N*-trimethylhomoserine (DGTS) and phosphatidylethanolamine (PtdEtn) (Giroud *et al.*, 1988; Kajikawa *et al.*, 2006).

The 16:4^{Δ4,7,10,13} in MGDG is catalyzed by the chloroplast-located Δ4 desaturase named CrΔ4FAD from 16:3^{Δ7,10,13} (Zäuner *et al.*, 2012). Down-regulation of *CrΔ4FAD* leads to a lower abundance of 16:4^{Δ4,7,10,13} and also MGDG. This indicates that a tight relationship may exist between the acyl group and the corresponding lipid, as reflected by the stable ratio of 16:4^{Δ4,7,10,13} and 18:3^{Δ9,12,15} within MGDG. Thus, the altered ratio of these two acyl groups leads to less MGDG being made. The importance of 16:4^{Δ4,7,10,13} to the synthesis of MGDG and to the photosynthetic membranes of *Chlamydomonas* is suggested in the Appendix of this dissertation. In that study, it is shown that desaturation of 16:3^{Δ7,10,13} to produce MGDG with 16:4^{Δ4,7,10,13} contributes to the ability to grow of the alga in the dark.

Synthesis of 18:3^{Δ5,9,12} and 18:4^{Δ5,9,12,15} takes place in the ER by the action of the Δ5 desaturase (CrDES) from 18:2^{Δ9,12} and 18:3^{Δ9,12,15}, respectively (Kajikawa *et al.*, 2006). Similar to CrΔ4FAD, CrDES contains a cytochrome *b₅* domain, which is commonly found in front-end desaturases in the ER (Petra Sperling & Heinz, 2001; P. Sperling *et al.*, 1995). In addition to their presence in *Chlamydomonas*, the 18:3^{Δ5,9,12} and 18:4^{Δ5,9,12,15} fatty acids are widely distributed in gymnosperms, but not in angiosperms, suggesting that the ability to desaturate the Δ5 position was lost from the angiosperm lineage.

Lipid species. *Chlamydomonas* and *Arabidopsis* contain similar lipid species, with three exceptions. Biochemical analysis by Giroud *et al.* (1988) revealed that phosphatidylcholine (PtdCho) and phosphatidylserine (PtdSer) were absent from the alga. Instead, *Chlamydomonas* contains DGTS that is not present in *Arabidopsis*. DGTS is thought to be a substitute for PtdCho due to their similarity in structural (Fig. 1.1 B & C) and biophysical properties (B. Liu & Benning, 2013; N. Sato & Murata, 1991). Although not found in seed plants, DGTS has been identified in other algae, bacteria, and non-seed plants (Moellering *et al.*, 2010).

Although DGTS has a structure and chemical properties similar to PtdCho, it might not be able to substitute for the biochemical function of PtdCho. Because DGTS contains an ether bond instead of an ester bond as in PtdCho, it is an inferior substrate for DAG synthesis (B. Liu & Benning, 2013). Hence, DGTS is not as versatile as PtdCho as a central metabolite for biosynthesis of different lipids.

The lack of PtdSer in *Chlamydomonas* is in accordance with an absence of the gene for its biosynthesis (Riekhof *et al.*, 2005). Since synthesis of PtdEtn relies on PtdSer as a substrate, the authors suggested that PtdEtn in *Chlamydomonas* is carried out through a transfer of phosphoethanolamine to a DAG moiety instead of through the decarboxylation of PtdSer as in yeasts, bacteria, and plants (Voelker, 1997).

Genes involved in lipid metabolism. In general, *Chlamydomonas* harbors fewer copies of lipid genes compared to *Arabidopsis* (Riekhof *et al.*, 2005). For example, *Arabidopsis* contains three and two copies of MGDG and digalactosyldiacylglycerol (DGDG) synthases, respectively; while *Chlamydomonas* has only one copy of each gene. In *Arabidopsis*, as summarized by Petroutsos *et al.* (2014) the major MGDG and DGDG synthase are MGD1 and DGD1, respectively; they are located in the inner and outer envelope membrane of the chloroplast, respectively. These two enzymes synthesize galactolipids for the thylakoid membrane in photosynthetic tissue. In contrast, two other MGDG synthases (MGD2 and MGD3) and DGDG synthase (DGD2) are located in the outer envelope membrane (Awai *et al.*, 2001). They are expressed in non-photosynthetic tissues and in response to phosphate limitation (Botte *et al.*, 2011a; Kobayashi *et al.*, 2004). A broad phylogenetic analysis of MGDG synthases indicates that the MGDG synthase in *Chlamydomonas* is a pre-angiosperm MGD1 orthologue (Botte *et al.*, 2011b; Petroutsos *et al.*, 2014; Yuzawa *et al.*, 2012). This implies that MGDG and DGDG synthases in *Chlamydomonas* are mainly responsible for synthesizing galactoglycerolipids of photosynthetic membranes. The absence of MGD2, MGD3, and DGD2 orthologues in the alga suggests the existence of a different response to phosphate limitation in the alga (Moellering *et al.*, 2010).

In contrast to the biosynthesis pathway for membrane lipids for which plants have a higher number of gene copies, algae have a higher number of genes for the pathway of TAG synthesis. In *Chlamydomonas*, six copies of diacylglycerol acyltransferases (DAGATs) were identified and categorized into two types; one DGAT, and five DGTs (Deng *et al.*, 2012; Merchant *et al.*, 2012). A more extreme case is seen in *Nannochloropsis* sp., an ologenous marine alga that has 13 copies of predicted DAGAT encoding genes (Vieler *et al.*, 2012). This higher number of gene copies for putative DAGATs in the algae compared to *Arabidopsis* could suggest gene loss during evolution due to the fact that vegetative tissues of higher plants do not accumulate TAG in high quantity.

LIPOLYSIS AND LIPASES

Lipolysis is a crucial reaction that results in the generation of lipid messengers, membrane remodeling and lipid homeostasis. Lipases hydrolyze either an ester or amide bond of an acyl chain from various types of lipids, resulting in a free fatty acid and the corresponding lysolipid. Lipases are diverse enzymes including TAG lipases, phospholipases, galactolipases, ceraminidases, cholesterol ester hydrolases and retinol ester hydrolases (M. Li & Wang, 2014). Figure 1.2 shows lipolysis of neutral lipids by TAG, DAG, or monoacylglycerol (MAG) lipase. For the purpose of TAG homeostasis in *Chlamydomonas* that is discussed in Chapter 3, I will focus on TAG lipase in this section.

Lipases are interfacial enzymes. This is due to the fact that the enzyme is hydrophilic whereas the substrate is lipophilic. This phenomenon was originally observed by Schönheyder and Volqvartz (1945) and then reinvestigated by Sarda and Desnuelle (1958). In a low concentration of substrate, lipase activity was almost undetectable. However, when the concentration of the hydrophobic substrate exceeded the solubility limit, thus allowing the substrate to be present in the form of micelles or emulsion drops, the lipase activity was increased sharply. The enzyme is activated by its interaction with the aqueous-hydrophobic interface. For this reason, kinetics of the TAG lipase does not follow normal Michaelis-Menten kinetics as reviewed by Gill and Parish (1997); Verger (1976); Reis *et al.* (2009). The mechanism of interfacial activation has been explained through a three dimensional structure of a *Mucor miehei* TAG lipase (Brady *et al.*, 1990) and of human pancreatic lipase (Winkler *et al.*, 1990). In the inactive stage, the active site of the lipase, containing serine, histidine, and aspartate residues, is protected from the hydrophilic environment by a lid structure. Upon interaction with aqueous-lipid interface, the enzyme undergoes a conformational change exposing the active site to the hydrophobic substrate.

Many TAG lipases contain a patatin domain. Patatins (Pfam01734) are potato tuber proteins that carry an evolutionarily conserved esterase box GX SXG (where G is glycine, X is any amino acid, and S is serine) and exhibit acyl-hydrolyzing activity (Andrews *et al.*, 1988). This group of proteins was classified into the patatin-related phospholipase A family (pPLA), which is a member of the phospholipase A₂ (PLA₂) superfamily (Scherer *et al.*, 2010). This PLA₂ superfamily is comprised of the cytosolic or Ca²⁺-activated cPLA₂, the Ca²⁺-independent iPLA₂

and the secreted sPLA₂ as summarized in (Scherer *et al.*, 2010). The pPLAs can be further classified into 4 groups; pPLAI, pPLAII (α , β , γ , δ , ϵ), pPLAIII (α , β , γ , δ) (Scherer *et al.*, 2010), and group 4 subclass (M. Li & Wang, 2014). Group 4 contains the only enzymes that catalyze hydrolysis of TAG while the other members of pPLAs hydrolyze phospholipids and/or galactoglycerolipids. Members of group 4 pPLAs are Arabidopsis SDP1, SDP1-like, and adipose triglyceride lipase-like (ATGL-L) (Eastmond, 2006). As discussed in detail in Chapter 3, SDP1 is responsible for TAG mobilization during seed germination and the establishment of photosynthesis.

Patatin-domain containing enzymes are unique lipases. As mentioned previously, patatin domain containing lipases contain an esterase motif and exhibit acylhydrolase activity as do typical lipases. However, crystallography of Pat17, an isozyme of potato patatin, revealed that patatin did not possess a canonical catalytic triad (Serine-Aspartate-Histidine) and did not adopt an α/β hydrolase fold structure as do other lipases (Rydel *et al.*, 2003). Instead Pat17 carries a catalytic dyad (Serine-Aspartate) with an $\alpha/\beta/\alpha$ structure. In addition, the study showed that Pat17 lacked a lid structure that was proposed to protect the catalytic site of a lipase. Therefore, the authors concluded that patatin did not likely interact interfacially, as opposed to other lipases. The activation of patatin was proposed to occur through translocation of the enzyme from the storage vacuole to the cytosol (H. Sato & Frank, 2004).

In the same study of Pat17 by Rydel *et al.* (2003), an amphipathic helical structure was identified within its topology that is equivalent to the lid structure of human cytosolic phospholipase A2 (cPLA₂) (Dessen *et al.*, 1999). Furthermore, low-resolution homology models of human patatin-like phospholipases (PNPLAs) suggested a loop structure that could function as a lid but with minimal flexibility (Wilson *et al.*, 2006). Since mammalian ATGL is a member of PNPLAs (Kienesberger *et al.*, 2009) and also a homologue of SDP1 (Eastmond, 2006) in group 4 pPLA, it is still unclear whether members of group 4 pPLA possesses a lid structure that allows the enzyme to be activated at the water-lipid interface. Biochemical and structural analyses are necessary to unravel this problem.

MUTANT SCREENING AND IDENTIFICATION OF A RESPONSIBLE GENE

Fundamental questions in biology have been studied through model organisms such as *Caenorhabditis elegans*, fruit fly, Arabidopsis, zebrafish and mouse. Knowledge from these studies can be further applied to other organisms including economically important ones, e.g. food crops and livestock as well as humans. For this purpose, genetic screening serves as a great tool to study gene function in model organisms. This approach can be classified into two types; forward and reverse genetics. Forward genetics starts with a particular phenotype and seeks to identify the responsible gene. In reverse genetics, the site of mutation is known, and the phenotype is characterized. While reverse genetics specifically studies the function of a particular gene, forward genetics allows one to discover a novel gene. In this section, I will focus on mutagenesis and gene identification through forward genetic screening.

Forward genetic screening

Forward genetic screens utilize chemical, physical or biological agents to mutate DNA of an organism. Chemical mutagens, such as ethylmethanol sulphonate (EMS) and nitrosomethylurea (NMU), yield a high mutation rate and depending on the mutagen, they generate various types of mutation including base substitutions and small insertions and deletions (Alonso & Ecker, 2006). The major disadvantage of using chemical mutagens is the unknown location of the mutated genes. This is due to the fact that point mutations are difficult to locate, especially in a large genome. Physical agents such as fast neutrons, X-rays or accelerated ions can be utilized to introduce large insertions/deletions and rearrangements in the genome (Alonso & Ecker, 2006). Finally, certain biological agents such as T-DNA and transposons can also be used to induce mutations. Selectable markers can also be used for mutagenesis by random insertional gene disruption. These include antibiotic or herbicide resistance, and genes that confer the ability to grow under specific conditions (prototrophy). Forward genetic screens using biological agents are widely used in *Chlamydomonas* because identification of the mutation is relatively easy. Using a specific DNA sequence that is carried by the biological agent, PCR-based techniques can be used to identify the mutation within adjacent DNA.

Once a population of transformants is generated, screening for mutants with a diagnostic phenotype is performed. For instance, *Chlamydomonas* mutants accumulating high amounts of TAG can be screened by Nile Red fluorescence staining which is specific for neutral lipids (Kimura *et al.*, 2004). The signal is detected with a plate reader (X. Li *et al.*, 2012) or a flow

cytometry (Cagnon *et al.*, 2013). In my study, the identification of the *Chlamydomonas* *tgd2* mutant in Chapter 2 was carried out following a random insertional mutagenesis with a DNA fragment carrying a hygromycin resistance gene (*AphVII*). The mutant population was screened by Western blot using an antibody against the major lipid droplet protein (MLDP). Its abundance is tightly correlated with the amount of TAG accumulating in the cells. A diagram of the screening procedure is depicted in Figure 1.3. After the mutants have been identified, the responsible genes that cause the phenotype need to be identified. Different methods are discussed below.

Map-based cloning. Before DNA sequencing and/or PCR became available, the method to identify mutations relied on map-based cloning (also called positional cloning) which was first introduced in 1913 (Sturtevant, 1913). The principle of this approach is that the distance between the gene of interest and the marker correlates to the recombination frequency. In general, the more infrequent the recombination events, the closer the gene of interest is to the marker. Therefore, this technique relies on the availability of markers, which were limited until the invention of ways to detect DNA differences between isolates or ecotypes including restriction fragment length polymorphisms (RFLPs) (Botstein *et al.*, 1980), random amplified polymorphic DNAs (RAPDs) (Williams *et al.*, 1990), simple sequence repeats (SSRs) (Bell & Ecker, 1994), single-nucleotide amplified polymorphisms (SNAP) (Drenkard *et al.*, 2000), and amplified fragment length polymorphisms (AFLP) (Vos *et al.*, 1995). The advantage of mapping with DNA-based markers is that no prior knowledge about a specific gene is required. The time for mapping a specific gene in *Arabidopsis* has been shortened from 3-5 years to a single year (Jander *et al.*, 2002), and most recently to months using combined mapping and sequencing strategies involving whole genome-resequencing techniques, which are discussed in the following sections.

PCR-based methods. PCR-based techniques exploit the known DNA sequence that was used for creating an insertional mutation as a key to identify the unknown flanking region. Only one defined primer-binding site is known, and it lies within the DNA insertion. Several different strategies are used to enable a second oligonucleotide to prime the reaction from the adjacent unknown DNA as discussed in three examples below.

The first example is inverse PCR, which is based on the inversion of an insert and flanking sequence to generate two primer-binding sites at both ends of the fragment (Triglia *et al.*, 1988). The technique employs one restriction enzyme, which cuts the genomic DNA outside the insertion. The digested product is ligated to itself to create a circular molecule. This molecule is then digested with a second restriction enzyme to produce a linearized DNA fragment having unknown sequence flanked by known DNA sequence at both 5' and 3' ends. With the known DNA sequence at both ends, PCR amplification can be carried out and the specific product can be amplified.

The second approach is to attach another known DNA fragment to the sequence that flanks the insertion. An example of this approach is called SiteFinding-PCR (Tan *et al.*, 2005). In this approach, the first round of PCR is carried out with a primer specific for the insertion and another primer attached to a SiteFinder that contains a restriction site and a semi-random sequence. The random sequence in the SiteFinder of the second primer allows semi non-specific amplification. More specific amplicons can be obtained through nested PCRs. The PCR product can then be digested with a restriction enzyme specific to the site at the SiteFinder and cloned into a vector for determining the sequence of a gene of interest.

The third method is thermal asymmetric interlaced (TAIL-) PCR (Y. G. Liu *et al.*, 1995; Y. G. Liu & Whittier, 1995). This method does not require any modification of DNA molecule. A series of PCRs are carried out with one specific primer that can bind to an insert fragment and an arbitrary degenerate primer. The alternating PCR cycles between high and low stringency are used to increase specificity of the amplification, followed by another two sets of PCR with nested primers to enhance specificity.

PCR-based methods are relatively easy and require less time compared to map-based cloning. However these approaches can be applied only to the mutants generated through biological mutagens with known sequence. In addition, high false positive rates can occur through the amplification of non-specific sequences due to the fact that only one primer-binding site is known. Finally, since this method relies on amplification at the insertion site, if the insertion is located in a high GC region, the amplification can be difficult. An example of the last case can be seen in the identification of the *tgd2* mutant in Chapter 2 in which inverse PCR and SiteFinding PCR both failed to identify the insertion site.

Whole genome resequencing. Both conventional and next generation DNA sequencing technologies have enabled many genome projects from diverse organisms starting with bacteriophage MS2 in 1976 (Fiers *et al.*, 1976). Twenty years later the first eukaryote to have its genome sequence was *Saccharomyces cerevisiae* (Goffeau *et al.*, 1996). From that point on, many genome projects of model organisms have been completed. These include *Caenorhabditis elegans* (Consortium, 1998), Arabidopsis (Arabidopsis Genome, 2000), fruitfly (Adams *et al.*, 2000), human (Venter *et al.*, 2001), and Chlamydomonas (Merchant *et al.*, 2007), etc. The availability of next generation sequencing, which offers high-throughput results at an affordable price, and an extensive genome database provided new tools for identifying all kinds of mutations by directly comparing genomes of mutants to that of the reference genome.

Resequencing allows direct comparison of the genome sequence of the mutant with the reference genome from the database. Sequencing reads of the mutant can be aligned with those of the reference genome through a computer program that uses algorithms based on the Burrows-Wheeler Transform such as Bowtie (Langmead *et al.*, 2009) and BWA (H. Li & Durbin, 2009). For example, 46 somatic mutations in four types of chronic lymphocytic leukemia were identified through an alignment between tumor DNA sequences and the human reference genome (Puente *et al.*, 2011). The major advantage of this method is that it can be applied to mutations with single nucleotide changes or short insertions/deletions depending on the parameter settings and software. However, the application of this approach is limited to a mutant generated in the same background as the reference genome. In addition, detection of large insertions/deletions or rearrangements can be challenging.

As a variation, the site of insertion of a specific DNA sequence can be identified based on construction of contigs that contain the alien DNA. This approach can overcome the drawbacks of the read alignment approach because it can be applied to a mutant that is not generated from a reference genome background. However, this method is also limited to insertional mutagenesis. An example of this approach is the identification of the Chlamydomonas *tgd2* mutant in Chapter 2. This mutant was generated in Chlamydomonas strain dw15.1 (CC-4619 cw15 nit1 mi⁺), which is not the same strain as the reference genome (CC-503 cw92 mt⁺). In this case, the huge number of polymorphisms between the two Chlamydomonas strains can overwhelm the real mutation. However, alignment of the insert sequence to the contigs of assembled reads allowed its site of insertion to be established. Figure 1.4 illustrates this process.

A point mutation that is generated in a non-reference background can be detected through a method called mapping by sequencing. The principle of this approach is to sequence a pooled group of the F₂ generation that carry the mutant phenotype produced from a cross between the mutant in the non-reference background to the reference genome. The read alignment between the mutants and the reference genome can identify both polymorphisms and mutations. These two types of reads can be distinguished based on the principle of genetic recombination as in the conventional mapping. More information about this technique can be found in a number of articles (Candela *et al.*, 2015; Ossowski *et al.*, 2008; Schneeberger *et al.*, 2009). An essential component of this method is the availability of a reference genome. Recently a new technique has been invented to eliminate this requirement. Based on the differences in frequency of *k*-mer (subsequence of length *k* from a sequencing read) between two closely related genomes, e.g. wild type and mutant, a single nucleotide change can be detected even in a mutant generated from non-reference background (Nordstrom *et al.*, 2013).

Forward genetic screening in *Chlamydomonas*

A number of forward genetic screens in *Chlamydomonas* have been carried out over the past 60 years. These screens led to identification of genes involved in photosynthesis, mobility, mating, nitrogen assimilation, and biosynthetic pathways, as summarized by Jinkerson and Jonikas (2015). Some of these genes were screened based on their lipid phenotype, i.e. *sqd1* (Riekhof *et al.*, 2003), *crfad7* (Nguyen *et al.*, 2013), and *pgd1* (X. Li *et al.*, 2012) and *cht7* (Tsai *et al.*, 2014). Mutations have been created by several mutagens, including chemicals (EMS and *N*-methyl-*N'*-nitro-*N*-nitrosoguanidine, MNNG), physical insult (UV, X-ray and gamma irradiation), and biological agents (e.g., using hygromycin and paromomycin resistance genes on a transforming DNA). The mutant alleles were mapped with various methods including classical genetic mapping and PCR-based techniques. In 2012, whole genome sequencing was first reported to identify mutations and polymorphisms in *Chlamydomonas* (Dutcher *et al.*, 2012), followed quickly by others (Lin *et al.*, 2013a; Lin *et al.*, 2013b; Tulin & Cross, 2014). Recently, two UV-induced *Chlamydomonas* mutants exhibiting high light tolerance were also identified through this approach (Schierenbeck *et al.*, 2015). These examples show that discovery of novel genes in *Chlamydomonas* can be accomplished through different types of forward genetic screening. In addition, many methods can be employed to identify a causative gene. Details about genetic screening in *Chlamydomonas* to discover genes in lipid metabolism can be found

in several recent articles (Cagnon *et al.*, 2013; Jinkerson & Jonikas, 2015; Terashima *et al.*, 2015).

AIM OF THE THESIS RESEARCH

As previously mentioned, unicellular microalgae are crucial for a well-balanced ecological system as primary producers and they have a great potential for alternative energy and bio-product production. Our current state of knowledge indicates that not all biological and biochemical processes in microalgae are identical to those of land plants or other kingdoms of life. With respect to lipids, microalgae produce unique fatty acids and lipids that are absent from plants. On the other hand, some lipids found in plants are missing in algae. Moreover, enzymes for some important metabolic functions have not been characterized. This thesis research attempts to resolve these discrepancies at least in part. *Chlamydomonas reinhardtii*, was selected as a model organism to represent unicellular microalgae and their lipid metabolism. The study is composed of two major parts. First, a forward genetic screen was performed to identify novel genes involved in lipid metabolism. The function of one gene in lipid metabolism of *Chlamydomonas* was then characterized. The details of this project can be found in Chapter 2. Second, a *Chlamydomonas* orthologue of a central triacylglycerol lipase in *Arabidopsis* seeds was characterized in Chapter 3. In addition, a collaborative project was carried out to study a gene important for synthesizing a unique fatty acid found in the chloroplast of *Chlamydomonas*. This topic will be addressed in the Appendix.

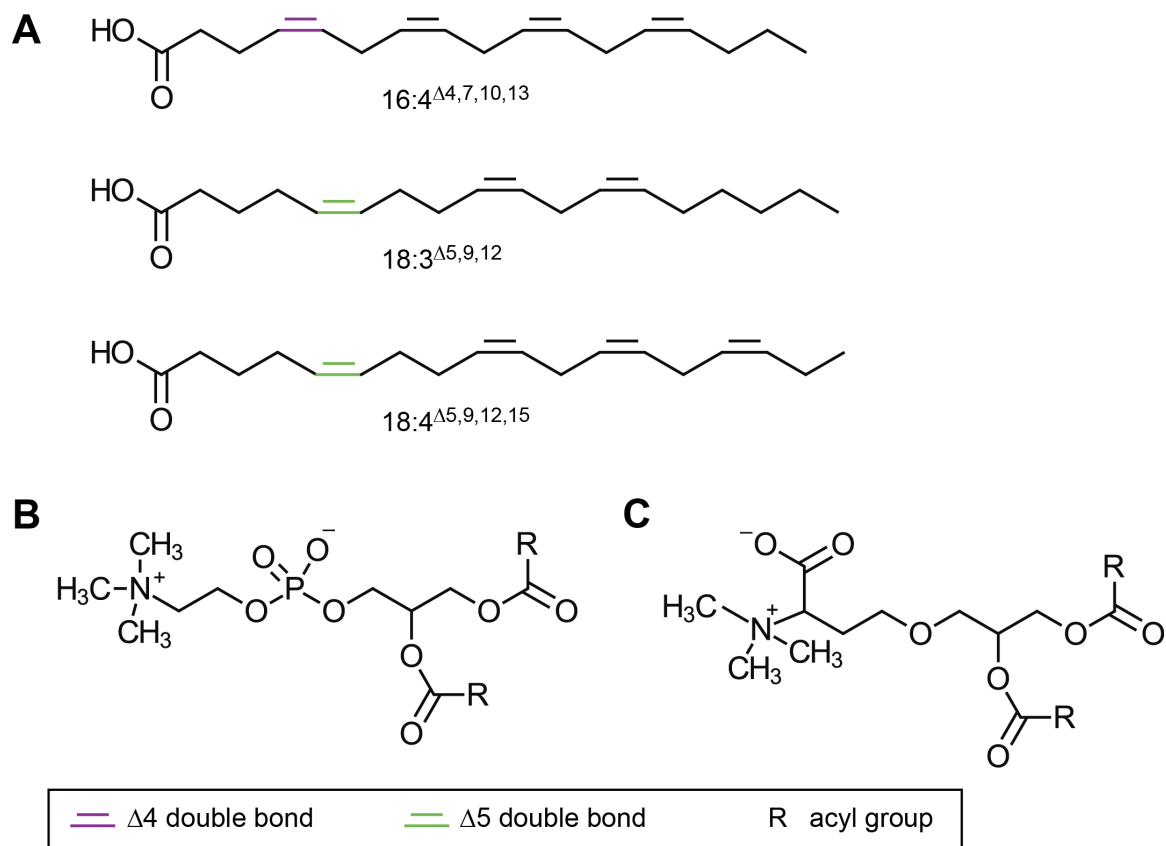


Figure 1.1. Chemical structures of fatty acids and lipids

(A) 16:4 $\Delta^{4,7,10,13}$, 18:3 $\Delta^{5,9,12}$, and 18:4 $\Delta^{5,9,12,15}$ fatty acids

(B) phosphatidylcholine (PtdCho)

(C) diacylglyceryl-*N,N,N*-trimethylhomoserine (DGTS)

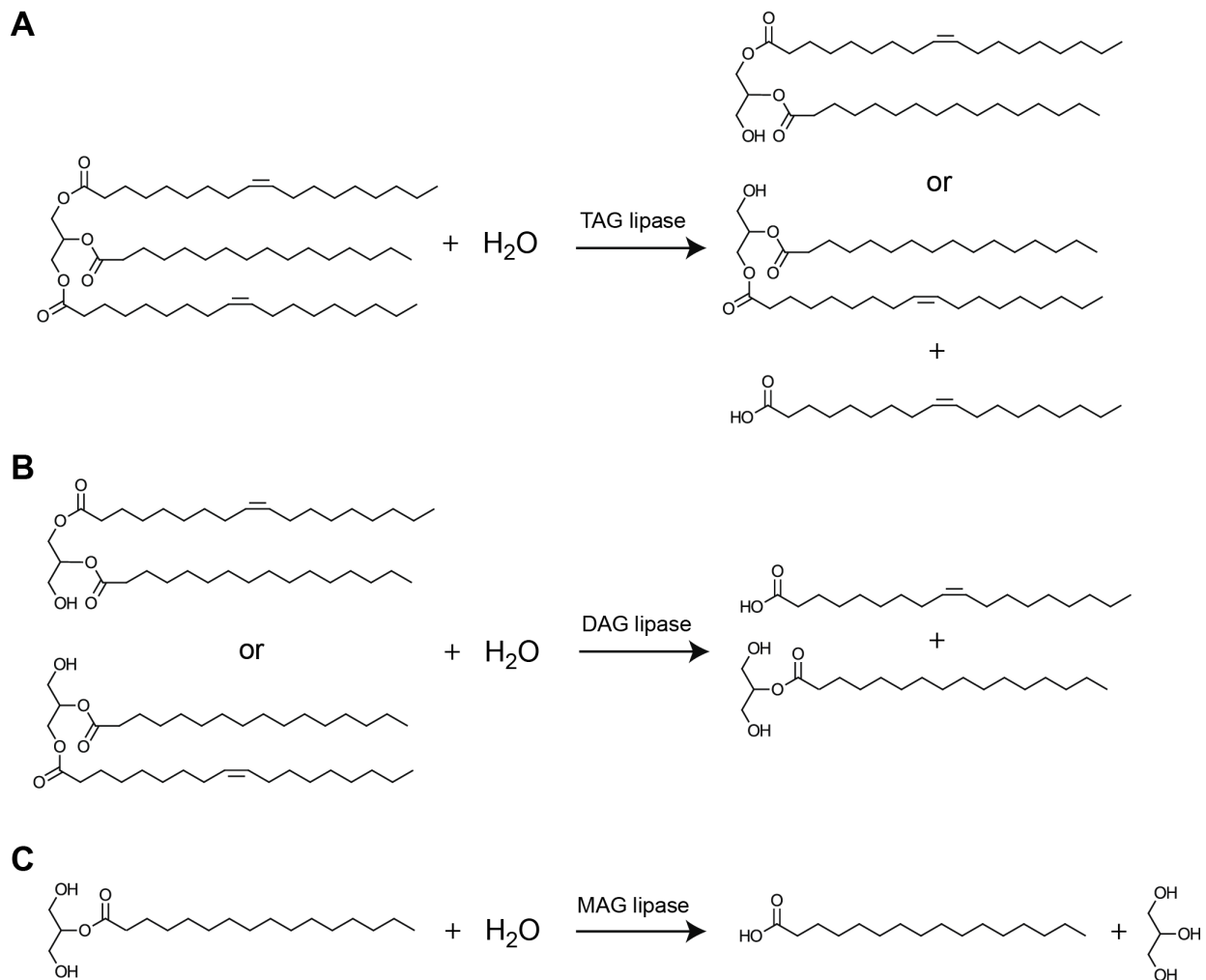


Figure 1.2. Lipolysis of neutral lipids

(A) Degradation of triacylglycerol (TAG) by TAG lipase yields 1,2- or 2,3-diacylglycerol (DAG) and free fatty acid (FFA). (B) Degradation of DAG by DAG lipase yields monoacylglycerol (MAG) and FFA. (C) Degradation of MAG by MAG lipase yields FFA and glycerol backbone.

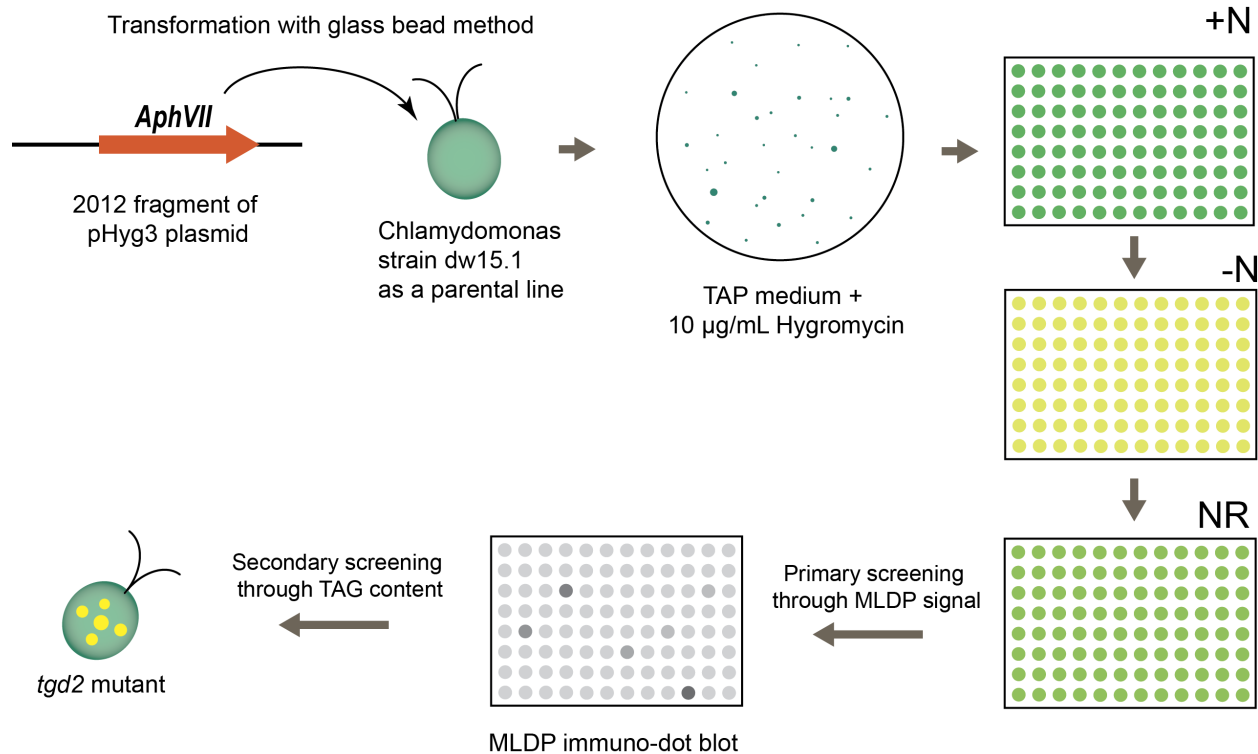


Figure 1.3. Screening of *Chlamydomonas* mutants

A random insertional mutagenesis was performed with the *AphVII* gene from the pHyg3 plasmid in the *Chlamydomonas* parental line (PL) strain dw15.1. The transformed colonies were selected on Tris-Acetate-Phosphate (TAP) medium with hygromycin. The transformants were picked and grown in liquid TAP medium (under nitrogen replete condition, N+) in 96-well culture plates. To induce TAG accumulation, the cultures were transferred to TAP medium without nitrogen (N-) and incubated for 48 hours. The cultures were then reintroduced into TAP medium with nitrogen (NR), in order to observe TAG degradation. A mutant defective in this process is expected to have a high level of TAG compared to the PL. The amount of TAG can be determined by immuno-dot blot against the major lipid droplet protein (MLDP). The MLDP signal was normalized with the density of the cells measured by a plate reader. Colonies showing a strong signal for MLDP were then tested for TAG content. During this screen the *tg d2* mutant was discovered and shown to have increased TAG levels. Further details of this screening procedure can be found in Chapter 2.

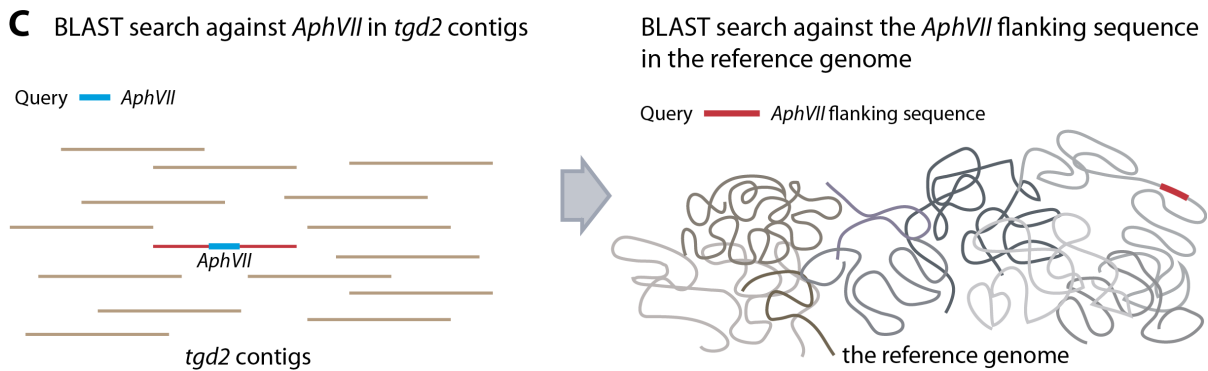
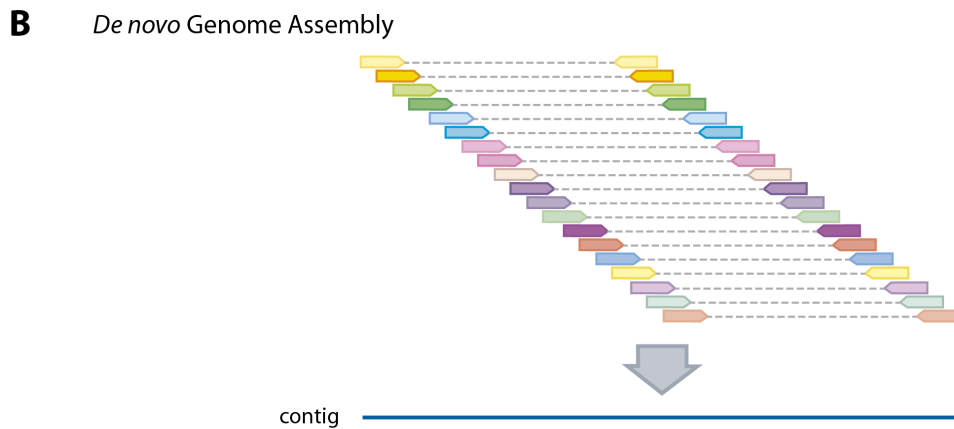
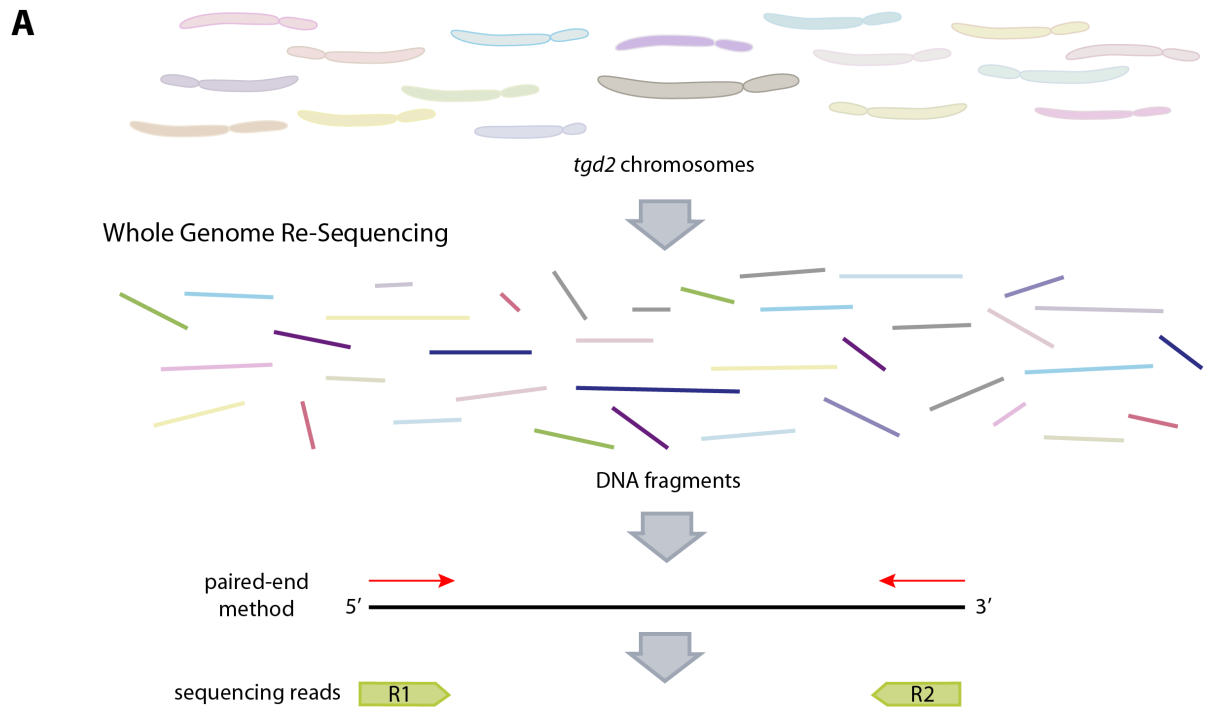


Figure 1.4. Identification of the insertion locus in the *Chlamydomonas tgd2* mutant using whole-genome resequencing.

Figure 1.4. (Continued)

The genome of the *Chlamydomonas tgd2* mutant was sequenced using the Illumina Hi-Seq paired-end method (A). Each DNA fragment was sequenced at both ends yielding 2 sequencing reads. Paired sequencing reads were used for *de novo* genome assembly (B) based on a known distance between the two reads illustrated as broken lines. This assembly yielded a number of contigs of the *tgd2* genome. Identification of the insertion site was carried out in two major steps (C). First, the *AphVII* sequence was located in the *tgd2* contigs by a BLAST search. Second, the *tgd2* sequence flanking the *AphVII* was used as a query for another BLAST search in the reference genome. Once the insertion was located, alignment between the *tgd2* contig containing the insertion and the reference genome in the corresponding location was carried out to determine the nature of the insertion site and possible deletions close by. The structure of the locus in the mutant was then further probed and confirmed with PCR. Further details of this process can be found in Chapter 2.

REFERENCES

REFERENCES

- Adams, M. D., Celniker, S. E., Holt, R. A., Evans, C. A., Gocayne, J. D., Amanatides, P. G., Scherer, S. E., Li, P. W., Hoskins, R. A., Galle, R. F., George, R. A., Lewis, S. E., Richards, S., Ashburner, M., Henderson, S. N., Sutton, G. G., Wortman, J. R., Yandell, M. D., Zhang, Q., Chen, L. X., Brandon, R. C., Rogers, Y. H., Blazej, R. G., Champe, M., Pfeiffer, B. D., Wan, K. H., Doyle, C., Baxter, E. G., Helt, G., Nelson, C. R., Gabor, G. L., Abril, J. F., Agbayani, A., An, H. J., Andrews-Pfannkoch, C., Baldwin, D., Ballew, R. M., Basu, A., Baxendale, J., Bayraktaroglu, L., Beasley, E. M., Beeson, K. Y., Benos, P. V., Berman, B. P., Bhandari, D., Bolshakov, S., Borkova, D., Botchan, M. R., Bouck, J., Brokstein, P., Brottier, P., Burtis, K. C., Busam, D. A., Butler, H., Cadieu, E., Center, A., Chandra, I., Cherry, J. M., Cawley, S., Dahlke, C., Davenport, L. B., Davies, P., de Pablos, B., Delcher, A., Deng, Z., Mays, A. D., Dew, I., Dietz, S. M., Dodson, K., Doup, L. E., Downes, M., Dugan-Rocha, S., Dunkov, B. C., Dunn, P., Durbin, K. J., Evangelista, C. C., Ferraz, C., Ferriera, S., Fleischmann, W., Fosler, C., Gabrielian, A. E., Garg, N. S., Gelbart, W. M., Glasser, K., Glodek, A., Gong, F., Gorrell, J. H., Gu, Z., Guan, P., Harris, M., Harris, N. L., Harvey, D., Heiman, T. J., Hernandez, J. R., Houck, J., Hostin, D., Houston, K. A., Howland, T. J., Wei, M. H., Ibegwam, C., Jalali, M., Kalush, F., Karpen, G. H., Ke, Z., Kennison, J. A., Ketchum, K. A., Kimmel, B. E., Kodira, C. D., Kraft, C., Kravitz, S., Kulp, D., Lai, Z., Lasko, P., Lei, Y., Levitsky, A. A., Li, J., Li, Z., Liang, Y., Lin, X., Liu, X., Mattei, B., McIntosh, T. C., McLeod, M. P., McPherson, D., Merkulov, G., Milshina, N. V., Mobarry, C., Morris, J., Moshrefi, A., Mount, S. M., Moy, M., Murphy, B., Murphy, L., Muzny, D. M., Nelson, D. L., Nelson, D. R., Nelson, K. A., Nixon, K., Nusskern, D. R., Pacleb, J. M., Palazzolo, M., Pittman, G. S., Pan, S., Pollard, J., Puri, V., Reese, M. G., Reinert, K., Remington, K., Saunders, R. D., Scheeler, F., Shen, H., Shue, B. C., Siden-Kiamos, I., Simpson, M., Skupski, M. P., Smith, T., Spier, E., Spradling, A. C., Stapleton, M., Strong, R., Sun, E., Svirskas, R., Tector, C., Turner, R., Venter, E., Wang, A. H., Wang, X., Wang, Z. Y., Wassarman, D. A., Weinstock, G. M., Weissenbach, J., Williams, S. M., WoodageT, Worley, K. C., Wu, D., Yang, S., Yao, Q. A., Ye, J., Yeh, R. F., Zaveri, J. S., Zhan, M., Zhang, G., Zhao, Q., Zheng, L., Zheng, X. H., Zhong, F. N., Zhong, W., Zhou, X., Zhu, S., Zhu, X., Smith, H. O., Gibbs, R. A., Myers, E. W., Rubin, G. M., & Venter, J. C. (2000). The genome sequence of *Drosophila melanogaster*. *Science*, 287(5461), 2185-2195.
- Alonso, J. M., & Ecker, J. R. (2006). Moving forward in reverse: genetic technologies to enable genome-wide phenomic screens in *Arabidopsis*. *Nat Rev Genet*, 7(7), 524-536. doi: 10.1038/nrg1893
- Andrews, D. L., Beames, B., Summers, M. D., & Park, W. D. (1988). Characterization of the lipid acyl hydrolase activity of the major potato (*Solanum tuberosum*) tuber protein, patatin, by cloning and abundant expression in a baculovirus vector. *Biochem J*, 252(1), 199-206.

- Arabidopsis Genome, I. (2000). Analysis of the genome sequence of the flowering plant *Arabidopsis thaliana*. *Nature*, 408(6814), 796-815. doi: 10.1038/35048692
- Awai, K., Marechal, E., Block, M. A., Brun, D., Masuda, T., Shimada, H., Takamiya, K., Ohta, H., & Joyard, J. (2001). Two types of MGDG synthase genes, found widely in both 16:3 and 18:3 plants, differentially mediate galactolipid syntheses in photosynthetic and nonphotosynthetic tissues in *Arabidopsis thaliana*. *Proc Natl Acad Sci U S A*, 98(19), 10960-10965. doi: 10.1073/pnas.181331498
- Bell, C. J., & Ecker, J. R. (1994). Assignment of 30 microsatellite loci to the linkage map of *Arabidopsis*. *Genomics*, 19(1), 137-144. doi: 10.1006/geno.1994.1023
- Botstein, D., White, R. L., Skolnick, M., & Davis, R. W. (1980). Construction of a genetic linkage map in man using restriction fragment length polymorphisms. *Am J Hum Genet*, 32(3), 314-331.
- Botte, C. Y., Deligny, M., Rocchia, A., Bonneau, A. L., Saidani, N., Hardre, H., Aci, S., Yamaro-Botte, Y., Jouhet, J., Dubots, E., Loizeau, K., Bastien, O., Brehelin, L., Joyard, J., Cintrat, J. C., Falconet, D., Block, M. A., Rousseau, B., Lopez, R., & Marechal, E. (2011a). Chemical inhibitors of monogalactosyldiacylglycerol synthases in *Arabidopsis thaliana*. *Nat Chem Biol*, 7(11), 834-842. doi: 10.1038/nchembio.658
- Botte, C. Y., Yamaro-Botte, Y., Janouskovec, J., Rupasinghe, T., Keeling, P. J., Crellin, P., Coppel, R. L., Marechal, E., McConville, M. J., & McFadden, G. I. (2011b). Identification of plant-like galactolipids in *Chromera velia*, a photosynthetic relative of malaria parasites. *J Biol Chem*, 286(34), 29893-29903. doi: 10.1074/jbc.M111.254979
- Brady, L., Brzozowski, A. M., Derewenda, Z. S., Dodson, E., Dodson, G., Tolley, S., Turkenburg, J. P., Christiansen, L., Hugel-Jensen, B., Norskov, L., & et al. (1990). A serine protease triad forms the catalytic centre of a triacylglycerol lipase. *Nature*, 343(6260), 767-770. doi: 10.1038/343767a0
- Cagnon, C., Mirabella, B., Nguyen, H. M., Beyly-Adriano, A., Bouvet, S., Cuine, S., Beisson, F., Peltier, G., & Li-Beisson, Y. (2013). Development of a forward genetic screen to isolate oil mutants in the green microalga *Chlamydomonas reinhardtii*. *Biotechnol Biofuels*, 6(1), 178. doi: 10.1186/1754-6834-6-178
- Candela, H., Casanova-Saez, R., & Micol, J. L. (2015). Getting started in mapping-by-sequencing. *J Integr Plant Biol*, 57(7), 606-612. doi: 10.1111/jipb.12305
- Consortium, C. e. S. (1998). Genome sequence of the nematode *C. elegans*: a platform for investigating biology. *Science*, 282(5396), 2012-2018.
- Day, A., & Goldschmidt-Clermont, M. (2011). The chloroplast transformation toolbox: selectable markers and marker removal. *Plant Biotechnol J*, 9(5), 540-553. doi: 10.1111/j.1467-7652.2011.00604.x

- Demirbas, A., & Fatih Demirbas, M. (2011). Importance of algae oil as a source of biodiesel. *Energy Convers Manage*, 52(1), 163-170. doi: 10.1016/j.enconman.2010.06.055
- Deng, X. D., Gu, B., Li, Y. J., Hu, X. W., Guo, J. C., & Fei, X. W. (2012). The roles of acyl-CoA: diacylglycerol acyltransferase 2 genes in the biosynthesis of triacylglycerols by the green algae *Chlamydomonas reinhardtii*. *Mol Plant*, 5(4), 945-947. doi: 10.1093/mp/sss040
- Dessen, A., Tang, J., Schmidt, H., Stahl, M., Clark, J. D., Seehra, J., & Somers, W. S. (1999). Crystal structure of human cytosolic phospholipase A2 reveals a novel topology and catalytic mechanism. *Cell*, 97(3), 349-360.
- Dismukes, G. C., Carrieri, D., Bennette, N., Ananyev, G. M., & Posewitz, M. C. (2008). Aquatic phototrophs: efficient alternatives to land-based crops for biofuels. *Curr Opin Biotechnol*, 19(3), 235-240. doi: 10.1016/j.copbio.2008.05.007
- Drenkard, E., Richter, B. G., Rozen, S., Stutius, L. M., Angell, N. A., Mindrinos, M., Cho, R. J., Oefner, P. J., Davis, R. W., & Ausubel, F. M. (2000). A simple procedure for the analysis of single nucleotide polymorphisms facilitates map-based cloning in *Arabidopsis*. *Plant Physiol*, 124(4), 1483-1492.
- Dutcher, S. K., Li, L., Lin, H., Meyer, L., Giddings, T. H., Jr., Kwan, A. L., & Lewis, B. L. (2012). Whole-Genome Sequencing to Identify Mutants and Polymorphisms in *Chlamydomonas reinhardtii*. *G3 (Bethesda)*, 2(1), 15-22. doi: 10.1534/g3.111.000919
- Eastmond, P. J. (2006). SUGAR-DEPENDENT1 encodes a patatin domain triacylglycerol lipase that initiates storage oil breakdown in germinating *Arabidopsis* seeds. *Plant Cell*, 18(3), 665-675. doi: 10.1105/tpc.105.040543
- Fiers, W., Contreras, R., Duerinck, F., Haegeman, G., Iserentant, D., Merregaert, J., Min Jou, W., Molemans, F., Raeymaekers, A., Van den Berghe, A., Volckaert, G., & Ysebaert, M. (1976). Complete nucleotide sequence of bacteriophage MS2 RNA: primary and secondary structure of the replicase gene. *Nature*, 260(5551), 500-507.
- Frentzen, M., Heinz, E., McKeon, T. A., & Stumpf, P. K. (1983). Specificities and selectivities of glycerol-3-phosphate acyltransferase and monoacylglycerol-3-phosphate acyltransferase from pea and spinach chloroplasts. *Eur J Biochem*, 129(3), 629-636.
- Gill, J., & Parish, J. H. (1997). Minireview: Lipases—enzymes at an interface. *Biochem Educ*, 25(1), 2-5. doi: 10.1016/S0307-4412(96)00125-2
- Giroud, C., Gerber, A., & Eichenberger, W. (1988). Lipids of *Chlamydomonas reinhardtii*. Analysis of Molecular Species and Intracellular Site(s) of Biosynthesis. *Plant Cell Physiol*, 29(4), 587-595.

- Goffeau, A., Barrell, B. G., Bussey, H., Davis, R. W., Dujon, B., Feldmann, H., Galibert, F., Hoheisel, J. D., Jacq, C., Johnston, M., Louis, E. J., Mewes, H. W., Murakami, Y., Philippsen, P., Tettelin, H., & Oliver, S. G. (1996). Life with 6000 genes. *Science*, 274(5287), 546, 563-547.
- Goodenough, U. (2015). Historical perspective on Chlamydomonas as a model for basic research: 1950-1970. *Plant J*, 82(3), 365-369. doi: 10.1111/tpj.12794
- Harris, E. H. (1989). *The Chlamydomonas sourcebook: a comprehensive guide to biology and laboratory use*. San Diego: Academic Press.
- Harris, E. H. (2001). Chlamydomonas as a Model Organism. *Annu Rev Plant Physiol Plant Mol Biol*, 52, 363-406. doi: 10.1146/annurev.arplant.52.1.363
- Heinz, E., & Roughan, P. G. (1983). Similarities and differences in lipid metabolism of chloroplasts isolated from 18:3 and 16:3 plants. *Plant Physiol*, 72(2), 273-279.
- James, G. O., Hocart, C. H., Hillier, W., Chen, H., Kordbacheh, F., Price, G. D., & Djordjevic, M. A. (2011). Fatty acid profiling of Chlamydomonas reinhardtii under nitrogen deprivation. *Bioresour Technol*, 102(3), 3343-3351. doi: 10.1016/j.biortech.2010.11.051
- Jander, G., Norris, S. R., Rounsley, S. D., Bush, D. F., Levin, I. M., & Last, R. L. (2002). Arabidopsis map-based cloning in the post-genome era. *Plant Physiol*, 129(2), 440-450. doi: 10.1104/pp.003533
- Jinkerson, R. E., & Jonikas, M. C. (2015). Molecular techniques to interrogate and edit the Chlamydomonas nuclear genome. *Plant J*, 82(3), 393-412. doi: 10.1111/tpj.12801
- Kajikawa, M., Yamato, K. T., Kohzu, Y., Shoji, S., Matsui, K., Tanaka, Y., Sakai, Y., & Fukuzawa, H. (2006). A front-end desaturase from Chlamydomonas reinhardtii produces pinolenic and coniferonic acids by omega13 desaturation in methylotrophic yeast and tobacco. *Plant Cell Physiol*, 47(1), 64-73. doi: 10.1093/pcp/pci224
- Kienesberger, P. C., Oberer, M., Lass, A., & Zechner, R. (2009). Mammalian patatin domain containing proteins: a family with diverse lipolytic activities involved in multiple biological functions. *J Lipid Res*, 50 Suppl, S63-68. doi: 10.1194/jlr.R800082-JLR200
- Kim, H. U., Li, Y., & Huang, A. H. (2005). Ubiquitous and endoplasmic reticulum-located lysophosphatidyl acyltransferase, LPAT2, is essential for female but not male gametophyte development in Arabidopsis. *Plant Cell*, 17(4), 1073-1089. doi: 10.1105/tpc.104.030403
- Kimura, K., Yamaoka, M., & Kamisaka, Y. (2004). Rapid estimation of lipids in oleaginous fungi and yeasts using Nile red fluorescence. *J Microbiol Methods*, 56(3), 331-338. doi: 10.1016/j.mimet.2003.10.018

- Kobayashi, K., Awai, K., Takamiya, K., & Ohta, H. (2004). Arabidopsis type B monogalactosyldiacylglycerol synthase genes are expressed during pollen tube growth and induced by phosphate starvation. *Plant Physiol*, *134*(2), 640-648. doi: 10.1104/pp.103.032656
- Koller, M., Muhr, A., & Brauneegg, G. (2014). Microalgae as versatile cellular factories for valued products. *Algal Res*, *6*, Part A, 52-63. doi: 10.1016/j.algal.2014.09.002
- Kunst, L., Browse, J., & Somerville, C. (1988). Altered regulation of lipid biosynthesis in a mutant of Arabidopsis deficient in chloroplast glycerol-3-phosphate acyltransferase activity. *Proc Natl Acad Sci U S A*, *85*(12), 4143-4147.
- Langmead, B., Trapnell, C., Pop, M., & Salzberg, S. L. (2009). Ultrafast and memory-efficient alignment of short DNA sequences to the human genome. *Genome Biol*, *10*(3), R25. doi: 10.1186/gb-2009-10-3-r25
- Li, H., & Durbin, R. (2009). Fast and accurate short read alignment with Burrows-Wheeler transform. *Bioinformatics*, *25*(14), 1754-1760. doi: 10.1093/bioinformatics/btp324
- Li, M., & Wang, X. (2014). pPLA: Patatin-Related Phospholipase As with Multiple Biological Functions. In X. Wang (Ed.), *Phospholipases in Plant Signaling* (Vol. 20, pp. 93-108): Springer Berlin Heidelberg.
- Li, X., Moellering, E. R., Liu, B., Johnny, C., Fedewa, M., Sears, B. B., Kuo, M. H., & Benning, C. (2012). A galactoglycerolipid lipase is required for triacylglycerol accumulation and survival following nitrogen deprivation in *Chlamydomonas reinhardtii*. *Plant Cell*, *24*(11), 4670-4686. doi: 10.1105/tpc.112.105106
- Li, Y., Han, D., Hu, G., Dauvillee, D., Sommerfeld, M., Ball, S., & Hu, Q. (2010). *Chlamydomonas* starchless mutant defective in ADP-glucose pyrophosphorylase hyperaccumulates triacylglycerol. *Metab Eng*, *12*(4), 387-391. doi: 10.1016/j.ymben.2010.02.002
- Li-Beisson, Y., Beisson, F., & Riekhof, W. (2015). Metabolism of acyl-lipids in *Chlamydomonas reinhardtii*. *Plant J*, *82*(3), 504-522. doi: 10.1111/tpj.12787
- Lin, H., Miller, M. L., Granas, D. M., & Dutcher, S. K. (2013a). Whole genome sequencing identifies a deletion in protein phosphatase 2A that affects its stability and localization in *Chlamydomonas reinhardtii*. *PLoS Genet*, *9*(9), e1003841. doi: 10.1371/journal.pgen.1003841
- Lin, H., Nauman, N. P., Albee, A. J., Hsu, S., & Dutcher, S. K. (2013b). New mutations in flagellar motors identified by whole genome sequencing in *Chlamydomonas*. *Cilia*, *2*(1), 14. doi: 10.1186/2046-2530-2-14

- Liu, B., & Benning, C. (2013). Lipid metabolism in microalgae distinguishes itself. *Curr Opin Biotechnol*, 24(2), 300-309. doi: 10.1016/j.copbio.2012.08.008
- Liu, Y. G., Mitsukawa, N., Oosumi, T., & Whittier, R. F. (1995). Efficient isolation and mapping of *Arabidopsis thaliana* T-DNA insert junctions by thermal asymmetric interlaced PCR. *Plant J*, 8(3), 457-463.
- Liu, Y. G., & Whittier, R. F. (1995). Thermal asymmetric interlaced PCR: automatable amplification and sequencing of insert end fragments from P1 and YAC clones for chromosome walking. *Genomics*, 25(3), 674-681.
- Merchant, S. S., Kropat, J., Liu, B., Shaw, J., & Warakanont, J. (2012). TAG, you're it! *Chlamydomonas* as a reference organism for understanding algal triacylglycerol accumulation. *Curr Opin Biotechnol*, 23(3), 352-363. doi: 10.1016/j.copbio.2011.12.001
- Merchant, S. S., Prochnik, S. E., Vallon, O., Harris, E. H., Karpowicz, S. J., Witman, G. B., Terry, A., Salamov, A., Fritz-Laylin, L. K., Marechal-Drouard, L., Marshall, W. F., Qu, L. H., Nelson, D. R., Sanderfoot, A. A., Spalding, M. H., Kapitonov, V. V., Ren, Q., Ferris, P., Lindquist, E., Shapiro, H., Lucas, S. M., Grimwood, J., Schmutz, J., Cardol, P., Cerutti, H., Chanfreau, G., Chen, C. L., Cognat, V., Croft, M. T., Dent, R., Dutcher, S., Fernandez, E., Fukuzawa, H., Gonzalez-Ballester, D., Gonzalez-Halphen, D., Hallmann, A., Hanikenne, M., Hippler, M., Inwood, W., Jabbari, K., Kalanon, M., Kuras, R., Lefebvre, P. A., Lemaire, S. D., Lobanov, A. V., Lohr, M., Manuell, A., Meier, I., Mets, L., Mittag, M., Mittelmeier, T., Moroney, J. V., Moseley, J., Napoli, C., Nedelcu, A. M., Niyogi, K., Novoselov, S. V., Paulsen, I. T., Pazour, G., Purton, S., Ral, J. P., Riano-Pachon, D. M., Riekhof, W., Rymarquis, L., Schroda, M., Stern, D., Umen, J., Willows, R., Wilson, N., Zimmer, S. L., Allmer, J., Balk, J., Bisova, K., Chen, C. J., Elias, M., Gendler, K., Hauser, C., Lamb, M. R., Ledford, H., Long, J. C., Minagawa, J., Page, M. D., Pan, J., Pootakham, W., Roje, S., Rose, A., Stahlberg, E., Terauchi, A. M., Yang, P., Ball, S., Bowler, C., Dieckmann, C. L., Gladyshev, V. N., Green, P., Jorgensen, R., Mayfield, S., Mueller-Roeber, B., Rajamani, S., Sayre, R. T., Brokstein, P., Dubchak, I., Goodstein, D., Hornick, L., Huang, Y. W., Jhaveri, J., Luo, Y., Martinez, D., Ngau, W. C., Otiillar, B., Poliakov, A., Porter, A., Szajkowski, L., Werner, G., Zhou, K., Grigoriev, I. V., Rokhsar, D. S., & Grossman, A. R. (2007). The *Chlamydomonas* genome reveals the evolution of key animal and plant functions. *Science*, 318(5848), 245-250. doi: 10.1126/science.1143609
- Michelet, L., Lefebvre-Legendre, L., Burr, S. E., Rochaix, J. D., & Goldschmidt-Clermont, M. (2011). Enhanced chloroplast transgene expression in a nuclear mutant of *Chlamydomonas*. *Plant Biotechnol J*, 9(5), 565-574. doi: 10.1111/j.1467-7652.2010.00564.x
- Moellering, E. R., Miller, R., & Benning, C. (2010). Molecular genetics of lipid metabolism in the model green alga *Chlamydomonas reinhardtii* *Lipids in photosynthesis* (pp. 139-155): Springer.

- Moroney, J. V., & Ynalvez, R. A. (2001). *Algal Photosynthesis eLS*: John Wiley & Sons, Ltd.
- Nguyen, H. M., Cuine, S., Beyly-Adriano, A., Legeret, B., Billon, E., Auroy, P., Beisson, F., Peltier, G., & Li-Beisson, Y. (2013). The green microalga *Chlamydomonas reinhardtii* has a single omega-3 fatty acid desaturase that localizes to the chloroplast and impacts both plastidic and extraplastidic membrane lipids. *Plant Physiol*, *163*(2), 914-928. doi: 10.1104/pp.113.223941
- Nordstrom, K. J., Albani, M. C., James, G. V., Gutjahr, C., Hartwig, B., Turck, F., Paszkowski, U., Coupland, G., & Schneeberger, K. (2013). Mutation identification by direct comparison of whole-genome sequencing data from mutant and wild-type individuals using k-mers. *Nat Biotechnol*, *31*(4), 325-330. doi: 10.1038/nbt.2515
- Ossowski, S., Schneeberger, K., Clark, R. M., Lanz, C., Warthmann, N., & Weigel, D. (2008). Sequencing of natural strains of *Arabidopsis thaliana* with short reads. *Genome Res*, *18*(12), 2024-2033. doi: 10.1101/gr.080200.108
- Petroutsos, D., Amiar, S., Abida, H., Dolch, L. J., Bastien, O., Rebeille, F., Jouhet, J., Falconet, D., Block, M. A., McFadden, G. I., Bowler, C., Botte, C., & Marechal, E. (2014). Evolution of galactoglycerolipid biosynthetic pathways--from cyanobacteria to primary plastids and from primary to secondary plastids. *Prog Lipid Res*, *54*, 68-85. doi: 10.1016/j.plipres.2014.02.001
- Puente, X. S., Pinyol, M., Quesada, V., Conde, L., Ordonez, G. R., Villamor, N., Escaramis, G., Jares, P., Bea, S., Gonzalez-Diaz, M., Bassaganyas, L., Baumann, T., Juan, M., Lopez-Guerra, M., Colomer, D., Tubio, J. M., Lopez, C., Navarro, A., Tornador, C., Aymerich, M., Rozman, M., Hernandez, J. M., Puente, D. A., Freije, J. M., Velasco, G., Gutierrez-Fernandez, A., Costa, D., Carrio, A., Guijarro, S., Enjuanes, A., Hernandez, L., Yague, J., Nicolas, P., Romeo-Casabona, C. M., Himmelbauer, H., Castillo, E., Dohm, J. C., de Sanjose, S., Piris, M. A., de Alava, E., San Miguel, J., Royo, R., Gelpi, J. L., Torrents, D., Orozco, M., Pisano, D. G., Valencia, A., Guigo, R., Bayes, M., Heath, S., Gut, M., Klatt, P., Marshall, J., Raine, K., Stebbings, L. A., Futreal, P. A., Stratton, M. R., Campbell, P. J., Gut, I., Lopez-Guillermo, A., Estivill, X., Montserrat, E., Lopez-Otin, C., & Campo, E. (2011). Whole-genome sequencing identifies recurrent mutations in chronic lymphocytic leukaemia. *Nature*, *475*(7354), 101-105. doi: 10.1038/nature10113
- Reis, P., Holmberg, K., Watzke, H., Leser, M. E., & Miller, R. (2009). Lipases at interfaces: a review. *Adv Colloid Interface Sci*, *147-148*, 237-250. doi: 10.1016/j.cis.2008.06.001
- Riediger, N. D., Othman, R. A., Suh, M., & Moghadasian, M. H. (2009). A systemic review of the roles of n-3 fatty acids in health and disease. *J Am Diet Assoc*, *109*(4), 668-679. doi: 10.1016/j.jada.2008.12.022
- Riekhof, W. R., Ruckle, M. E., Lydic, T. A., Sears, B. B., & Benning, C. (2003). The sulfolipids 2'-O-acyl-sulfoquinovosyldiacylglycerol and sulfoquinovosyldiacylglycerol are absent

- from a *Chlamydomonas reinhardtii* mutant deleted in SQD1. *Plant Physiol*, 133(2), 864-874. doi: 10.1104/pp.103.029249
- Riekhof, W. R., Sears, B. B., & Benning, C. (2005). Annotation of genes involved in glycerolipid biosynthesis in *Chlamydomonas reinhardtii*: discovery of the betaine lipid synthase BTA1Cr. *Eukaryot Cell*, 4(2), 242-252. doi: 10.1128/EC.4.2.242-252.2005
- Rochaix, J. D. (2002). The three genomes of *Chlamydomonas*. *Photosynth Res*, 73(1-3), 285-293. doi: 10.1023/A:1020484105601
- Roughan, P. G., & Slack, C. R. (1982). Cellular Organization of Glycerolipid Metabolism. *Ann Rev Plant Physiol*, 33(1), 97-132. doi: 10.1146/annurev.pp.33.060182.000525
- Rydel, T. J., Williams, J. M., Krieger, E., Moshiri, F., Stallings, W. C., Brown, S. M., Pershing, J. C., Purcell, J. P., & Alibhai, M. F. (2003). The crystal structure, mutagenesis, and activity studies reveal that patatin is a lipid acyl hydrolase with a Ser-Asp catalytic dyad. *Biochemistry*, 42(22), 6696-6708. doi: 10.1021/bi027156r
- Sarda, L., & Desnuelle, P. (1958). Actions of pancreatic lipase on esters in emulsions. *Biochim Biophys Acta*, 30(3), 513-521.
- Sato, H., & Frank, D. W. (2004). ExoU is a potent intracellular phospholipase. *Mol Microbiol*, 53(5), 1279-1290. doi: 10.1111/j.1365-2958.2004.04194.x
- Sato, N., & Murata, N. (1991). Transition of lipid phase in aqueous dispersions of diacylglyceryltrimethylhomoserine. *Biochim Biophys Acta*, 1082(1), 108-111.
- Scherer, G. F., Ryu, S. B., Wang, X., Matos, A. R., & Heitz, T. (2010). Patatin-related phospholipase A: nomenclature, subfamilies and functions in plants. *Trends Plant Sci*, 15(12), 693-700. doi: 10.1016/j.tplants.2010.09.005
- Schierenbeck, L., Ries, D., Rogge, K., Grewe, S., Weisshaar, B., & Kruse, O. (2015). Fast forward genetics to identify mutations causing a high light tolerant phenotype in *Chlamydomonas reinhardtii* by whole-genome-sequencing. *BMC Genomics*, 16, 57. doi: 10.1186/s12864-015-1232-y
- Schneeberger, K., Ossowski, S., Lanz, C., Juul, T., Petersen, A. H., Nielsen, K. L., Jorgensen, J. E., Weigel, D., & Andersen, S. U. (2009). SHOREmap: simultaneous mapping and mutation identification by deep sequencing. *Nat Methods*, 6(8), 550-551. doi: 10.1038/nmeth0809-550
- Schönheyder, F., & Volqvartz, K. (1945). On the affinity of pig pancreas lipase for tricaproin in heterogeneous solution. *Acta Physiol Scand*, 9(1), 57-67. doi: 10.1111/j.1748-1716.1945.tb03084.x

- Sheehan, J., Dunahay, T., Benemann, J., & Roessler, P. (1998). *A look back at the US Department of Energy's aquatic species program: biodiesel from algae* (Vol. 328): National Renewable Energy Laboratory Golden.
- Sperling, P., & Heinz, E. (2001). Desaturases fused to their electron donor. *Eur J Lipid Sci Technol*, *103*(3), 158-180. doi: 10.1002/1438-9312(200103)103:3<158::AID-EJLT158>3.0.CO;2-1
- Sperling, P., Schmidt, H., & Heinz, E. (1995). A cytochrome-b5-containing fusion protein similar to plant acyl lipid desaturases. *Eur J Biochem*, *232*(3), 798-805.
- Spolaore, P., Joannis-Cassan, C., Duran, E., & Isambert, A. (2006). Commercial applications of microalgae. *J Biosci Bioeng*, *101*(2), 87-96. doi: 10.1263/jbb.101.87
- Sturtevant, A. H. (1913). The linear arrangement of six sex-linked factors in *Drosophila*, as shown by their mode of association. *J Exp Zool*, *14*(1), 43-59. doi: 10.1002/jez.1400140104
- Tan, G., Gao, Y., Shi, M., Zhang, X., He, S., Chen, Z., & An, C. (2005). SiteFinding-PCR: a simple and efficient PCR method for chromosome walking. *Nucleic Acids Res*, *33*(13), e122. doi: 10.1093/nar/gni124
- Terashima, M., Freeman, E. S., Jinkerson, R. E., & Jonikas, M. C. (2015). A fluorescence-activated cell sorting-based strategy for rapid isolation of high-lipid *Chlamydomonas* mutants. *Plant J*, *81*(1), 147-159. doi: 10.1111/tpj.12682
- Triglia, T., Peterson, M. G., & Kemp, D. J. (1988). A procedure for in vitro amplification of DNA segments that lie outside the boundaries of known sequences. *Nucleic Acids Res*, *16*(16), 8186.
- Tsai, C. H., Warakanont, J., Takeuchi, T., Sears, B. B., Moellering, E. R., & Benning, C. (2014). The protein Compromised Hydrolysis of Triacylglycerols 7 (CHT7) acts as a repressor of cellular quiescence in *Chlamydomonas*. *Proc Natl Acad Sci U S A*, *111*(44), 15833-15838. doi: 10.1073/pnas.1414567111
- Tulin, F., & Cross, F. R. (2014). A microbial avenue to cell cycle control in the plant superkingdom. *Plant Cell*, *26*(10), 4019-4038. doi: 10.1105/tpc.114.129312
- Venter, J. C., Adams, M. D., Myers, E. W., Li, P. W., Mural, R. J., Sutton, G. G., Smith, H. O., Yandell, M., Evans, C. A., Holt, R. A., Gocayne, J. D., Amanatides, P., Ballew, R. M., Huson, D. H., Wortman, J. R., Zhang, Q., Kodira, C. D., Zheng, X. H., Chen, L., Skupski, M., Subramanian, G., Thomas, P. D., Zhang, J., Gabor Miklos, G. L., Nelson, C., Broder, S., Clark, A. G., Nadeau, J., McKusick, V. A., Zinder, N., Levine, A. J., Roberts, R. J., Simon, M., Slayman, C., Hunkapiller, M., Bolanos, R., Delcher, A., Dew, I., Fasulo, D., Flanigan, M., Florea, L., Halpern, A., Hannenhalli, S., Kravitz, S., Levy, S., Mobarry, C., Reinert, K., Remington, K., Abu-Threideh, J., Beasley, E., Biddick, K.,

Bonazzi, V., Brandon, R., Cargill, M., Chandramouliswaran, I., Charlab, R., Chaturvedi, K., Deng, Z., Di Francesco, V., Dunn, P., Eilbeck, K., Evangelista, C., Gabrielian, A. E., Gan, W., Ge, W., Gong, F., Gu, Z., Guan, P., Heiman, T. J., Higgins, M. E., Ji, R. R., Ke, Z., Ketchum, K. A., Lai, Z., Lei, Y., Li, Z., Li, J., Liang, Y., Lin, X., Lu, F., Merkulov, G. V., Milshina, N., Moore, H. M., Naik, A. K., Narayan, V. A., Neelam, B., Nusskern, D., Rusch, D. B., Salzberg, S., Shao, W., Shue, B., Sun, J., Wang, Z., Wang, A., Wang, X., Wang, J., Wei, M., Wides, R., Xiao, C., Yan, C., Yao, A., Ye, J., Zhan, M., Zhang, W., Zhang, H., Zhao, Q., Zheng, L., Zhong, F., Zhong, W., Zhu, S., Zhao, S., Gilbert, D., Baumhueter, S., Spier, G., Carter, C., Cravchik, A., Woodage, T., Ali, F., An, H., Awe, A., Baldwin, D., Baden, H., Barnstead, M., Barrow, I., Beeson, K., Busam, D., Carver, A., Center, A., Cheng, M. L., Curry, L., Danaher, S., Davenport, L., Desilets, R., Dietz, S., Dodson, K., Doup, L., Ferriera, S., Garg, N., Gluecksmann, A., Hart, B., Haynes, J., Haynes, C., Heiner, C., Hladun, S., Hostin, D., Houck, J., Howland, T., Ibegwam, C., Johnson, J., Kalush, F., Kline, L., Koduru, S., Love, A., Mann, F., May, D., McCawley, S., McIntosh, T., McMullen, I., Moy, M., Moy, L., Murphy, B., Nelson, K., Pfannkoch, C., Pratts, E., Puri, V., Qureshi, H., Reardon, M., Rodriguez, R., Rogers, Y. H., Romblad, D., Ruhfel, B., Scott, R., Sitter, C., Smallwood, M., Stewart, E., Strong, R., Suh, E., Thomas, R., Tint, N. N., Tse, S., Vech, C., Wang, G., Wetter, J., Williams, S., Williams, M., Windsor, S., Winn-Deen, E., Wolfe, K., Zaveri, J., Zaveri, K., Abril, J. F., Guigo, R., Campbell, M. J., Sjolander, K. V., Karlak, B., Kejariwal, A., Mi, H., Lazareva, B., Hatton, T., Narechania, A., Diemer, K., Muruganujan, A., Guo, N., Sato, S., Bafna, V., Istrail, S., Lippert, R., Schwartz, R., Walenz, B., Yooseph, S., Allen, D., Basu, A., Baxendale, J., Blick, L., Caminha, M., Carnes-Stine, J., Caulk, P., Chiang, Y. H., Coyne, M., Dahlke, C., Mays, A., Dombroski, M., Donnelly, M., Ely, D., Esparham, S., Fosler, C., Gire, H., Glanowski, S., Glasser, K., Glodek, A., Gorokhov, M., Graham, K., Gropman, B., Harris, M., Heil, J., Henderson, S., Hoover, J., Jennings, D., Jordan, C., Jordan, J., Kasha, J., Kagan, L., Kraft, C., Levitsky, A., Lewis, M., Liu, X., Lopez, J., Ma, D., Majoros, W., McDaniel, J., Murphy, S., Newman, M., Nguyen, T., Nguyen, N., Nodell, M., Pan, S., Peck, J., Peterson, M., Rowe, W., Sanders, R., Scott, J., Simpson, M., Smith, T., Sprague, A., Stockwell, T., Turner, R., Venter, E., Wang, M., Wen, M., Wu, D., Wu, M., Xia, A., Zandieh, A., & Zhu, X. (2001). The sequence of the human genome. *Science*, 291(5507), 1304-1351. doi: 10.1126/science.1058040

Verger, R. (1976). Interfacial enzyme kinetics of lipolysis. *Annu Rev Biophys Bioeng*, 5, 77-117. doi: 10.1146/annurev.bb.05.060176.000453

Vieler, A., Wu, G., Tsai, C. H., Bullard, B., Cornish, A. J., Harvey, C., Reza, I. B., Thornburg, C., Achawanantakun, R., Buehl, C. J., Campbell, M. S., Cavalier, D., Childs, K. L., Clark, T. J., Deshpande, R., Erickson, E., Armenia Ferguson, A., Handee, W., Kong, Q., Li, X., Liu, B., Lundback, S., Peng, C., Roston, R. L., Sanjaya, Simpson, J. P., Terbush, A., Warakanont, J., Zäuner, S., Farre, E. M., Hegg, E. L., Jiang, N., Kuo, M. H., Lu, Y., Niyogi, K. K., Ohlrogge, J., Osteryoung, K. W., Shachar-Hill, Y., Sears, B. B., Sun, Y., Takahashi, H., Yandell, M., Shiu, S. H., & Benning, C. (2012). Genome, functional gene annotation, and nuclear transformation of the heterokont oleaginous alga *Nannochloropsis oceanica* CCMP1779. *PLoS Genet*, 8(11), e1003064. doi: 10.1371/journal.pgen.1003064

- Voelker, D. R. (1997). Phosphatidylserine decarboxylase. *Biochim Biophys Acta*, 1348(1-2), 236-244.
- Vos, P., Hogers, R., Bleeker, M., Reijans, M., van de Lee, T., Hornes, M., Frijters, A., Pot, J., Peleman, J., Kuiper, M., & et al. (1995). AFLP: a new technique for DNA fingerprinting. *Nucleic Acids Res*, 23(21), 4407-4414.
- Wang, Z. T., Ullrich, N., Joo, S., Waffenschmidt, S., & Goodenough, U. (2009). Algal lipid bodies: stress induction, purification, and biochemical characterization in wild-type and starchless *Chlamydomonas reinhardtii*. *Eukaryot Cell*, 8(12), 1856-1868. doi: 10.1128/EC.00272-09
- Williams, J. G., Kubelik, A. R., Livak, K. J., Rafalski, J. A., & Tingey, S. V. (1990). DNA polymorphisms amplified by arbitrary primers are useful as genetic markers. *Nucleic Acids Res*, 18(22), 6531-6535.
- Wilson, P. A., Gardner, S. D., Lambie, N. M., Commans, S. A., & Crowther, D. J. (2006). Characterization of the human patatin-like phospholipase family. *J Lipid Res*, 47(9), 1940-1949. doi: 10.1194/jlr.M600185-JLR200
- Winkler, F. K., D'Arcy, A., & Hunziker, W. (1990). Structure of human pancreatic lipase. *Nature*, 343(6260), 771-774. doi: 10.1038/343771a0
- Work, V. H., Radakovits, R., Jinkerson, R. E., Meuser, J. E., Elliott, L. G., Vinyard, D. J., Laurens, L. M., Dismukes, G. C., & Posewitz, M. C. (2010). Increased lipid accumulation in the *Chlamydomonas reinhardtii* sta7-10 starchless isoamylase mutant and increased carbohydrate synthesis in complemented strains. *Eukaryot Cell*, 9(8), 1251-1261. doi: 10.1128/EC.00075-10
- Yuzawa, Y., Nishihara, H., Haraguchi, T., Masuda, S., Shimojima, M., Shimoyama, A., Yuasa, H., Okada, N., & Ohta, H. (2012). Phylogeny of galactolipid synthase homologs together with their enzymatic analyses revealed a possible origin and divergence time for photosynthetic membrane biogenesis. *DNA Res*, 19(1), 91-102. doi: 10.1093/dnares/dsr044
- Zäuner, S., Jochum, W., Bigorowski, T., & Benning, C. (2012). A cytochrome b5-containing plastid-located fatty acid desaturase from *Chlamydomonas reinhardtii*. *Eukaryot Cell*, 11(7), 856-863. doi: 10.1128/EC.00079-12

CHAPTER 2

Chloroplast lipid transfer processes in *Chlamydomonas reinhardtii* involving a TRIGALACTOSYLDIACYLGLYCEROL 2 (TGD2) orthologue*

*This project was carried out in the collaboration with several colleagues and has been published in the Plant Journal in Jaruswan Warakanont, Chia-Hong Tsai, Elena J. S. Michel, George R. Murphy III, Peter Y. Hsueh, Rebecca L. Roston, Barbara B. Sears, and Christoph Benning (2015) Chloroplast lipid transfer processes in *Chlamydomonas reinhardtii* involving a TRIGALACTOSYLDIACYLGLYCEROL 2 (TGD2) orthologue. Plant J. 84: 1005-1020, doi: 10.1111/tpj.13060. In collaboration with me, Chia-Hong Tsai screened the mutants. Elena J. S. Michel was an undergraduate student under my supervision. She contributed to Figure 2.1B, 2.S1B, 2.S9, and 2.S10. George R. Murphy III and Peter Y. Hsueh were undergraduate students under the supervision of Rebecca L. Roston. They contributed in liposome binding assay in Figure 2.7, and made *DsRED-CrTGD2* pLW01 construct used in Figure 2.7 and in the production of antiserum against CrTGD2. Barbara B. Sears performed crossing between the *tgd2* mutant and CC-198 wild type, providing progenies for genetic analysis in Figure 2.S5 and for electron microscopy in Figure 2.3.

ABSTRACT

In plants, lipids of the photosynthetic membrane are synthesized by parallel pathways associated with the endoplasmic reticulum (ER) and the chloroplast envelope membranes. Lipids derived from the two pathways are distinguished by their acyl-constituents. Following this plant paradigm, the prevalent acyl composition of chloroplast lipids suggests that *Chlamydomonas* does not use the ER pathway. However, the *Chlamydomonas* genome encodes presumed plant orthologues of a chloroplast lipid transporter consisting of TGD (TRIGALACTOSYLDIACYLGLYCEROL) proteins that are required for ER-to-chloroplast lipid trafficking in plants. To resolve this conundrum, we identified a mutant of *Chlamydomonas* deleted in the *TGD2* gene and characterized the respective protein, CrTGD2. Notably, the mutant's viability was reduced showing the importance of CrTGD2. Galactoglycerolipid metabolism was altered in the *tgd2* mutant with monogalactosyldiacylglycerol (MGDG) synthase activity being strongly stimulated. We hypothesize this to be a result of phosphatidic acid accumulation in the chloroplast outer envelope membrane, the location of MGDG synthase in *Chlamydomonas*. Concomitantly, increased conversion of MGDG into triacylglycerol (TAG) was observed. This TAG accumulated in lipid droplets in the *tgd2* mutant under normal growth conditions. Labeling kinetics indicate that *Chlamydomonas* can import lipid precursors from the ER, a process that is impaired in the *tgd2* mutant.

SIGNIFICANCE STATEMENT

In plants, lipids in the chloroplast membrane are synthesized both in the ER and in the chloroplast envelope membranes. However, in *Chlamydomonas*, the chloroplast lipid composition has suggested that the ER pathway was not involved. Here, analyzing a mutant in a chloroplast lipid transporter, we show that the *Chlamydomonas* chloroplast does likely import precursors from the ER for thylakoid lipid biosynthesis.

INTRODUCTION

Microalgae play an important role as primary biomass producers in diverse ecosystems due to their ability to efficiently convert solar into chemical energy. In fact, estimates based on radioactive bicarbonate labeling of sea water samples from the Atlantic ocean suggest that marine algae account for nearly a quarter of total global carbon fixation (Jardillier *et al.*, 2010), which is in part due to their high photosynthetic efficiency (Melis, 2009; Weyer *et al.*, 2010). In addition to their importance in natural ecosystems, microalgae have received special attention as biofuel feedstocks due to their rapid life cycle and their potential to accumulate high levels of biomass in limited space.

Chlamydomonas reinhardtii (Chlamydomonas) is a unicellular green alga, which has served for many decades as an instructive model in studies of photosynthesis, flagella development and function, and more recently to explore the regulation of metabolism in response to different growth conditions. Chlamydomonas cells are haploid during vegetative growth and the Chlamydomonas genome often has a single copy of many plant orthologous genes facilitating genotype-phenotype relationship studies. Finally, availability of multiple resources including a sequenced genome (Merchant *et al.*, 2007) facilitates research on this microalga.

Photosynthesis takes place in thylakoid membranes in bacterial cells or inside chloroplasts present in algae and land plants. Photosynthetic membranes from cyanobacteria, the presumed predecessor of chloroplasts, algae, and plants analyzed to date contain four lipids: the two galactoglycerolipids mono- (MGDG) and digalactosyldiacylglycerol (DGDG), the sulfoglycerolipid sulfoquinovosyldiacylglycerol (SQDG), and the only phosphoglycerolipid phosphatidylglycerol (PtdGro) (Boudière *et al.*, 2014). Due to their different properties, each lipid class plays distinct roles in photosynthetic membranes. Therefore, these four lipids are present in a conserved ratio in order to maintain the structure and function of photosynthetic membranes (Boudière *et al.*, 2014).

Among these conserved lipids, the galactoglycerolipids MGDG and DGDG are the most abundant throughout Viridiplantae (Boudière *et al.*, 2014). In plants, the galactoglycerolipids are synthesized either through the eukaryotic or the prokaryotic pathways (Roughan & Slack, 1982). In the case of the eukaryotic pathway, fatty acids synthesized in the chloroplast are exported, converted to acyl-CoAs and incorporated at the endoplasmic reticulum (ER) into membrane

lipids, e.g. phosphatidic acid (PtdOH) or phosphatidylcholine (PtdCho). ER-assembled lipids then return to the chloroplast and are converted to diacylglycerol (DAG), which is then galactosylated in the two envelope membranes to form MGDG and subsequently DGDG. In contrast, the prokaryotic pathway in plants and algae occurs entirely in the chloroplast envelope membranes. Fatty acyl groups attached to acyl carrier proteins (ACPs) synthesized in the chloroplast are incorporated directly into lipid precursors to give rise to PtdOH, DAG and then galactoglycerolipids. In plants, the bulk of MGDG is synthesized in the inner envelope while DGDG is synthesized at the outer envelope requiring exchange of lipids between the two envelope membranes (C Benning, 2009).

In plants, lipids derived from either pathway can be distinguished by the number of carbons at the *sn*-2 position of the glyceryl backbone; 16-carbon fatty acids (C16) for the prokaryotic and 18-carbon fatty acids (C18) for the eukaryotic pathway-derived lipids, respectively (Heinz & Roughan, 1983). This is thought to be due to the substrate specificity of lyso-PtdOH acyltransferases located in the chloroplast that prefer C16, while those at the ER prefer C18 (Frentzen *et al.*, 1983; H. U. Kim *et al.*, 2005; Kunst *et al.*, 1988; Roughan & Slack, 1982). Because *Chlamydomonas* has exclusively C16 fatty acids at the *sn*-2 position of its galactoglycerolipids, it is thought to not utilize the eukaryotic pathway for galactoglycerolipid synthesis and therefore should not require ER-to-chloroplast lipid trafficking (Giroud & Eichenberger, 1988). However, this conclusion is based on the untested assumption that the lyso-PtdOH acyltransferases at the ER and the chloroplast membranes in plants and *Chlamydomonas* have the same distinct substrate specificity.

In *Arabidopsis*, the ER-to-chloroplast lipid trafficking of the eukaryotic pathway is mediated through TRIGALACTOSYLDIACYLGLYCEROL (TGD1, -2, -3 and -4) proteins (Koichiro Awai *et al.*, 2006; Lu *et al.*, 2007; Xu *et al.*, 2008; Xu *et al.*, 2003) and a recently discovered TGD5 protein (J. Fan *et al.*, 2015). Mutations in any of the respective *Arabidopsis* genes cause a secondary phenotype resulting in the accumulation of oligogalactolipids, e.g. trigalactosyldiacylglycerol (TGDG), after which the mutants were named. These oligogalactolipids are synthesized by activation of a galactolipid : galactolipid galactosyltransferase encoded by *SENSITIVE TO FREEZING2* (*SFR2*), a gene absent from *Chlamydomonas*, which, therefore, presumably does not synthesize oligogalactolipids. In *Arabidopsis*, TGD1, -2 and -3 form an ABC (ATP-binding cassette) transporter complex in the

inner envelope membrane of the chloroplast and function as a permease, a substrate binding protein, and an ATPase, respectively (C Benning, 2009; R. L. Roston *et al.*, 2012). TGD4 is localized in the outer envelope membrane of the chloroplast as a homodimer (Wang *et al.*, 2012). It has been suggested that TGD4 transports the ER lipid precursor from ER to the TGD1, -2, -3 complex (C Benning, 2009; Hurlock *et al.*, 2014) and that TGD5 links this complex to TGD4 (J. Fan *et al.*, 2015). The TGD1, 2, 3 complex then transfers the ER lipid precursor to the inner envelope membrane of the chloroplast. It should be noted that the exact nature of the transported lipid species for the TGD1, 2, 3 complex or TGD4 is not known at this time.

Bacterial orthologues of TGD proteins have been suggested to be involved in resistance to organic solvents or toxic chemicals. In *Pseudomonas putida*, TtgA, -B, -C (toluene tolerance genes) and SrpA, -B, -C (solvent-resistant pump) have been proposed to act as toluene efflux pumps, although their direct biochemical function has yet to be demonstrated (Kieboom *et al.*, 1998a; Kieboom *et al.*, 1998b; K. Kim *et al.*, 1998; Ramos *et al.*, 1998). Loss of function of these proteins leads to toluene sensitivity. In *Escherichia coli*, MlaD, -E, -F proteins are proposed to function in maintaining an asymmetric lipid distribution in the outer membrane (Malinverni & Silhavy, 2009). Loss of function of any of these proteins results in increased outer membrane permeability, possibly due to an inability to remodel the outer membrane lipid composition in response to chemical stress. The implication is that the bacterial orthologues of the plant TGD proteins transport lipids between the cell membrane and the outer membrane to allow remodeling in response to chemical insults.

The genome of *Chlamydomonas* harbors genes encoding putative TGD1, -2 and -3 orthologues (Merchant *et al.*, 2007). This raises two possibilities: 1. If *Chlamydomonas* does not require the import of lipids from the ER for thylakoid lipid assembly as suggested by the molecular species composition of its thylakoid lipids, these proteins may be primarily involved in transferring lipids between the two envelope membranes as in bacteria. 2. Alternatively, these proteins are involved in lipid trafficking from the ER to the chloroplast, in which case the plant paradigm for distinguishing thylakoid lipid species derived from the ER versus the chloroplast species does not apply to *Chlamydomonas*. To test these possibilities, we identified and studied a *Chlamydomonas* mutant deleted in *TGD2*.

RESULTS

The *tgd2* mutant accumulates triacylglycerol enriched in MGDG acyl groups.

Triacylglycerols (TAGs) typically accumulate to high levels in *Chlamydomonas* only following nutrient deprivation and are degraded following refeeding. The *tgd2* mutant was generated by insertional mutagenesis and identified during a screen for mutants delayed in TAG degradation following nitrogen (N) deprivation and refeeding (Tsai *et al.*, 2014). When TAG levels were monitored during N-replete, N-deprived and N-resupplied growth conditions, the *tgd2* mutant showed elevated levels under all conditions tested (Figure 2.1A). Therefore, we focused the subsequent analysis on cells grown in N-replete medium. When the steady-state levels of all glycerolipids and free fatty acids (FFA) were analyzed during N-replete growth, only TAG and PtdOH were increased with statistical significance in *tgd2* compared to the parental line (PL, Figure 2.1B). The central lipid intermediate PtdOH was the least abundant lipid included in the analysis and was identified based on its relative co-chromatography with standards (Figure 2.S1A) and its distinct acyl composition. While the ratios of different acyl groups in the total lipid fraction did not obviously change (Figure 2.1C), the TAG fraction of *tgd2* was enriched in 16:4^{Δ4,7,10,13} and 18:3^{Δ9,12,15} acyl groups (number of carbons : number of double bonds with ^{ΔNumber} indicating the position of the double bond counted from the carboxyl end), with a concomitant reduction in 16:0 acyl groups (Figure 2.1D) normally found in TAG synthesized following nutrient deprivation. These highly unsaturated acyl groups are found typically only in MGDG (Figure 2.1E) and their abundance in TAG of *tgd2* suggests that its DAG moiety or its acyl groups are derived from MGDG.

Subtle changes in MGDG and DGDG molecular species were notable as well. In MGDG of *tgd2* higher levels of 16:0, 16:1 and 18:1, and lower levels of 16:4^{Δ4,7,10,13} and 18:3^{Δ9,12,15} were observed (Figure 2.1E). In the case of DGDG of *tgd2*, the levels of 16:0 and 16:3 were reduced, while those of the 16:1 and 16:4 were increased (Figure 2.1F). We specifically tested whether the *Chlamydomonas tgd2* mutant accumulates TGDG, as observed for *Arabidopsis tgd* mutants. However, none of the *Chlamydomonas* samples showed TGDG detectable by thin-layer chromatography (Figure 2.S1B), consistent with the absence of an SFR2-like activity from *Chlamydomonas*.

Cultures of *tgd2* show early senescence. During routine maintenance of long-term cultures on agar-solidified medium, we observed that the *tgd2* mutant had a shorter culture lifespan than the PL. Subsequently, viability assays were carried out to further investigate this phenotype. Liquid cultures of PL, *tgd2*, and *TGD2 tgd2* cells (a complemented line expressing *TGD2* in the *tgd2* mutant background, see below) were inoculated at 0.5×10^6 cells/mL. Cultures were examined after 3, 7, 14, 21 and 28 days. After 21 days, the *tgd2* culture began to turn yellow which was even more obvious on day 28 (Figure 2.2A). This observation correlated with a continuously increasing fraction of dead cells over time observed in the *tgd2* culture using live cell stains (methylene blue and phenosafranin) (Figure S2a). The *tgd2* culture accumulated more TAG throughout the culturing time (Figure 2.2B), and at day 3 substantial levels of MGDG derived acyl groups were detected in the TAG fraction (Figure 2.S2B). It seems likely that initially TAG is derived from turnover of fully desaturated MGDG peaking at day 3, while later during prolonged culturing, as nutrients are depleted, *de novo* TAG synthesis is induced. This is indicated by a steady increase of 16:0 and 18:1^{Δ9} acyl groups characteristic of *de novo* synthesized TAG. The prolonged culturing of *tgd2* also led to an accumulation of high levels of malondialdehyde, which is a product of the reaction between polyunsaturated acyl groups and reactive oxygen species (ROS) (Figure 2.2C). As cells die, ROS typically accumulates consistent with the observed decrease in viability of the *tgd2* mutant.

Changes in the ultrastructure of *tgd2* cells. The original *tgd2* mutant was isolated in the cell wall mutant background dw15.1. However, strains with cell walls (*cw*⁺) are more amenable to ultra-thin sectioning for transmission electron microscopy (TEM) than are *cw*⁻ lines, such as dw15.1. Hence, we moved the *tgd2* mutation into a *cw*⁺ line, by crossing it with wild-type strain CC-198. For the TEM studies, the *tgd2* mutant was compared with CC-198, to determine ultrastructural changes caused by the *tgd2* mutation at mid-log, stationary and late stationary phases. In contrast to CC-198 (Figure 2.3A-C), which contained lipid droplets during late stationary phase (black arrows), *tgd2* showed lipid droplets at every time point (Figure 2.3D-F, black arrows). The *tgd2* mutant had more lipid droplets, which were larger in size over time. These lipid droplets were observed in the cytoplasm of *tgd2* also harboring mitochondria and were often adjacent to the chloroplast outer envelope membrane (Figure 2.3G). In addition, lipid droplets from the *tgd2* mutant stained darker (Figure 2.3D-G compared to 2.3C, black arrows), which is consistent with a higher desaturation level of TAGs as osmium tetroxide stains

unsaturated lipids more intensely. During late stationary phase at day 17, membranes of *tgd2* became disorganized (Figure 2.3H, white arrows) compared to PL and earlier stages of *tgd2* (Figure 2.S3). About half of the population appeared to be dead ghost cells, lighter in color and with less distinct internal structures (Figure 2.3I). Although a *cw*⁺ complemented line was not available for this experiment, these ultrastructural changes corroborate observations made on the *tgd2* mutant and complemented lines in the *dw15.1* background described above and are likely due to the ablation of the *TGD2* gene.

Molecular and genetic analysis of the *tgd2* mutant locus. The *tgd2* mutant was generated by random genomic insertion of a plasmid carrying the Hygromycin B resistant gene (*AphVII*). Southern blot analysis of genomic DNA of *tgd2* cut with *Bam*HI and using a probe covering a region of *AphVII* that does not contain the *Bam*HI restriction site indicated the presence of a single insertion (Figure 2.S4). As a first step to identify the mutant locus, a genetic analysis was carried out to determine linkage of the primary lipid phenotype and the Hygromycin B resistance marker. For this purpose, CC-198 as already mentioned above was crossed with *tgd2* in the *dw15.1* background. The progenies of this cross were tested for TAG content, TAG acyl profile and sensitivity to Hygromycin B. Without exception, all Hygromycin B resistant progenies tested (11 resistant and 12 susceptible progenies from 6 zygotes) showed high TAG levels and TAGs with highly unsaturated acyl groups (Figure 2.S5A and B). This result suggested close linkage of the Hygromycin B resistant marker and the mutation that caused the TAG phenotype of the *tgd2* mutant.

Because PCR-based methods were not successful in identifying DNA flanking the Hygromycin B marker, whole genome resequencing was used to determine the location of the mutation responsible for the primary phenotype in the genome of the *tgd2* mutant. Towards this end, genomic DNA of the *tgd2* mutant was subjected to Illumina-HiSeq paired-end sequencing. The reads were assembled *de novo* with velvet 1.2.07 (Zerbino & Birney, 2008) using the *k*-mer length of 21. Contigs containing *AphVII* were searched against the Chlamydomonas reference genome (v5.3) to identify flanking sequences revealing a possible insertion site in chromosome 16. When the respective section of the reference genome of chromosome 16 was used as a template for the assembled contigs from the *tgd2* genome, a 31 kb deletion in chromosome 16 of *tgd2* became apparent. This deletion, which was confirmed by PCR probing, affected six genes either fully or partially as shown in Figure 2.S6A.

We introduced into *tgd2* genomic DNA fragments containing each affected gene (from approximately 1 kb 5' of the start codon to about 0.5 kb 3' of the stop codon) derived from a bacterial artificial chromosome covering the region. Each genomic DNA fragment was co-introduced into *tgd2* along with a linearized Paromomycin resistance gene (*AphVIII*), which was under selection. Of the six genes disrupted or missing from the *tgd2* genome, only introduction of *CrTGD2* was able to restore TAG content, TAG acyl group profile, cell viability, and PtdOH content close to PL levels (Figure 2.S6). Therefore, deletion of *TGD2* is the cause of at least the four phenotypes of the *tgd2* mutant discussed. Because the phenotype of complemented line C3 was nearly fully restored to that of the PL (Figure 2.S6C and C), this line was included in all subsequent analyses, except where indicated otherwise, and is designated *TGD2 tgd2*.

***CrTGD2* is a presumed orthologue of *AtTGD2*.** The translated sequence of the Chlamydomonas *CrTGD2* gene has 40% amino acid identity with the Arabidopsis protein *AtTGD2*. Both are similar to substrate binding protein components of bacterial ABC transporters (Casali & Riley, 2007). Both also contain a Mammalian Cell Entry (MCE) domain (Figure 2.S7), which in the respective *Mycobacterium tuberculosis* protein for which this domain was named, is required for pathogenesis. In addition phylogenetic analysis of the MCE domain of predicted *CrTGD2* orthologues across plants, green algae, and bacteria revealed that *CrTGD2* falls into the same clade as the respective plant proteins and is divergent from bacterial orthologues (Figure 2.S8 and APPENDIX C. for the alignment). Using TMHMM (Krogh *et al.*, 2001), *CrTGD2* is predicted to contain one transmembrane domain (Figure 2.S7), similar to the Arabidopsis orthologue *AtTGD2* (Koichiro Awai *et al.*, 2006). Based on these similarities, we hypothesized that *CrTGD2* may have similar functions as *AtTGD2* and, hence, those two proteins may be true orthologues. To more directly test their functional equivalence, we introduced (i) codon optimized Arabidopsis *TGD2* in the Chlamydomonas *tgd2* mutant, and (ii) Chlamydomonas *TGD2* in Arabidopsis *tgd2-1* mutant. However, despite the presence of the recombinant proteins, lipid phenotypes were not restored (Figure 2.S9 and 2.S10). Thus, the two *TGD2* proteins seem to be sufficiently divergent to not substitute for each other in a heterologous protein complex.

Altered galactoglycerolipid labeling and impaired ER-to-plastid lipid trafficking in *tgd2*. Pulse chase analysis provides a proven *in vivo* method to examine general substrate-product relationships in metabolic pathways and lipid trafficking in plants in particular, and it was used in the original analysis of the *tgd1-1* mutant of Arabidopsis, e.g. (Xu *et al.*, 2003). Here, we

carried out pulse-chase labeling experiments with [^{14}C]-acetate using mid-log phase cultures of PL, *tgd2* and *TGD2 tgd2*. The cells were incubated in the presence of labeled substrate until 20-40% incorporation of label was observed before the labeled medium was replaced for the chase. Total lipids were extracted at different times during the chase phase and individual lipids were separated by thin-layer chromatography followed by liquid scintillation counting to determine the fraction of incorporation of radiolabel into all lipids analyzed. Multiple individual repetitions of this experiment were carried out and all of these replicates showed similar trends, but the absolute values differed making it difficult to average results from the different experiments. Therefore, a representative experiment is shown in Figure 2.4.

The most noticeable differences in labeling between the different cell lines were observed for MGDG and DGDG. MGDG in *tgd2* was labeled to much higher levels with a subsequent rapid decrease in label during the chase phase (Figure 2.4, top panels). In contrast, MGDG labeling in PL and in the *TGD2 tgd2* line was lower, and less of a decrease in label was observed during the chase. As the bulk-steady-state levels of MGDG in *tgd2* did not significantly change compared to the PL (Figure 2.1b), the result suggests that MGDG was more rapidly synthesized and metabolized in *tgd2*. Since DGDG is derived from MGDG, one would expect that its labeling would follow that of MGDG at least in the initial chase phase (within the first five hours) and that label would appear to move from MGDG to DGDG as was the case for the PL and *TGD2 tgd2* lines during the first five hours of the chase. However, DGDG labeling was severely delayed and not as high in *tgd2* (Figure 2.4, top panels) suggesting a disruption in the conversion of MGDG to DGDG in *tgd2* or the activation of pathways competing for MGDG as a substrate.

The detailed shape of the time course for MGDG labeling also was different in the mutant. In the PL and *TGD2 tgd2* lines the MGDG labeling time course showed a “dip” and rebound during the first five hours of the initial stage of the chase, but in the *tgd2* mutant, MGDG labeling declined steadily (Figure 2.4, top panel). This result was not a chance observation of this particular experiment, because independent repeats showed this phenomenon reproducibly (Figure 2.S11). The equivalent experiment with wild-type Arabidopsis leaves shows a comparable MGDG labeling time course which is interpreted as initial rapid labeling of MGDG by the chloroplast pathway, followed by label dilution during the initial chase phase decreasing the label followed by a gradual increase in labeling of MGDG over time as lipids move back from the ER as part of the ER pathway of galactoglycerolipid biosynthesis (Xu *et al.*, 2003). In

the Arabidopsis *tgdl-1* mutant MGDG labeling is also very high and steadily declines during the chase phase, interpreted as a reduction in lipid species returning from the ER to the chloroplast. The observation of the typical “dip” in MGDG labeling in the Chlamydomonas PL is currently the most direct indicator for ER-to-chloroplast lipid trafficking in this alga. The lack of the “dip” in the *tgdl2* mutant suggests that TGD2 is involved in this process.

Altered labeling of non-galactoglycerolipids in *tgdl2*. In addition to the differences in MGDG and DGDG labeling, the labeling time course of the betaine lipid diacylglyceryl-trimethylhomoserine (DGTS) and PtdGro also showed changes in the *tgdl2* mutant. In contrast to the PL, DGTS labeling during the chase in *tgdl2* started at a lower level and continued to increase without leveling off (Figure 2.4, middle panels). This result would be consistent with a decreased rate of precursor conversion into DGTS in the *tgdl2* mutant. Less label was also found in PtdGro in *tgdl2* (Figure 2.4, top panels), although the shape of the labeling time course looked similar to that of the PL and the *TGD2 tgdl2* complemented line. It should be noted that DGTS and PtdGro steady state levels were not altered in the mutant (Figure 2.1B). Therefore the relative rate of synthesis of these two lipids was decreased (or turnover increased) compared to that of MGDG in *tgdl2*.

While incorporation of label into the TAG fraction in the PL and the complemented line *TGD2 tgdl2* was minimal, label in TAG of the *tgdl2* mutant steadily increased during the chase phase in parallel with a decrease in label in MGDG (Figure 2.4 lower panel). Given also the observation that MGDG specific acyl groups were found in TAG under steady-state conditions in *tgdl2* (Figure 2.1A, B, D and E), the labeling result was consistent with a conversion of mature MGDG to TAG in the *tgdl2* mutant. The labeling of other lipids did not show much difference in the *tgdl2* mutant (Figure 2.4).

Biosynthesis of MGDG is increased in the *tgdl2* mutant. The increase in acetate labeling of MGDG prompted us to investigate MGDG synthesis directly by using a more specific substrate, UDP-galactose. Intact chloroplasts from PL and *tgdl2* were fed with 300 mCi/mmol UDP-[¹⁴C]-galactose. Total lipids were extracted and incorporation of labeled galactose into MGDG and DGDG was monitored and normalized based on an equal number of chloroplasts. We observed higher levels of labeled MGDG and DGDG in chloroplasts from *tgdl2* than from the PL (Figure 2.5A) consistent with a higher galactolipid synthesis activity in the *tgdl2* mutant. It is important to

note that MGDG is synthesized by addition of one galactose from UDP-galactose to DAG and DGDG is synthesized by transfer of one galactose from UDP-galactose to MGDG. Thus in the case of DGDG, four different molecular species can be obtained during this experiment, depending on whether only the distal or the proximal galactose, or both or none of the galactoses are labeled. This makes it challenging to directly determine the MGDG-to-DGDG precursor product relationship. However, in order to compare rates of conversion of MGDG to DGDG, ratios of labeled DGDG/labeled MGDG were calculated. This ratio is significantly lower in *tgd2* (Figure 2.5B), which indicates a lower rate of conversion of MGDG to DGDG in *tgd2*.

In *Arabidopsis*, MGDG synthases can be localized in either of the two chloroplast envelope membranes (K. Awai *et al.*, 2001), but the bulk of MGDG synthesis involves MGD1 at the inner envelope membrane (Jarvis *et al.*, 2000). To test whether the observed MGDG synthase activity of isolated chloroplasts might be associated with the outer envelope membrane in *Chlamydomonas*, we treated the chloroplasts with Thermolysin, a large protease that cannot penetrate the outer envelope membrane (see also below). As shown in Figure 2.5A, MGDG and DGDG syntheses were sensitive to Thermolysin suggesting that both, the MGDG and DGDG synthases are located in the outer envelope membrane in *Chlamydomonas*.

CrTGD2 is present in the chloroplast inner envelope membrane. Based on amino acid sequence analysis with different online prediction tools including PredAlgo (Tardif *et al.*, 2012), the location of CrTGD2 was initially ambiguous, but likely in the chloroplast. Fractions containing chloroplasts, mitochondria and microsomal membranes were isolated from whole cell lysates and CrTGD2 was detected using immunoblotting with antiserum raised against the recombinant protein. Antisera against marker proteins for each cell compartment were tested as well. Whole cell lysate of the *tgd2* mutant lacking CrTGD2 was used as a negative control to confirm the presence of the CrTGD2 signal in the PL extracts. As shown in Figure 2.6A each subfraction was enriched with its respective marker protein, while CrTGD2 was clearly detected in the chloroplast fraction and whole cell lysate. This suggests that CrTGD2 is localized in the chloroplast.

Because CrTGD2 was predicted to contain one transmembrane domain (Figure 2.S7), a protease protection assay was carried out to determine the possible insertion of CrTGD2 into one of the chloroplast envelope membranes. This assay takes advantage of size difference between

Thermolysin and Trypsin (Cline *et al.*, 1984). In general, Thermolysin is too big to penetrate the outer envelope membrane of the chloroplast. In contrast, Trypsin is sufficiently small to gain access to the intermembrane space and proteins in the inner envelope membrane. Different concentrations of either Thermolysin or Trypsin were used to treat isolated intact chloroplasts of the PL. Antisera against three markers for specific compartments were: anti-Toc34 detecting an outer envelope membrane protein, anti-ARC6 detecting an inner envelope membrane protein facing the intermembrane space, and anti-Tic40 detecting an inner envelope membrane protein facing the stroma, respectively. As a result of Thermolysin treatment at increasing concentrations, Toc34 decreased in abundance as predicted for an outer envelope membrane protein, but the other markers and CrTGD2 did not (Figure 2.6B, left panel). Following treatment with Trypsin, all proteins were susceptible at increasing concentrations of the protease (Figure 2.6B, right panel). This result suggests that CrTGD2 is localized in the inner envelope membrane as was previously observed for the AtTGD2 orthologue (Koichiro Awai *et al.*, 2006).

CrTGD2 binds PtdOH *in vitro*. The Arabidopsis orthologue AtTGD2 binds PtdOH *in vitro* (Koichiro Awai *et al.*, 2006; Lu & Benning, 2009). Therefore, a liposome binding assay was used to test for lipid binding by CrTGD2. As done for AtTGD2, a recombinant CrTGD2 protein truncated from the N-terminus to just beyond the membrane-spanning domain was fused to the C-terminus of DsRED to improve solubility (Lu & Benning, 2009) and was produced in *E. coli*. This fusion protein also contained a His-tag at its C-terminus and was designated DsRED-CrTGD2-His-tag. In parallel, DsRED-AtTGD2-His-tag was used as a positive control. As an internal negative control, DsRED by itself, which does not bind lipids, was included with the samples. Both AtTGD2 and CrTGD2 showed strongest binding to PtdOH of all lipids tested (Figure 2.7A and B). The double band is due to an internal autocatalytic cleavage of DsRED as previously reported (Gross *et al.*, 2000).

DISCUSSION

Lipid metabolism of *Chlamydomonas* was thought to differ from that of *Arabidopsis* in at least three aspects: 1. *Chlamydomonas* does not synthesize phosphatidylcholine (PtdCho); 2. It has the betaine lipid DGTS; and 3. It is thought to not utilize the ER-pathway for precursors of thylakoid lipid assembly (Giroud & Eichenberger, 1988). In fact, because the lipid precursor transported from the ER to the chloroplast is still unknown (Hurlock *et al.*, 2014), but might involve PtdCho, these three differences could be related. However, the genome of *Chlamydomonas* encodes TGD1, 2, and 3 proteins, which have been shown to be involved in lipid trafficking from the ER to the chloroplasts in *Arabidopsis* (C Benning, 2009; Hurlock *et al.*, 2014). Thus, if *Chlamydomonas* were truly lacking ER-to-plastid lipid transport, the presence of these proteins in *Chlamydomonas* presents an interesting conundrum.

The analysis of the *tgd* mutants of *Arabidopsis* is complicated by the fact that loss of function of *TGD* genes is lethal and that in the available leaky mutants a galactoglycerolipid synthesizing enzyme, SFR2, is induced. Its activity leads to the formation of di- and higher order oligogalactoglycerolipids from MGDG. Therefore, the absence of SFR2 activity from *Chlamydomonas* allows us to reevaluate more directly the function of TGD proteins in the biosynthesis of the thylakoid lipids MGDG and DGDG in this organism without having to consider the competing SFR2-based pathway present in *Arabidopsis*. Thus, studying the role of TGD2 in *Chlamydomonas* with a loss-of-function *tgd2* mutant that is not lethal, but has a rapid senescence phenotype, provides a unique opportunity to more fully understand the role(s) of TGD proteins in the chloroplast envelope membranes. Moreover, only single genes for MGDG and DGDG synthases respectively have been identified in the *Chlamydomonas* genome further simplifying the analysis of its galactoglycerolipid metabolism. One caveat is that we do not yet know the exact location of the two galactoglycerolipid synthases in *Chlamydomonas*, but our analysis based on the sensitivity of the two activities in isolated chloroplasts to Thermolysin (Figure 2.5A) suggests that they are both associated with the outer envelope membrane. In *Arabidopsis*, the main MGDG synthase activity encoded by *MGDI* is associated with the inner envelope membrane facing the intermembrane space, while the DGDG synthase, *DGDI*, is associated with the outer envelope membrane facing the cytosol (C. Benning & Ohta, 2005). Additional MGDG synthases MGD2 and MGD3 are present in the outer envelope membrane in *Arabidopsis*, but are thought to be conditionally involved in synthesis of galactoglycerolipids

during phosphate starvation or in specific tissues (Kobayashi *et al.*, 2009). How the products of the two enzymes move between the envelope membranes in Arabidopsis or any other organism is currently unknown.

Galactoglycerolipid metabolism is altered in *tgd2*. A first indication that MGDG synthesis and turnover are affected in the *tgd2* mutant arises from the fact that *tgd2* accumulates TAG with 16:4 and 18:3 acyl groups typically found only in MGDG (Figure 2.1D and E). Moreover, osmium tetroxide-stained lipid droplets of *tgd2* (Figure 2.3D-F) appeared darker compared to those of the PL (Figure 2.3C) consistent with an increased desaturation of acyl groups associated with lipid droplets (Bahr, 1954; Korn, 1967).

Second, altered MGDG metabolism in the *tgd2* mutant became obvious during acetate pulse-chase labeling studies. While the steady state bulk levels of MGDG and DGDG in *tgd2* were similar to those of the PL (Figure 2.1B), acetate-labeling experiments and subsequently direct measurements of MGDG synthase activity in isolated chloroplasts showed that MGDG is more actively synthesized in *tgd2* (Figure 2.4 and 2.5A). Interestingly, this higher level of MGDG labeling did not translate into higher or more rapid labeling of DGDG presumably formed by galactosylation of MGDG. In fact, this result would be consistent with an impairment in the conversion of MGDG into DGDG in the *tgd2* mutant. Similarly, UDP-galactose labeling of isolated chloroplasts showed a decrease in the conversion of MGDG into DGDG in the *tgd2* mutant as the ratio of labeled DGDG to MGDG strongly decreased (Figure 2.5B). It should be noted that in this assay DGDG is more highly labeled than MGDG, which is opposite to what is observed with isolated Arabidopsis chloroplasts (Xu *et al.*, 2005). One reason could be that in *Chlamydomonas* substrate channeling occurs between the MGDG and DGDG synthases, which is decreased in the *tgd2* mutant indicated by the strongly decreased ratio of labeled DGDG to MGDG. Another reason might be the absence of SFR2 from *Chlamydomonas*, such that there is no further redistribution of label from MGDG into higher order galactoglycerolipids.

How TGD2 might be affecting galactoglycerolipid metabolism in *Chlamydomonas* is outlined in Figure 2.8. Formally based on the labeling data alone, TGD2 could provide MGDG substrate to the DGDG synthase. However, TGD2 is likely a component of a lipid transporter shuttling lipids between the outer and the inner envelope membranes while the two galactoglycerolipid synthases appear to be both localized in the outer envelope membrane in

Chlamydomonas. Because we do not know the lipid substrate of this transporter, it might well be that the TGD1, 2, 3 complex transfers galactoglycerolipids from the outer to the inner envelope membrane. An alternative possibility is that TGD2 as proposed for Arabidopsis is involved in transferring PtdOH from the outer to the inner envelope membrane. After all, it is similar to substrate binding proteins associated with ABC transporters and binds primarily PtdOH just like the TGD2 orthologue from Arabidopsis (Figure 2.7). Its absence could lead to an increase in PtdOH in the outer envelope membrane. We indeed observed an increase in cellular PtdOH content in the *tgd2* mutant (Figure 2.1B), although we could not determine the membrane association of this additional PtdOH. As is known for the Arabidopsis MGDG synthase (Dubots *et al.*, 2010), this increased PtdOH content if associated with the outer envelope membrane could stimulate MGDG synthase activity leading to increased MGDG biosynthesis as observed in the *tgd2* mutant (Figure 2.8). In fact, there is some resemblance in the labeling results obtained for Arabidopsis *tgd* mutants (Xu *et al.*, 2005; Xu *et al.*, 2003). First, Arabidopsis *tgdl-1* showed initially a strongly increased incorporation of label into MGDG during acetate pulse-chase labeling (Xu *et al.*, 2003). Second, differences in the labeling of MGDG and DGDG are increased as well in the Arabidopsis *tgdl-1* mutant (Xu *et al.*, 2003). Thirdly, during UDP-galactose labeling of isolated chloroplasts, MGD1 activity of *tgdl-1* was increased while DGDG labeling did not increase (Xu *et al.*, 2005). Thus disruption of the TGD complex in both organisms seems to stimulate MGDG synthesis without stimulating DGDG synthesis and formally could appear as a disruption of transfer of precursors to the DGDG synthase in labeling experiments.

What happens to MGDG as it is metabolized in the *tgd2* mutant? It is critical for the cell to maintain a set ratio of the non-bilayer forming lipid, MGDG, and the bilayer forming lipid, DGDG, in its photosynthetic membrane (Dörmann & Benning, 2002). Because MGDG synthesis is increased over that of DGDG in the *tgd2* mutant, to maintain lipid homeostasis and prevent accumulation of bulk MGDG, its turnover rate must also be increased as suggested by the acetate pulse-chase labeling experiment (Figure 2.4). As acyl groups normally specifically found in MGDG of the PL are present in TAG accumulating in the *tgd2* mutant (Figure 2.1D and E), it appears that some of the DAG moieties of MGDG or its acyl groups are converted to TAG and are sequestered in lipid droplets (Figure 2.3D-F). In plants, MGDG can be hydrolyzed and its DAG or acyl groups are converted to TAG that is stored in plastoglobuli inside the plastid during

photosynthetic stress (Youssef *et al.*, 2010) or during leaf senescence (Kaup *et al.*, 2002). Thus lipid droplets may serve as buffer for storing otherwise toxic acyl groups derived from membrane lipids. In addition, TAG synthesis in *Chlamydomonas* may involve the release of acyl groups from newly formed MGDG by the activity of the lipase PGD1 (Figure 2.8), as has been shown to occur during N deprivation (Li *et al.*, 2012).

In case of the *tgd2* mutant of *Chlamydomonas*, lipid droplets were observed in the cytosol in contact with the outer envelope membrane of the chloroplast (Figure 2.3G). This observation supports the hypothesis that *Chlamydomonas* can synthesize TAG in its chloroplast membranes (Jilian Fan *et al.*, 2011; Liu & Benning, 2013). The *Arabidopsis* *tgd* mutants, e.g. *tgd1-1*, also accumulate TAG in the cytosol of leaves (Xu *et al.*, 2005). However, the TAG accumulating in the *Arabidopsis* *tgd1-1* mutant has an acyl profile more similar to that of PtdCho, but not MGDG as in the case of *Chlamydomonas* *tgd2*. It was concluded that accumulation of TAG in the *tgd1-1* mutant was the result of increased conversion of lipid precursors accumulating at the ER due to impaired ER to chloroplast lipid trafficking. TAG accumulation in *Arabidopsis* *tgd1-1* involves the conversion of PtdCho by phospholipid : DAG acyltransferase (PDAT, Jilian Fan *et al.*, 2013). In addition, studies on the *Arabidopsis* *tgd1-1 sfr2* double mutant revealed that the DAG moiety of TAG accumulating in the *Arabidopsis* *tgd1-1* mutant is derived from DAG generated by SFR2 activity (Jilian Fan *et al.*, 2014). However, as *Chlamydomonas* lacks SFR2 activity, the mechanism of TAG biosynthesis in the *Chlamydomonas* *tgd2* mutant must be different.

It seems also likely that acyl groups derived from MGDG undergo a different fate as they can become oxidized as seen in the higher level of malondialdehyde derived from fatty acid peroxidation in the *tgd2* mutant (Figure 2.2C). It is largely accepted that polyunsaturated fatty acids are targets for oxidation by autooxidation or lipoxygenases (Feussner & Wasternack, 2002). Products of lipid peroxidation are mainly aldehydes, which are toxic to nucleic acids and proteins (Esterbauer *et al.*, 1991). Thus, it seems possible that increased oxidization of MGDG derived acyl groups in *tgd2* leads to lower viability of *tgd2* in prolonged cultures (Figure 2.2A and 2.3I).

Does CrTGD2 play a role in the transfer of lipids from the ER to the chloroplast? In the *Arabidopsis* *tgd1,2,3,4* mutants, increase in the ratio of C16/C18 acyl groups of thylakoid lipids indicates lack of lipid trafficking from the ER to the chloroplast (Koichiro Awai *et al.*, 2006; Lu

et al., 2007; Xu *et al.*, 2008; Xu *et al.*, 2003). In addition, changes in acetate pulse-chase labeling of MGDG in *tgdl-1* seedlings (a lack of a transient decrease in MGDG labeling in the mutant as lipid precursors move from the chloroplast to the ER and then return) also indicates the lack of lipid transfer between the two compartments (Xu *et al.*, 2003). A similar, albeit more subtle change in the labeling time course for MGDG was observed for the *Chlamydomonas* *tgd2* mutant (Figure 2.4, top panel, Figure 2.S11). Thus these labeling data suggest that lipid precursors could be transferred from the ER to the chloroplast envelope membranes for the synthesis of thylakoid lipids. If this conclusion is correct, the ER located lyso-PtdOH acyl transferase must have a different substrate specificity in *Chlamydomonas* compared to *Arabidopsis* to explain the absence of 18 carbon fatty acids at the *sn-2* position of thylakoid lipids in *Chlamydomonas*. Thus, a thorough analysis of the acyltransferases in *Chlamydomonas* will be required to ultimately solve this conundrum.

Like in *Arabidopsis*, subcellular localization and protease protection assays suggested that CrTGD2 is localized in the inner envelope membrane of the chloroplast (Figure 2.6A and B). Furthermore, similar to AtTGD2 (Koichiro Awai *et al.*, 2006; Lu & Benning, 2009; R. Roston *et al.*, 2011), *in vitro* lipid binding assays showed that CrTGD2 binds primarily to PtdOH (Figure 2.7A and B), which is a candidate for transferred lipid species. Phylogenetic analysis showed that CrTGD2 is in the same clade as those of land plants but not bacteria (Figure 2.S8), but TGD2 proteins from either *Arabidopsis* or *Chlamydomonas* were not functional in the opposite host in our hands, respectively (Figure 2.S9 and 2.S10), perhaps because both proteins are too divergent to function in a heterologous complex. However, based on all other data presented here, it is likely that the TGD2 protein of *Chlamydomonas* is also a component of a lipid transporter transferring lipid precursors between the envelope membranes as proposed for the homologous system in *Arabidopsis*. However, because TGD4 and TGD5 are seemingly absent from *Chlamydomonas*, it remains to be seen what proteins might be involved in lipid transfer between the ER and the outer envelope membrane in *Chlamydomonas*. Furthermore, because the actual lipid species transported is not yet known, a possibility remains that the TGD1, 2, 3 complex of *Chlamydomonas* also plays a role in the transfer of the galactoglycerolipids synthesized at the outer chloroplast envelope membrane to the inner envelope membrane in *Chlamydomonas*.

MATERIALS AND METHODS

Algal strains and growth conditions. *Chlamydomonas reinhardtii* cell wall-less strain dw15.1 (cw15, nit1, mt⁺) provided by Arthur Grossman (Carnegie Institute for Science, Department of Plant Biology, Stanford University) was used as wild-type PL with regard to *TGD2* to generate the *tgd2* mutant. A cell-walled strain CC-198 (er-u-37, str-u-2-60, mt⁻) obtained from the Chlamydomonas Resource Center (<http://www.chlamycollection.org>) was used to generate *tgd2* cell-walled progenies for linkage analysis and for TEM. Unless specified, the algal cultures were grown in Tris-acetate-phosphate (TAP) medium (Gorman & Levine, 1965). For all experiments except for chloroplast preparation, algal cultures were grown under continuous light at 80 $\mu\text{mol m}^{-2} \text{s}^{-1}$ and at 22°C. The cell concentration was monitored with a Z2 Coulter Counter (Beckman Coulter).

Generation of *tgd2* mutant and genetic analyses. The *tgd2* mutant was generated by insertional mutagenesis in the same experiment as described previously for the *cht7* mutant (Tsai *et al.*, 2014). The details of the genetic analysis are described under APPENDIX D. Details about the Bacterial Artificial Chromosomes used for genetic complementation can be found in Table 2.S1. Sequences of primers used for testing genetic complementation are listed in Table 2.S2.

DNA isolation and Southern blot analysis. DNA isolation was carried out as previously described (Keb-Llanes *et al.*, 2002) with some modifications as detailed in the APPENDIX D. Southern blot analysis was done with the same probe as described in (Li *et al.*, 2012).

Whole genome resequencing. The genome of the *tgd2* mutant was sequenced by Illumina Hi-Seq using the paired-end method at the MSU-Research Technology Support Facility. Details of the analysis are described under APPENDIX D. Sequences of primers used for identifying the deletion can be found in Table 2.S2.

Lipid analysis. Total lipid was extracted as previously described (Bligh & Dyer, 1959) from pellets of either freshly harvested cultures or from pellets stored at -80°C. In general, pellets from 15 mL algal culture were resuspended in 3 mL extraction solvent. The extracted lipids were dried under an N₂ stream and stored at -20°C. Individual lipids were separated on thin layer chromatography (TLC) plates (TLC Silica gel 60, EMD). For PtdOH separation, ammonium sulfate treated TLC plates (C Benning & Somerville, 1992) were employed. Different solvents were used for different lipid classes: for neutral lipids petroleum ether, diethyl ether, acetic acid

(80:20:1 v/v); for polar lipids chloroform, methanol, acetic acid and water (75: 13: 9: 3 v/v); for PtdOH chloroform, methanol, ammonium hydroxide (65: 25: 5); and for oligogalactolipids chloroform, methanol, 0.9% sodium chloride and water (60: 35: 4: 4 v/v). Lipids on TLC plates were visualized by briefly staining with iodine vapor. Alternatively, galactoglycerolipids were stained with α -naphthol as described in (Wang & Benning, 2011). Lipids were isolated and processed for generation of fatty acid methyl esters (FAMES) as described in (C Benning & Somerville, 1992). Quantifications of FAMES were performed by gas liquid chromatography using an HP6890 instrument equipped with a DB-23 column (both Agilent Technologies, Santa Clara, CA) with a temperature profile and running conditions as described in (Zäuner *et al.*, 2012).

Viability assay. The PL (dw15.1), *tgd2* mutant and *TGD2 tgd2* inoculated at 0.5 million cells/mL were grown in TAP medium. Cells were harvested at day 3, 7, 14, 21 and 28 for viability staining, lipid analysis, and thiobarbituric acid-reactive-substances (TBARS) assay. Viability staining was performed as described (Chang *et al.*, 2005) with minor modifications. The cell samples were mixed with an equal volume of staining solution (0.0252% methylene blue, 0.0252% phenosafranin and 5% ethanol) and incubated for 5 min. The two dyes are excluded from living cells, which remain green, while dead cells taking up the dyes stain purple. The two cell types were counted with a hemocytometer. For lipid analysis, cell were harvested as described above, flash frozen in liquid N₂, and stored at -80°C for later lipid analysis (see above).

Lipid peroxidation was estimated with a TBARS assay. Two aliquots of 5 to 10 ml of algal culture were harvested by centrifugation as described and the algal pellets were resuspended in 1 mL of 20% trichloroacetic acid either with or without 0.5% thiobarbituric acid. The mixtures were heated at 95°C for 15 min. Absorbance was measured at 440, 532 and 600 nm. The concentration of malondialdehyde was calculated as described in (Hodges *et al.*, 1999).

Transmission Electron Microscopy. Walled strains were fixed as previously described (Harris, 1989). Images were taken with a JEOL100 CXII instrument (Japan Electron Optics Laboratories, Tokyo, Japan).

Phylogenetic analysis. The analysis was done as detailed under APPENDIX D.

Heterologous complementation analysis. The heterologous complementation analysis of the *tgd2* mutant was performed as described in detail under APPENDIX D. Sequences of primers used for generating constructs are listed in Table 2.S3.

[¹⁴C]-Acetate pulse-chase labeling. The different lines were grown in 200 mL TAP medium to mid-log phase. After 10-fold concentration into 20 mL TAP medium, 10 µL of 1 mCi/mL [¹⁴C] sodium acetate (55 mCi/mmol) were added to the culture. The cultures were incubated at room temperature for 1-2 h until the incorporation of label reached 20-40%. To initiate the chase, the cultures were centrifuged at 3,000 X g for 3 min. The cell pellets were then resuspended in 200 mL unlabeled TAP medium and the cultures were incubated at room temperature. At given intervals, 20 mL of the cultures were harvested. Individual lipids were separated on TLC plates as described above. Silica powder containing each lipid was isolated from the TLC plates and subjected to liquid scintillation counting in 10 mL complete counting cocktail 4a20TM (Research Products International Corp.). Radioactivity was measured with a PerkinElmer Liquid Scintillation Analyzer Tri-Carb 2800TR.

***DsRED-CrTGD2* pLW01, *DsRED-AiTGD2* pLW01 and *DsRED* pLW01 constructs, recombinant protein expression and purification.** Details of the construction of the plasmids and recombinant protein production are as described under APPENDIX D. Primers used in this experiment are listed in Table 2.S3.

CrTGD2 antibody. DsRED-CrTGD2 fusion protein was used as antigen to raise antiserum in rabbits (Cocalico Biologicals). The antigen was prepared with Freund's adjuvant and inoculated in rabbits with 3 additional boosts. Two test bleeds were tested for immunoreaction against pre-bleed with *Chlamydomonas* PL and *tgd2* mutant proteins. Final bleed antiserum was used as primary antibody for detection of immunoreactions.

Immunoblotting. Protein samples for localization of CrTGD2 and for heterologous *tgd2* complementation analysis were resuspended in protein extraction buffer (0.1 M Tris-HCl pH 6.8, 1% SDS, 15% glycerol and 5% β-mercaptoethanol). The mixtures were incubated at 95°C for 5 min. The protein was cooled down on ice and centrifuged at 20,000 X g for 10 min at 4°C. Pellets were discarded. Protein concentrations were determined with bovine serum albumin (BSA) as a standard according to (Bradford, 1976). In general, equivalents of 10 µg protein (2 µg chlorophyll equivalents for experiments described in Figure 2.6B and 40 µg of protein in Figure

2.S9B) were separated by SDS-PAGE. The proteins were then transferred to polyvinylidene difluoride (PVDF) membranes. The membranes were incubated in blocking solution (5% non-fat dry milk in TBST containing 20 mM Tris-HCl pH 7.5, 150 mM NaCl and 0.05% Tween 20 (v/v)) for 30 min. Following the addition of primary antiserum in blocking solution, the membranes were incubated at 4°C overnight. The membranes were washed 6 times with TBST at 5 min intervals. Secondary antisera conjugated with horseradish peroxidase were incubated with the membranes for 1-2 h at room temperature. The membranes were washed again as described previously prior to detection of immunoreaction with Clarity™ Western ECL Substrate (BIO-RAD) as a substrate using a ChemiDoc™ MP Imaging System (BIO-RAD). Antibodies against CrTGD2, Tic40 (provided by John Froehlich, Michigan State University), BIP (Santa Cruz Biotechnology), cytochrome C (BD Pharmingen™), Toc34 (Agrisera), ARC6 (provided by Katherine W. Osteryoung, Michigan State University) and AtTGD2 (Koichiro Awai *et al.*, 2006) were used at 1:500, 1:2000, 1:1000, 1:250, 1: 10,000, 1:2500 and 1:2000 dilutions, respectively. Secondary anti-rabbit antibodies were used for each primary antibody, except for anti-cytochrome C, for which an anti-mouse antibody (SIGMA) was used.

In case of the lipid binding assay described below, the protein samples were resuspended in 2x SDS sample buffer (0.12 M Tris-HCl pH 6.8, 4% SDS, 20% glycerol, 10% β-Mercaptoethanol and 0.05% bromophenol blue) and processed as described above. The protein samples were separated by SDS-PAGE and transferred to PVDF membranes. These membranes were processed in the same manner as described above. Primary and secondary antibodies were the His-tag antibody (GenScript) and anti-mouse conjugated with horseradish peroxidase, respectively. The immunoreaction was detected as described above.

Subcellular fractionation. *Chlamydomonas* PL dw15.1 was grown under 12 h light and 12 h dark cycles to mid-log phase. A 500 mL culture was harvested by centrifugation at 3000 X g for 10 min at 4°C. Isolation of chloroplast, mitochondrial and microsomal membranes was based on a procedure described in (Klein *et al.*, 1983) with modifications. In brief, cells were broken by digitonin. The pellet from an 800 X g centrifugation was considered the chloroplast fraction. The chloroplasts were further purified on a 20-40-65% Percoll step gradient made with isotonic solution. Intact chloroplasts were obtained at the transition between 40% and 65% Percoll layers following centrifugation at 4,000 X g for 15 min at 4°C. The supernatant of the 800 X g centrifugation contained mitochondria and microsomal membranes. This supernatant was

centrifuged at 5,000 X g for 10 min at 4°C. The pellet from this centrifugation contained a mitochondrial crude fraction which was further purified as previously described in (Eriksson *et al.*, 1995) using a 20% Percoll gradient made from isotonic solution compatible with the chloroplast isolation buffer. The supernatant from the 5,000 X g centrifugation was further centrifuged at 100,000 X g for 90 min at 4°C. The pellet from this centrifugation was considered the microsomal membrane fraction. All fractions were processed by immunoblotting as described above.

Protease protection assay. Isolated chloroplasts were treated with Thermolysin or Trypsin. For Thermolysin treatment, 50 µg/mL chlorophyll equivalent of chloroplasts were incubated with 0-200 µg/mL Thermolysin in buffer containing 20 mM Tricine-NaOH pH 7.7, 150 mM mannitol, 1 mM MgCl₂, 1 mM MnCl₂, 2 mM EDTA and 0.5 mM CaCl₂. The treatment was carried out on ice for 15 min. The reaction was stopped with the above buffer by adding 10 mM EDTA. The treated chloroplasts were overlaid on a 40% Percoll gradient made from treatment buffer with the addition of 5 mM EDTA. The chloroplasts were centrifuged at 1,500 X g for 5 min. The pellet was washed with treatment buffer containing 5 mM EDTA. Trypsin treatment was carried out in a similar manner with a few modifications. The Trypsin treatment buffer was the same as the Thermolysin buffer without 0.5 mM CaCl₂. The reaction was stopped with buffer containing 200 µg/mL Trypsin inhibitor. Instead of 5 mM EDTA in the 40% Percoll gradient and in the wash buffer 100 µg/mL Trypsin inhibitor were added. Protease-treated chloroplasts were processed for immunoblotting as described above or assayed for MGDG synthase activity.

MGDG synthase assay. Intact chloroplasts either treated with 100 µg/mL Thermolysin or left untreated as described above were resuspended at 125 µg chlorophyll equivalent in 100 µL assay buffer containing 20 mM Tricine-NaOH pH 7.7, 150 mM mannitol, 5 mM MgCl₂, 2.5 mM EDTA. The reaction was started by adding 0.3 µCi of UDP-[¹⁴C] galactose (300 mCi/mmol) and incubated at room temperature under light for 2 min. Lipid was extracted as a means to stop the reaction. MGDG and DGDG were separated by TLC and radioactive lipids analyzed as described above.

Lipid binding assay. Liposomes consisting of different test lipids were prepared with dioleoyl PtdCho at a 40:60% molar ratio. The mixtures of tested lipid and PtdCho were dried under a stream of N₂. Dried lipids were resuspended in 200 µL of TBS (50 mM Tris-HCl pH 7.0 and 0.1

M NaCl). The mixtures were incubated in a water bath at the highest lipid transition temperature (37°C for dioleoyl lipids) for 1 h. The liposomes were washed one time and resuspended in 95 μ L TBS. Five μ L of 3.7 μ g DsRED-AtTGD2-6xHis and 2 μ g of DsRED, or 3.6 μ g of DsRED-CrTGD2-6xHis and 2 μ g DsRED were added to the liposomes. DsRED served as internal negative control. The mixtures were incubated at room temperature for 30 min. Liposome-protein complexes were recovered by centrifugation at 13,000 X g for 10 min at 4°C. The pellets were washed twice in TBS. The liposome-protein pellets were processed to detect the DsRED proteins by immunoblotting as described above.

ACCESSION NUMBERS

Read sequences of the *tgd2* mutant obtained from whole genome resequencing can be found in the Sequence Read Archive of the National Center for Biotechnology Information under accession number SRP061379. Chlamydomonas TGD2 sequence accession number Cre16.g694400.t1.2 was obtained from the Joint Genome Institute. Arabidopsis TGD2 sequence accession number AT3G20320 was obtained from The Arabidopsis Information Resource (www.arabidopsis.org). Accession numbers used for phylogenetic tree reconstruction are shown in Figure 2.S8 following the species names.

ACKNOWLEDGMENTS

We are grateful to Dr. Simone Zäuner and Dr. Yang Yang for valuable discussions. We would like to thank Dr. Likit Preeyanon for helping with *de novo* genome assembly and Alicia Pastor for helping with electron microscopy. We thank Tomomi Takeuchi and Dr. Shin-Han Shiu for helping with phylogenetic tree construction. We thank Dr. Setsuko Wakao and Dr. John Froehlich for valuable suggestions for subcellular fractionation and the protease protection assay, respectively. We appreciate Dr. Pawin Ittisamai of photographs in Figure 2.2A. J. W. has been supported by a Royal Thai Government Scholarship. This work was supported in parts by grants to C.B. from the US NSF (MCB 1157231), the US AFOSR (FA9550-11-1-0264), by a Strategic Partnership grant from the MSU Foundation, and by MSU AgBioResearch.

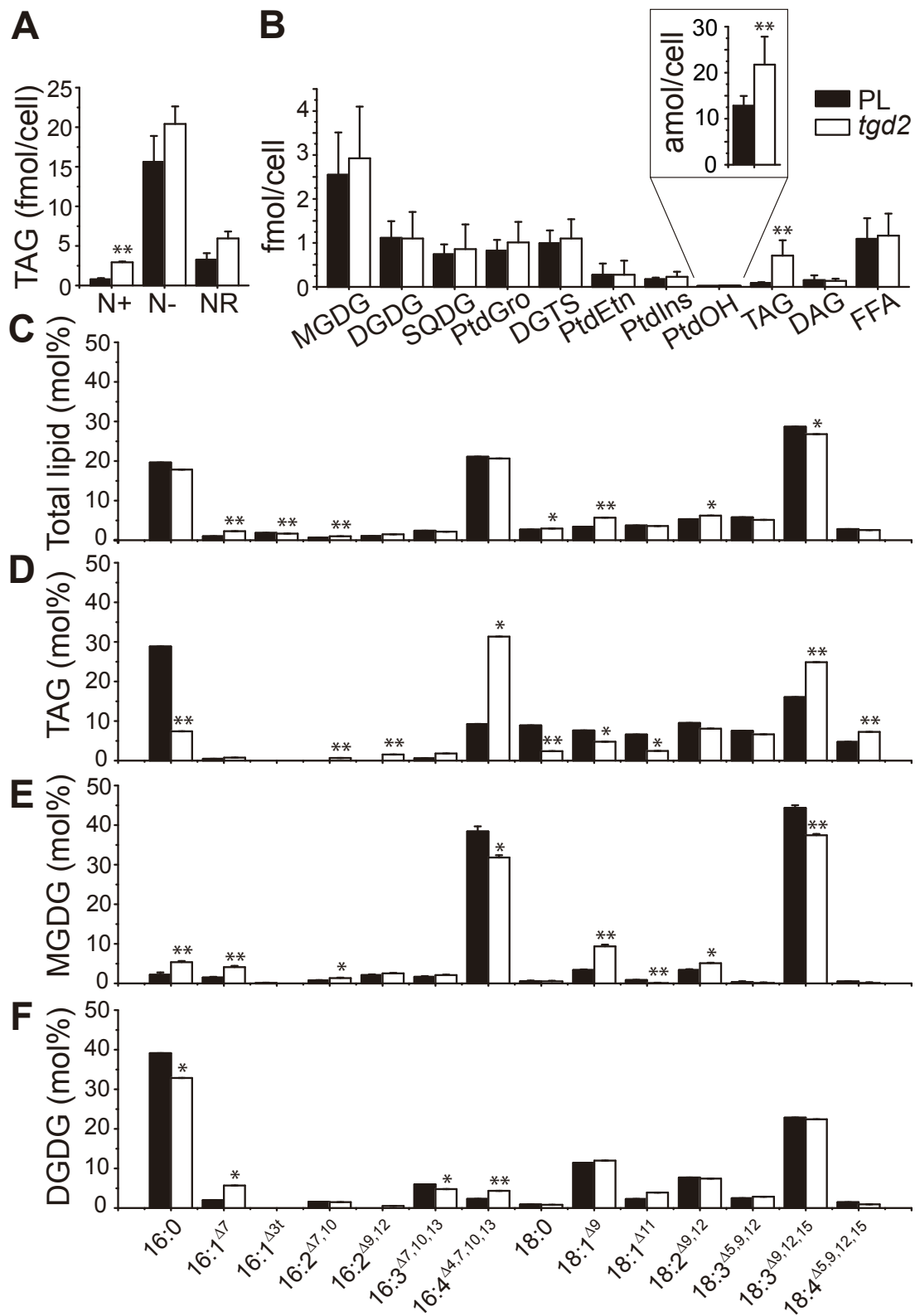


Figure 2.1. Lipid phenotypes of *Chlamydomonas tgd2* mutant.

Figure 2.1. (cont'd)

(A) Triacylglycerol (TAG) concentration in fmol/cell of parental line (dw15.1) PL (solid bars) and *tgd2* (open bars) grown in N-replete medium (N+) until mid-log phase, followed by 48 h of N-deprivation (N-), followed by 24 h of N-resupply (NR). (B) Cellular concentration of lipids of the PL and *tgd2* during mid-log phase grown in N-replete medium in order of presentation: monogalactosyldiacylglycerol, MGDG; digalactosyldiacylglycerol, DGDG; sulfoquinovosyldiacylglycerol, SQDG; phosphatidylglycerol, PtdGro; digalactosyl-*N,N,N*-trimethylhomoserine; DGTS; phosphatidylethanolamine, PtdEtn; phosphatidylinositol, PtdIns; phosphatidic acid, PtdOH; triacylglycerol, TAG; diacylglycerol, DAG; and free fatty acids, FFA. (C) Acyl group profile of total lipids of the PL and *tgd2* during mid-log phase grown in N-replete medium. Standard nomenclature for fatty acids is used and indicated at the bottom axis in (F): number of carbons : number of double bonds with position of double bounds indicated counting from the carboxyl end. (D) Acyl group profile of TAG of the PL and *tgd2* during mid-log phase grown in N-replete medium. (E) Acyl group profile of MGDG of the PL and *tgd2* during mid-log phase grown in N-replete medium. (F) Acyl group profile of DGDG of the PL and *tgd2* during mid-log phase grown in N-replete medium. In all cases, three biological replicates were averaged and standard deviations are shown. Differences in means of PL and *tgd2* were compared with a paired-sample student *t*-test (* p-value ≤ 0.05 , ** p-value ≤ 0.01).

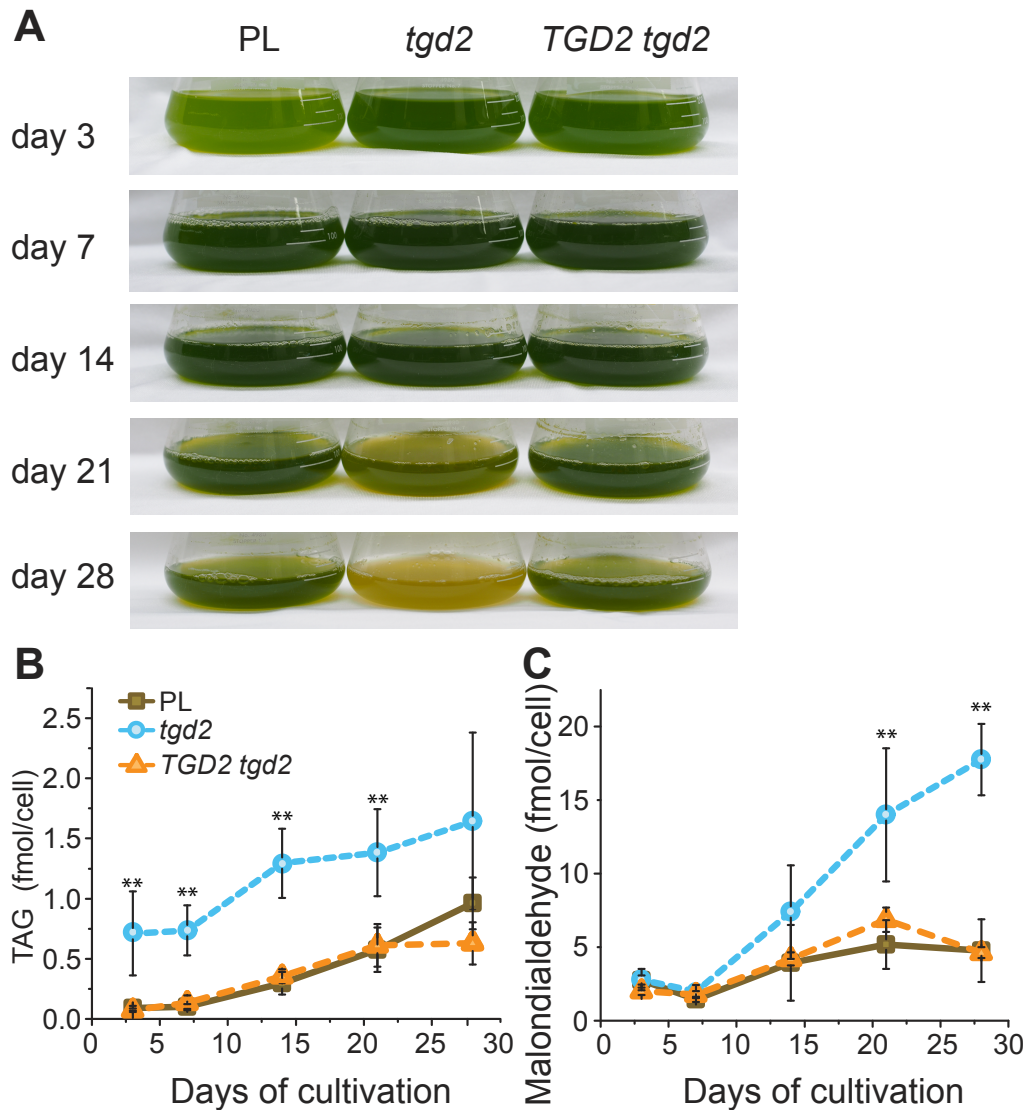


Figure 2.2. Viability assay for the PL (dw15.1), *tgd2* and complemented line *TGD2 tgd2* grown in N-replete medium.

(A) Images of cultures of PL, *tgd2* and *TGD2 tgd2* at days 3, 7, 14, 21 and 28 of cultivation. The culture was inoculated at 0.5×10^6 cells/ml at day 1. (B) Cellular concentration of triacylglycerol (TAG, fmol/cell) of the PL, *tgd2* and *TGD2 tgd2* at days 3, 7, 14, 21 and 28 of cultivation. (C) Cellular concentration of malondialdehyde (fmol/cell) of the PL, *tgd2* and *TGD2 tgd2* at day 3, 7, 14, 21 and 28. In all cases error bars indicate standard deviations based on three replicates. Analysis of variance was performed with Origin Pro 8.0 (** p-value ≤ 0.01).

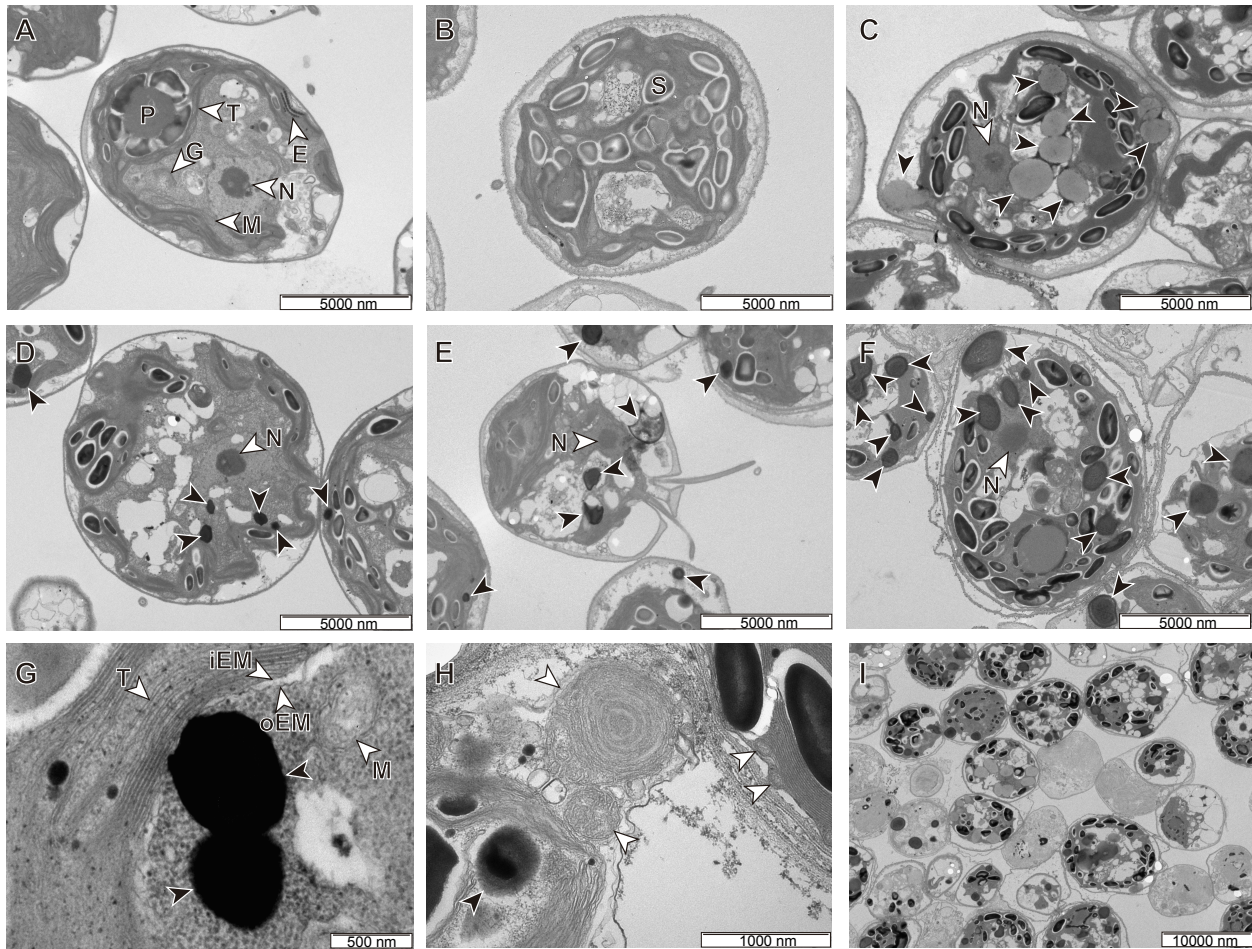


Figure 2.3. Ultrastructural changes in the *tgd2* mutant.

Electron micrographs of the wild-type cw^+ strain (CC-198) and *tgd2* grown in N-replete medium are shown during mid-log phase (day 3), stationary phase (day 10) and late stationary phase (day 17). Black and white arrows indicate lipid droplets and other organelles, respectively. Bars represent size as indicated. (A) Cells of CC-198 during mid-log growth with subcellular structures abbreviated: eyespots, E; Golgi apparatus, G; mitochondria, M; nucleus, N; pyrenoid, P; and thylakoid membrane, T. (B) Cells of CC-198 during stationary phase with starch granules (S). (C) Cells of CC-198 during late stationary phase. (D) Cells of *tgd2* during mid-log phase. (E) Cells of *tgd2* during stationary phase. (F) Cells of *tgd2* during late stationary phase. (G) Representative *tgd2* cell during mid-log phase showing the thylakoid membrane (T), inner envelope membrane (iEM), outer envelope membrane (oEM), mitochondria (M) and electron-dense lipid droplets (black arrows). (H) Representative *tgd2* cell during late stationary phase showing compromised membrane structures (white arrows). (I) Population of *tgd2* cells during late stationary phase showing dead and living cells.

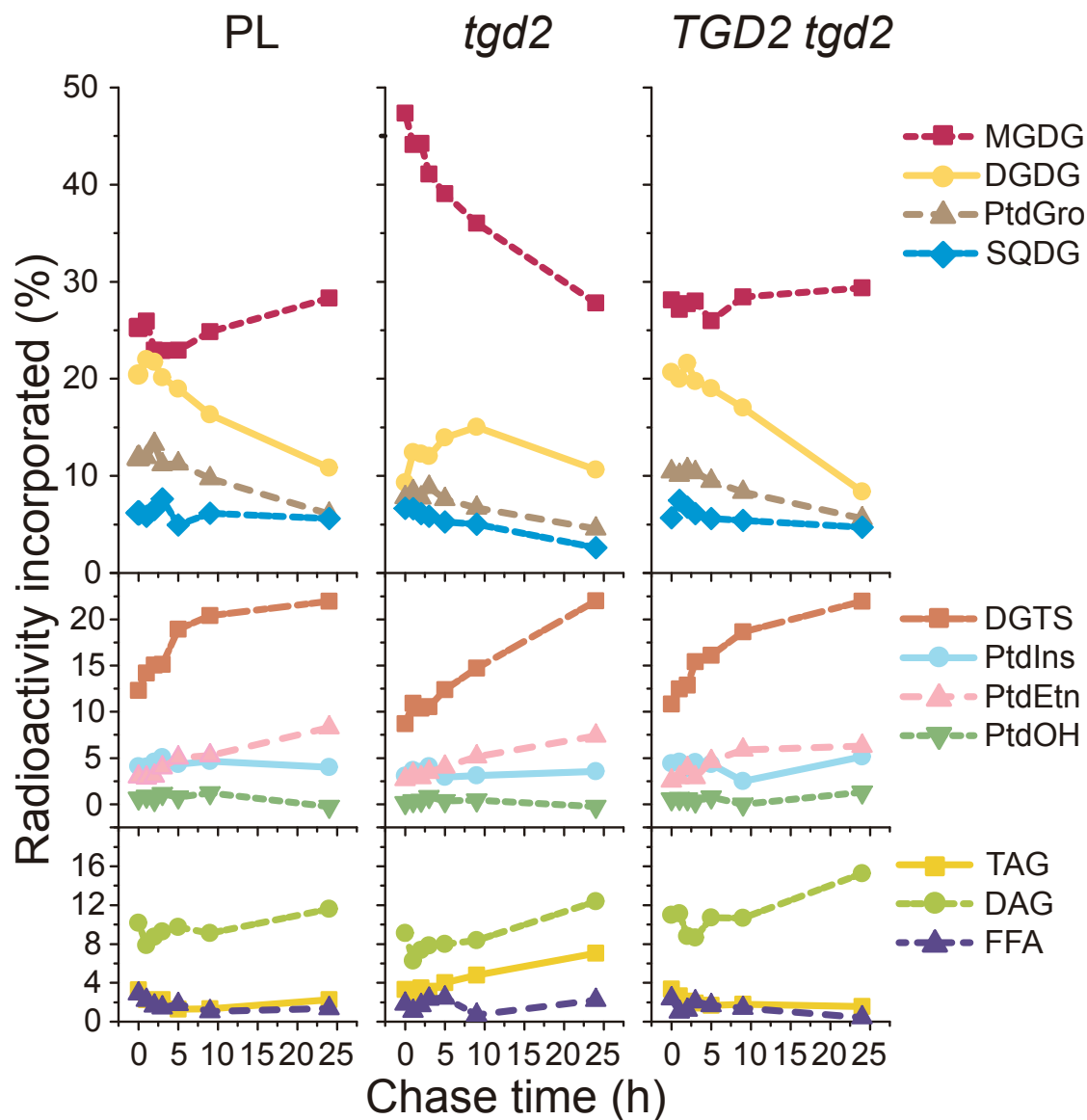


Figure 2.4. $[^{14}\text{C}]$ -Acetate pulse-chase labeling of PL (dw15.1), *tgd2* mutant, and *TGD2 tgd2* complemented line.

Cells were labeled with $[^{14}\text{C}]$ -acetate until 20-40% of label was incorporated (pulse). The chase shown here beginning at time 0 (h) was initiated by changing to unlabeled medium. The fraction of label found in each lipid (%) relative to the total label incorporated in the lipid fraction is shown during the 24 h chase time course. Abbreviations of lipid are as defined in the legend to Figure 2.1. Results from one representative experiment of four are shown.

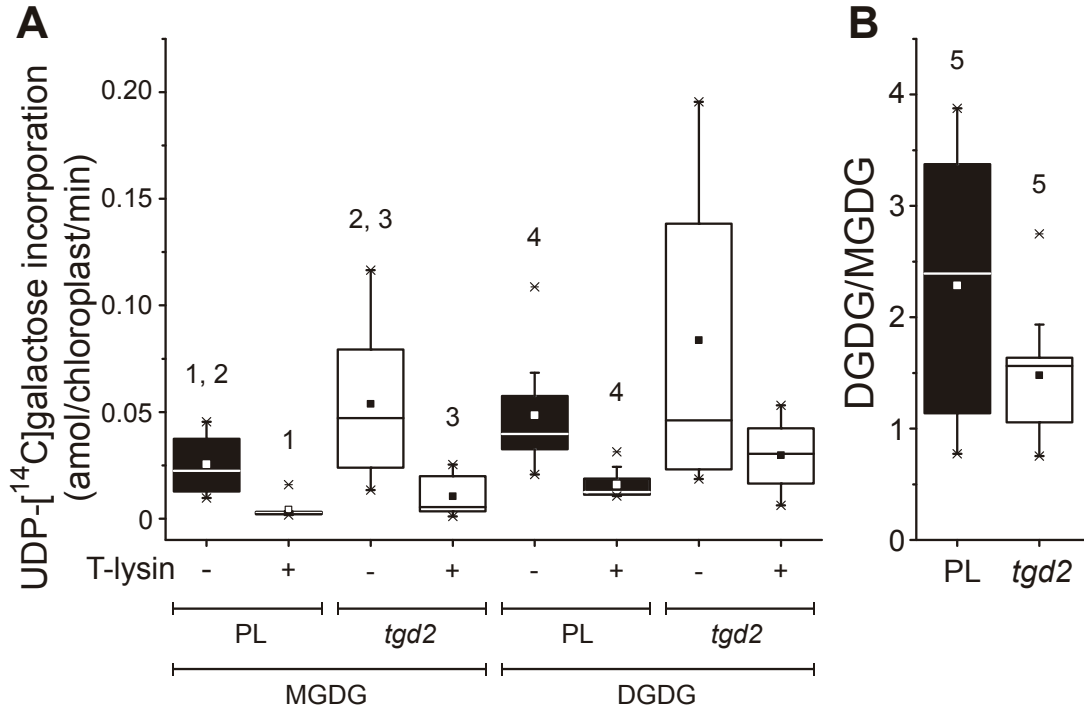


Figure 2.5. Galactoglycerolipid synthesis of PL (15.1) and *tgd2* chloroplasts.

(A) UDP-[¹⁴C]-galactose incorporation into monogalactosyldiacylglycerol (MGDG) and digalactosyldiacylglycerol (DGDG) of PL and *tgd2* chloroplasts. All samples were either not treated with protease (-) or treated (+) with Thermolysin (T-lysin) as indicated. (B) Ratio of labeled DGDG/labeled MGDG from non-protease treated chloroplasts for the PL and the *tgd2* mutant. In each case nine replicates from different experiments were statistically analyzed for each treatment and the results displayed as box plots (solid for PL, open for *tgd2*). A central square within each box plot represents the mean, the line the median. The extreme values are indicated by *. Statistical tests of different means were performed using a paired-sample student *t*-test (*p*-value ≤ 0.05). The following pairs indicated by numbers were significantly different: ¹MGDG PL (-) was significantly higher than MGDG PL (+). ²MGDG PL (-) was significantly lower than MGDG *tgd2* (-). ³MGDG *tgd2* (-) was significantly higher than MGDG *tgd2* (+). ⁴DGDG PL (-) was significantly higher than DGDG PL (+). ⁵DGDG/MGDG PL (-) was significantly higher than DGDG/MGDG *tgd2* (-).

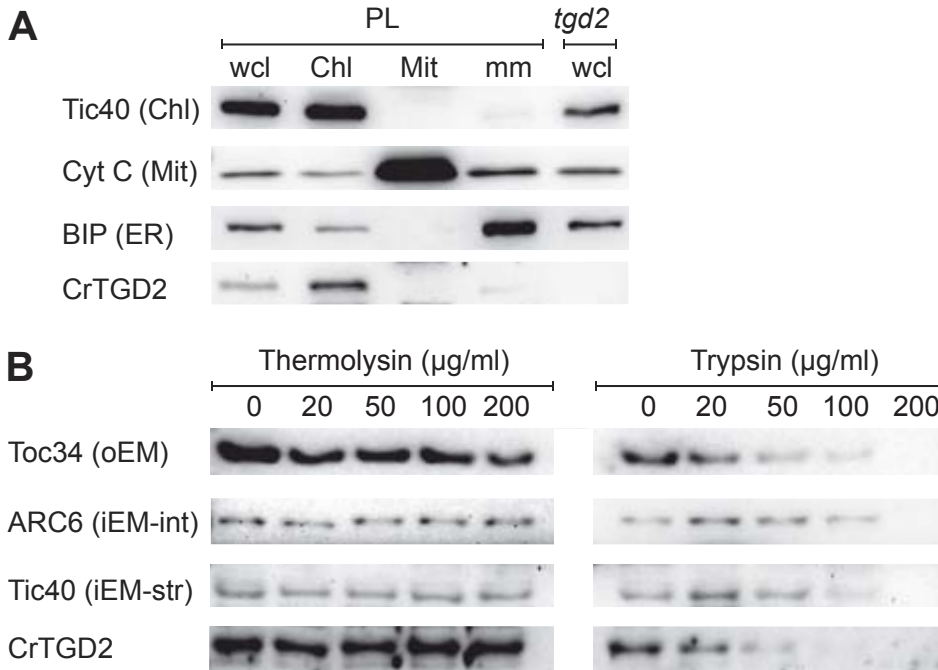


Figure 2.6. Localization of CrTGD2.

(A) Subcellular fractionations of the PL (dw15.1) were compared to whole cell lysates of *tgd2*. Fractions of the PL were as follows: whole cell lysate, wcl; chloroplasts, Chl; mitochondria, Mit; and microsomal membrane, mm. A Western blot is shown. Total protein of each fraction was used to detect Tic40, a chloroplast marker (Chl), cytochrome C (Cyt C), a mitochondrial marker (Mit), BIP, an endoplasmic reticulum (ER) marker, and CrTGD2 using the respective antisera.

(B) Protease treatment of PL chloroplasts to determine envelope membrane association of TGD2. Chloroplasts were treated with various concentrations of Thermolysin or Trypsin as indicated. A western blot is shown detecting Toc34, a chloroplast outer envelope membrane (oEM) marker, ARC6, a chloroplast inner envelope membrane marker facing the intermembrane space (iEM-int), Tic40, a chloroplast inner envelope membrane marker facing the stroma (iEM-str), and CrTGD2.

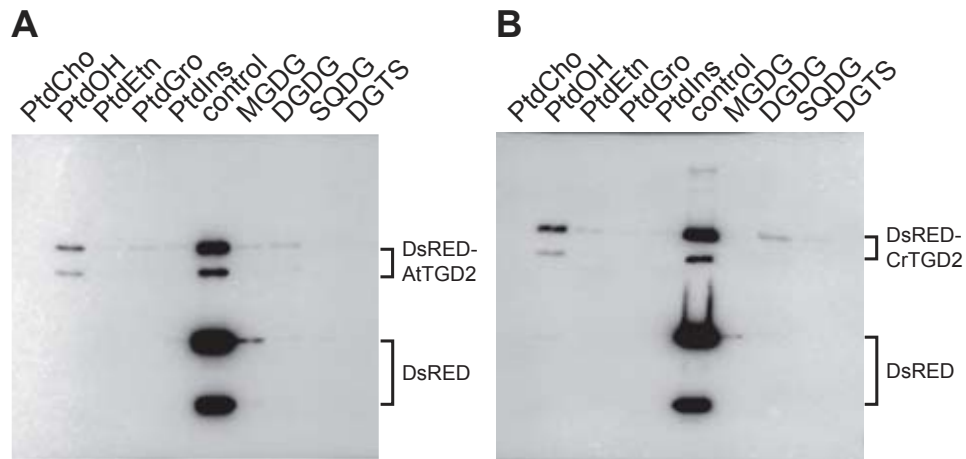


Figure 2.7. Lipid binding assay.

Liposomes made from different lipids as indicated (see legend of Figures 2.1 for lipid abbreviations) were incubated with DsRED-TGD2 recombinant proteins from Arabidopsis (**A**) or Chlamydomonas (**B**). Proteins associated with the liposomes were detected by Western blotting using a His-tag antibody. Each reaction contained DsRED protein as an internal negative control. A control lane containing 10% of the proteins without liposomes used in each assay is shown in the middle of each blot.

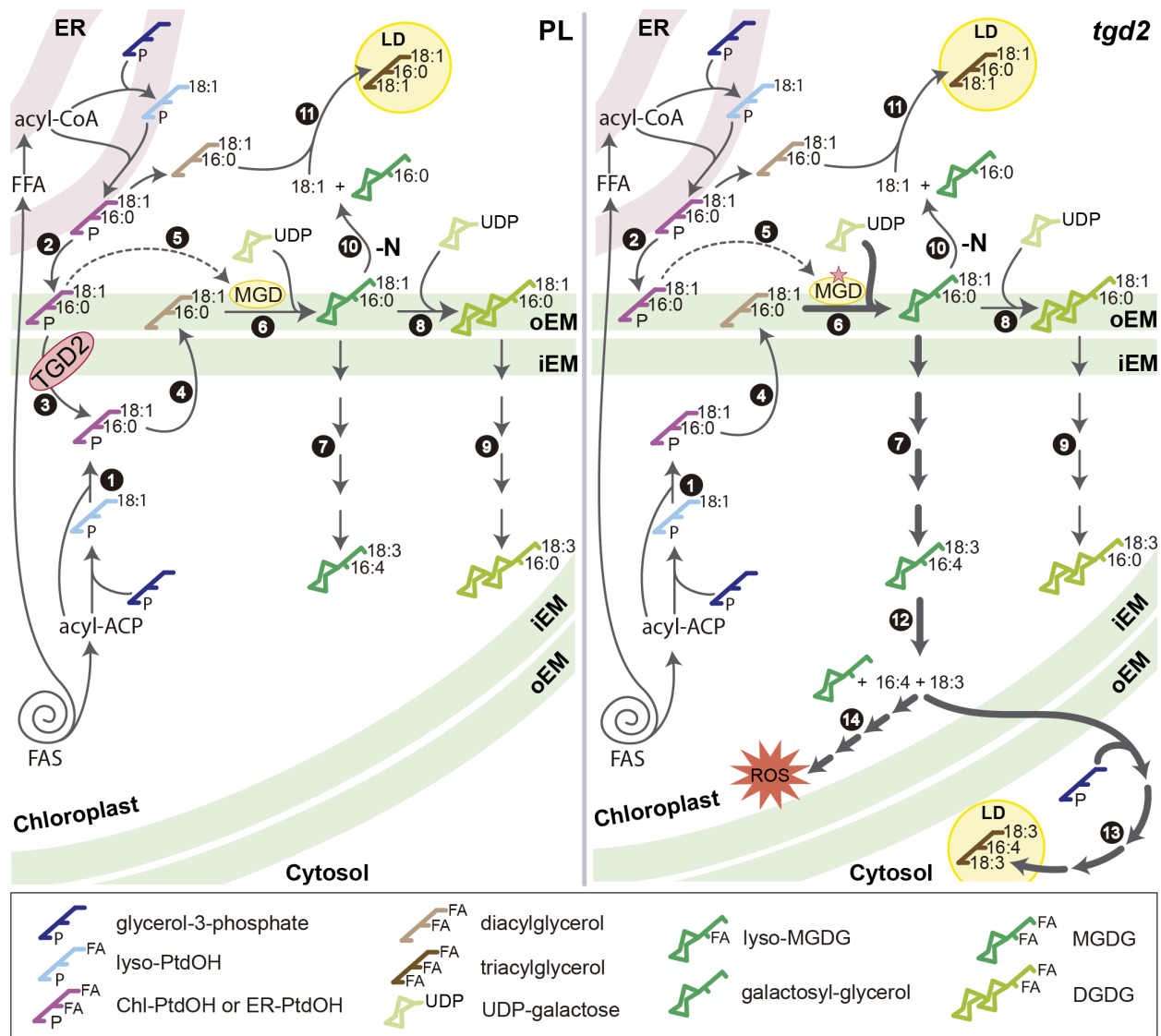


Figure 2.8. Proposed model of CrTGD2 function.

Different steps (as numbered in solid circles) involved in galactoglycerolipid synthesis are shown in the PL (left panel) and in the *tgd2* mutant (right panel). Lipid molecular species symbols are explained in a box below the scheme. Fatty acid synthesis (FAS) takes place in the chloroplast generating acyl groups bound to acyl carrier protein (acyl-ACP) used for the synthesis of chloroplast-derived phosphatidic acid (Chl-PtdOH) (1). Free fatty acids (FFA) are also exported to endoplasmic reticulum (ER) and activated to acyl-CoAs for the synthesis of ER-derived PtdOH (ER-PtdOH), which is then returned to the chloroplast outer envelope membrane (oEM) (2). It is postulated that the two PtdOHs derived from the two different pathways in *Chlamydomonas* cannot be distinguished unlike those produced in plants. TGD2 situated in the

Figure 2.8. (cont'd) chloroplast inner envelope membrane (iEM) transports ER-PtdOH from the oEM to the stroma side of the iEM (Loria *et al.*). PtdOH from both sources can give rise to diacylglycerol (4). On the oEM, PtdOH stimulates MGDG synthase (MGD) (5) to produce MGDG from diacylglycerol and UDP-galactose (6). This newly synthesized MGDG composed of 18:1 and 16:0 acyl chains is a common substrate for three reactions. First, desaturation by MGDG specific desaturases (7) produces mature MGDG with 18:3 and 16:4 acyl chains. Second, DGDG synthesis (8) yields newly synthesized DGDG with 18:1 and 16:0 acyl chains, which then undergoes desaturation (9) resulting in mature DGDG with mainly 18:3 and 16:0 acyl chains. Third, under N deprivation (Villena *et al.*), newly synthesized MGDG is degraded (10) by the action of PLASTID GALACTOGLYCEROLIPID DEGRADATION1 (PGD1). Fatty acids derived from PGD1 degradation is then used for the synthesis of triacylglycerol (11) containing 18:1 and 16:0 acyl chains which is stored in lipid droplets (LD).

In the *tgd2* mutant lacking TGD2, ER-PtdOH accumulates in the oEM and hyper-stimulates MGDG synthase (5) indicated by the star. This results in higher MGDG synthesis (6) indicated as thick arrows. Note that MGDG in the *tgd2* mutant is primarily synthesized from Chl-PtdOH. Under normal growth conditions, desaturation of MGDG is more efficient than degradation by PGD1 or synthesis of DGDG leading to an increased formation of mature MGDG. To avoid an accumulation of mature MGDG it is then degraded by galactolipase(s) (12) yielding 16:4 and 18:3 fatty acids or diacylglycerol with these two acyl groups. These lipid precursors are exported to the cytosol to give rise to triacylglycerol unique to the *tgd2* mutant (13). The additional MGDG molecules produced or fatty acids derived from them can also be substrates for lipid peroxidation (14) resulting in the accumulation of reactive oxygen species (ROS), presumably causing lower viability of the *tgd2* mutant.

APPENDICES

APPENDIX A. SUPPORTING FIGURES

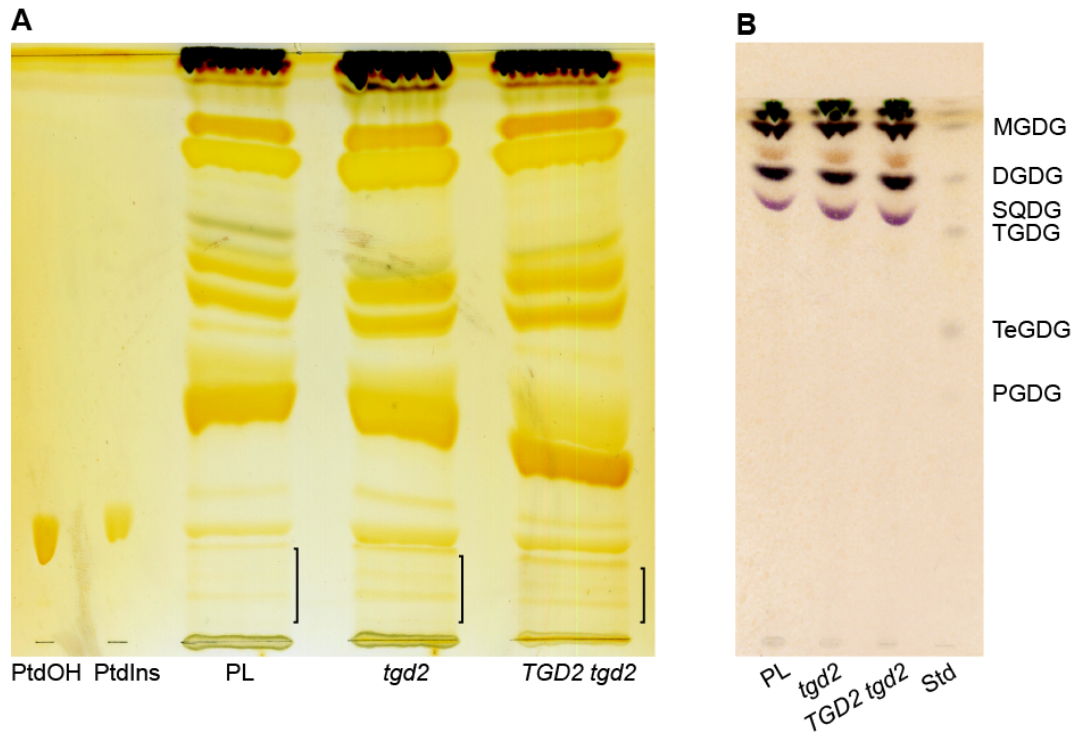


Figure 2.S1. Separation of Phosphatidic acid (PtdOH) and oligogalactoglycerolipids by thin layer chromatography (TLC).

(A) Lipids from the PL (dw15.1), the *tgd2* mutant, and the *TGD2 tgd2* complemented line were separated by TLC and stained with iodine vapor. PtdOH and phosphatidylinositol (PtdIns) standards were loaded on the left of the plate to indicate positions of the lipids. Brackets indicate the areas from which silica containing PtdOH was isolated and used for quantification of PtdOH by gas chromatography in Figure 2.1B. The number of cells used for lipid loading of each lane was not equal. (B) Lipids from the same cell lines as in (A) were separated by TLC and stained with α -naphthol. A lipid extract from *E. coli* producing galactoglycerolipids was included as standard (Std) containing MGDG, DGDG, trigalactosyldiacylglycerol (TGDG), tetragalactosyldiacylglycerol (TeGDG), and pentagalactosyldiacylglycerol (PGDG).

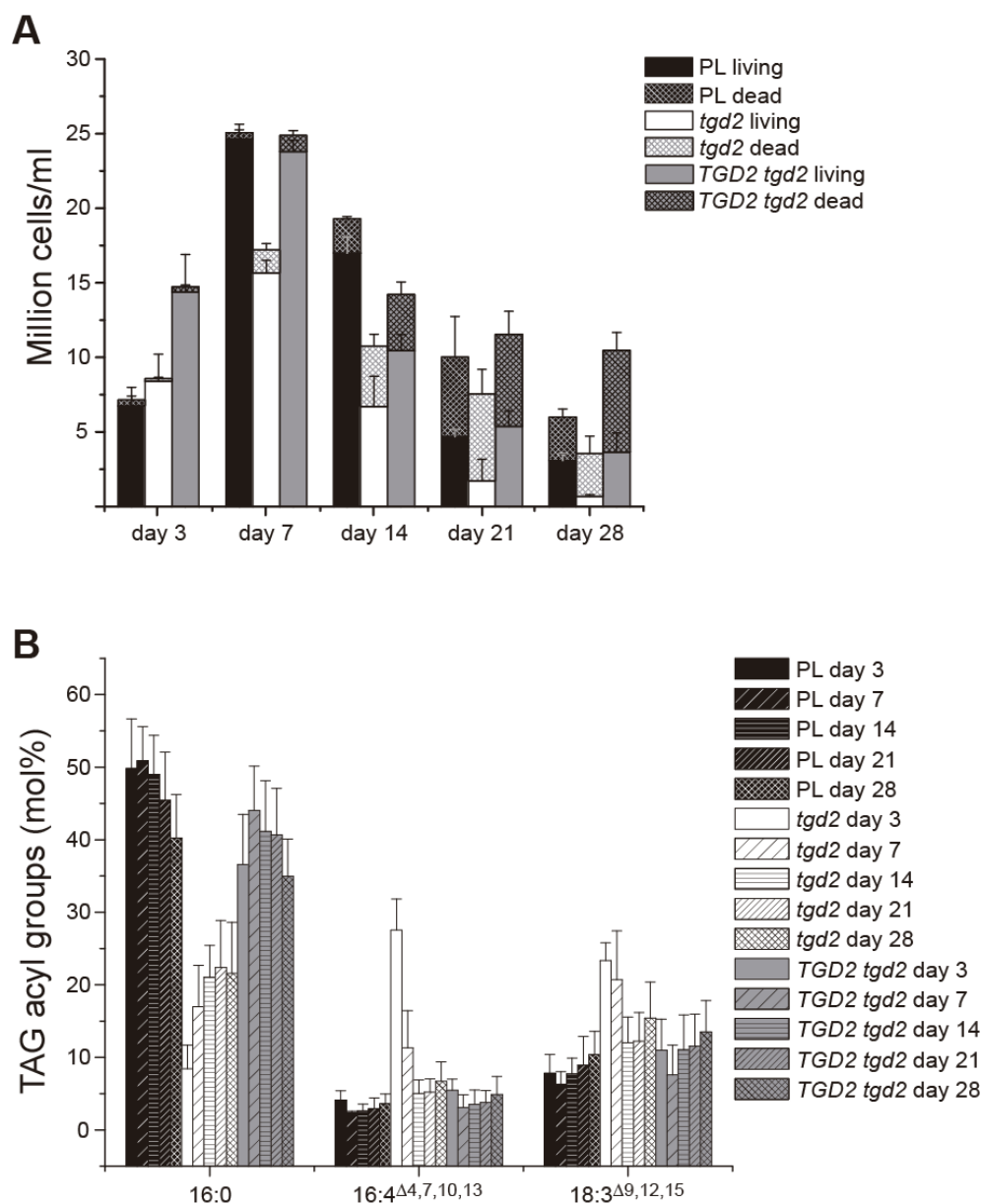


Figure 2.S2. Cell viability and acyl group composition of TAGs during extended culturing time.

(A) Numbers of living and dead cells of the PL (dw15.1), the *tgd2* mutant, and the *TGD2 tgd2* complemented line kept in N-replete medium for 3, 7, 14, 21 and 28 days. The cells were stained with methylene blue and phenosafranin to distinguish living and dead cells. Cells were counted with a hemocytometer. (B) TAG acyl group profile of the PL (dw15.1), the *tgd2* mutant, and the *TGD2 tgd2* complemented line kept in N-replete medium for 3, 7, 14, 21 and 28 days. Three biological replicates were averaged and standard deviations are shown.

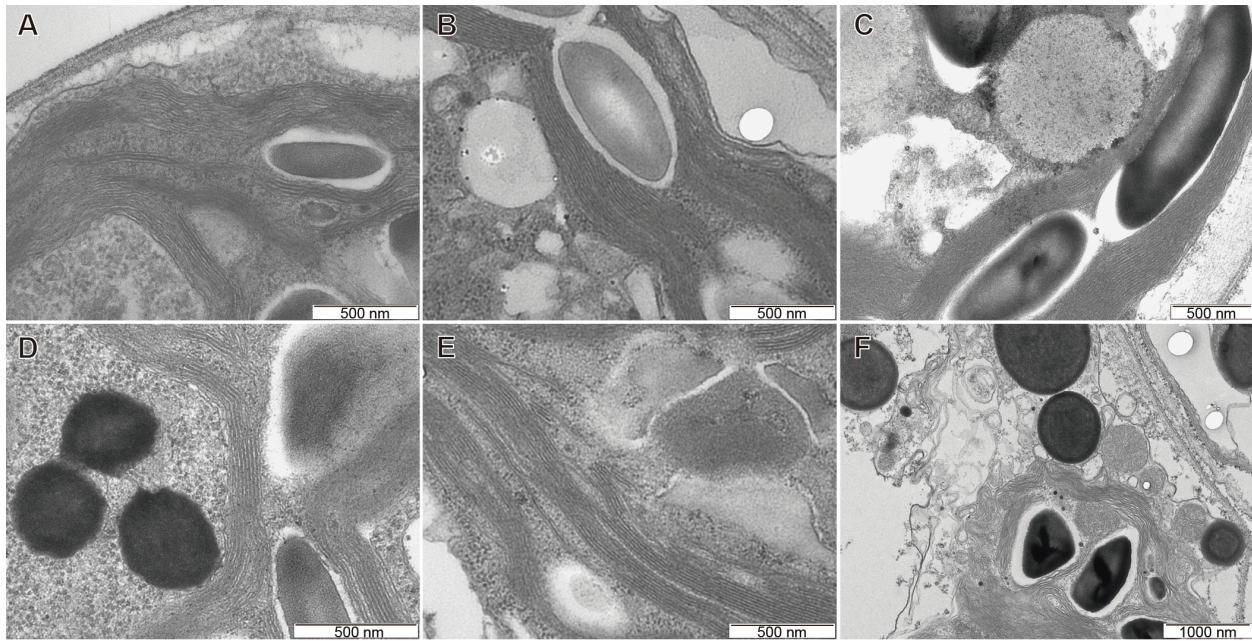


Figure 2.S3. Ultrastructure of chloroplast membranes

Electron micrographs of chloroplast membranes of the wild-type cw^+ strain (CC-198) and *tgd2* grown in N-replete medium are shown during mid-log phase (day 3), stationary phase (day 10) and late stationary phase (day 17). (A) Chloroplast membranes of a representative CC-198 cell during mid-log phase. (B) Chloroplast membranes of a representative CC-198 cell during stationary phase. (C) Chloroplast membranes of a representative CC-198 cell during late stationary phase. (D) Chloroplast membranes of a representative *tgd2* during mid-log phase. (E) Chloroplast membranes of a representative *tgd2* cell during stationary phase. (F) Chloroplast membranes of a representative *tgd2* cell during late stationary phase.

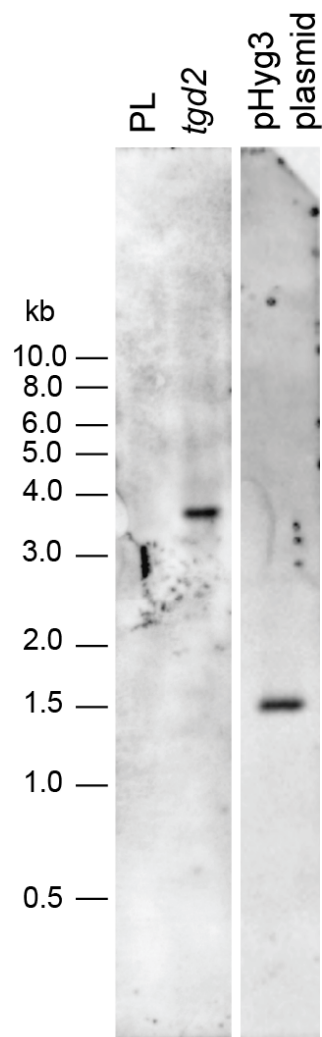


Figure 2.S4. Southern blot analysis of the *tgd2* mutant and the PL (dw15.1).

Genomic DNA was restriction digested with *Bam*HI. Linearized pHyg3 plasmid was used as a control. The probe was complementary to a fragment from the pHyg3 plasmid (see Methods). A line between *tgd2* and pHyg3 plasmid indicates different exposure times of the same blot.

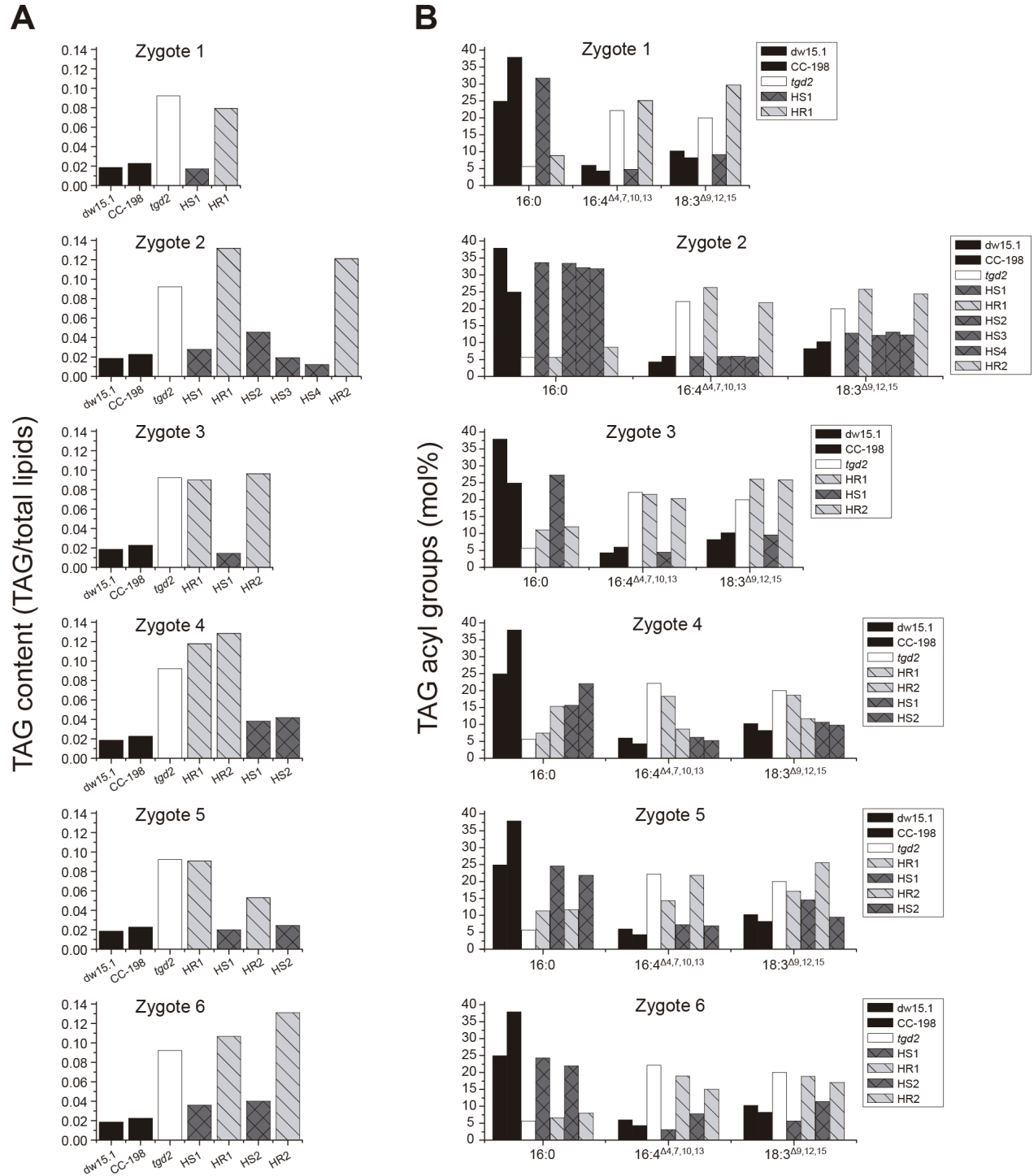


Figure 2.S5. (cont'd)

(A) TAG content of the PLs (dw15.1) and (CC-198), the original *tgd2* mutant in the dw15.1 background, and progenies from 6 zygotes with HS indicating Hygromycin B-sensitive and HR Hygromycin B-resistant progenies. (B) TAG acyl group profiles of the same lines as described under (A).

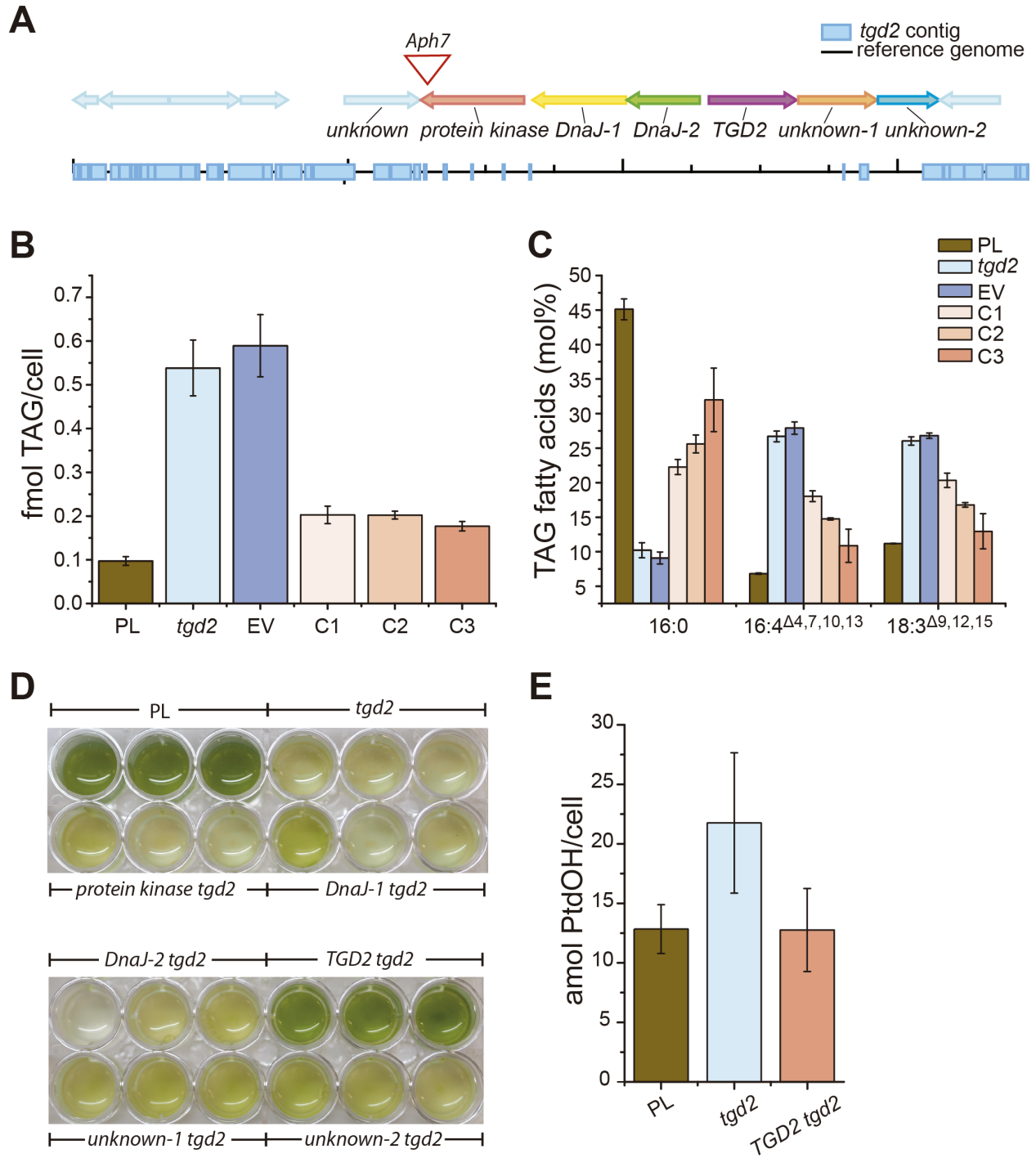


Figure 2.S6. Mutant locus in the *tg2* genome and complementation.

Figure 2.S6. (cont'd)

(A) Alignment of *tgd2* assembled contigs with chromosome 16 of the *Chlamydomonas* reference genome (v5.3). The *AphVII* gene insertion, affected genes and their annotation are shown. (B) Cellular TAG concentrations of parental line (PL, dw15.1), *tgd2* mutant, *CrTGD2* complemented lines (C1-C3) and empty vector control (EV). (c) TAG acyl groups (16:0, 16:4 and 18:3) of the same lines as described under (B). (B, C) Three replicates were averaged and standard deviations are shown. (D) Cultures (30 day-old) of the PL (dw15.1), the *tgd2* mutant and transgenic lines into which the six deleted genes were individually introduced into the *tgd2* mutant. Three independent lines per gene introduced are shown. (E) Cellular PtdOH concentrations of the PL, the *tgd2* mutant and *CrTGD2* complemented lines (*TGD2 tgd2*, C3).

AtTGD2	MIGNPVIQVP	SSLMPSSSMI	ACPRVSPNGV	PYLPPKPRTR	HLVVRAASNS
CrTGD2MVIHASASQ
AtTGD2	DAAHGQPSSD	GGKNPLTVVL	DVPRNIWRQT	LKPLSDFGFG	KRSIWEGGVG
CrTGD2	GDAESQPGFK	QG.....LFGSI	AKSLSDYGIG	KKSLWEGGVG
Transmembrane Domain					
AtTGD2	LFI VSGATLL	ALSWAWLRGF	QMRSKFRKYQ	TVFELSHASG	ICTGTPVRIR
CrTGD2	LFVLAGGGAA	VALVAWARGN	ALRTG.TPYQ	ATIEFPLACG	IQIGTPVRIR
Mammalian Cell Entry Domain					
AtTGD2	GVTVGTIIRV	NPSLKNIEAV	AEIEDDKIII	PRNSLVEVNQ	SGLLMETMID
CrTGD2	GVQVGQVLAV	KPSLERVDVL	VEVNDVSTVI	PRNSVIEANQ	SGLIAEPLVD
AtTGD2	IMPRNPIPEP	SVGPLHPECG	KEGLIVCDRQ	TIKGVQGVSL	DELVGIFTRI
CrTGD2	ITPQVPVPDY	RALPHEPRCQ	DESLIVCSNG	HIQGRQGVAL	DDLVIYIMTRL
AtTGD2	GREVEAIGVA	NTYSLAERAA	SVIEEARPLL	KKIQA MAEDA	QPLLSEFRDS
CrTGD2	ARQAENDGVD	KVFAAAESAT	QLMEKAAPLV	SSAAELVEQL	TPLMAELRGG
AtTGD2	GLLKEVECLT	RSLTQASDDL	RKVNSSIMTP	ENTE LIQKSI	YTLVYTLKNV
CrTGD2	GLVGNIEALT	RTAADAAADI	RRLQGSVLTE	DNVRALRQAV	LTLCKTLDHV
AtTGD2	ESISSDILGF	TGDEATRKNL	KLLIKLSRL	L..	
CrTGD2	ESISADVSIL	ARDSGVQRNL	KTLVQALSRL	LDD	

Figure 2.S7. Amino acid sequence alignment of AtTGD2 and CrTGD2.

The alignment shows transmembrane and Mammalian Cell Entry (MCE) domains. The alignment was carried out with MUSCLE (3.8).

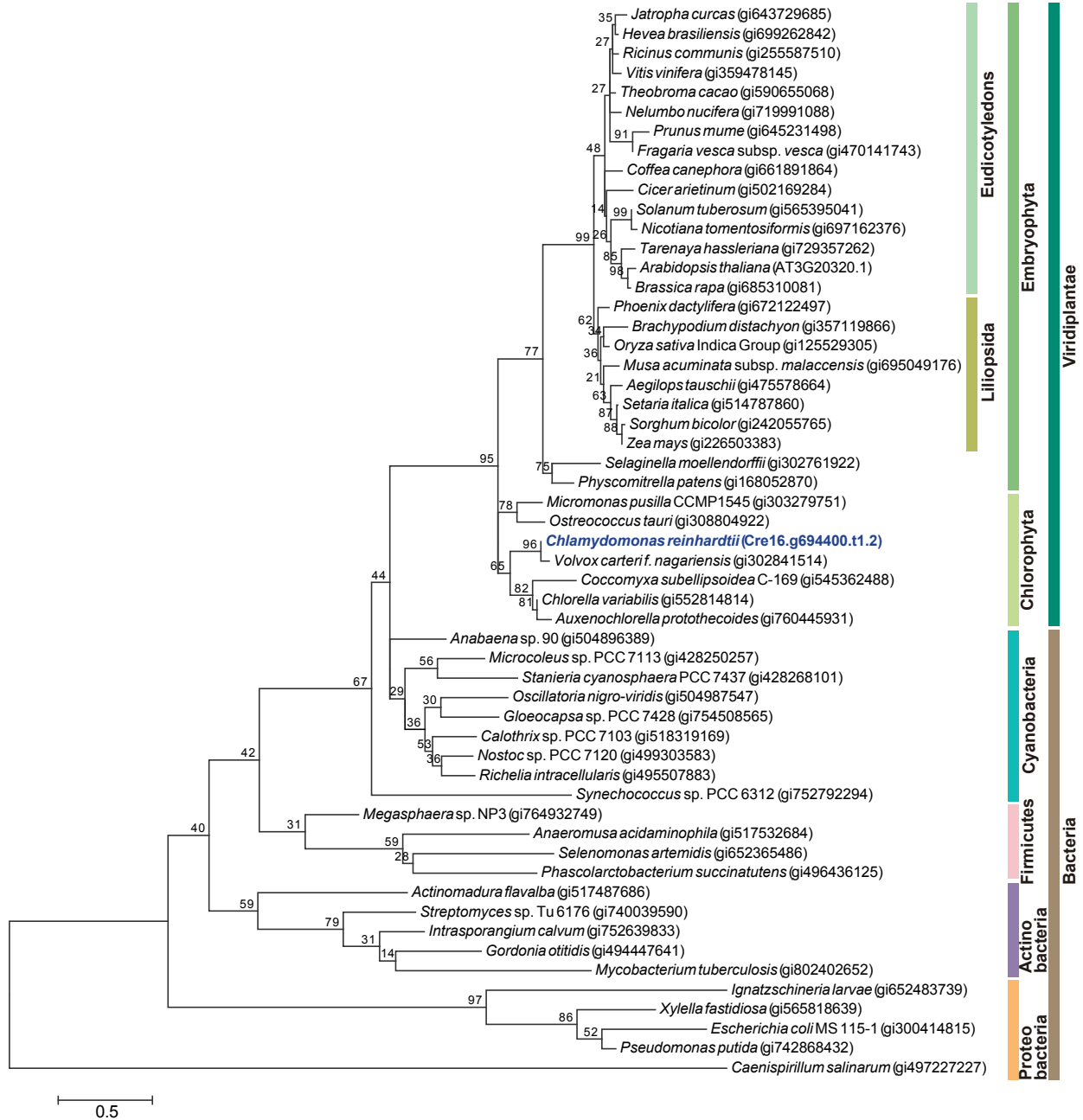


Figure 2.S8. Phylogenetic analysis of CrTGD2 homologues.

Figure 2.S8. (cont'd)

The evolutionary history was inferred based on Maximum Likelihood. The tree with the highest log likelihood (-4302.1023) is shown. The percentage of trees in which the associated taxa clustered together (1000 repeats) is shown above the branches. The tree is drawn to scale, with branch lengths corresponding to the number of substitutions per site. The accession number for each protein is given in the parenthesis following the scientific name. Accession numbers for *Chlamydomonas*, *Arabidopsis* and other organisms are from the Joint Genome Institute (JGI), the Arabidopsis Information Resource (TAIR), and National Center for Biotechnology Information (NCBI), respectively. Groups of organisms are shown as colored bars.

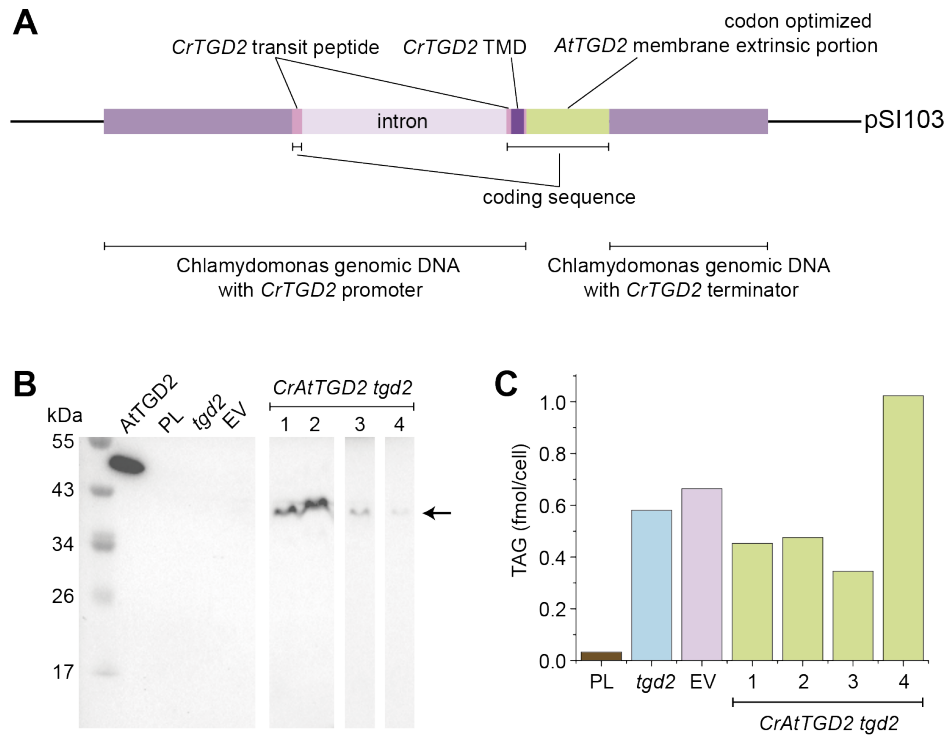


Figure 2.S9. Lack of Arabidopsis TGD2 complementation in Chlamydomonas *tgd2* mutant.

(A) *CrAtTGD2*-pSI103 construct. Genomic DNA of Chlamydomonas *TGD2* (*CrTGD2*) containing promoter region, intron, transit peptide and transmembrane domain (TMD) was assembled with codon optimized Arabidopsis *TGD2* (*AtTGD2*) membrane extrinsic portion, followed by Chlamydomonas genomic DNA containing the terminator of *CrTGD2*. The assembled sequence was cloned into pSI103-AphVIII containing the *AphVIII* Paromomycin resistance gene. (B) Western blot analysis of CrAtTGD2 protein expression in the *tgd2* mutant background (*AtTGD2 tgd2*). Arabidopsis TGD2 recombinant protein (AtTGD2) was used as a positive control. White lines separate irrelevant lanes removed from the blot. (C) TAG concentration (fmol/cell) of the PL, the *tgd2* mutant, the empty vector control in *tgd2* mutant background (EV), and *AtTGD2 tgd2* line 1-4.

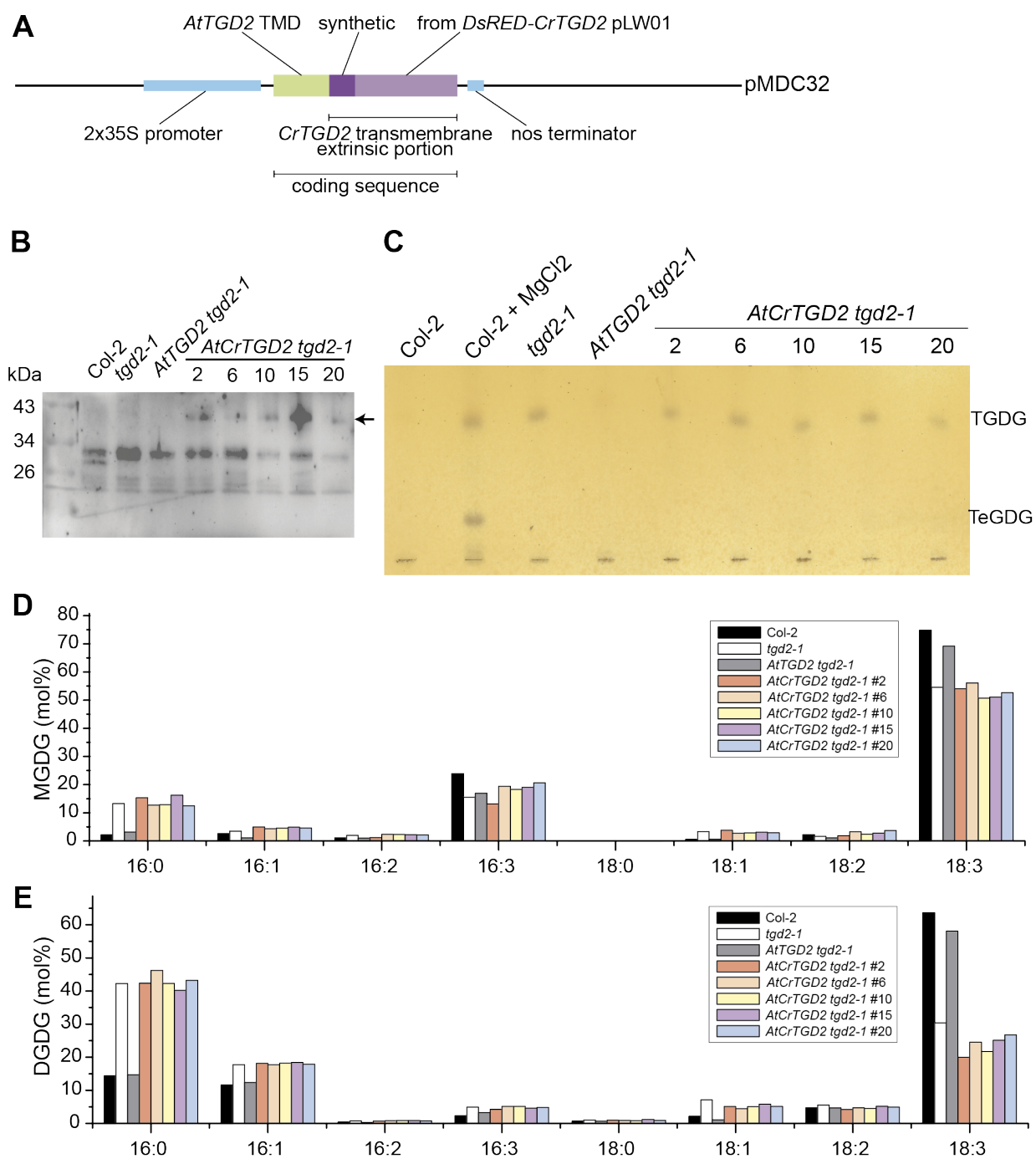


Figure S10. Lack of Chlamydomonas TGD2 complementation in Arabidopsis *tgd2* mutant.

Figure S10. (cont'd)

(A) *AtCrTGD2*-pMDC32 construct. Genomic DNA of Arabidopsis *TGD2* (*AtTGD2*) containing transit peptide and transmembrane domain (TMD) was assembled with *Chlamydomonas TGD2* (*CrTGD2*) transmembrane extrinsic portion. The assembled sequence was cloned into pMDC32 containing 2x35S promoter and nos terminator. (B) Western blot analysis of *AtCrTGD2* fusion protein expression in the Arabidopsis *tgd2* mutant background (*AtCrTGD2 tgd2*) line 2, 6, 10, 15 and 20 compared to Col-2, *tgd2-1* and the *AtTGD2* cDNA complemented line (*AtTGD2 tgd2-1*). (C) TLC plate separating oligogalactoglycerolipids shows trigalactosyldiacylglycerol (TGDG) and tetragalactosyldiacylglycerol (TeGDG) of Arabidopsis lines as shown in (B). (D) Acyl group composition of monogalactosyldiacylglycerol (MGDG) of lines in (B). (E) Acyl group composition of digalactosyldiacylglycerol (DGDG) of lines in (B).

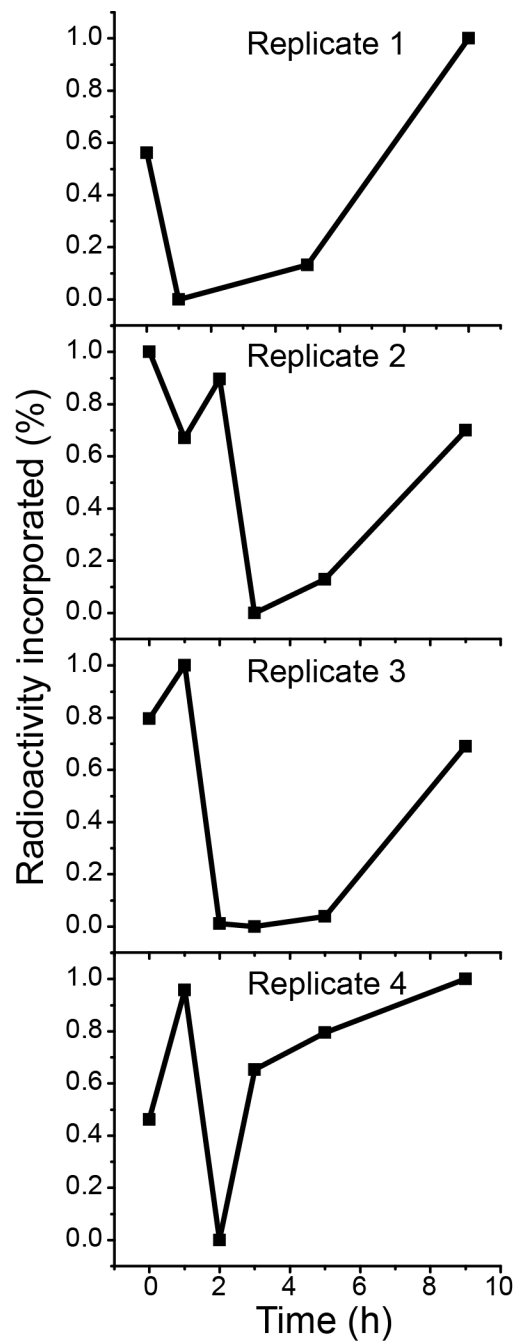


Figure 2.S11. Pulse chase [^{14}C]-acetate labeling of MGDG in the PL (dw15.1).

Replicates from four independent experiments during a 0-9 h chase are shown. The highest radioactivity incorporations were set as 1, while the lowest were set as 0.

APPENDIX B. SUPPORTING TABLES

Table 2.S1. Bacterial Artificial Chromosomes (BACs) used in the *tgd2* complementation analysis.

Corresponding BAC identifiers from the Joint Genome Institute (JGI) and from the Clemson University Genomics Institute (CUGI) are shown. Restriction endonucleases used for isolating genomic DNA fragments containing individual genes and corresponding product sizes are shown. The amount of genomic DNA and that of the *AphVIII* gene used for transformation as well as names of primers used for testing the insertion are listed. The primer sequences are given in Table 2.S2.

Phytozome, (V5.3) Number	JGI number	CUGI number	Restriction endonuclease	Product size (kb)	Amount of DNA used		Testing primers
					DNA from BAC (µg)	<i>AphVIII</i> from pSI103 (ng)	
Cre16.g694550	PTQ2066	6C14	<i>DraI</i> and <i>XhoI</i>	9.5	1.6	34.8	ch16-1, ch16-4, ch16-8 and ch16-14
Cre16.g694500	PTQ2066	6C14	<i>SnaBI</i> , <i>RsrII</i> and <i>EcoRI</i>	9.9	1.5	30.0	ch16-16, ch16-20 and ch16-21
Cre16.g694450	PTQ12548	33H17	<i>DraIII</i> and <i>KpnI</i>	8.0	0.5	11.0	ch16-21, ch16-22, ch16-25 and ch16- 26
Cre16.g694400	PTQ12548	33H17	<i>ApoI</i> , <i>MscI</i> and <i>MluI</i>	8.1	1.0	25.0	ch16-29, ch16-32, TGD2_5' and TGD2_3'
g15584	PTQ12548	33H17	<i>ApaI</i> , <i>Bsu36I</i> and <i>SfiI</i>	7.5	1.0	25.0	ch16-32 and ch16- 33
g15585	PTQ12548	33H17	<i>DraIII</i> , <i>ZraI</i> and <i>NcoI</i>	6.5	0.5	25.0	ch16-37, ch16-38 and ch16-40

Table 2.S2. Sequences of primers for probing the deletion in chromosome 16 of the *td2* mutant.

Gene/ primer names	Forward primer sequence (5'-3')	Reverse primer sequence (5'-3')	Covered region on chromosome 16	
			From	To
Hygromycin	ACTTCGAGGTGTTTCGAGGAG AC	GCTGCAAGGCGATTAAGTTGGG	N/A	N/A
ch16-1	GATTAACGGTGCCTGATG	GGAAGTAGCGTGATGATG	230406	231550
ch16-2	CGACACATGGCGCTTGAT	CGATTGGCCAGTATTCGT	231416	232578
ch16-3	CCGCACCTTGCCAATCT	AGCGATGGCCGATGTCA	232058	233209
ch16-4	ATAGCAGTCCGCGAGTG	ACGTGTGCTTGGTAATGG	233056	234297
ch16-5	GCGTGCAACCAACTAGTA	CAACATCACCACCACAAC	234095	235303
ch16-7	ACACCTACCTGGAATTCG	CGTACACGCGCAATAA	236170	237339
ch16-8	GCACCTATCCGCACCTTATT	TGTCCGGTGTTCAGTC	237309	238693
ch16-9	GCTGAGTATGCAGCTTCCA	GTGCGAACCGTGAAGACA	225080	226389
ch16-14	GGCTCAGCTGTTCTTGTC	CCATTGGTCCAGTGTCTA	238609	239330
ch16-15	CGGCTGCTTAACTCGTTG	GCAGGTGGAGGTGTTCA	239168	240594
ch16-16	GTTGTAGCTCAGGCTGTA	CTGGAGCGACTTCAACT	240227	241327
ch16-18	GCTGCTGCTGCTACTTCT	GCAGCATGTGTCGTTATCG	242251	243390
ch16-20	GTGTCGTACGCTCCTTGA	CAGCAGCCTCGGTTGACTA	244128	245414
ch16-21	GTTACGCTCAGCTTGTCTGTT	AATGTCATGCGGCCTTG	245224	246297
ch16-22	CGACCAGACTACCACTTA	GCAGGAGGAGGTTGATGT	246223	247360
ch16-23	GCAGCTGTTGCAGTTCTT	CGATTGGAGCACGAGCTA	247377	248719
ch16-24	TAGCTCGTGTCCAATCGT	TGTCGCATCGTGTCTTGA	248702	249668
ch16-25	CTCGCTGCCAAGTACCAT	GCGTCTGAGTCAGCTTGTAG	249183	250444
ch16-26	GCGTTACCGCTGTGTAAGG	GCAGGCGGTTAAGCGAA	250253	251488
ch16-29	TCAAGCAGTGGTGGTAGTG	ACGGTGAAGTCCGTGAT	253446	254368
ch16-32	CCTTGCCGTCTCTGTTGTT	CAGTGCCTGGTACTTGCTA	256655	257724
ch16-33	GGTGCCATGTGAGGAACGAT	AGGTGCGTCACCGACTTGT	258158	259348
ch16-34	GCATCGCATCGCATAAC	CCAGGTCCTCACTCCACTT	259233	260470
ch16-37	GTGGAGAACGGAGTGAGTA	GTGGACCGACATCGCATT	263345	264599
ch16-38	CGCGTCTGTCTTAAGAT	TGCGGTAGGTGGCCTAATA	264324	265679
ch16-40	GGCGTTGCCAACCTCTT	CTCCGCTGCGATGTTA	267314	268421
ch16-43	CGCGCAGTATGTACGGTT	CCATCAGGCACCGTTAATCC	229674	230424
ch16-44	CGGCATTGCGCCTTACAAGA	TGCGGAGTGTGGACATAGTG	230638	231246
ch16-45	GCGGCGGCTTATTATT	ACATGGCGGTCTATCT	265814	266436
ch16-46	CGGCATTGCGCCTTACAAGA	ATGCGGCTTAGGCGGAATAC	230638	231091
ch16-47	CGACCACCGTCATATAGT	CGGTAGTCAGCGCATT	230779	231072
ch16-48	GGCATTGCGCCTTACAAGA	TGCTGTGCCAGTATGCTTC	230639	230975
ch16-49	GCTGCCGTGGCTGAGTATT	GACCTCGGCTGTGTCTGTAA	230237	230554
TGD2_3'	CATGCCTGACGGTGAATCCT	GTAGCACGGTGAAGCTCTGT	251097	251804
TGD2_5'	GTCCATGTGAGGAACGATT	TGTCGAGGACGGAGTTACAA	258159	258814

Table 2.S3. Sequences of primers used for constructing plasmids as indicated.

Plasmids	Purpose	Forward (5'-3')	Reverse (5'-3')
<i>DsRED-CrTGD2</i> pLW01	<i>CrTGD2</i> cloning	ATGGTCATCCACGCCAGCG	TCAGTCGTCCAGCAGCCTG
<i>DsRED-CrTGD2</i> pLW01	<i>CrTGD2</i> amplification for <i>DsRED-CrTGD2</i> pLW01	CAGGATCCGCTCGCGGCAAC GCGCT	TGGTCGACGAGTCGTCCAGCA GCCTGCTG
<i>CrAtTGD2</i> pSI103	<i>AtTGD2</i> amplification	TGGTGGCGTGGGCTCGCGAAT TCGGCTTCCAGATGCGGAGCA AGTTCCGCAAGTACCAA	AAGCTTTCAGAGCAGGCCGGA CAGGCTCTTGATCAGCAGCTTC AGGTTCTTGCGGGTGGC
<i>CrAtTGD2</i> pSI103	Amplification of <i>CrTGD2</i> containing promoter and transmembrane domain	TCAGGCTGCGCAACTGTTGGG AAGGGCGATCGGTGCGGGCG TTCAGGGGTTTCGAGGGT	CTCCGCATCTGGAAGCCGAAT TCGCGAGCCCACGCCACCAGC GCCACCGCCGCGCCGCCG
<i>CrAtTGD2</i> pSI103	pSI103 amplification	GCCCCACCGATCGCCCTTCC CAACAGTTGCGCAGCCTGAAT GGCGAATGGGACGCGCCC	TGGCGGCCGCTCTAGAACTAG TGGATCCCCCGGGCTGCAGGA CGGCGGGGAGCTCGCTGA
<i>CrAtTGD2</i> pSI103	Amplification of <i>CrTGD2</i> containing terminator	GCTGCTGATCAAGAGCCTGTC GCGCCTGCTCTGAAAGCTTGG CGCGCGAGGGGCGAGGAG	CTGCAGCCCCGGGGATCCACT AGTTCTAGAGCGGCCGCCAAG TGCGCCACGCCGCCACGC
<i>AtCrTGD2</i> pDONR221	Amplifying pDONR221	GATGCTGCCAACTTAGTC	GCTGGATACGACGATTCC
<i>AtCrTGD2</i> pDONR221	Amplifying <i>AtTGD2</i> Annealing synthesis portion of <i>CrTGD2</i> and pDONR	GCAGCGCGTTACCTCGCAAC CAAGCCCA	ACGGAATCGTCGTATCCAGC ATGATTGGGAATCCAGTAATT CAAGTCC
<i>AtCrTGD2</i> pDONR221	Amplifying <i>CrTGD2</i> synthetic, overlapping <i>AtTGD2</i> and <i>CrTGD2</i> from <i>DsRED</i>	GTTGCGAGGTAACGCGCTGC GCACCGGC	CCGTGGACACGTCGTTACCT CCACCAGCACGTC
<i>AtCrTGD2</i> pDONR221	Amplifying <i>CrTGD2</i> from <i>DsRED</i> , overlapping <i>CrTGD2</i> synthetic and pDONR	GGTGAACGACGTGTCCACGG TCATCCCG	TCGACTAAGTTGGCAGCATCT CAGTGGTGGTGGTGGTG

APPENDIX C. APPENDIX C.

Amino acid sequence alignment of Mammalian Cell Entry domains of CrTGD2 homologues used for building the phylogenetic tree in Figure 2.S7.

MUSCLE (3.8) multiple sequence alignment

```
Ignatzschineria larvae      IEYKVTITN-ESVAGLSINSPIIDYRGVNVGKVA AIELNNNDPRVYTILLNI--DVGTPIKR
Xylella fastidiosa         --YRVVFR-EAVTGLSVGSPVQYNGIAIGSITQLTLPNDPRQVIAHLRV--NATTPIKK
Escherichia coli MS 115-1  --FN-----EPVSGLSQGSTVQYSGIRVGEVTLQLRLDRDNPKNVWARIRV--SASTPIRE
Pseudomonas putida         --YTI---YDNVGGVKFGTVPVLYEGYTVGQVEDVEPQMTD-EGTRFRVEMSVQEGWPIPE
Caenispirillum salinarum  -PYNISVEFASSPGLHPGFVEDYDLGLRIGKIDSVRLAGDK---VVVKLDI--DKDVEVPR
Actinomadura flavalba     --NTVVAYFTQANALYVGDVKVQIMGLPVGSIIDKIEPAGDK---MKVTFHY--QNKYKQVA
Mycobacterium tuberculosis -TKTITAYFPSVNGLYTGTPTVRVRLGVKVGKVA AITPRSGD---VKVTLDV--DRSTPIPA
Gordonia otitidis         -GTRVTAYFDRAVGIYAGSDLRILGVVRAGAVKSVRPQGTQ---VRVELEL--DDGIQVPR
Streptomyces sp. Tu_6176   -PTTISADFTRAVGLYPGSDVRILGVKVGQVDVVEFPQGRH---VRVTFVS--DSRHRIPA
Intrasporangium calvum   -TYEVTITLADAPGLVVGTPTVRYRQVVRVGSISDVQVQVPMG---IAKAKLR-D--VVIIPR
Synechococcus sp. PCC 6312 -EYTLVYVGFRAVGLNPEAQVLLSGVPVGHVEKVGSDGTG---VTVAISVS-DD-VKIPR
Selenomonas artemidis     -GYELRINYQVSGLMPGHVVRYAGVQVGTVKKINVAHDK---VEVITEIN-DD-IKIPQ
Phascolarctobacterium succinatutens -SYQVIAQFPNVNGIQVGDVRYRGLKVGKITDIMPGTNG---VDVMMETS-SSDLLIPK
Stanieria cyanosphaera PCC 7437 -PYQATIEFPLACGIQIGTPTVIRIRGVQVGVQLAVKPSLER---VDVLVEVN-DVSTVIPR
Chlamydomonas reinhardtii -PYKATIEFPLACGIQIGTPTVIRIRGVQVGVQLAVKPSLER---VDVLVEVN-DVSTVIPR
Volvox carteri f. nagariensis -GYQCVLEFPLACGITVGTPTVIRIRGVPIGSLVNLNASLEK---VEVLTEVK-KSTTVIPR
Coccomyxa subellipsoidea C-169 -GYQAILLEFPVACGITVGTPTVIRIRGVVPGVLSVQPSLEK---VDVLVEMK-DSTTVIPR
Chlorella variabilis     -SYQAILLEFPVACGISVGTPTVIRIRGVVPGVLSVQPSLEK---VEVLVEIR-DSTTVIPR
Auxenochlorella protothecoides -YQAFVEFPFACGIQVGTQVRVIRGVKVGNVLSVSRPNLER---VEVLVEMD-DDGIVIPR
Ostreococcus tauri       --YQAFIEFEPVACGITVGTPTVIRIRGVKAGTVLSVQPSLEK---VDVLVEMD-DKNVPIPR
Tarenaya hassleriana     -KYQTVFEFPQASGICTGTPTVIRIRGVNVGNVIRVNP SLKN---IEAVTEID-DDKIIIPR
Arabidopsis thaliana     -KYQTVFELSASGICTGTPTVIRIRGVTVGTIIRVNP SLKN---IEAVAEIE-DDKIIIPR
Brassica rapa            -KYQTVFELSASGICTGTPTVIRIRGVTVGTIIRVNP SLKN---IEAVAEIE-DDKIIIPR
Solanum tuberosum       --YLAVLEFEPQACGICTGTPTVIRIRGVSIGNVIRVNP SLRN---IEAVVEVE-DDKIIIPR
Nicotiana tomentosiformis -KYLA VLQFEQACGICTGTPTVIRIRGVNIGNVIRVNP SLRN---VEAVVEVE-DDKIIIPR
Cicer arietinum         -KYTATIEFEPQACGICTGTPTVIRIRGVTVGDVIRVNP SLRS---IEAVVEIE-DDKTIIPR
Brachypodium distachyon -KYQAVLEFEGQACGICVGTPTVIRIRGVTVGNVVRVDS SLRS---IDAVEVD-DEKIVVPR
Musa acuminata subsp. malaccensis -KYQAVFEFPQACGICVGTPTVIRIRGVNVGNVVRVDS TLRN---IDATAEVD-DDKIIIPR
Phoenix dactylifera     -KYQAVFEFPQACGICVGTPTVIRIRGVTVGSVVQVNS SLKS---IDATVEVE-DDKIIIPQ
Aegilops tauschii      -KYNAVFEFPQACGICVGTPLRIRGVTIGSVVRVDS SLRS---IDAYVEVE-DDKIIIPR
Oryza sativa Indica Group -KYQAVFEFPQACGICVGTPTVIRIRGVTVGNVVRVDS SLKS---IDAYVEVE-DDKIIIPR
Sorghum bicolor         -KYNTVFEFPQACGICVGTPTVIRIRGVTVGSVVRVDS SLRS---IDATVEVE-DDKIIIPR
Zea mays                -KYNTVFEFPQACGICVGTPTVIRIRGVTVGSVVRVDS SLRS---IDATVEVE-DDKIIIPR
Setaria italica        -KYNTVFEFPQACGICVGTPTVIRIRGVTVGSVVRVDS SLRS---IDALVEVE-DDKIIIPR
Prunus mume            --YFAVFEFPQACGISTGTPTVIRIRGVNVGSVVRVNS SLES---IEAVVEVE-DDKTVIPR
Fragaria vesca subsp. vesca -YFAVFEFPQACGISTGTPTVIRIRGVTVGNVIRVNS SLSQ---IEAVVEVE-DDKTVIPR
Coffea canephora       --YLAVFEFEQACGICTGTPTVIRIRGVNVGSVIRVNP SLNS---IEAVVEVD-DDKVIIPR
Theobroma cacao        --YLAVFEFAQASGICTGTPTVIRIRGVTVGNVVRVNP SLKS---IEAVVEVE-DDKIFIPR
Jatropha curcas        --YLAVFEFAQAGGICTGTPTVIRIRGVTVGNVIKVNPS LRC---IEAVVEVE-DDKIIIPR
Nelumbo nucifera       -KYQAVFEFAQACGICTGTPTVIRIRGVTVGNVIRINPS LKS---IEAVVEVE-DDKVIIPR
Hevea brasiliensis     --YVAVFEFAQACGICTGTPTVIRIRGVTVGNVIQVNPS LRS---IEAVVEVE-DDKIIIPR
Ricinus communis       -KYTAVLEFAQACGICTGTPTVIRIRGVTVGNVIQVNPS LKS---IEAVVEVE-DDKIIIPR
Vitis vinifera         --YLAVFEFPQACGICKGTPTVIRIRGVTVGNVIQVNPS LKS---IEAVVEVE-DDKIIIPQ
Selaginella moellendorffii -KYFATFEFAKAWGITVGTPTVIRIRGVTVGTVIRVKPTLEK---LDVEVQIV-DANLVIIPR
Physcomitrella patens  -KYEAVFEFQLAQGITVGTPTVIRIRGVTVGNVVRVNP SLEK---IDVVVLEL-DAGIVVPR
Microcoleus sp. PCC 7113 -SYQFIVKFNANVAGMKTGAMVRYRGVVKVGRIT E VTPETNG---VNATVEIS-DPDLIIPK
Oscillatoria nigro-viridis -SYKFAVEFASAQGMQIGTPIRYRGVAVGKITALKPGSNG---VDVTLEIA-PGTLVIIPR
Anabaena sp. 90         -SYQATIEFANAGGMQKGA VPRFRGVKVGRIAAIRPGPNN---VEVELEIS-QRDLIIPR
Gloeocapsa sp. PCC 7428 --YSAIEFANVGGMQEGGVVRYRGVNVGNIAAIRPGPNG---VEVDVEIA-PANLIIPR
Calothrix sp. PCC 7103  -NYKIFVDFSNAGGMQKGA VPRFRGVKVGRIAAIRPGPNN---VEVELEIS-QRDLIIPR
Nostoc sp. PCC 7120    --YKAVVEFANAGGMQRGATVRYRGVVKVGRISQIQPGPNA---VEVEIEFA-QSNLIIPR
Richelia intracellularis -TYKVIVEFTNAGGMQKGA VPRFRGVKVGVRVNSIQPGPNT---VEVEIEIS-QSELIIPK
Megasphaera sp. NP3    ----IHTEFNDANGLQKGNVRYVGVHVGKVEKVTPSRNG---VDVTMKI--DKGTEIPR
Anaeromusa acidaminophila -GYPIQAVFSQVGGKLDGAI VRYAGVDVGRVQSVEMTATG---VTVNLRI-F-DH-VRIIPR
. :      : * * : :
```

```
Ignatzschineria larvae      DTEAVLMSRGITGIVNVSLTG-
Xylella fastidiosa         DTRAKLAITSLTGPSIIQLSG-
Escherichia coli MS_115-1  DTQARLTVAGITGTSNIQFSS-
```

<i>Pseudomonas putida</i>	DTQAKLTLTGITGTSFIQLSG-
<i>Caenispirillum salinarum</i>	DSSADVAASGFLGGMMINITGG
<i>Actinomadura flavalba</i>	GVHAAAARKSAVGEVVELTP-
<i>Mycobacterium tuberculosis</i>	NASAVILNPTLVASRNIQLEP-
<i>Gordonia otitidis</i>	DARAVVVAQSLVSGRFVQLTP-
<i>Streptomyces</i> sp. Tu_6176	GAHAVIVAPSVVADRFRVQLTP-
<i>Intrasporangium calvum</i>	DARAAIVAPSLVSDRYVQLLP-
<i>Synechococcus</i> sp. PCC_6312	DAIPEVRQSGFVGSFLDF---
<i>Selenomonas artemidis</i>	GSSVTIAQPGIMGDKFVVIITP-
<i>Phascolarctobacterium succinatutens</i>	GATFTISSDGMGEKRVSVIP-
<i>Stanieria cyanosphaera</i> PCC 7437	NALIQAASSGLIGETFVAIIP-
<i>Chlamydomonas reinhardtii</i>	NSVIEANQSGLIAEPLVDITP-
<i>Volvox carteri</i> f. nagariensis	NSVIEANQSGLIAEPLVDITP-
<i>Coccomyxa subellipsoidea</i> C-169	NSHIEANQSGLIAEPLIDITP-
<i>Chlorella variabilis</i>	NSLIEANQSGLIAEPLIDITP-
<i>Auxenochlorella protothecoides</i>	NSLIEANQSGLIAEPLIDITP-
<i>Micromonas pusilla</i> CCMP1545	NSLVEANQSGLIAETIIDITP-
<i>Ostreococcus tauri</i>	NSVIEANQSGLIAETIIDITP-
<i>Tarenaya hassleriana</i>	NSLVEVNSGGLMETMIDVTP-
<i>Arabidopsis thaliana</i>	NSLVEVNSGGLMETMIDIMP-
<i>Brassica rapa</i>	NSLVEVNSGGLMETMIDITP-
<i>Solanum tuberosum</i>	NSLVEVNSGGLMETMIDITP-
<i>Nicotiana tomentosiformis</i>	NSLVEVNSGGLMETMIDITP-
<i>Cicer arietinum</i>	NSSVEVNSGGLMETVIDITP-
<i>Brachypodium distachyon</i>	NSVVEVNSGGLMIDLIDITP-
<i>Musa acuminata</i> subsp. <i>malaccensis</i>	NSLVEVNSGGLMETLIDITP-
<i>Phoenix dactylifera</i>	NSLVEVNSGGLMETLIDITP-
<i>Aegilops tauschii</i>	NSLVEVNSGGLMETMIDITP-
<i>Oryza sativa</i> Indica Group	NSVVEVNSGGLMETLIDITP-
<i>Sorghum bicolor</i>	NSVVEVNSGGLMETLIDITP-
<i>Zea mays</i>	NSMVEVNSGGLMETLIDITP-
<i>Setaria italica</i>	NSLVEVNSGGLMETLIDITP-
<i>Prunus mume</i>	NSLIEVNSGGLMETRIDVTP-
<i>Fragaria vesca</i> subsp. <i>vesca</i>	NSLIEVNSGGLMETRIDITP-
<i>Coffea canephora</i>	NSLVEVNSGGLMETLIDITP-
<i>Theobroma cacao</i>	NSLIEVNSGGLMETLIDITP-
<i>Jatropha curcas</i>	NSLIEVNSGGLMETIIDITP-
<i>Nelumbo nucifera</i>	NSLIEVNSGGLMETLIDITP-
<i>Hevea brasiliensis</i>	NSLIEVNSGGLMETLIDITP-
<i>Ricinus communis</i>	NSLIEVNSGGLMETLIDITP-
<i>Vitis vinifera</i>	NSLIEVNSGGLMETLIDITP-
<i>Selaginella moellendorffii</i>	NALVEVNSGGLVSETLIDITP-
<i>Physcomitrella patens</i>	NALVEVNSGGLVSETLIDVTP-
<i>Microcoleus</i> sp. PCC 7113	DVVIEANQAGLVGETSIDITP-
<i>Oscillatoria nigro-viridis</i>	DVTIEANKSGLIGESSIDITP-
<i>Anabaena</i> sp. 90	NSIIEANQSGLISENIIDITP-
<i>Gloeocapsa</i> sp. PCC 7428	DVQIAANQSGLISEVSDITP-
<i>Calothrix</i> sp. PCC 7103	DVKVEANQSGLIAESLIDITP-
<i>Nostoc</i> sp. PCC 7120	DVVIEANQTGLISESIIDITP-
<i>Richelia intracellularis</i>	NIVVEANQSGLIGESVIDITP-
<i>Megasphaera</i> sp. NP3	DSKIVITTDGLLGEKIVSISPG
<i>Anaeromusa acidaminophila</i>	GSVFTIASEGLLGEKYITILP-

. : .

APPENDIX D. SUPPORTING METHODS

Generation of *tgd2* mutant and genetic analyses. The *tgd2* mutant was generated by insertional mutagenesis in the same experiment as described previously for the *cht7* mutant (Tsai *et al.*, 2014). For genetic analysis, the original *tgd2* mutant (in dw15.1) was crossed with the cell-walled strain CC-198 as previously described (Li *et al.*, 2012). The progenies were tested for cosegregation of Hygromycin B resistance and TAG lipid phenotype. Genetic complementation analysis was initiated by generating *tgd2* lines into which fragments of genomic DNA were introduced that were derived from bacterial artificial chromosomes (Clemson University Genomics Institute). Genomic DNA fragments covering individually each affected gene with ~ 1 kb 5' of the start codon and 0.5 kb 3' of the stop codon were cut from BACs with restriction endonucleases (for details refer to Table 2.S1). Approximately 0.5-2.0 µg of purified genomic DNA was co-introduced into the *tgd2* mutant with the Paramomycin resistance gene *AphVIII* at a 1/10 molar ratio. *AphVIII* was prepared by *KpnI/PstI* digestion from plasmid pSI103 (Chlamydomonas Resource Center; <http://chlamycollection.org/>). The amounts of DNA used for the transformations are listed in Table 2.S1. The transformants were selected on TAP agar containing 20 µg/mL Paramomycin. Single colonies were picked and grown in 200 µL TAP medium in 96-well culture plates. Of the mid-log phase culture 150 µL were transferred into 96-well PCR plates and centrifuged at 3000 X g for 5 min. The supernatant was removed. The pellet was used to extract DNA with Chelex-100 (SIGMA) as previously described (Cao *et al.*, 2009). Presence of the introduced DNA was confirmed by PCR using primers and sequences listed in Tables 2.S1 and 2.S2, respectively. Colonies positive for the introduced gene were then grown in TAP liquid medium for lipid analysis.

DNA isolation and Southern blot analysis. DNA isolation was carried out as previously described (Keb-Llanes *et al.*, 2002) with some modifications. A mid-log phase culture (15 mL) was harvested by centrifugation at 3,000 X g for 5 min. The pellet was resuspended in 400 µL extraction buffer A without polyvinylpyrrolidone, ascorbic acid and β-mercaptoethanol. The mixture was then incubated at 60°C for 1 h. 400 µL of phenol/chloroform (1:1 v/v) was added. The mixture was then mixed by repeated inverting and centrifuged at 13,000 X g for 1 min. The upper phase was transferred to a new tube. The process was repeated with chloroform. DNA was precipitated by adding 1 volume of isopropanol, followed by centrifugation at 13,000 X g for 5 min. The supernatant was discarded. The pellet was washed with 70% ethanol, dried and

resuspended in 200 μ L of 10 mM Tris-HCl pH 8.0. The isolated DNA was treated with 10 μ L of 0.5 mg/mL DNase-free RNase (Roche). The treated DNA was purified, precipitated, and resuspended again as mentioned above. Southern blot analysis was done with the same probe as described in (Li *et al.*, 2012).

Whole genome resequencing. The genome of the *tgd2* mutant was sequenced by Illumina Hi-Seq using the paired-end method at the MSU-Research Technology Support Facility. Reads were quality checked and trimmed with the FASTX toolkit 0.0.13 (Patel & Jain, 2012). Read assembly was performed with velvet 1.2.07 (Zerbino & Birney, 2008) using the 21 *k*-mer length of 21. The presence of the *AphVII* gene was detected in assembled reads with BLASTN 2.2.26+ (Park *et al.*, 2012) using the default setting. Reads containing the *AphVII* gene were analyzed for flanking genomic sequences against the *Chlamydomonas reinhardtii* V5.3 reference genome using BLAST (Altschul *et al.*, 1997). The identified deletion was confirmed by PCR using primers as listed in Table 2.S2.

Phylogenetic analysis. Amino acid sequences were obtained from blastp searches with CrTGD2 as query against the amino acid sequence database through BLASTP 2.2.31+ at the National Center for Biotechnology Information website (www.ncbi.nlm.nih.gov/, Altschul *et al.*, 1997; Altschul *et al.*, 2005). Protein domain searches were carried out against the Pfam protein families database (Finn *et al.*, 2014) with hmmscan 3.1b1 (Eddy, 2009). Mammalian Cell Entry (MCE) domain (PF02470.15) was a common domain for every amino acid sequence and was used for alignment with MUSCLE (Edgar, 2004). The gap penalty was set to -9 for gap open and to -3 for gap extension. The aligned amino acid sequences were then used for phylogenetic tree reconstruction with MEGA6 (Tamura *et al.*, 2013) using Maximum Likelihood method based on the JTT matrix-based model (Jones *et al.*, 1992). Test of phylogeny was carried out with the Bootstrap method (Felsenstein, 1985) set for 1000 replicates.

Heterologous complementation analysis. In order to test the activity of AtTGD2 in the *Chlamydomonas tgd2* mutant, a fusion protein containing the CrTGD2 transmembrane domain and the AtTGD2 extrinsic portion was expressed from a construct assembled into the pSI103 vector (Sizova *et al.*, 2001). The *CrTGD2* transmembrane domain encoding portion also contained 1 kb 5' of the start codon including an intron followed by the extra membrane portion encoded by codon-optimized *AtTGD2*. In addition, 1 kb *CrTGD2* sequence 3' of the stop codon

was included (Figure 2.S9). This construct was produced using a Gibson's assembly kit (New England Biolabs). Primers used are listed in Table 2.S3. Two μg of this construct was used to transform the *Chlamydomonas tgd2* mutant.

For testing *CrTGD2* complementation of the *Arabidopsis tgd2* mutant, a fusion protein consisting of the transmembrane domain encoded by *AtTGD2* and the membrane extrinsic portion encoded by *CrTGD2* was expressed from a construct assembled into the pMDC32 vector (Curtis & Grossniklaus, 2003) (Figure 2.S10). The *CrTGD2* fragment was obtained by gene synthesis (165 bp) and *DsRED-CrTGD2* pLW01 (672 bp). *AtTGD2* and *CrTGD2* fragments were introduced by Gibson assembly (New England Biolabs) into pDONRTM221 (InvitrogenTM). This construct was then used as a template for assembly into pENTRTM/D-TOPO[®] (InvitrogenTM) eliminating the His-tag. *At-CrTGD2* pENTR was used as a donor vector to construct *At-CrTGD2* in pMDC32 using Gateway[®] LR ClonaseTM II enzyme mix (InvitrogenTM). Primers used to make this construct are listed in Table 2.S3. *At-CrTGD2* pMDC32 was introduced into *Agrobacterium* strain G3101. *Agrobacterium* containing *At-CrTGD2* pMDC32 was used for *Arabidopsis tgd2* mutant transformation using the floral dip method as previously described (Clough & Bent, 1998).

***DsRED-CrTGD2* pLW01, *DsRED-AtTGD2* pLW01 and *DsRED* pLW01 constructs, recombinant protein expression and purification.** *DsRED-AtTGD2* pLW01 and *DsRED* pLW01 were obtained from Binbin Lu (Lu & Benning, 2009). *DsRED-CrTGD2* pLW01 was constructed in order to test the function of CrTGD2. Based on sequence alignment between CrTGD2 and AtTGD2 and hydrophobicity analysis the C-terminal membrane external portion of CrTGD2 was identified (Figure 2.S7). The corresponding DNA fragment was amplified with Phusion polymerase using primers listed in Table 2.S3. The CrTGD2 fragment and pLW01 (a provided by Dr. Michael Garavito, Michigan State University) containing *DsRED* and a His-tag were digested with *Bam*HI and *Sal*I. The products were ligated together to produce *DsRED-CrTGD2* pLW01.

Protein expression was carried out according to (Lu & Benning, 2009) with minor modifications. Protein expression was induced with 100 μM instead of 50 μM IPTG. For protein purification, the supernatant from the cell lysate was incubated with HisPur Ni-NTA resin (Thermo SCIENTIFIC). The eluted protein was dialyzed in dialysis buffer containing 125 mM

NaCl in addition to 10 mM KH_2PO_4 . The protein was stored in 50% (v/v) glycerol at -20°C until used.

REFERENCES

REFERENCES

- Altschul, S. F., Madden, T. L., Schäffer, A. A., Zhang, J., Zhang, Z., Miller, W., & Lipman, D. J. (1997). Gapped BLAST and PSI-BLAST: a new generation of protein database search programs. *Nucleic Acids Res*, 25(17), 3389-3402. doi: 10.1093/nar/25.17.3389
- Altschul, S. F., Wootton, J. C., Gertz, E. M., Agarwala, R., Morgulis, A., Schäffer, A. A., & Yu, Y.-K. (2005). Protein database searches using compositionally adjusted substitution matrices. *FEBS Journal*, 272(20), 5101-5109. doi: 10.1111/j.1742-4658.2005.04945.x
- Awai, K., Marechal, E., Block, M. A., Brun, D., Masuda, T., Shimada, H., Takamiya, K., Ohta, H., & Joyard, J. (2001). Two types of MGDG synthase genes, found widely in both 16:3 and 18:3 plants, differentially mediate galactolipid syntheses in photosynthetic and nonphotosynthetic tissues in *Arabidopsis thaliana*. *Proc Natl Acad Sci U S A*, 98(19), 10960-10965. doi: 10.1073/pnas.181331498
- Awai, K., Xu, C., Tamot, B., & Benning, C. (2006). A phosphatidic acid-binding protein of the chloroplast inner envelope membrane involved in lipid trafficking. *Proc Natl Acad Sci U S A*, 103(28), 10817-10822. doi: 10.1073/pnas.0602754103
- Bahr, G. F. (1954). Osmium tetroxide and ruthenium tetroxide and their reactions with biologically important substances: Electron stains III. *Exp Cell Res*, 7(2), 457-479. doi: [http://dx.doi.org/10.1016/S0014-4827\(54\)80091-7](http://dx.doi.org/10.1016/S0014-4827(54)80091-7)
- Benning, C. (2009). Mechanisms of lipid transport involved in organelle biogenesis in plant cells. *Ann Rev Cell Dev Biol*, 25(1), 71-91. doi: doi:10.1146/annurev.cellbio.042308.113414
- Benning, C., & Ohta, H. (2005). Three enzyme systems for galactoglycerolipid biosynthesis are coordinately regulated in plants. *J Biol Chem*, 280(4), 2397-2400. doi: 10.1074/jbc.R400032200
- Benning, C., & Somerville, C. (1992). Isolation and genetic complementation of a sulfolipid-deficient mutant of *Rhodobacter sphaeroides*. *J Bacteriol*, 174(7), 2352-2360.
- Bligh, E. G., & Dyer, W. J. (1959). A rapid method of total lipid extraction and purification. *Can J Biochem Physiol*, 37(8), 911-917. doi: 10.1139/o59-099
- Boudière, L., Michaud, M., Petroutsos, D., Rébeillé, F., Falconet, D., Bastien, O., Roy, S., Finazzi, G., Rolland, N., Jouhet, J., Block, M. A., & Maréchal, E. (2014). Glycerolipids in photosynthesis: Composition, synthesis and trafficking. *Biochim Biophys Acta*, 1837(4), 470-480. doi: <http://dx.doi.org/10.1016/j.bbabi.2013.09.007>

- Bradford, M. M. (1976). A rapid and sensitive method for the quantitation of microgram quantities of protein utilizing the principle of protein-dye binding. *Anal Biochem*, 72(1–2), 248-254. doi: [http://dx.doi.org/10.1016/0003-2697\(76\)90527-3](http://dx.doi.org/10.1016/0003-2697(76)90527-3)
- Cao, M., Fu, Y., Guo, Y., & Pan, J. (2009). Chlamydomonas (Chlorophyceae) colony PCR. *Protoplasma*, 235(1-4), 107-110. doi: 10.1007/s00709-009-0036-9
- Casali, N., & Riley, L. W. (2007). A phylogenomic analysis of the Actinomycetales mce operons. *Bmc Genomics*, 8(1), 60.
- Chang, C. W., Moseley, J. L., Wykoff, D., & Grossman, A. R. (2005). The LPB1 gene is important for acclimation of *Chlamydomonas reinhardtii* to phosphorus and sulfur deprivation. *Plant Physiol*, 138(1), 319-329. doi: 10.1104/pp.105.059550
- Cline, K., Werner-Washburne, M., Andrews, J., & Keegstra, K. (1984). Thermolysin is a suitable protease for probing the surface of intact pea chloroplasts. *Plant Physiol*, 75(3), 675-678. doi: 10.1104/pp.75.3.675
- Clough, S. J., & Bent, A. F. (1998). Floral dip: a simplified method for *Agrobacterium*-mediated transformation of *Arabidopsis thaliana*. *The Plant Journal*, 16(6), 735-743. doi: 10.1046/j.1365-3113.1998.00343.x
- Dörmann, P., & Benning, C. (2002). Galactolipids rule in seed plants. *Trends Plant Sci*, 7(3), 112-118. doi: 10.1016/S1360-1385(01)02216-6
- Curtis, M. D., & Grossniklaus, U. (2003). A gateway cloning vector set for high-throughput functional analysis of genes in planta. *Plant Physiol*, 133(2), 462-469. doi: 10.1104/pp.103.027979
- Dubots, E., Audry, M., Yamaryo, Y., Bastien, O., Ohta, H., Breton, C., Marechal, E., & Block, M. A. (2010). Activation of the chloroplast monogalactosyldiacylglycerol synthase MGD1 by phosphatidic acid and phosphatidylglycerol. *J Biol Chem*, 285(9), 6003-6011. doi: 10.1074/jbc.M109.071928
- Eddy, S. R. (2009). *A new generation of homology search tools based on probabilistic inference*. Paper presented at the Genome Inform.
- Edgar, R. C. (2004). MUSCLE: multiple sequence alignment with high accuracy and high throughput. *Nucleic Acids Res*, 32(5), 1792-1797. doi: 10.1093/nar/gkh340
- Eriksson, M., Gardstrom, P., & Samuelsson, G. (1995). Isolation, purification, and characterization of mitochondria from *Chlamydomonas reinhardtii*. *Plant Physiol*, 107(2), 479-483. doi: 10.1104/pp.107.2.479

- Esterbauer, H., Schaur, R. J., & Zollner, H. (1991). Chemistry and biochemistry of 4-hydroxynonenal, malonaldehyde and related aldehydes. *Free Radic Biol Med*, *11*(1), 81-128. doi: [http://dx.doi.org/10.1016/0891-5849\(91\)90192-6](http://dx.doi.org/10.1016/0891-5849(91)90192-6)
- Fan, J., Andre, C., & Xu, C. (2011). A chloroplast pathway for the de novo biosynthesis of triacylglycerol in *Chlamydomonas reinhardtii*. *Febs Letters*, *585*(12), 1985-1991. doi: 10.1016/j.febslet.2011.05.018
- Fan, J., Yan, C., Roston, R., Shanklin, J., & Xu, C. (2014). Arabidopsis lipins, PDAT1 acyltransferase, and SDP1 triacylglycerol lipase synergistically direct fatty acids toward β -oxidation, thereby maintaining membrane lipid homeostasis. *Plant Cell*, *26*(10), 4119-4134.
- Fan, J., Yan, C., & Xu, C. (2013). Phospholipid: diacylglycerol acyltransferase - mediated triacylglycerol biosynthesis is crucial for protection against fatty acid - induced cell death in growing tissues of Arabidopsis. *Plant J*, *76*(6), 930-942.
- Fan, J., Zhai, Z., Yan, C., & Xu, C. (2015). Arabidopsis TRIGALACTOSYLDIACYLGLYCEROL5 Interacts with TGD1, TGD2, and TGD4 to Facilitate Lipid Transfer from the Endoplasmic Reticulum to Plastids. *Plant Cell*. doi: 10.1105/tpc.15.00394
- Felsenstein, J. (1985). Confidence limits on phylogenies: an approach using the bootstrap. *Evolution*, *39*, 783-791.
- Feussner, I., & Wasternack, C. (2002). The lipoxygenase pathway. *Ann Rev Plant Biol*, *53*(1), 275-297. doi: doi:10.1146/annurev.arplant.53.100301.135248
- Finn, R. D., Bateman, A., Clements, J., Coggill, P., Eberhardt, R. Y., Eddy, S. R., Heger, A., Hetherington, K., Holm, L., Mistry, J., Sonnhammer, E. L. L., Tate, J., & Punta, M. (2014). Pfam: the protein families database. *Nucleic Acids Res*, *42*(D1), D222-D230. doi: 10.1093/nar/gkt1223
- Frentzen, M., Heinz, E., McKeon, T. A., & Stumpf, P. K. (1983). Specificities and selectivities of glycerol-3-phosphate acyltransferase and monoacylglycerol-3-phosphate acyltransferase from pea and spinach chloroplasts. *Eur J Biochem*, *129*(3), 629-636. doi: 10.1111/j.1432-1033.1983.tb07096.x
- Giroud, C., & Eichenberger, W. (1988). Fatty acids of *Chlamydomonas reinhardtii* - Structure, positional distribution and biosynthesis. *Biol Chem*, *369*(1), 18-19.
- Gorman, D. S., & Levine, R. P. (1965). Cytochrome *f* and plastocyanin: their sequence in the photosynthetic electron transport chain of *Chlamydomonas reinhardtii*. *Proc Natl Acad Sci U S A*, *54*(6), 1665-1669.

- Gross, L. A., Baird, G. S., Hoffman, R. C., Baldrige, K. K., & Tsien, R. Y. (2000). The structure of the chromophore within DsRed, a red fluorescent protein from coral. *Proc Natl Acad Sci U S A*, *97*(22), 11990-11995. doi: 10.1073/pnas.97.22.11990
- Harris, E. H. (1989). *The Chlamydomonas sourcebook: A comprehensive guide to biology and laboratory use*. San Diego: Academic Press.
- Heinz, E., & Roughan, P. G. (1983). Similarities and differences in lipid metabolism of chloroplasts isolated from 18:3 and 16:3 plants. *Plant Physiol*, *72*(2), 273-279.
- Hodges, D. M., DeLong, J. M., Forney, C. F., & Prange, R. K. (1999). Improving the thiobarbituric acid-reactive-substances assay for estimating lipid peroxidation in plant tissues containing anthocyanin and other interfering compounds. *Planta*, *207*(4), 604-611. doi: 10.1007/s004250050524
- Hurlock, A. K., Roston, R. L., Wang, K., & Benning, C. (2014). Lipid trafficking in plant cells. *Traffic*, *15*(9), 915-932. doi: 10.1111/tra.12187
- Jardillier, L., Zubkov, M. V., Pearman, J., & Scanlan, D. J. (2010). Significant CO₂ fixation by small prymnesiophytes in the subtropical and tropical northeast Atlantic Ocean. *ISME J*, *4*(9), 1180-1192. doi: <http://www.nature.com/ismej/journal/v4/n9/supinfo/ismej201036s1.html>
- Jarvis, P., Dormann, P., Peto, C. A., Lutes, J., Benning, C., & Chory, J. (2000). Galactolipid deficiency and abnormal chloroplast development in the Arabidopsis MGD synthase 1 mutant. *Proc Natl Acad Sci U S A*, *97*(14), 8175-8179. doi: 10.1073/pnas.100132197
- Jones, D. T., Taylor, W. R., & Thornton, J. M. (1992). The rapid generation of mutation data matrices from protein sequences. *CABIOS*, *8*(3), 275-282.
- Kaup, M. T., Froese, C. D., & Thompson, J. E. (2002). A role for diacylglycerol acyltransferase during leaf senescence. *Plant Physiol*, *129*(4), 1616-1626.
- Keb-Llanes, M., González, G., Chi-Manzanero, B., & Infante, D. (2002). A rapid and simple method for small-scale DNA extraction in Agavaceae and other tropical plants. *Plant Mol Biol Rep*, *20*(3), 299-299. doi: 10.1007/bf02782465
- Kieboom, J., Dennis, J. J., de Bont, J. A. M., & Zylstra, G. J. (1998a). Identification and molecular characterization of an efflux pump involved in *Pseudomonas putida* S12 solvent tolerance. *J Biol Chem*, *273*(1), 85-91. doi: 10.1074/jbc.273.1.85
- Kieboom, J., Dennis, J. J., Zylstra, G. J., & de Bont, J. A. M. (1998b). Active efflux of organic solvents by *Pseudomonas putida* S12 is induced by solvents. *J Bacteriol*, *180*(24), 6769-6772.

- Kim, H. U., Li, Y., & Huang, A. H. C. (2005). Ubiquitous and endoplasmic reticulum–located lysophosphatidyl acyltransferase, LPAT2, is essential for female but not male gametophyte development in Arabidopsis. *Plant Cell*, 17(4), 1073-1089. doi: 10.1105/tpc.104.030403
- Kim, K., Lee, S., Lee, K., & Lim, D. (1998). Isolation and characterization of toluene-sensitive mutants from the toluene-resistant bacterium *Pseudomonas putida* GM73. *J Bacteriol*, 180(14), 3692-3696.
- Klein, U., Chen, C., Gibbs, M., & Platt-Aloia, K. A. (1983). Cellular fractionation of *Chlamydomonas reinhardtii* with emphasis on the isolation of the chloroplast. *Plant Physiol*, 72(2), 481-487. doi: 10.1104/pp.72.2.481
- Kobayashi, K., Awai, K., Nakamura, M., Nagatani, A., Masuda, T., & Ohta, H. (2009). Type-B monogalactosyldiacylglycerol synthases are involved in phosphate starvation-induced lipid remodeling, and are crucial for low-phosphate adaptation. *Plant J*, 57(2), 322-331. doi: 10.1111/j.1365-313X.2008.03692.x
- Korn, E. D. (1967). A chromatographic and spectrophotometric study of the products of the reaction of osmium tetroxide with unsaturated lipids. *J Cell Biol*, 34(2), 627-638. doi: 10.1083/jcb.34.2.627
- Krogh, A., Larsson, B., Von Heijne, G., & Sonnhammer, E. L. (2001). Predicting transmembrane protein topology with a hidden Markov model: application to complete genomes. *J Mol Biol*, 305(3), 567-580.
- Kunst, L., Browse, J., & Somerville, C. (1988). Altered regulation of lipid biosynthesis in a mutant of Arabidopsis deficient in chloroplast glycerol-3-phosphate acyltransferase activity. *Proc Natl Acad Sci U S A*, 85(12), 4143-4147.
- Li, X., Moellering, E. R., Liu, B., Johnny, C., Fedewa, M., Sears, B. B., Kuo, M.-H., & Benning, C. (2012). A galactoglycerolipid lipase is required for triacylglycerol accumulation and survival following nitrogen deprivation in *Chlamydomonas reinhardtii*. *Plant Cell*, 24, 4670-4686. doi: 10.1105/tpc.112.105106
- Liu, B., & Benning, C. (2013). Lipid metabolism in microalgae distinguishes itself. *Curr Opin Biotech*, 24(2), 300-309. doi: <http://dx.doi.org/10.1016/j.copbio.2012.08.008>
- Loria, J. P., Rance, M., & Palmer, A. G., 3rd. (1999). A TROSY CPMG sequence for characterizing chemical exchange in large proteins. *J Biomol NMR*, 15(2), 151-155.
- Lu, B., & Benning, C. (2009). A 25-amino acid sequence of the Arabidopsis TGD2 protein is sufficient for specific binding of phosphatidic acid. *J Biol Chem*, 284(26), 17420-17427. doi: 10.1074/jbc.M109.016014

- Lu, B., Xu, C., Awai, K., Jones, A. D., & Benning, C. (2007). A small ATPase protein of Arabidopsis, TGD3, involved in chloroplast lipid import. *J Biol Chem*, 282(49), 35945-35953. doi: 10.1074/jbc.M704063200
- Malinverni, J. C., & Silhavy, T. J. (2009). An ABC transport system that maintains lipid asymmetry in the Gram-negative outer membrane. *Proc Natl Acad Sci U S A*, 106(19), 8009-8014. doi: 10.1073/pnas.0903229106
- Melis, A. (2009). Solar energy conversion efficiencies in photosynthesis: Minimizing the chlorophyll antennae to maximize efficiency. *Plant Sci*, 177(4), 272-280. doi: <http://dx.doi.org/10.1016/j.plantsci.2009.06.005>
- Merchant, S. S., Prochnik, S. E., Vallon, O., Harris, E. H., Karpowicz, S. J., Witman, G. B., Terry, A., Salamov, A., Fritz-Laylin, L. K., Maréchal-Drouard, L., Marshall, W. F., Qu, L.-H., Nelson, D. R., Sanderfoot, A. A., Spalding, M. H., Kapitonov, V. V., Ren, Q., Ferris, P., Lindquist, E., Shapiro, H., Lucas, S. M., Grimwood, J., Schmutz, J., Cardol, P., Cerutti, H., Chanfreau, G., Chen, C.-L., Cognat, V., Croft, M. T., Dent, R., Dutcher, S., Fernández, E., Fukuzawa, H., González-Ballester, D., González-Halphen, D., Hallmann, A., Hanikenne, M., Hippler, M., Inwood, W., Jabbari, K., Kalanon, M., Kurat, R., Lefebvre, P. A., Lemaire, S. D., Lobanov, A. V., Lohr, M., Manuell, A., Meier, I., Mets, L., Mittag, M., Mittelmeier, T., Moroney, J. V., Moseley, J., Napoli, C., Nedelcu, A. M., Niyogi, K., Novoselov, S. V., Paulsen, I. T., Pazour, G., Purton, S., Ral, J.-P., Riaño-Pachón, D. M., Riekhof, W., Rymarquis, L., Schroda, M., Stern, D., Umen, J., Willows, R., Wilson, N., Zimmer, S. L., Allmer, J., Balk, J., Bisova, K., Chen, C.-J., Elias, M., Gendler, K., Hauser, C., Lamb, M. R., Ledford, H., Long, J. C., Minagawa, J., Page, M. D., Pan, J., Pootakham, W., Roje, S., Rose, A., Stahlberg, E., Terauchi, A. M., Yang, P., Ball, S., Bowler, C., Dieckmann, C. L., Gladyshev, V. N., Green, P., Jorgensen, R., Mayfield, S., Mueller-Roeber, B., Rajamani, S., Sayre, R. T., Brokstein, P., Dubchak, I., Goodstein, D., Hornick, L., Huang, Y. W., Jhaveri, J., Luo, Y., Martínez, D., Ngau, W. C. A., Otiillar, B., Poliakov, A., Porter, A., Szajkowski, L., Werner, G., Zhou, K., Grigoriev, I. V., Rokhsar, D. S., & Grossman, A. R. (2007). The Chlamydomonas Genome Reveals the Evolution of Key Animal and Plant Functions. *Science*, 318(5848), 245-250. doi: 10.1126/science.1143609
- Park, Y., Sheetlin, S., Ma, N., Madden, T. L., & Spouge, J. L. (2012). New finite-size correction for local alignment score distributions. *BMC Res Notes*, 5, 286-286. doi: 10.1186/1756-0500-5-286
- Patel, R. K., & Jain, M. (2012). NGS QC Toolkit: A Toolkit for Quality Control of Next Generation Sequencing Data. *PLoS ONE*, 7(2), e30619. doi: 10.1371/journal.pone.0030619
- Ramos, J. L., Duque, E., Godoy, P., & Segura, A. (1998). Efflux pumps involved in toluene tolerance in *Pseudomonas putida* DOT-T1E. *J Bacteriol*, 180(13), 3323-3329.

- Roston, R., Gao, J., Xu, C., & Benning, C. (2011). Arabidopsis chloroplast lipid transport protein TGD2 disrupts membranes and is part of a large complex. *Plant J*, *66*(5), 759-769. doi: 10.1111/j.1365-313X.2011.04536.x
- Roston, R. L., Gao, J., Murcha, M. W., Whelan, J., & Benning, C. (2012). TGD1, -2, and -3 proteins involved in lipid trafficking form ATP-binding cassette (ABC) transporter with multiple substrate-binding proteins. *J Biol Chem*, *287*(25), 21406-21415. doi: 10.1074/jbc.M112.370213
- Roughan, P. G., & Slack, C. R. (1982). Cellular organization of glycerolipid metabolism. *Ann Rev Plant Physiol*, *33*(1), 97-132. doi: doi:10.1146/annurev.pp.33.060182.000525
- Sizova, I., Fuhrmann, M., & Hegemann, P. (2001). A *Streptomyces rimosus* aphVIII gene coding for a new type phosphotransferase provides stable antibiotic resistance to *Chlamydomonas reinhardtii*. *Gene*, *277*(1-2), 221-229. doi: http://dx.doi.org/10.1016/S0378-1119(01)00616-3
- Tardif, M., Atteia, A., Specht, M., Cogne, G., Rolland, N., Brugière, S., Hippler, M., Ferro, M., Bruley, C., Peltier, G., Vallon, O., & Cournac, L. (2012). PredAlgo: A new subcellular localization prediction tool dedicated to green algae. *Mol Biol Evol*, *29*(12), 3625-3639. doi: 10.1093/molbev/mss178
- Tamura, K., Stecher, G., Peterson, D., Filipowski, A., & Kumar, S. (2013). MEGA6: Molecular Evolutionary Genetics Analysis Version 6.0. *Mol Biol Evol*, *30*(12), 2725-2729. doi: 10.1093/molbev/mst197
- Tsai, C.-H., Warakanont, J., Takeuchi, T., Sears, B. B., Moellering, E. R., & Benning, C. (2014). The protein Compromised Hydrolysis of Triacylglycerols 7 (CHT7) acts as a repressor of cellular quiescence in *Chlamydomonas*. *Proc Natl Acad Sci U S A*, *111*(44), 15833-15838. doi: 10.1073/pnas.1414567111
- Villena, J. A., Roy, S., Sarkadi-Nagy, E., Kim, K. H., & Sul, H. S. (2004). Desnutrin, an adipocyte gene encoding a novel patatin domain-containing protein, is induced by fasting and glucocorticoids: ectopic expression of desnutrin increases triglyceride hydrolysis. *J Biol Chem*, *279*(45), 47066-47075. doi: 10.1074/jbc.M403855200
- Wang, Z., & Benning, C. (2011). *Arabidopsis thaliana* polar glycerolipid profiling by thin layer chromatography (TLC) coupled with gas-liquid chromatography (GLC). *J Visual Exp*, *49*(49), e2518-e2523.
- Wang, Z., Xu, C., & Benning, C. (2012). TGD4 involved in endoplasmic reticulum-to-chloroplast lipid trafficking is a phosphatidic acid binding protein. *Plant J*, *70*(4), 614-623. doi: 10.1111/j.1365-313X.2012.04900.x
- Weyer, K., Bush, D., Darzins, A., & Willson, B. (2010). Theoretical maximum algal oil production. *BioEnergy Res*, *3*(2), 204-213. doi: 10.1007/s12155-009-9046-x

- Xu, C., Fan, J., Cornish, A. J., & Benning, C. (2008). Lipid trafficking between the endoplasmic reticulum and the plastid in Arabidopsis requires the extraplastidic TGD4 protein. *Plant Cell*, 20(8), 2190-2204. doi: 10.2307/25224323
- Xu, C., Fan, J., Froehlich, J. E., Awai, K., & Benning, C. (2005). Mutation of the TGD1 chloroplast envelope protein affects phosphatidate metabolism in Arabidopsis. *Plant Cell*, 17(11), 3094-3110. doi: 10.1105/tpc.105.035592
- Xu, C., Fan, J., Riekhof, W., Froehlich, J. E., & Benning, C. (2003). A permease-like protein involved in ER to thylakoid lipid transfer in Arabidopsis. *EMBO J*, 22(10), 2370-2379. doi: 10.1093/emboj/cdg234
- Youssef, A., Laizet, Y. h., Block, M. A., Maréchal, E., Alcaraz, J.-P., Larson, T. R., Pontier, D., Gaffé, J., & Kuntz, M. (2010). Plant lipid-associated fibrillin proteins condition jasmonate production under photosynthetic stress. *Plant J*, 61(3), 436-445. doi: 10.1111/j.1365-313X.2009.04067.x
- Zäuner, S., Jochum, W., Bigorowski, T., & Benning, C. (2012). A Cytochrome b5-containing plastid-located fatty acid desaturase from *Chlamydomonas reinhardtii*. *Euk Cell*, 11(7), 856-863. doi: 10.1128/ec.00079-12
- Zerbino, D. R., & Birney, E. (2008). Velvet: algorithms for *de novo* short read assembly using de Bruijn graphs. *Genome Res*, 18(5), 821-829.

CHAPTER 3

Characterization of *Chlamydomonas* LIP4, a putative triacylglycerol lipase[†]

[†] This project was conducted in collaboration with Witawas Handee who contributed to Figure 3.8.

ABSTRACT

The metabolism of triacylglycerol (TAG) is not only important for maintaining an organism's homeostasis, but it is also key for coping with environmental stress. In microalgae, TAG accumulates in lipid droplets during stress conditions such as nutrient deprivation. When normal growth conditions resume, TAG is degraded to free fatty acids, which can be used for membrane synthesis or further metabolism to supply carbon in the form of acetyl-CoA and energy in the form of ATP and NADH to support growth and development. TAG lipase is the first enzyme of TAG degradation. Whole genome sequencing of *Chlamydomonas* has identified 130 genes for putative lipases; however none of these candidates has been directly shown to possess TAG lipase activity. A transcriptomic study revealed nine putative lipases, CrLIP1 through CrLIP9, which are differentially expressed during nitrogen deprivation. Based on its amino acid sequence, one of these, CrLIP4, is a homologue of a major Arabidopsis seed TAG lipase, SDP1. The goal of this study was to assess the TAG lipase activity of the CrLIP4 protein. Down-regulation of *CrLIP4* through artificial microRNA showed reduced TAG degradation in *Chlamydomonas*. The coding sequence of the gene was cloned and used for heterologous expression in both Arabidopsis and yeast and *in vitro* lipase assays. Introduction of *CrLIP4* cannot rescue the Arabidopsis *sdp1* mutant nor yeast TAG lipase mutants. However, the CrLIP4 recombinant protein showed TAG lipase activity toward triolein and *Chlamydomonas* TAG substrates *in vitro*. In summary, CrLIP4 showed TAG lipase activity in both *Chlamydomonas* and *in vitro* assays, but not in heterologous systems.

INTRODUCTION

All eukaryotic and some prokaryotic cells (such as *Mycobacterium*, *Streptomyces*, *Rhodococcus*, and *Nocardia*, Alvarez & Steinbuchel, 2002) sequester triacylglycerol (TAG) inside lipid droplets (LDs) in the cytosol as a way to store both energy and substrates for membrane lipid synthesis. During normal growth and development, TAG will be synthesized, stored, and broken down in response to the needs of the cell. In animals imbalanced LD homeostasis and TAG metabolism can lead to diseases such as lipodystrophies, obesity, insulin resistance and type 2 diabetes as summarized by Gross and Silver (2014). In angiosperms, TAG accumulates mainly in seeds. During germination, TAG is degraded to support growth of seedlings prior to the establishment of photosynthesis. In leaves, TAG is synthesized from membrane lipids in response to stress, e.g. freezing (Moellering *et al.*, 2010) and ozone fumigation (Sakaki *et al.*, 1990a; Sakaki *et al.*, 1990b). Senescence can also stimulate TAG accumulation in vegetative tissue as discussed in Troncoso-Ponce *et al.* (2013). In microalgae, TAG accumulation is observed in many stress responses such as high light and hypoxia as summarized by Goold *et al.* (2015), and nutrient deprivation, including nitrogen (N), iron (Fe), zinc (Zn), sulfur (S) and phosphorus (P) (Boyle *et al.*, 2012; Kropat *et al.*, 2011; Matthew *et al.*, 2009).

TAG breakdown is mediated through TAG lipase yielding diacylglycerol (DAG) and free fatty acid. In some cases, TAG lipase can further hydrolyze DAG or monoacylglycerol (MAG) yielding free fatty acids and the glycerol backbone. TAG lipase is a patatin-related phospholipase A (pPLA) (Scherer *et al.*, 2010), which has an esterase box GX SXG containing a serine in it as an active site. Lipases hydrolyze ester bonds at the interface of organic and aqueous phases as originally monitored by Schönheyder and Volqvartz (1945). This is due to the difference in solubility of the enzyme and its substrate. In addition, conformational changes are required for the enzyme to function properly (reviewed in Gill & Parish, 1997; Verger, 1976). In the inactive conformation, the catalytic motif is hidden. Upon exposure to an interface, the catalytic motif is exposed for substrate interaction. This process is controlled by a short helical fragment that acts as a lid covering the catalytic domain (Brady *et al.*, 1990; Brzozowski *et al.*, 1991; Kim *et al.*, 1997). Many lipases have been discovered in several organisms; examples of some of these are described below.

In yeast, Tgl3p, Tgl4p and Tgl5p were identified as having the conserved lipase motif and patatin domain (Athenstaedt & Daum, 2003, 2005; Kurat *et al.*, 2006). These three TAG lipases

are associated with LDs and contain hydrophobic domains but not transmembrane domains. An *in vitro* study revealed that Tgl3p acts on both TAG and DAG. Deletion of *TGL3*, the gene that encodes Tgl3p, resulted in increased amounts of TAG and hypersensitivity to cerulenin, a fatty acid synthase inhibitor (Athenstaedt *et al.*, 1999). Lipase assays showed that Tgl4p degrades TAG (preferentially TAG-containing myristic and palmitic acids) but not DAG (Kurat *et al.*, 2006). In contrast to Tgl3p and Tgl4p, which both showed lipase activity *in vitro* and *in vivo*, Tgl5p only showed activity *in vitro* on TAG that contains 26:0 fatty acid (Athenstaedt & Daum, 2005). The *tgl3Δtgl4Δtgl5Δ* triple mutant accumulated high levels of TAG; furthermore, no TAG degradation was observed in the presence of cerulenin (Athenstaedt & Daum, 2005).

Adipose Triglyceride Lipase (ATGL), a major intracellular TAG lipase in mammals, was discovered for its TAG lipase activity by three different groups (Jenkins *et al.*, 2004; Villena *et al.*, 2004; Zimmermann *et al.*, 2004). The transcript level of ATGL in mice and humans is highest in adipose tissue, for which the enzyme was named. ATGL contains a lipase motif and patatin domain and is localized in LDs. Mice deficient in ATGL exhibited increased adipose mass that led to accumulation of TAG in several tissues (Haemmerle *et al.*, 2006). High levels of TAG in the heart of these mice led to cardiac dysfunction and premature death. ATGL is regulated through hormonal stimulation by the protein Comparative Gene Identification-58 (CGI-58). During inactivation, CGI-58 binds to perilipin A; once stimulated, perilipin A is phosphorylated, and CGI-58 is free to bind ATGL and induce TAG lipase activity (Zechner *et al.*, 2009).

The major TAG lipase in seeds of Arabidopsis is named SUGAR-DEPENDENT 1 (SDP1) (Eastmond, 2006). SDP1 was discovered through ethyl methanesulfonate (EMS) mutagenesis. The *sdp1-1* point mutant is impaired in TAG degradation in the seed, which is important for seedling growth. *SDP1* encodes a protein containing a patatin-like acyl-hydrolase domain, which is also found in yeast Tgl3p and human ATGL. Recombinant SDP1 hydrolyzed TAG and DAG *in vitro*. Fusion of SDP1 with the green fluorescent protein revealed that SDP1 is associated with the surface of LDs. An attempt to identify other TAG lipases in Arabidopsis was carried out in double, triple and quadruple mutants of *SDP1-LIKE* (*SDP1L*), *ATGL-LIKE* and *CGI-58-LIKE* in the *sdp1-5* (a T-DNA insertion line) background (Kelly *et al.*, 2011). Only SDP1 and SDP1L were found to be required for seedling growth.

Although more than one hundred putative lipases are encoded in the *Chlamydomonas* genome (Merchant *et al.*, 2007), none of the TAG lipases has been characterized. Transcriptomic analysis in *Chlamydomonas* revealed nine putative lipases, named *CrLIP1-CrLIP9*, that are either up or down regulated during N-replete and N-deprived conditions (Miller *et al.*, 2010). Based on *in vitro* analyses, CrLIP1 has been shown to possess DAG lipase activity and it can hydrolyze polar lipids *in vitro* (Li *et al.*, 2012). Down-regulation of *CrLIP1* resulted in slower degradation of TAG in the mutant relative to wild type when N is resupplied to starved cells, in which TAG has accumulated in LDs. In addition, expression of *CrLIP1* in a yeast *tgl3Δtgl4Δ* double mutant can rescue the TAG phenotype, which is similar to that of the *tgl3Δtgl4Δtgl5Δ* triple mutant. Among the nine lipases, CrLIP4 shares the most sequence identity to the well-characterized *Arabidopsis* SDP1. The current study sought to determine if CrLIP4 has TAG lipase activity.

RESULTS

***CrLIP4* is down-regulated during N-deprivation.** A transcriptomic study of *Chlamydomonas* showed that expression of *CrLIP4* was down-regulated during N-deprivation, during which TAG accumulates (Miller *et al.*, 2010). In order to monitor the expression pattern of this gene in detail, quantitative reverse transcription PCR (qRT-PCR) was used to analyze *CrLIP4* transcript levels at different time points. The culture of the parental line *Chlamydomonas* strain dw15.1 (PL) was grown in N-replete Tris-Acetate-Phosphate (TAP) medium until mid-log phase (0 h) was achieved. The culture was N-deprived for 48 h and then resupplied with N and grown for another 48 h. RNA was isolated from samples taken at 24 h intervals; qRT-PCR of *CrLIP4* was performed and normalized to an internal standard. The level of *CrLIP4* transcript dropped sharply after 24 h of N deprivation and remained low throughout this condition (Figure 3.1). After N-resupply, the *CrLIP4* transcript increased to about 30% of the initial level. The level of *CrLIP4* transcript was inversely related to the TAG level (Figure 3.1), pointing to its potential role as a TAG lipase.

CrLIP4 contains DUF3336, transmembrane, and patatin domains and a large IDR at its C terminus.

Structure and domains of CrLIP4 were predicted based on the amino acid sequence translated from the coding sequence through hmmscan 3.1b1 (Eddy, 2009). Apparently, CrLIP4 contains a

DUF3336 (domain of unknown function) and a patatin domain (Figure 3.2A). These two domains are also present in Arabidopsis SDP1 and yeast Tgl3p – 5p (Figure 3.3). The domain homology allowed us to hypothesize that CrLIP4 may function as a TAG lipase. In addition, the carboxyl end of CrLIP4 contains a large intrinsically disordered region (IDR) as predicted by four different programs (Figure 3.2B-3.2E). Furthermore, more phosphorylation sites were predicted to be localized in the IDR compared to the rest of the protein by the Disorder Enhanced Phosphorylation Predictor (DEPP) (Iakoucheva *et al.*, 2004) (Figure 3.2F). A transmembrane domain search through the transmembrane hidden Markov model (TMHMM) (Krogh *et al.*, 2001; Sonnhammer *et al.*, 1998) revealed that CrLIP4 contains one transmembrane domain (TMD) (Figure 3.3A). Although the gene sequences are divergent (Fig 3B), the GX SXG motif of the patatin domain is consistently preceded by a TMD in CrLIP4, Tgl3p, Tgl5p and ATGL, and by hydrophobic regions in SDP1 and Tgl4p (Figure 3.3A), suggesting that the patatin domain needs to be anchored and/or situated close to a membrane. Note that SDP1, Tgl4p and Tgl5p also contain IDRs (Figure 3.3A), however, sequence alignments show no similarity among these regions (Figure 3.3B). In addition, secondary structure prediction revealed that CrLIP4, SDP1, Tgl3p, Tgl4p, Tgl5p, and ATGL contain multiple helices (α -, π -, and 3_{10} -helix) upstream of IDR regions (Figure 3.3A).

Phylogenetic analysis of CrLIP4. Based on a homology search using the CrLIP4 sequence against sequences deposited at the National Center for Biotechnology Information (NCBI), 45 orthologues were selected for further analysis. A domain search through hmmscan 3.1b1 (Eddy, 2009) revealed that all of the homologues contain a patatin domain (Table 3.1). The DUF3336 domain is also common to all presumed homologues except ATGL. For this reason, human ATGL was excluded from the alignment and phylogenetic tree reconstruction. Structurally, the DUF3336 domain is always present at the N terminus followed by a few amino acids and the patatin domain. Protein alignment was performed for the regions containing DUF3336 and the patatin domains with MUSCLE (Edgar, 2004) using the same criteria as described in Chapter 2. Phylogenetic tree reconstruction was undertaken from the protein alignment with the same setting as described in Chapter 2. This analysis revealed that CrLIP4 is grouped with presumed orthologues from plants but not with those from fungi or bacteria (Figure 3.4).

Down-regulation of *CrLIP4* transcript resulted in slower TAG degradation.

In vivo analysis of *CrLIP4* was conducted through artificial microRNA (amiRNA) knockdown in *Chlamydomonas*. Two constructs of amiRNA vectors targeting *CrLIP4* at either the 5' or 3' region were designed based on WMD3- Web MicroRNA Designer (<http://wmd3.weigelworld.org/cgi-bin/webapp.cgi?page=Home;project=stdwmd>). The linearized plasmid containing *AphVIII*, a paromomycin resistance gene, was introduced with the glass bead method as described in the Materials and Methods section into the *Chlamydomonas* PL genome. The mRNA levels of the transformants were first tested with qRT-PCR. From 15 tested transformants of each construct, amiRNA targeting the 3' region of *CrLIP4* provided more clones with reduced *CrLIP4* transcript level than did the amiRNA targeting the 5' region (Figure 3.5A).

Eleven amiRNA knockdown lines showed highly reduced levels (less than 75% of PL level) of the *CrLIP4* transcript from both constructs (Figure 3.5A). Among these eleven lines, seven of them were screened for TAG degradation during N-resupply. From the seven, four lines accumulated more TAG than did the empty vector control. TAG levels in these four lines were then tested at different time points: 48 h after removal of N (time 0); 10 and 24 h after N-resupply. Three of the four lines showed higher TAG levels at 24 h after N-resupply. Another experiment was carried out to include additional time points at 12, 16 and 20 h after N-resupply. The result confirmed that these three lines showed higher TAG levels at 24 h after N-resupply (Figure 3.5B). This result suggested that lowering the expression level of *CrLIP4* resulted in a delay in TAG degradation. Note that the three lines contain amiRNA targeting the 3' region of *CrLIP4*. This suggested that knocking down *CrLIP4* was more effective when the 3' region of the gene was targeted.

***CrLIP4* coding sequence cloned from *Chlamydomonas* dw15.1 contains four amino acid changes and a five amino acid insertion compared to the gene model.** The *CrLIP4* nucleotide sequence contains a region with extremely high GC content (79%). The overall GC content of the coding sequence is 72%. This high GC content made cloning of the full *CrLIP4* coding sequence very challenging. Thus, the coding sequence of *CrLIP4* was cloned in five overlapping fragments from *Chlamydomonas* PL cDNA. These five segments were joined two fragments at a time by PCR using the forward primer from the 5' piece and the reverse primer from the 3' piece. The sequence of the cloned *CrLIP4* differs from the gene model 319691 available in the

JGI v.4 database, with differences in the identity of four amino acids and with a five amino acid insertion in the IDR region (Figure 3.6). These differences are likely to be due to the unusually high GC content of the gene, which causes technical difficulties for standard sequencing. Indeed, I was unable to sequence this region with the normal Sanger procedures. To eliminate DNA secondary structure during the sequencing reactions, dimethyl sulfoxide, betaine and 7-deaza-dGTP were added to the sequencing reaction mix (Musso *et al.*, 2006). The cloned coding sequence was used for all subsequent experiments.

CrLIP4 was not able to rescue yeast *tgl3Δ*, *tgl4Δ*, or *tgl3Δtgl4Δ* mutants. CrLIP4 shares 26, 45 and 32% amino acid identity with yeast Tgl3p, Tgl4p and Tgl5p, respectively. Tgl5p was reported to exhibit only *in vitro* TAG lipase activity toward TAG with 26-carbon acyl groups (Athenstaedt & Daum, 2005). In addition, the phenotype of the *tgl3Δtgl4Δtgl5Δ* triple mutant and *tgl3Δtgl4Δ* double mutant are the same. Therefore, functional analysis was conducted by overexpressing CrLIP4 with an HA tag in the yeast *tgl3Δtgl4Δ* double mutant. Yeast WT strain yMK839 (Kuo *et al.*, 1998) and/or *tgl3Δtgl4Δ* were transformed with either pMK595 empty vector or pMK595-CrLIP4. Expression of CrLIP4 was detected with HA antibodies in *tgl3Δtgl4Δ* transformed with pMK595-CrLIP4 (*CrLIP4-HA tgl3Δtgl4Δ*) but not the WT or *tgl3Δtgl4Δ* transformed with the pMK595 empty vector (Figure 3.7A). Note that multiple bands were detected with the HA antibody in the *CrLIP4-HA tgl3Δtgl4Δ* lines. These multiple bands could be a result of protein degradation in the yeast cell, multiple start codons or early termination of mRNA translation. The yeast cultures were then grown until stationary phase was achieved. Cerulenin (an inhibitor of fatty acid synthesis) or the same volume of ethanol was added to the cultures. Cell density (cells/ml) and TAG concentration (fmol/ml) were monitored at 0, 3 and 7 h after addition of cerulenin or ethanol.

In the presence of cerulenin, all cell types remained in stationary phase (Figure 3.7B, upper left), however TAG concentrations in all cell lines dropped as the cells metabolized their storage lipids. The TAG concentration of *CrLIP4 tgl3Δtgl4Δ* was essentially identical to the *tgl3Δtgl4Δ* double mutant (Figure 3.7B, lower left), and both were higher than TAG levels of wild-type cells. At 7 h after cerulenin addition, TAG concentrations of *CrLIP4 tgl3Δtgl4Δ* and *tgl3Δtgl4Δ* were reduced to less than half of the original value.

Without cerulenin, cell numbers of all cell types were constant during the first 3 h and then increased to almost double (Figure 3.7B, upper right). The TAG concentration of *CrLIP4*

tgl3Δtgl4Δ was similar to that of the double mutant and higher than that of WT (Figure 3.7B, lower right). At 3 h, the TAG concentration of all three lines dropped, while at 0 and 7 h, TAG concentration of all was relatively unchanged. This drop in TAG concentration at 3 h could be due to smaller cell size of newly budded cells as mentioned above. It is crucial to note that this TAG analysis in *CrLIP4 tgl3Δtgl4Δ* experiment was carried out only once. Without more replicates, a solid conclusion cannot be drawn from this result.

These experiments showed that *CrLIP4* was unable to rescue the TAG phenotype of the yeast *tgl3Δtgl4Δ* double mutant. However, it was possible that the impact of the loss of lipase activity in the *tgl3Δtgl4Δ* double mutant is greater than any compensation *CrLIP4* activity could provide. Therefore, introduction of pMK595-*CrLIP4* into each single mutant (*tgl3Δ* or *tgl4Δ*) was carried out. Stationary phase cultures of *tgl3Δ* and *tgl4Δ* with pMK595 empty vector (EV) or pMK595-*CrLIP4* were used to determine TAG concentration. The HA antibody detected a smaller than expected size of *CrLIP4*-HA in both *CrLIP4 tgl3Δ* and *CrLIP4 tgl4Δ* mutants (Figure 3.8A). TAG concentrations in both *CrLIP4 tgl3Δ* and *CrLIP4 tgl4Δ* were higher than the mutants with empty vector controls (Figure 3.8B). Despite the large error bars, these results were similar to that of *CrLIP4* overexpression in the yeast double mutant.

***CrLIP4* could not complement Arabidopsis *sdp1* mutants.** Since the *CrLIP4* amino acid sequence shares 41% identity to *SDP1* and carries patatin and DUF3336 domains similar to *SDP1*, I hypothesized that *CrLIP4* would rescue the Arabidopsis *sdp1* mutant phenotype. In order to test this hypothesis, *CrLIP4* cDNA under the control of the CaMV 35S promoter was introduced into *sdp1-4* or *-5* null mutants, which are T-DNA insertion lines. Expression of the *CrLIP4* transcript was measured in the first generation of transgenic plants (Figure 3.9A). Transgenic plants were selected and self-crossed. Only the transgenic lines that contain a single insertion and are homozygous were selected for further analysis. Since the original *sdp1-1* mutant was reported to have a post-germination growth phenotype, root length of four-day old seedlings grown in Murashige and Skoog (MS) medium without sucrose was measured (Figure 3.9B). The *sdp1* mutants and the *sdp1* mutants expressing *CrLIP4* (*CrLIP4 sdp1*) had shorter roots than did Col-0 WT when grown in no sucrose medium (Figure 3.9B and 3.9C). This difference in root length was not observed in seedlings grown in regular medium (Figure 3.9D). I conclude that *CrLIP4* was unable to rescue the *sdp1* mutant phenotype.

Recombinant CrLIP4 and SDP1 protein production in *Escherichia coli*. Despite the unsuccessful attempts to complement phenotypes of yeast and Arabidopsis TAG lipase mutants, the amiRNA experiment pointed to the role of *CrLIP4* as a TAG lipase. To test for lipase activity *in vitro*, a recombinant His-tagged CrLIP4 was expressed in *E. coli* strain BL21-CodonPlus(DE3)-RP (Stratagene), which contains extra tRNAs corresponding to rare codons usually present in GC-rich genomes. To prevent leaky expression before induction, glucose was added to the medium. Recombinant CrLIP4 was mainly in the insoluble fraction after both lysis buffer extraction and re-extraction with 0.25% Tween 20 (Figure 3.10A, middle and right panels). This could be due to either high level of expression or to the insertion of CrLIP4 into membranes. The latter case is possible since CrLIP4 is predicted to contain one transmembrane domain at the N-terminus (Figure 3.3A). A minute amount of recombinant CrLIP4 was detected with anti-His antibody in the soluble fraction (s1 in Figure 3.10A). In order to avoid protein denaturation, protein purification with an Ni-NTA column was carried out from this soluble fraction. In addition, neutral lipids from *E. coli* expressing CrLIP4 were separated by thin layer chromatography (TLC). CrLIP4 expression caused changes in the pattern of neutral lipids and free fatty acids on the TLC plate (Figure 3.10B).

SDP1 recombinant protein was also produced to use as a positive control in the lipase assay. Recombinant His-tagged SDP1 was expressed in *E. coli* strain BL21-CodonPlus(DE3)-RIPL (Stratagene), containing extra tRNAs for AT-rich genomes. The SDP1 protein was also mostly insoluble (Figure 3.10C). Note that the protein was degraded over time (Figure 3.10C). Since SDP1 is not predicted to contain a transmembrane domain (Figure 3.3A), lack of protein solubility could be due to its high level of expression. Despite the very low amounts of recombinant protein in the soluble fraction, SDP1 was detected and purified (Figure 3.10C).

Recombinant CrLIP4 showed TAG lipase activity *in vitro*. Different TAG substrates (*Chlamydomonas* TAG or triolein) were used to assay for lipase activity of various amounts of recombinant CrLIP4, with recombinant SDP1 as a positive control. The reactions were incubated at room temperature for 6 h. Total lipids were extracted and separated on a TLC plate. In the presence of recombinant SDP1 or CrLIP4, DAG and free fatty acid (FFA) were present at higher levels compared to the negative control (no protein) for both types of substrate (Figure 3.11A). DAG and FFA bands were stronger for 2 μ g of protein than 1 μ g of protein and stronger TAG lipase activity was observed when triolein was used as a substrate (Figure 3.11A). Therefore,

further characterizations were conducted with 2 μg of triolein as a substrate and 2 μg of recombinant protein. Longer incubation times yielded more FFA (Figure 3.11B). The pH optimum was tested from 5.0 to 11.0. CrLIP4 showed TAG lipase activity from pH 5.0 to 9.0 (Figure 3.11C), with the highest activity detected at pH 8.0.

DISCUSSION

Metabolism of neutral lipids, e.g. triacylglycerol (TAG), is not only essential to cellular homeostasis, but it is also a key part of survival for an organism undergoing stress. TAG mobilization serves as the initial step of energy utilization for growth and development. TAG lipases are responsible for the first step of TAG catabolism. This study has been focused on characterization of a putative TAG lipase in *Chlamydomonas*.

Despite the fact that *Chlamydomonas* has been studied intensely, TAG lipase has not been identified in *Chlamydomonas* (Li-Beisson *et al.*, 2015). A transcriptomic study of *Chlamydomonas* growing under N-deprived compared to N-replete conditions revealed 9 differentially-expressed putative lipases named *CrLIP1* through *CrLIP9* (Miller *et al.*, 2010). Eight of these were cloned and tested for TAG lipase activity in a yeast *tgl3 Δ tgl4 Δ* double mutant (Li *et al.*, 2012). One of the putative lipases CrLIP1 not only rescued the yeast mutant but showed lipase activity toward diacylglycerol. Only one of the eight putative lipases, *CrLIP4*, was not amenable to clone at the time. Since CrLIP4 is a homologue of the Arabidopsis major seed TAG lipase, SDP1, it deserved further attention, and the gene was ultimately cloned and characterized in this study.

As mentioned earlier, two transcriptomic experiments showed that CrLIP4 transcript is reduced during N-deprivation (Miller *et al.*, 2010; Tsai *et al.*, 2014). This observation was confirmed by gene-specific amplification through quantitative reverse transcription PCR (Figure 3.1). In addition, gene-expression is reduced when the cell enters stationary and later declining phase and during the period of TAG accumulation (Lv *et al.*, 2013). Furthermore, dark anoxia can induce transcription of *CrLIP4* within 30 minutes of treatment (Hemschemeier *et al.*, 2013).

Since the transcript of *CrLIP4* is less abundant during N-deprivation, it was expected that when N was resupplied, the transcript of *CrLIP4* would increase to the same level as during the N-replete condition. However, while TAG levels recovered to original amounts, the transcript level of *CrLIP4* did not fully recover (Figure 3.1). Conceivably, transcription of *CrLIP4* requires more time than allowed in this experiment. In addition to transcriptional regulation, post-

translational regulation could also play a role in CrLIP4 activity. By analogy, the Arabidopsis homologue *SDP1* has transcript levels that do not correlate with enzyme activity during seed maturation (Eastmond, 2006). The author suggested that SDP1 is regulated posttranscriptionally. Finally, it is possible that one or more additional TAG lipases could be (fully or partially) responsible for TAG degradation during N-resupply. In order to investigate the contribution of CrLIP4 to TAG metabolism, a combination of Western blot analysis of CrLIP4 and lipase activity assays was used.

Knocking down *CrLIP4* transcript through artificial miRNA resulted in slower degradation of TAG during N-resupply following N-starvation (Figure 3.5). Therefore, I concluded that CrLIP4 likely acts as a TAG lipase during N-resupply.

CrLIP4 contains patatin and DUF3336 domains, which typify TAG lipases in other biological systems, including Arabidopsis SDP1 and yeast Tgl3p, Tgl4p and Tgl5p (Figure 3.3A and Table 3.1). The patatin domain is well established for its esterase/hydrolase activity (Scherer *et al.*, 2010), while the DUF3336 domain is of unknown function. CrLIP4 shares 41% amino acid identity with Arabidopsis SDP1. Based on TMHMM, CrLIP4 contains one hydrophobic region, which could be a transmembrane domain (Figure 3.3A). This hydrophobic region is located at the beginning of the patatin domain before the GX SXG motif. The presence of a hydrophobic region and its position and α -helices are conserved in CrLIP4 homologues including SDP1, Tgl3p, Tgl4p, Tgl5p, and ATGL (Figure 3.3A). As summarized by Thiam *et al.* (2013), three types of proteins can be targeted to lipid droplets; amphiphathic helix-containing proteins, unfolded helix-containing proteins, and hairpin-containing proteins. Since the Arabidopsis, yeast, and human lipases associate with lipid droplets (Athenstaedt & Daum, 2003, 2005; Eastmond, 2006; Gronke *et al.*, 2005; Zimmermann *et al.*, 2004), their hydrophobic regions and α -helices are likely to be responsible for their targeting to lipid droplets. However, the mechanisms for protein targeting to lipid droplets are largely unknown and more conclusive evidence is needed to test this hypothesis. Since the catalytic site of TAG lipase is in the soluble portion of the protein, it is possible that the enzyme undergoes conformational changes upon interaction with the hydrophobic region in lipid droplets, which would allow the hydrophobic substrate (TAG) to enter the active site of the enzyme.

A lipase assay showed that recombinant CrLIP4 exhibited TAG lipase activity toward triolein and *Chlamydomonas* TAG substrates (Figure 3.11). This *in vitro* activity supports the

conclusions of *in vivo* activity in the artificial miRNA experiment (Figure 3.5B). For future experiments, the kinetics of CrLIP4 activity should be tested.

Despite these similarities to the Arabidopsis and yeast proteins, introduction of *CrLIP4* into the Arabidopsis *sdp1* mutant and the yeast *tgl3Δ*, *tgl4Δ*, *tgl3Δtgl4Δ* mutants failed to rescue the phenotypes. These unsuccessful attempts to complement the phenotypes could be due to the fact that these proteins are too evolutionarily divergent. The failure to obtain heterologous complementation using *CrLIP4* is similar to our results from attempts to introduce *CrTGD2* into different organisms as shown in Chapter 2. In the cases of both CrLIP4 and CrTGD2, amino acid similarity between the Arabidopsis and the Chlamydomonas proteins are about 40%. The divergence of intrinsic disorder regions (IDRs) in CrLIP4 (Figure 3.2 and 3.3A) could also contribute to the failure of the attempts at heterologous complementation. Although IDRs were also predicted in SDP1, Tgl4p and Tgl5p, sequence alignments showed lack of similarity in these regions (Figure 3.3B). IDRs can function in protein-protein interaction or serve as a regulatory or signaling region (Dunker *et al.*, 2002; Uversky, 2013a, 2013b). This is also indicated by the presence of many predicted phosphorylation sites (Figure 3.2F). Therefore, function of CrLIP4 could be dependent on a protein partner, which may not be present in divergent organisms. Another possible explanation is the high GC content of the Chlamydomonas gene, which can cause poor protein expression especially in the case of the Arabidopsis *sdp1* mutant, since the Arabidopsis genome is AT rich. Although I could monitor transcription of the recombinant gene, in the absence of an epitope tag or antiserum against CrLIP4, I could not determine if the protein was expressed.

MATERIALS AND METHODS

Algal strain and growth condition. Chlamydomonas cell wall-less strain dw15.1 (cw15, nit1, mt⁺) was used in this study. Growth conditions were the same as previously described in Chapter 2.

Artificial microRNA (amiRNA) knockdown. Target sequences of amiRNA were determined through the Target function of WMD3- Web MicroRNA Designer (<http://wmd3.weigelworld.org/cgi-bin/webapp.cgi?page=Home;project=stdwmd>). Primers for amiRNA of CrLIP4 were designed at either the 5' or 3' ends of the transcript through the Designer page of WMD3. Sequences of amiRNA and primers can be found in Table 3.2.

Oligonucleotides were then cloned into the pChlamiRNA3int vector according to (Molnar *et al.*, 2009). The resulting amiRNA constructs were linearized with *KpnI* restriction enzyme. The digested products were separated via agarose gel electrophoresis. The bands were cut and purified. The linearized plasmids were then used to transform a *Chlamydomonas* culture by the glass bead method based on (Kindle, 1990) with minor modifications; the cells were grown in Tris-acetate-phosphate (TAP) liquid medium, and the use of polyethyleneglycol (PEG) was omitted. The transformants were selected on TAP medium with 10 µg/mL Paromomycin. Selected colonies were grown on TAP liquid medium and used to test transcript level by real-time PCR and TAG level by thin layer chromatography (TLC) and gas chromatography (GC) as described below.

RNA isolation and cDNA synthesis. RNA was prepared from 5-10 ml mid-log phase culture of *Chlamydomonas* with RNeasy Plant Mini Kit (QIAGEN) following the manual's instruction. The isolated RNA was treated with Rnase-Free DNase (QIAGEN) to eliminate genomic DNA contamination. Two µg of RNA were then used for cDNA synthesis with either RETROscript[®] Reverse Transcription Kit (Ambion) or Quantiscript Reverse Transcription (QIAGEN).

Quantitative reverse transcription PCR (qRT-PCR). The transcript level of *CrLIP4* was monitored with qRT-PCR on either the Applied Biosystems 7500 Fast real-time PCR system or Eppendorf realplex². Primers Lip4-jw2 F and Lip4-jw2 R were used to amplify the *CrLIP4* transcript. Sequences of these primers are given in Table 3.3. The reference gene used for *Chlamydomonas* samples was *Receptor of activated protein kinase C (RACK1)*, while *Isopentenyl-diphosphate Delta-isomerase II (IPP2)* was used as a reference gene for *Arabidopsis* samples. Sequences of primers used in these experiments are shown in the Table 3.2. The qRT-PCR data were calculated based on the $2^{-\Delta\Delta C_T}$ method as previously described (Livak & Schmittgen, 2001).

Bioinformatic analysis. A homology search of CrLIP4 was carried out by BLASTP at the web site of the National Center for Biotechnology Information (NCBI) (Altschul *et al.*, 1997). Amino acid sequences that had more than 60% coverage and had an e-value lower than e-10 were selected for further analysis. Protein domains were searched against amino acid sequences from the blast search result with hmmscan 3.1b1 (Eddy, 2009). Disorder prediction was carried out with 4 different programs; PONDR-VSL2, PONDR-VLXT, PONDR-VL3

(<http://www.pondr.com/cgi-bin/PONDR/pondr.cgi>), and IUPred (<http://iupred.enzim.hu/>) (Dosztanyi *et al.*, 2005). Phosphorylation sites associated with intrinsically disordered regions were predicted by DEPP (<http://www.pondr.com/cgi-bin/PONDR/depp.cgi>). Transmembrane helices were predicted with TMHMM (<http://www.cbs.dtu.dk/services/TMHMM/>). Protein secondary structure was analyzed with PredictProtein (<https://www.predictprotein.org/home>) (Yachdav *et al.*, 2014).

Phylogenetic reconstructions Amino acid sequence alignment of CrLIP4 homologues in the region encompassing the patatin domains through DUF3336 was performed with MUSCLE3.8 as described in Chapter 2. The phylogenetic reconstruction was carried out through MEGA6 as described in Chapter 2.

Lipid analysis. Lipid analysis of TAG for *Chlamydomonas* was carried out as described in Chapter 2. For the lipase assays, the solvent for neutral lipid separation consisted of chloroform, acetone and acetic acid (96: 4: 1 v/v/v). Lipid extraction from yeast was carried out in a similar manner to lipid extraction from *Chlamydomonas* except glass beads (425-600 μm , Sigma-Aldrich) were added to the cells resuspended in extraction solvent.

Cloning of the *CrLIP4* coding sequence. Because *CrLIP4* has a region with high GC content (about 70%), cloning the entire cDNA in one experiment was not successful. Therefore, the cDNA was cloned as five overlapping fragments. PCR reactions were carried out with either GoTaq[®] DNA polymerase (Promega) or Phusion[®] High-Fidelity DNA Polymerase (New England Biolab). In addition to dNTP and MgCl₂, 0-8% dimethyl sulfoxide (DMSO) was added to the PCR reactions. Sequences of primers used for amplifying each fragment, joining fragments and sequencing are provided in Table 3.3. Each fragment, including joined fragments, was ligated with pGEM[®]-T Easy Vector (Promega) and transformed into *E. coli* strain DH5 α . Transformed bacteria were selected on Luria Bertani (LB) medium with 100 $\mu\text{g}/\text{ml}$ ampicillin, 5 mmol of Isopropyl β -D-1-thiogalactopyranoside (IPTG) and 1 mg of 5-bromo-4-chloro-3-indolyl- β -D-galactopyranoside (X-Gal). Plasmids were prepared from *E. coli* transformants and sent for sequencing. Clones containing the correct DNA sequence were used for fragment joining.

Fragments of *CrLIP4* were cut out from the pGEM-T Easy plasmid with *EcoRI*. Fragment joining was performed sequentially two fragments at a time with PCR. Fragments 1 and 2, and

fragments 3 and 4 were joined with primers F-1 and R2, and primers F3 and F4.3, respectively. The resulting fragment, 3-4, was joined to fragment 5 with primers F3 and R6. The 2 large fragments, 1-2 and 3-4-5, were joined using primers F-1 and R6. The full *CrLIP4* fragment was cloned into the pGEM[®]-T Easy vector for sequence determination. The clone containing the correct sequence was then used as a template for PCR amplification for pENTR[™]/D-TOPO (Invitrogen[™]) cloning with Lip4-F1 kozak and Lip4-R6 primers.

Expression of CrLIP4 in yeast *tgl3Δtgl4Δ* double, *tgl3Δ*, and *tgl4Δ* single mutants. *CrLIP4* from pENTR/D-CrLIP4 was amplified with Phusion polymerase using 595Lip4 F and R primers. 10% DMSO was added to the reaction. The sequence was determined with MHK98 and MHK99 primers. Sequences of cloning and sequencing primers are provided in Table 3.3. A restriction digest of the pMK595 vector (Luo *et al.*, 2010) was performed with *NotI*. Linearized pMK595 and *CrLIP4* DNA from PCR amplification were co-transformed into the yeast WT strain yMK839 following the method from (Gietz *et al.*, 1992). The linearized vector and *CrLIP4* were then joined by endogenous homologous recombination of the yeast cell (Ma *et al.*, 1987). The yeast transformants were selected on synthetic complete medium without uracil (SC-U). A few single colonies were picked and grown on liquid SC-U medium for testing protein expression. Colonies showing expression of the *CrLIP4* cDNA were used for plasmid isolation. Plasmids from the WT yeast were then transformed into *E. coli* DH5 α for sequencing the plasmid pMK595-*CrLIP4*. The pMK595 plasmid and the pMK595-*CrLIP4* plasmid of correct DNA sequence were then used to transform the yeast *tgl3Δtgl4Δ* double mutant, strain yXL005 (Li *et al.*, 2012) and the yeast *tgl3Δ* and *tgl4Δ* single mutants. The transformants were tested for CrLIP4 expression by western blot analysis against HA-tag.

Western blot analysis. Total protein extracts for yeast were prepared from either freshly harvested or frozen yeast cell pellets as previously described in Chapter 2 with some modifications. The cell pellets were resuspended in 2X sample buffer, and acid washed glass beads were added. The mixture was vortexed vigorously, followed the same remaining steps as described in Chapter 2. Total protein preparation from *E. coli* was carried out in a similar manner without addition of glass beads. Protein quantification, gel electrophoresis, blotting and immuno detection were performed similarly to that described in Chapter 2. Primary antibodies for yeast and *E. coli* samples were anti-HA and anti-His mouse antibodies, respectively. The secondary antibody was anti-mouse, conjugated with horseradish peroxidase.

Analysis of CrLIP4 overexpression in yeast *tgl3Δtgl4Δ* double, and *tgl3Δ* and *tgl4Δ* single mutants. Single colonies of yeast WT or double mutant containing pMK595 empty vector or pMK595-*CrLIP4* were inoculated in SC-U liquid medium. The cultures were grown at 30°C for 20 h (stationary phase). The cultures were then diluted with fresh SC-U liquid medium at OD₆₀₀ = 3 for a total volume of 25 ml. Either 25 μl of ethanol or 10 mg/ml cerulenin was added to the culture. Cells were harvested at 0, 1, 3, 5 and 7 h after addition of cerulenin for TAG separation, and direct FAME and cell concentration monitoring with Z2 Coulter Counter (Beckman Coulter) were performed. In the case of *tgl3Δ* and *tgl4Δ* single mutants, 4-day-old cells were harvested for lipid analysis after growth in casamino acid medium lacking uracil (CAA-U).

Plant materials and growth conditions. Arabidopsis *sdp1-4* (SALK_102887) and *sdp1-5* (SALK_076697) mutants were obtained from the Salk Institute for Genomic Analysis Laboratory. Arabidopsis Col-0 was used as a wild-type control in all Arabidopsis experiments throughout this study. The plants were germinated on Murashige and Skoog (MS) solid medium either with or without 1% (w/v) sucrose. The seeds were stratified for at least 48 h prior to incubation in a growth chamber to induce germination. One- to two-week old seedlings were transferred to soil. The plants were maintained in a 16/8 h light/dark cycle with temperatures of 22/20°C and light intensity at 120/0 μmol.m⁻².sec⁻¹.

Genomic DNA isolation from Arabidopsis leaves. A young leaf of Arabidopsis was used to isolate genomic DNA. The leaf was ground in 200 μl of extraction buffer (0.2 M Tris-HCl, pH 7.5, 0.25 M NaCl, 25 mM EDTA and 0.5% SDS) followed by addition of 400 μl of absolute ethanol. The mixture was then shaken gently and centrifuged at 13,000 X g for 5 min. The supernatant was discarded. The pellet was washed with 200 μl of 70% ethanol, centrifuged at 13,000 X g for 1 min and air dried. The dried pellet was resuspended in TE buffer (10 mM Tris-HCl, pH7.5 and 1 mM EDTA) and stored at 4°C until further use.

Genotyping of *sdp1* T-DNA insertion lines. Determination of homozygosity for the *sdp1-4* and *sdp1-5* mutants was carried out based on <http://signal.salk.edu/tdnaprimers.2.html>. Primers used in this analysis are listed in Table 3.3. PCR amplification of the WT gene was carried out with primers LP-sdp1-4 or LP-sdp1-5 and RP-sdp1-4 or RB-sdp1-5. The T-DNA inserted gene was amplified with primers LBb1.3 and RP-sdp1-4 or RP-sdp1-5. Two separate PCR reactions were carried out for each plant tested; one for amplifying the WT locus and another for amplifying the

T-DNA insertion. The WT plants show one band for LP and RP primers. Heterozygous plants show a band for LBB1.3 and RP primers in addition to another band for LP and RP primers. Homozygous plants show only one band for primers LBB1.3 and RP.

Construction of pMDC32-*CrLIP4* plasmid. *CrLIP4* was cloned into pMDC32 vector through a clonase reaction from pENTR/D-*CrLIP4* following instructions from Invitrogen.

Preparation of Agrobacterium competent cells. A single colony of *Agrobacterium tumefaciens* strain GV3101 was grown in 5 ml of LB medium with 25 µg/ml gentamycin and 34 µg/ml rifampicin overnight at 28°C. This culture was then inoculated into a larger volume of fresh medium and grown until OD₆₀₀ reached 0.3-0.6. One ml of this culture was then aliquoted into a 1.5 ml centrifuge tube and chilled on ice for 2-3 min before centrifugation at 13,000 X g for 3 min at 4°C. The supernatant was removed, and the pellet was resuspended into 1 ml cold 10 mM Tris-HCl, pH 7.5. The cells were then centrifuged at 13,000 X g for 3 min at 4°C to remove the supernatant. The pellet was then resuspended in 100 µL of cold LB medium. The cells were flash frozen with liquid N₂ and stored at -80°C.

Agrobacterium transformation. Agrobacterium competent cells were thawed on ice. One to two µg of pMDC32-*CrLIP4* plasmid DNA was added to the cells. The mixture was frozen in liquid N₂ for 5 min and quickly transferred to a 37°C water bath for 5 min. One ml of LB medium was added to the cell mixture which was then incubated at 28°C with shaking for 2.5 h. After incubation, the cells were centrifuged at 5,000 X g for 5 min to remove the supernatant. The cell pellet was then resuspended in 100 µl LB medium and spread onto LB medium containing Bacto agar. The cells were incubated at 28°C for 2 days until colonies formed.

Arabidopsis transformation. Transformation of Agrobacterium containing pMDC32-*CrLIP4* plasmid into Arabidopsis was carried out with the floral dip method as described previously (Clough & Bent, 1998). Seeds obtained from transformed plants were screened for transformants with Hygromycin B resistance as described previously (Harrison *et al.*, 2006). The number of insertions and homozygosity were tested in the second and third generations by determining the ratio of seedlings resistant and susceptible to Hygromycin B. Transgenic plants were grown and self-crossed until homozygosity was obtained in the third generation. Transgenic plants with a single insertion were selected for further analysis.

Construction of pET28-*AtSDP1* and pET28-*CrLIP4* plasmids. *AtSDP1* coding sequence was cloned into pENTR/D-TOPO with SDP1-pENTR F and SDP1-pENTR R primers using Q5[®] High-Fidelity DNA Polymerase (New England Biolabs). Sequences of primers are provided in Table 3.3. The *AtSDP1*-pENTR/D-TOPO plasmid was transformed into *E. coli* strain DH5 α . Single colonies were picked and grown in liquid LB medium for plasmid preparation. Sequences of the plasmids were determined with primers listed in Table 3.3. A clone containing the correct sequence was then used as a template for pET28-*AtSDP1* construction with primers SDP1-pET28_NheI F and SDP1-pET28_NotI R. pENTR/D-*CrLIP4* was used as a template to construct pET28-*CrLIP4* with Lip4-pET28-F4 and Lip4-pET28-R2 primers. *AtSDP1* and *CrLIP4* were cloned into pET28b+ (Novagen), an *E. coli* expression vector, with a restriction digestion and ligation method. For *AtSDP1*, the pET28b+ vector and the PCR product of SDP1 were digested with *NheI* and *NotI*. In the case of *CrLIP4*, the PCR product and pET28b+ vector were digested with *HindIII* and *XhoI*. After digestion, ligations of the two sets of genes and vectors were carried out. The ligation products were transformed into *E. coli* DH5 α for recovery of plasmids.

Recombinant *AtSDP1* and *CrLIP4* protein production. Since *AtSDP1* could not be produced in the BL21(DE3) strain of *E. coli*, it was produced in the *E. coli* strain BL21-CodonPlus(DE3)-RIPL (Stratagene), which can express proteins from AT-rich genomes. After transformation, a single colony was inoculated into 100 mL LB medium with 50 μ g/mL kanamycin at 37°C for 8 h. Eight mL of the seed culture was then inoculated into 50 mL fresh medium and incubated for another 75 min. Protein expression was induced by adding 1 mM IPTG into the culture. The cells were harvested for protein purification after 30 min of induction at 37°C.

CrLIP4 was also unable to be produced in the *E. coli* strain BL21(DE3). As an alternative, *E. coli* strain BL21-CodonPlus(DE3)-RP (Stratagene), which is able to express proteins from GC-rich genomes, was used. The culture of *E. coli* containing pET28-*CrLIP4* was grown in LB medium containing 50 μ g/mL kanamycin and 1% glucose at 37°C for 8 h. The seed culture was used to inoculate into fresh medium with 1% glucose and was grown overnight. Expression of the cloned cDNA was induced in fresh medium without glucose with addition of 0.1 mM IPTG. The cells were incubated at 37°C for 6 h and harvested by centrifugation for protein purification.

Recombinant protein purification. The cell pellet was resuspended in an equal volume of lysis buffer (50 mM NaH₂PO₄, 300 mM NaCl and 10 mM imidazole) to the original culture volume. Cells were lysed by addition of 1 mg/ml lysozyme and shaken for 30 min on ice. The cells were

then sonicated on ice at power level 4.0 for 10 sec a total of 6 times (MISONIX Sonicator 3000). The soluble and non-soluble fractions were separated by centrifugation at 10,000 X g for 30 min at 4°C. The supernatant was then collected and mixed with 1 volume of Ni-NTA slurry to 4 volumes of supernatant. The mixture was incubated with shaking at 4°C for 30 min and loaded into a column. The flow-through was allowed to drain. The column was washed with 4 volumes of wash buffer (50 mM NaH₂PO₄, 300 mM NaCl and 20 mM imidazole) to the initial lysate-Ni slurry volume. Finally, the protein was eluted from the column with elution buffer (50 mM NaH₂PO₄, 300 mM NaCl and 250 mM imidazole) 6 times. A small volume from each step was collected for further analysis by western blot.

Lipase assay. TAG substrates were prepared from either *Chlamydomonas* total lipids or commercial triolein. *Chlamydomonas* TAG was separated from total lipids as described in Chapter 2. Triolein was separated on a TLC plate to remove free fatty acids and other products of TAG degradation. The silica powder containing the TAG band from triolein separation was scraped and used for lipid extraction. Both *Chlamydomonas* TAG and triolein were dried and resuspended in chloroform. The concentration of TAG was determined by GC. Dry TAG was resuspended at 100 mM with 5% (w/v) gum arabic in water. The mixture was sonicated at 20 W for 30 sec.

A lipase assay was carried out according to (Eastmond, 2006). TAG substrate in gum arabic was mixed with assay buffer (50 mM Bis-Tris propane-HCl pH 8.0) at 1-2 μM final concentration. In addition, 2 mM dithiothreitol (DTT) and 2 mM CaCl₂ were added to the reaction. The mixture was incubated at room temperature with shaking for 6 h. The reaction was stopped by adding lipid extraction solvent. The lipid was separated on a TLC plate with a neutral lipid solvent system as described above. The resulting TLC plate was stained with iodine vapor.

ACCESSION NUMBERS

CrLIP4 accession number, 319691, was obtained from Joint Genome Institute (JGI) v4. Arabidopsis SDP1 accession number, AT5G04040.1, was obtained from The Arabidopsis Information Resource (TAIR, www.arabidopsis.org). Accession numbers of amino acid sequences used for the phylogenetic tree reconstruction in Figure 3.4 were given in the parenthesis following the scientific name.

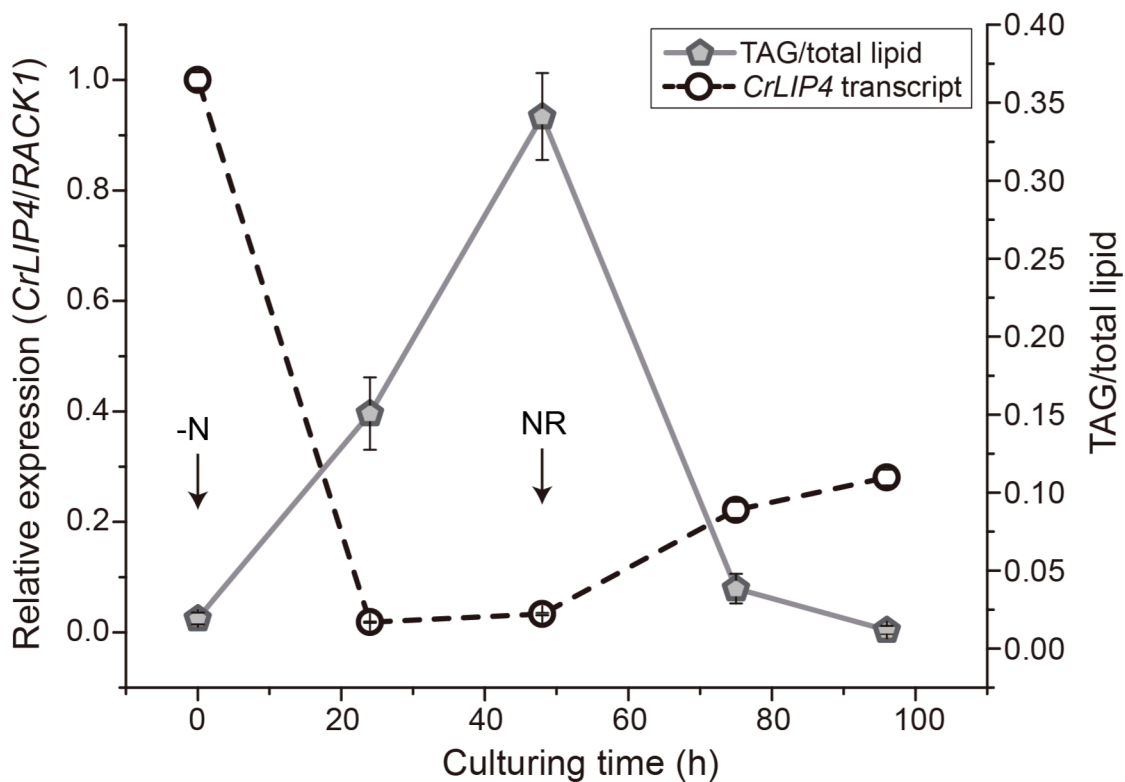


Figure 3.1. Relative expression of *CrLIP4* transcript compared to TAG concentration during N deprivation and N resupply.

Relative expression of *CrLIP4* transcript compared to the *Receptor of activated protein kinase C (RACK1)* (left y-axis), and relative TAG level (right y-axis) compared to total lipid fatty acids of *Chlamydomonas* PL. Arrows indicate the times when N was deprived (-N) and resupplied (NR). Three biological replicates were averaged and standard deviations are shown.

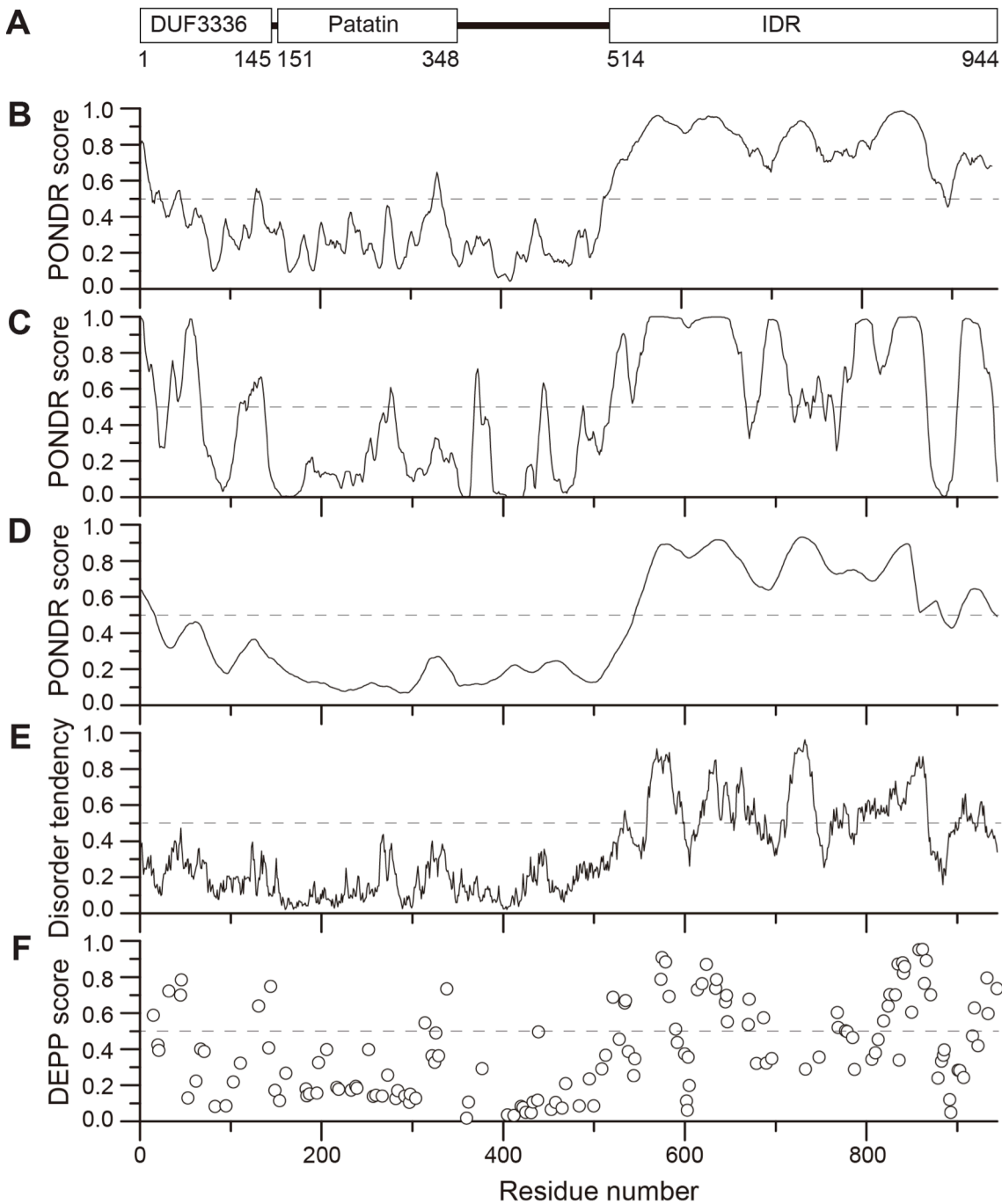


Figure 3.2. Amino acid sequence analysis of CrLIP4.

(A) Protein domains present in CrLIP4. Disorder prediction by (B) PONDRL-VSL2, (C) PONDRL-VLXT, (D) PONDRL-VL3, and (E) IUPred. (F) Phosphorylation prediction sites predicted by DEPP. The broken line at value 0.5 indicates the threshold of disorder or putative phosphorylation sites.

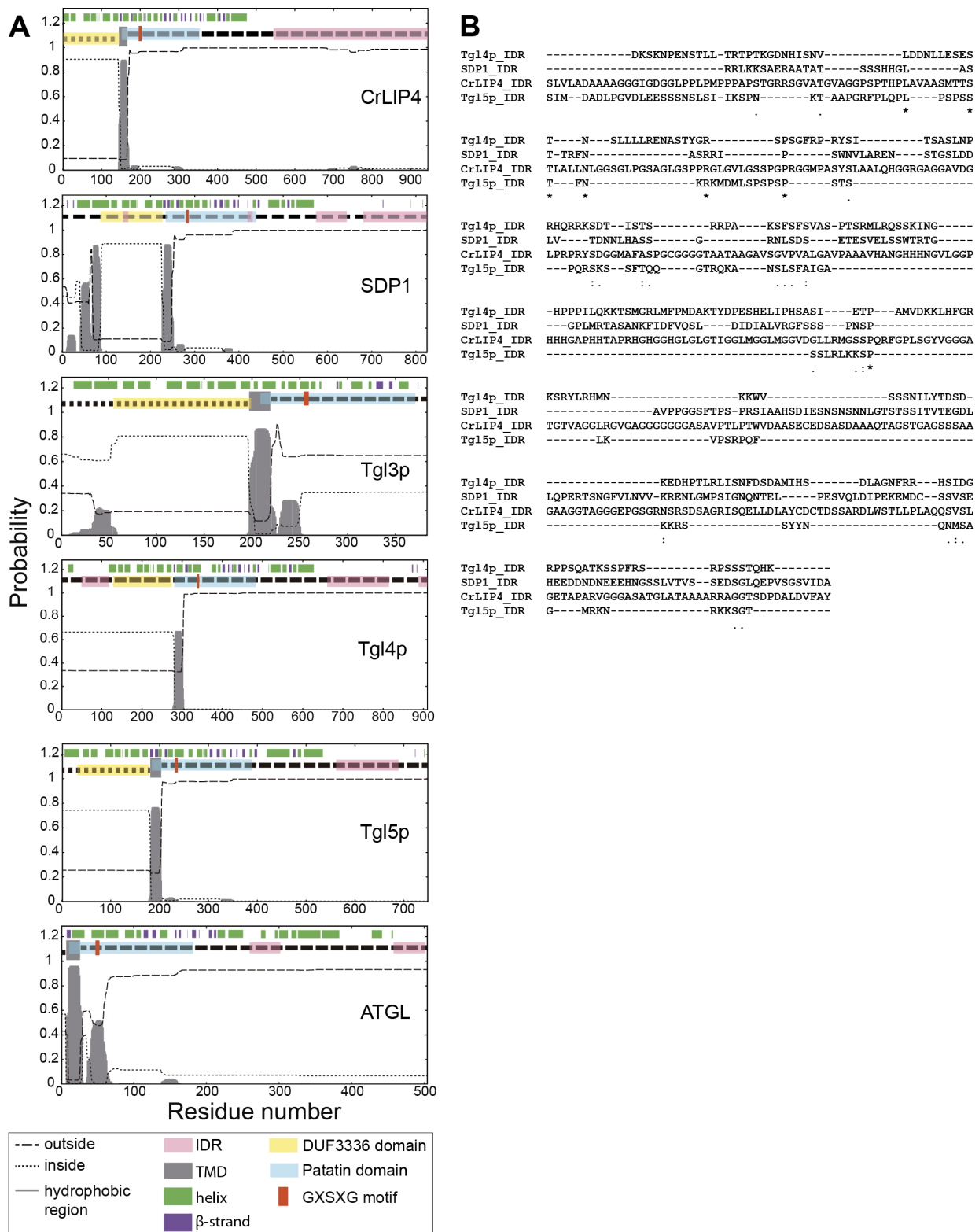


Figure 3.3. Prediction of transmembrane helices (TMD) and alignment of intrinsic disorder regions (IDRs) of CrLIP4 homologues.

Figure 3.3. (cont'd)

(A) Prediction of TMD of amino acid sequences through TMHMM Topology, secondary structures (helix and β -strand), domains and conserved motives of each protein are shown above the plots. (B) Amino acid sequence alignment of IDRs as shown in (A) from CrLIP4, Arabidopsis SDP1, yeast Tgl4p and Tgl5p and human? ATGL. The alignment was carried out through MUSCLE3.8.

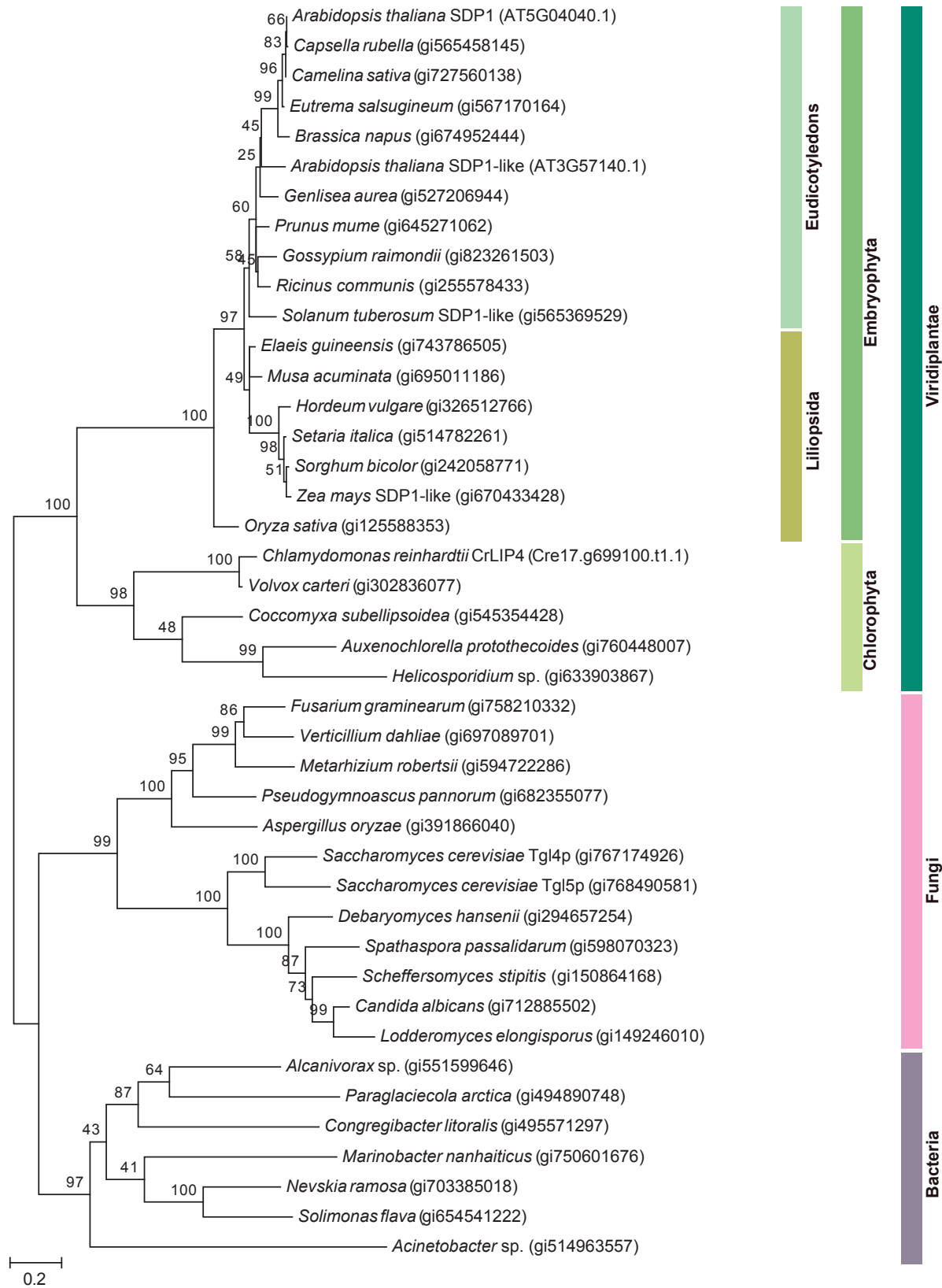


Figure 3.4. Phylogenetic analysis of CrLIP4 homologues.

Figure 3.4. (cont'd)

The evolutionary history was inferred based on Maximum Likelihood. The tree with the highest log likelihood (-12809.1964) is shown. The percentage of trees in which the associated taxa clustered together (1000 repeats) is shown above the branches. The tree is drawn to scale with branch lengths corresponding to the number of substitutions. The accession number for each protein is given in the parenthesis following the scientific name. Accession numbers for *Chlamydomonas*, *Arabidopsis* and other organisms are from the Joint Genome Institute (JGI), the Arabidopsis Information Resource (TAIR), and National Center for Biotechnology Information (NCBI), respectively. Groups of organisms are indicated by colored bars.

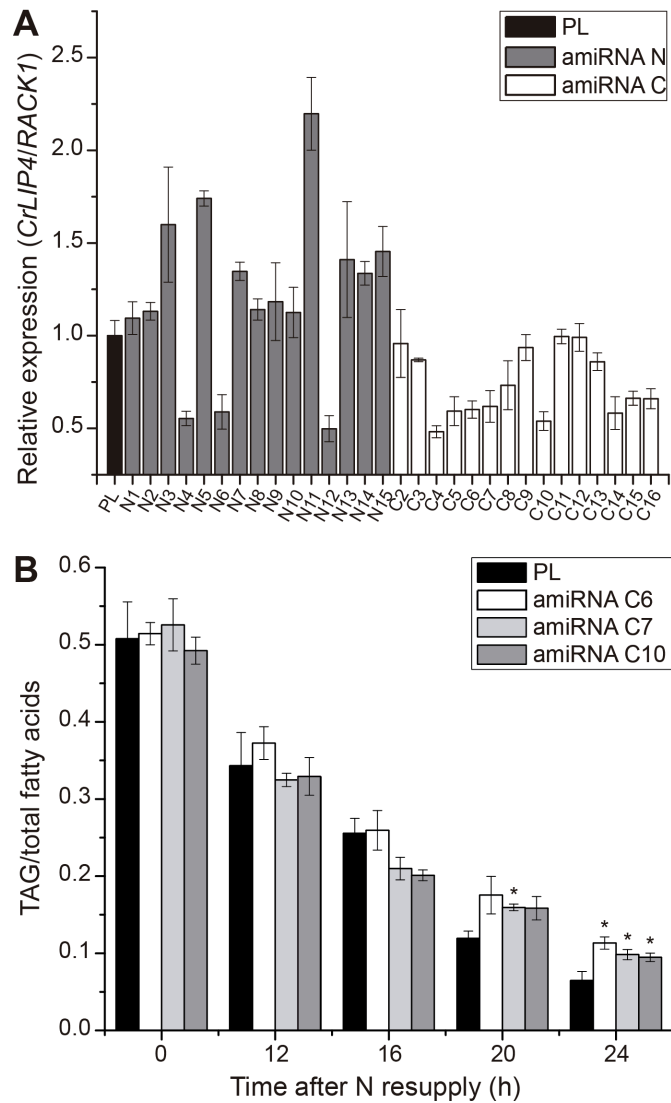


Figure 3.5. Down regulation of *CrLIP4* transcript with artificial microRNA (amiRNA).

(A) Relative expression of *CrLIP4* transcript compared to the *RACK1* of the PL and amiRNA knockdown lines. The amiRNA knockdown lines targeting the 5' or 3' regions were named with N or C followed by number, respectively. (B) TAG concentration (TAG/total fatty acids) of selected amiRNA knockdown lines from (A) at various time points after N-resupply following N-deprivation. Three technical (A) or biological (B) replicates were averaged and standard deviations are shown. Differences in means of PL and amiRNA lines in (B) were compared with a paired-sample student *t*-test (* p-value ≤ 0.05).

MUSCLE (3.8) multiple sequence alignment

```

CrLIP4      MDARHRRRACLRRLLSAANSYEQWREIAEQLYALEEADMPAGDVSTRRAARLYDRKLLLE
319691_JGI_v4 MDARHRRRACLRRLLSAANSYEQWREIAEQLYALEEADMPAGDVSTRRAARLYDRKLLLE
*****
                DUF3336
CrLIP4      KTNHLRSVRATGNVKEIMLALRTDLIRNIANIAKSQLHEHFVSI PDDIGRYLAEMKEQLA
319691_JGI_v4 KTNHLRSVRATGNVKEIMLALRTDLIRNIANIAKSQLHEHFVSI PDDIGRYLAEMKEQLA
*****
CrLIP4      QLVWEPEDELSAEKLAFFRETRHTFGRTALLSGGGGLGTFHIGVVKALFERQLLPRVL
319691_JGI_v4 QLVWEPEDELSAEKLAFFRETRHTFGRTALLSGGGGLGTFHIGVVKALFERQLLPRVL
*****
CrLIP4      AGSSVGSIVCGIIATKTDALERDLFSRLDEFDVGFFSNSRAVELVQHLINKGSLQDMSYM
319691_JGI_v4 AGSSVGSIVCGIIATKTDALERDLFSRLDEFDVGFFSNSRAVELVQHLINKGSLQDMSYM
*****
                Patatin
CrLIP4      IKKLRGLMGDATFLEAYERTGRILNVTVC PADTNEPPRLNLYLTAPNALIWSAVAASSAF
319691_JGI_v4 IKKLRGLMGDATFLEAYERTGRILNVTVC PADTNEPPRLNLYLTAPNALIWSAVAASSAF
*****
CrLIP4      PGLYPAQHILARNSRGEIIRFSAQSTNDSLERRWRDGSLELDLPVQALGEMFNCNHFLVS
319691_JGI_v4 PGLYPAQHILARNSRGEIIRFSAQSTNDSLERRWRDGSLELDLPVQALGEMFNCNHFLVS
*****
CrLIP4      QTNPHIVPLLNKKALSRKWANVLEAELKHRCQVAQWLLPEWVPSKWMLMFTQAWEGDIT
319691_JGI_v4 QTNPHIVPLLNKKALSRKWANVLEAELKHRCQVAQWLLPEWVPSKWMLMFTQAWEGDIT
*****
CrLIP4      MTLPSALWHL SKTIVNPTTEELIRNVKVEG VATWEKISAIECNCSIEATLDKCLANIANQ
319691_JGI_v4 MTLPSALWHL SKTIVNPTTEELIRNVKVEG VATWEKISAIECNCSIEATLDKCLANIANQ
*****
CrLIP4      VRGYRLQRMHNRI PSWLHMSAVGLPAVASWGDSEFAEAAAASIAAAAASGGARGT SWGTPH
319691_JGI_v4 VRGYRLQRMHNRI PSWLHMSAVGLPAVASWGDSEFAEAAAASIAAAAASGGARGT SWGTPH
*****
CrLIP4      AAATSLVLADAAAAGGGIGDGGLPFLPMPPPPAPSTGRRSGVATGVAGGSPSPHPLAVAAS
319691_JGI_v4 AAATSLVLADAAAAGGGIGDGGLPFLPMPPPPAPSTGRRSGVATGVAGGSPSPHPLAVAAS
*****
CrLIP4      MTTSTLALLNLGGSGLPGSAGLGSPPRGLGVLGSSPGPRGMPASYS LAALQHGGRGAGG
319691_JGI_v4 MTTSTLALLNLGGSGLPGSAGLGSPPRGLGVLGSSPGPRGMPASYS LAALQHGGRGAGG
*****
CrLIP4      AVDGLPRPRYSDGGMAFASPGCGGGGTAATAAGAVSGVPVALGAVPAAAVHANGHHHNGV
319691_JGI_v4 AVDGLPRPRYSDGGMAFASPGCGGGGTAATAAGAVSGVPVALGAVPAAAVHANGHHHNGV
*****
                IDR
CrLIP4      LGGPHHHGAPHHTAPRHGGHGLGLGTIGGLMGGLMGGVDGLLRMGSSPQRFGLSGYV
319691_JGI_v4 LGGPHHHGAPHHTAPRHGGHGLGLGTIGGLMGGLMGGVDGLLRMGSSPQRFGLSGYV
*****
CrLIP4      GGGATGTVAGGLRGVAGGGGGGASAVPTLPTWVDAASECEDSASDAAAQTAGSTGAGS
319691_JGI_v4 GGGATGTVAGGLRGVAGGGGGGASAVPTLPTWVDAASECEDSASDAAAQTAGSTGAGS
*****
CrLIP4      SSAAGAAGGTAGGGEFGSGRNSRSDSAGRISQELLDLAYCDCTDSSARDLWSTLLPLAQQ
319691_JGI_v4 SSAAGAAGGTAGGGEFGSGRNSRSDSAGRISQELLDLAYCDCTDSSARDLWSTLLPLAQQ
*****
CrLIP4      SVSLGETAPARVGGGASATGLATAAAARRAGGTSDFDALDVFAY
319691_JGI_v4 SVSLGETAPARVGGGASATGLATAAAARRAGGTSDFDALDVFAY
*****

```

Figure 3.6. Sequence alignment of the *CrLIP4*.

Sequence alignment of the *CrLIP4* coding sequence cloned from *Chlamydomonas* strain dw15.1 and the *CrLIP4* gene model (accession number 319691 from JGI v4). Boxes show DUF3336 and patatin domains and the intrinsically disordered region (IDR). A conserved lipase domain (GX SXG) is underlined.

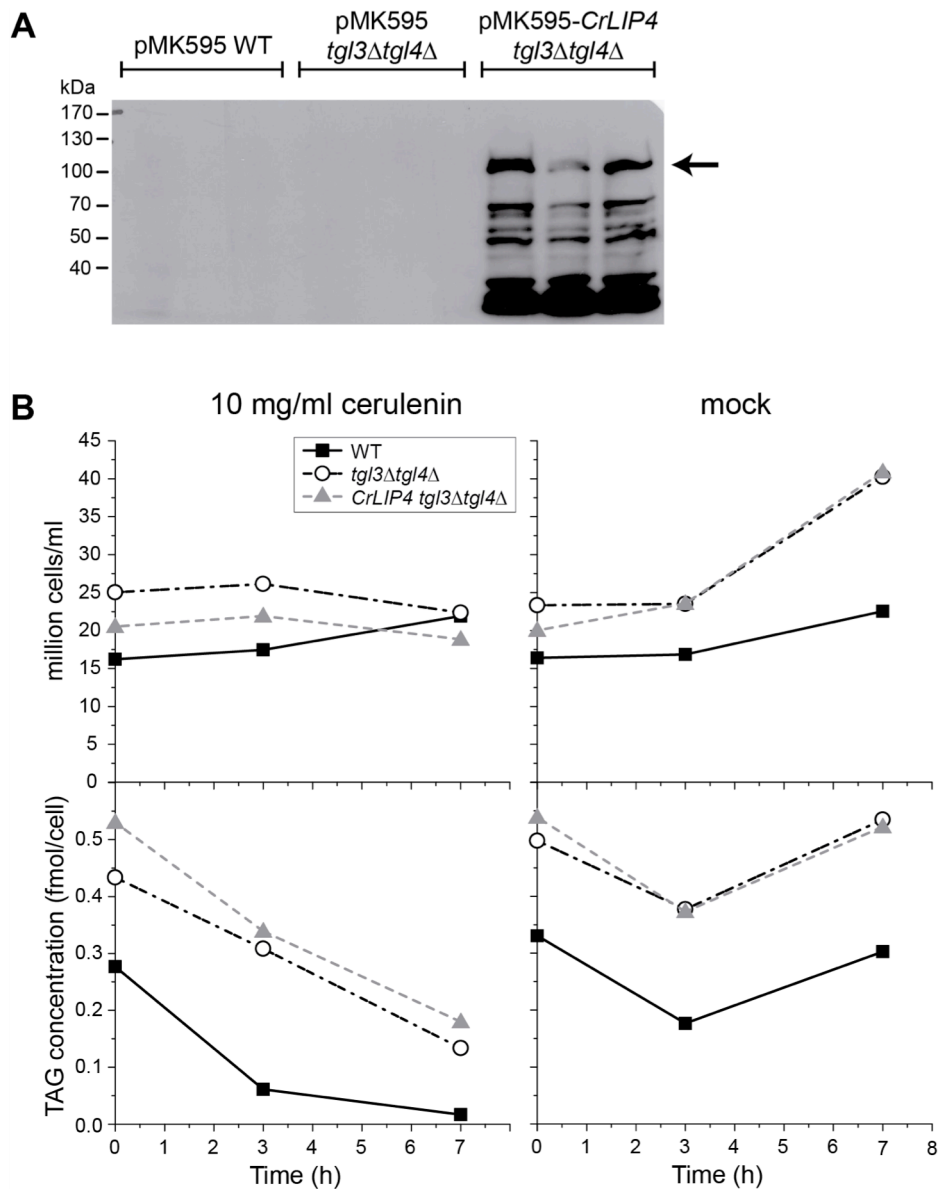


Figure 3.7. Heterologous expression of *CrLIP4* in the yeast *tgl3Δtgl4Δ* double mutant.

(A) Western blot analysis of pMK595 or pMK595-*CrLIP4* introduced into WT or the *tgl3Δtgl4Δ* yeast double mutant. An arrow indicates the size of the expected *CrLIP4* protein. (B) Growth (million cells/ml) and TAG concentration (fmol/cell) of yeast WT, *tgl3Δtgl4Δ* double mutant, and the double mutant expressing *CrLIP4* (*CrLIP4 tgl3Δtgl4Δ*). Cerulenin (10 mg/ml, left panel) or equal volume of ethanol (mock, right panel) was added to the stationary phase cultures at time 0.

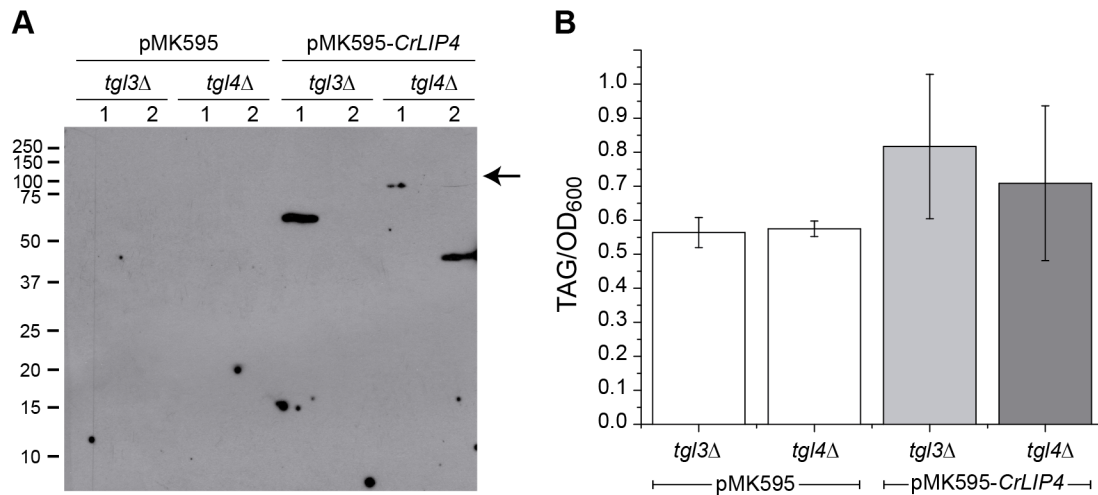


Figure 3.8. Heterologous expression of *CrLIP4* in yeast *tgl3Δ* and *tgl4Δ* mutants.

(A) Western blot analysis against HA tag of pMK595 or pMK595-*CrLIP4* introduced into the yeast *tgl3Δ* and *tgl4Δ* mutants. Two biological replicates were shown. Numbers on the left indicate molecular weight distribution in kDa. An arrow indicates expected size of *CrLIP4* at 115 kDa. (B) TAG concentration of *tgl3Δ* and *tgl4Δ* with either pMK595 or pMK595-*CrLIP4* introduced into their genomes. Two biological replicates were averaged and standard deviations are shown.

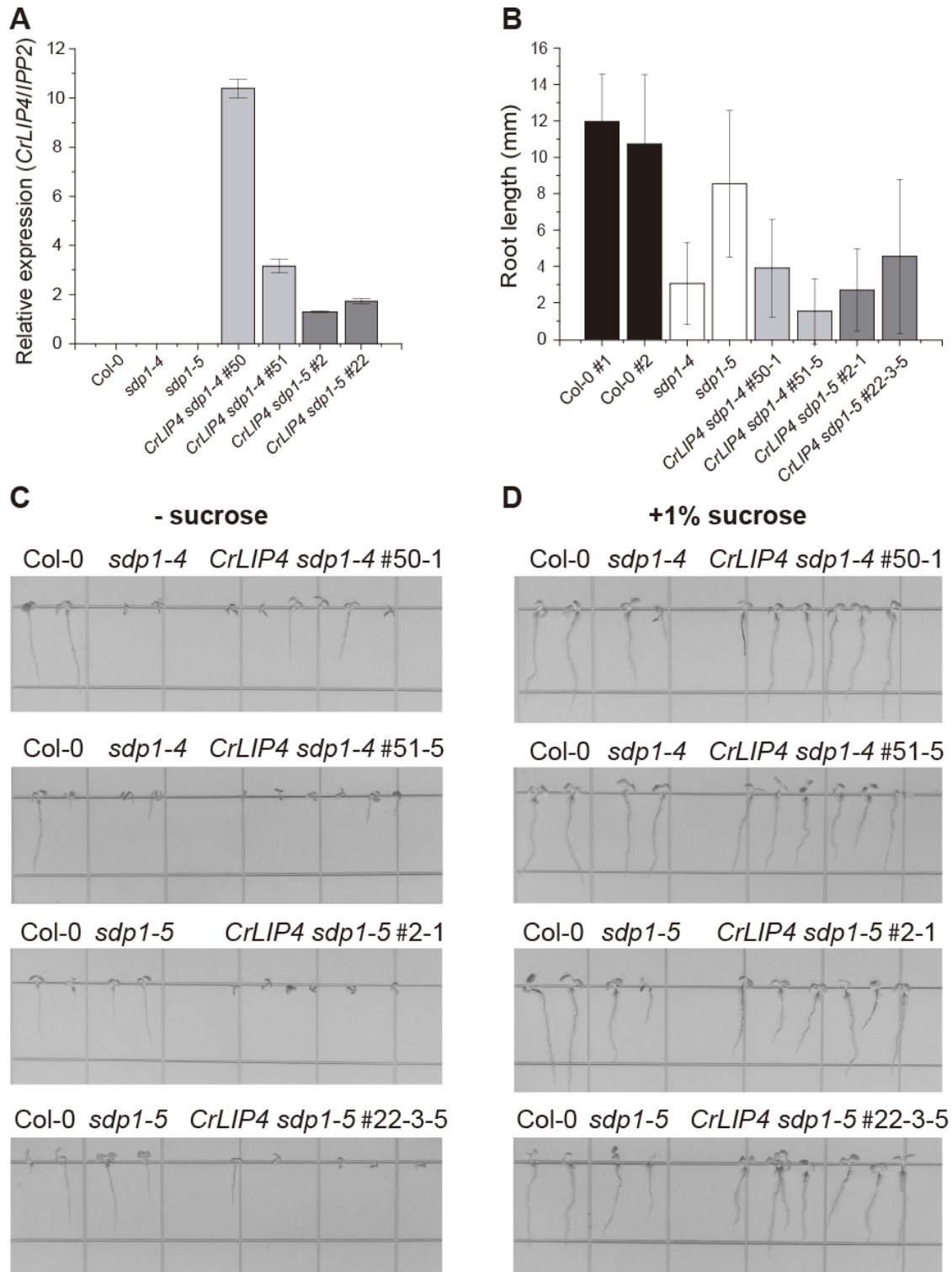


Figure 3.9. Heterologous expression of CrLIP4 in Arabidopsis *sdp1* mutants.

Figure 3.9. (cont'd)

Seeds were germinated in the absence (A, B, C) or presence (D) of 1% sucrose.

(A) Relative expression of *CrLIP4* transcript compared to *Isopentenyl-diphosphate Delta-isomerase II (IPP2)* in the T1 generation by RT-PCR. Three technical replicates were averaged and standard deviations are shown. (B) Root length (mm) of seedlings of WT (Col-0), the *sdp1-4* and *sdp1-5* mutants, and the T2 or T3 generations of *CrLIP4* expressed in either the *sdp1-4* or *sdp1-5* background (*CrLIP4 sdp1-4* or *CrLIP4 sdp1-5*). In all cases, one hundred biological replicates were averaged and standard deviations are shown. (C) Photographs of seedlings of lines in (B) grown in ½ MS medium without sucrose. (D) Photographs of seedlings of lines in (B) grown in ½ MS medium with 1% sucrose.

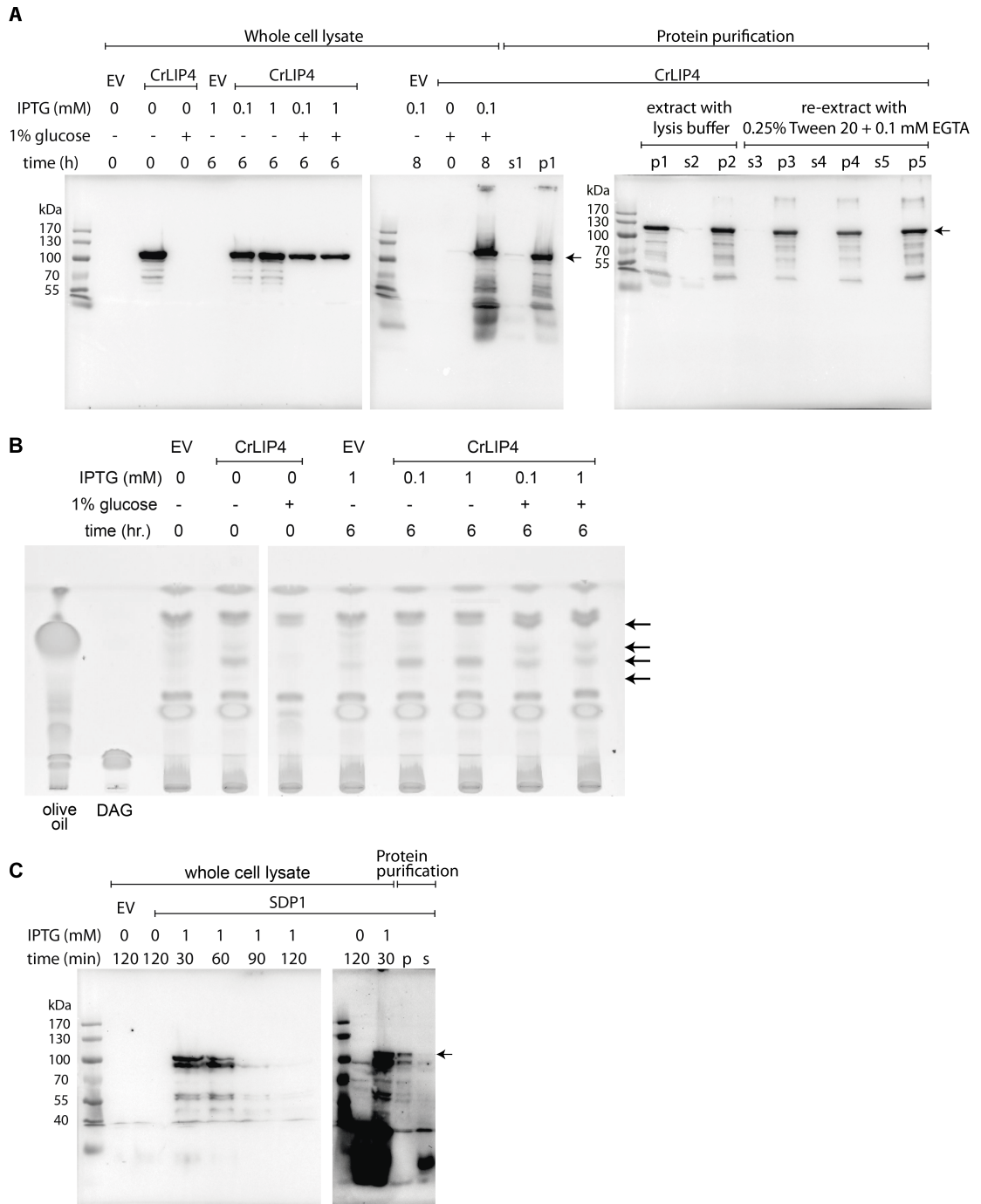


Figure 3.10. CrLIP4 recombinant protein expression in *E. coli*.

Figure 3.10. (cont'd)

(A) Western blot analysis of CrLIP4 recombinant protein expression compared to an empty vector (EV, pET28b+) with addition of IPTG and/or 1% glucose at different time points (left and middle panels), and recombinant protein purification (middle and right panels) showing supernatant (s) and pellet (p) at different steps. White lines separate different membranes or indicate removal of irrelevant lanes. (B) Separation of neutral lipids on TLC plates isolated from *E. coli* cells expressing CrLIP4 or EV. The solvent system was petroleum ether, diethyl ether, acetic acid (80:20:1 v/v). The lipid bands were visualized by staining with iodine vapor. Arrows indicate changes in abundance of lipids or free fatty acids due to the presence of the recombinant CrLIP4 at various concentrations of IPTG, with or without 1% glucose inhibition at different time points. The white line indicates removal of irrelevant lanes. (C) Western blot analysis of AtSDP1 recombinant protein expression compared to an empty vector (EV, pET28b+) with addition of IPTG at different time points (left and right panels) and recombinant protein purification (right panel) showing supernatant (s) and pellet (p). The white line indicates two different membranes.

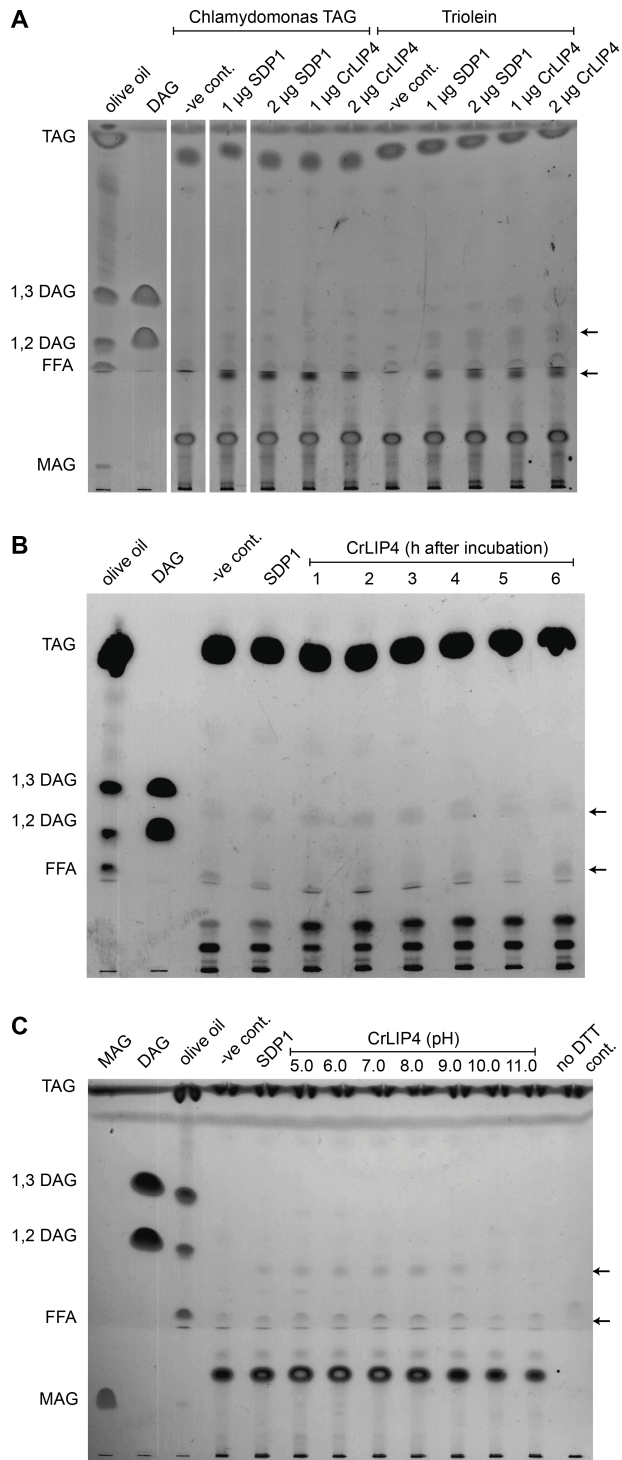


Figure 3.11. Lipase assay.

Figure 3.11. (cont'd)

Separation of neutral lipids with chloroform, acetone and acetic acid (96:4:1 v/v/v) on a TLC plate. Lipids were stained with iodine vapor. Olive oil, diacylglycerol (DAG) and monoacylglycerol (MAG) were used as standards. Each assay had a negative control (-ve cont'd) containing no protein. Arrows indicate DAG and free fatty acid (FFA) bands.

(A) Chlamydomonas TAG or triolein was used as a substrate for 1-2 μg of either recombinant SDP1 or CrLIP4. The reactions were carried out for six hours. White lines indicate reordering of -ve cont'd and 1 μg SDP1 lanes from the same plate. **(B)** TAG lipase activity of CrLIP4 was tested at different time points. Triolein was used as a substrate. **(C)** TAG lipase activity of CrLIP4 was tested against different pH levels from 5.0 to 11.0. No dithiothreitol (DTT) control (cont'd) was included.

Table 3.1. Protein domains identified in CrLIP4 homologues.

Query name	Domain					
	Patatin		DUF3336		Overall	
	From	To	From	To	From	To
<i>Acinetobacter</i> sp. (gi514963557)	4	151	157	343	4	343
<i>Alcanivorax</i> sp. (gi551599646)	1	139	145	331	1	331
<i>Arabidopsis thaliana</i> SDP1 (AT5G04040.1)	86	226	232	436	86	436
<i>Arabidopsis thaliana</i> SDP1-like (AT3G57140.1)	87	227	233	435	87	435
<i>Aspergillus oryzae</i> (gi391866040)	1	129	138	334	1	334
<i>Auxenochlorella protothecoides</i> (gi760448007)	94	235	241	424	94	424
<i>Brassica napus</i> (gi674952444)	88	234	240	444	88	444
<i>Camelina sativa</i> (gi727560138)	86	226	232	435	86	435
<i>Candida albicans</i> (gi712885502)	59	205	211	416	59	416
<i>Capsella rubella</i> (gi565458145)	86	226	232	435	86	435
<i>Chlamydomonas reinhardtii</i> CrLIP4 (Cre17.g699100.t1.1)	1	145	151	348	1	348
<i>Coccomyxa subellipsoidea</i> (gi545354428)	1	68	74	270	1	270
<i>Congregibacter litoralis</i> (gi495571297)	1	140	146	333	1	333
<i>Debaryomyces hansenii</i> (gi294657254)	62	205	211	416	62	416
<i>Elaeis guineensis</i> (gi743786505)	86	226	232	435	86	435
<i>Eutrema salsugineum</i> (gi567170164)	86	226	232	435	86	435
<i>Fusarium graminearum</i> (gi758210332)	63	207	218	414	63	414
<i>Genlisea aurea</i> (gi527206944)	89	229	235	437	89	437
<i>Gossypium raimondii</i> (gi823261503)	86	226	232	435	86	435
<i>Helicosporidium</i> sp. (gi633903867)	23	120	126	306	23	306
<i>Homo sapiens</i> (gi58759051)	-	-	10	179	10	179
<i>Hordeum vulgare</i> (gi326512766)	85	225	231	433	85	433
<i>Lodderomyces elongisporus</i> (gi149246010)	77	220	226	432	77	432
<i>Marinobacter nanhaiticus</i> (gi750601676)	3	141	147	333	3	333
<i>Metarhizium robertsii</i> (gi594722286)	69	211	225	421	69	421
<i>Mortierella verticillata</i> (gi672823045)	194	340	346	540	194	540
<i>Musa acuminata</i> (gi695011186)	87	228	234	437	87	437
<i>Nevskia ramosa</i> (gi703385018)	3	140	146	332	3	332
<i>Nevskia soli</i> (gi659872973)	3	140	146	332	3	332
<i>Oryza sativa</i> (gi125588353)	83	223	229	432	83	432
<i>Paraglaciecola arctica</i> (gi494890748)	2	140	146	331	2	331
<i>Prunus mume</i> (gi645271062)	86	226	232	434	86	434
<i>Pseudogymnoascus pannorum</i> (gi682355077)	62	208	221	418	62	418
<i>Ricinus communis</i> (gi255578433)	86	226	232	435	86	435
<i>Saccharomyces cerevisiae</i> Tgl3p (gi323346999)	56	198	204	364	56	364
<i>Saccharomyces cerevisiae</i> Tgl4p (gi767174926)	132	276	282	482	132	482
<i>Saccharomyces cerevisiae</i> Tgl5p (gi768490581)	32	177	183	387	32	387

Table 3.1. (cont'd)

Query name	Domain					
	Patatin		DUF3336		Overall	
	Position		Position			
From	To	From	To	From	To	
<i>Scheffersomyces stipitis</i> (gi150864168)	14	155	161	366	14	366
<i>Setaria italica</i> (gi514782261)	85	226	232	434	85	434
<i>Solanum tuberosum</i> SDP1-like (gi565369529)	90	230	236	440	90	440
<i>Solimonas flava</i> (gi654541222)	3	146	152	338	3	338
<i>Sorghum bicolor</i> (gi242058771)	85	226	232	434	85	434
<i>Spathaspora passalidarum</i> (gi598070323)	45	187	193	398	45	398
<i>Verticillium dahliae</i> (gi697089701)	59	206	218	414	59	414
<i>Volvox carteri</i> (gi302836077)	124	274	280	477	124	477
<i>Zea mays</i> SDP1-like (gi670433428)	85	226	232	434	85	434

Table 3.2. Target and primer sequences for artificial microRNA of CrLIP4.

Target position on the CrLIP4 transcript	Target sequence/Primer name	Sequence from 5' to 3'
5'	Target sequence	TGAAACCCACGTCTAACTCGA
	Lip4AmiRNA_b_Fwd	CTAGTTCGAGTTAGACGTGGGATTTCATCTCGCTG ATCGGCACCATGGGGGTGGTGGTGATCAGCGCT ATGAAACCCACGTCTAACTCGAG
	Lip4AmiRNA_b_Rev	CTAGCTCGAGTTAGACGTGGGTTTCATAGCGCTG ATCACCACCACCCCATGGTGCCGATCAGCGAG ATGAATCCCACGTCTAACTCGAA
		TTTCACAATGGTCTTCCTCAA
3'	Target sequence	TTTCACAATGGTCTTCCTCAA
	Lip4AmiRNA_e_Fwd	CTAGTTTGAGGAAGACCATTGAGAAATCTCGCTG ATCGGCACCATGGGGGTGGTGGTGATCAGCGCT ATTCACAATGGTCTTCCTCAAG
	Lip4AmiRNA_e_Rev	CTAGCTTGAGGAAGACCATTGTGAAATAGCGCT GATCACCACCACCCCATGGTGCCGATCAGCGA GATTTCTCAATGGTCTTCCTCAA

Table 3.3. Sequences of Primers used for various purposes as indicated.

Purpose	Name	Sequence (5' to 3' direction)
qPCR of <i>CrLIP4</i>	Lip4-jw2-fwd	CTTCTCCAACAGCCGCGC
	Lip4-jw2-rev	CGCTCGTACGCCTCCAGG
qPCR of <i>RACK1</i>	BEN3433	GTCATCCACTGCCTGTGCTT
	BEN3434	CCTTCTTGCTGGTGTGTTG
qPCR of <i>IPP2</i>	QK194	GTATGAGTTGCTTCTCCAGCAAAG
	QK195	GAGGATGGCTGCAACAAGTGT
Cloning of <i>CrLIP4</i> fragment 1	Lip4-F0	TGGAGGAGGCCGATATG
	Lip4-R0	GGCTGCCCTTGTTGATG
Cloning of <i>CrLIP4</i> fragment 2	Lip4-F2	GGTTTCTTCTCCAACAGC
	Lip4-R2	CACCAGGAAGTGGTTGC
Cloning of <i>CrLIP4</i> fragment 3	Lip4-F3	CCACCAATGACTCGCTG
	Lip4-R3	AATGGTCTTGCTCAGGTG
Cloning of <i>CrLIP4</i> fragment 4	Lip4-F4.3	GTGGCTCATGCTGTTTAC
	Lip4-R4.3	TCTGAAGCGCTGTCTC
Cloning of <i>CrLIP4</i> fragment 5	Lip4-F5	TGAGGACAGCGCTTCAGAC
	Lip4-R5	CCTCCTCAGTACGCAAACAC
Joining <i>CrLIP4</i> fragment 1 and 2 and 3-4-5	Lip4_F-1	ATGGACGCCCGCCAC
Joining <i>CrLIP4</i> fragment 5 with 3-4 and 1-2	Lip4-R6	GTACGCAAACACGTCCAGAGCA
<i>CrLIP4</i> sequencing	Lip4-1424	CCAACATCGCCAACCAGGTC
	Lip4-1817	TGGCCCTTCTGAACCTG
	Lip4-1924	ATGCCGGCCTCTTACAG
pENTR TM /D-TOPO cloning	Lip4-F kozak	GAAATGGACGCCCGC
pMK595 cloning	595Lip4 F	TATCCATATGACGTTCCAGATTACGCTGC TCAGTGCGGCCGCATGGACGCCCGCCACA GA
	595Lip4 R	GAATTTGACGGTATCGGGGGGATCCACT AGTTCTAGCTAGATCAGTACGCAAACACG TC

Table 3.3. (cont'd)

Purpose	Name	Sequence (5' to 3' direction)
pMK595 sequencing	MHK98	CAAGTATAAATAGACCTG
	MHK99	CAAGTATAAATAGACCTG
Genotyping of T-DNA insertion lines	LBb1.3	ATTTTGCCGATTCGGAAC
	LP-sdp1-4	CGAGCCTGTCTTATCTCGTTG
	RP-sdp1-4	GCCGTGTTTCATGCATAAAAG
	LPb-sdp1-5	TGGTTGAAGCCAATCCGTGAT
	RP-sdp1-5	TTGGTGTGGTTAGGACTTTGG
pENTR/D- <i>AtSDP1</i>	SDP1-pENTR F	CACCATGGATATAAGTAATGAGGCTAGT
	SDP1-pENTR R	CTAAGCATCTATAACACTACCAGACAC
<i>AtSDP1</i> sequencing	SDP1 seq F1	CAGGAGCTTCGTCATCGTC
	SDP1 seq F2	CGGAGGCGTGTTCTCAATAG
	SDP1 seq F3	ATGGTGGTAGATTTCGCAGC
	SDP1 seq F4	AGTGAAACAGAGAGCGTGG
pET28b+- <i>AtSDP1</i>	SDP1-pET28_NheI F	CATTGAGCTAGCATGGATATAAGTAATGAGGC
	SDP1-pET28-NotI R	CAATTAGCGGCCCGCCTAAGCATCTATAACACT
pET28b+- <i>CrLIP4</i>	Lip4-pET28-F4	GTCGACAAGCTTATGGACGCCCGC
	Lip4-pET28-R2	CACCACCTCGAGTCAGTACGCAAACACG

REFERENCES

REFERENCES

- Altschul, S. F., Madden, T. L., Schaffer, A. A., Zhang, J., Zhang, Z., Miller, W., & Lipman, D. J. (1997). Gapped BLAST and PSI-BLAST: a new generation of protein database search programs. *Nucleic Acids Res*, 25(17), 3389-3402.
- Alvarez, H. M., & Steinbuchel, A. (2002). Triacylglycerols in prokaryotic microorganisms. *Appl Microbiol Biotechnol*, 60(4), 367-376. doi: 10.1007/s00253-002-1135-0
- Athenstaedt, K., & Daum, G. (2003). YMR313c/TGL3 encodes a novel triacylglycerol lipase located in lipid particles of *Saccharomyces cerevisiae*. *J Biol Chem*, 278(26), 23317-23323. doi: 10.1074/jbc.M302577200
- Athenstaedt, K., & Daum, G. (2005). Tgl4p and Tgl5p, two triacylglycerol lipases of the yeast *Saccharomyces cerevisiae* are localized to lipid particles. *J Biol Chem*, 280(45), 37301-37309. doi: 10.1074/jbc.M507261200
- Athenstaedt, K., Zweytick, D., Jandrositz, A., Kohlwein, S. D., & Daum, G. (1999). Identification and characterization of major lipid particle proteins of the yeast *Saccharomyces cerevisiae*. *J Bacteriol*, 181(20), 6441-6448.
- Boyle, N. R., Page, M. D., Liu, B., Blaby, I. K., Casero, D., Kropat, J., Cokus, S. J., Hong-Hermesdorf, A., Shaw, J., Karpowicz, S. J., Gallaher, S. D., Johnson, S., Benning, C., Pellegrini, M., Grossman, A., & Merchant, S. S. (2012). Three acyltransferases and nitrogen-responsive regulator are implicated in nitrogen starvation-induced triacylglycerol accumulation in *Chlamydomonas*. *J Biol Chem*, 287(19), 15811-15825. doi: 10.1074/jbc.M111.334052
- Brady, L., Brzozowski, A. M., Derewenda, Z. S., Dodson, E., Dodson, G., Tolley, S., Turkenburg, J. P., Christiansen, L., Huge-Jensen, B., Norskov, L., & et al. (1990). A serine protease triad forms the catalytic centre of a triacylglycerol lipase. *Nature*, 343(6260), 767-770. doi: 10.1038/343767a0
- Brzozowski, A. M., Derewenda, U., Derewenda, Z. S., Dodson, G. G., Lawson, D. M., Turkenburg, J. P., Bjorkling, F., Huge-Jensen, B., Patkar, S. A., & Thim, L. (1991). A model for interfacial activation in lipases from the structure of a fungal lipase-inhibitor complex. *Nature*, 351(6326), 491-494. doi: 10.1038/351491a0
- Clough, S. J., & Bent, A. F. (1998). Floral dip: a simplified method for *Agrobacterium*-mediated transformation of *Arabidopsis thaliana*. *Plant J*, 16(6), 735-743.
- Dosztanyi, Z., Csizmok, V., Tompa, P., & Simon, I. (2005). IUPred: web server for the prediction of intrinsically unstructured regions of proteins based on estimated energy content. *Bioinformatics*, 21(16), 3433-3434. doi: 10.1093/bioinformatics/bti541

- Dunker, A. K., Brown, C. J., Lawson, J. D., Iakoucheva, L. M., & Obradovic, Z. (2002). Intrinsic disorder and protein function. *Biochemistry*, *41*(21), 6573-6582.
- Eastmond, P. J. (2006). SUGAR-DEPENDENT1 encodes a patatin domain triacylglycerol lipase that initiates storage oil breakdown in germinating Arabidopsis seeds. *Plant Cell*, *18*(3), 665-675. doi: 10.1105/tpc.105.040543
- Eddy, S. R. (2009). A new generation of homology search tools based on probabilistic inference. *Genome Inform*, *23*(1), 205-211.
- Edgar, R. C. (2004). MUSCLE: multiple sequence alignment with high accuracy and high throughput. *Nucleic Acids Res*, *32*(5), 1792-1797. doi: 10.1093/nar/gkh340
- Gietz, D., St Jean, A., Woods, R. A., & Schiestl, R. H. (1992). Improved method for high efficiency transformation of intact yeast cells. *Nucleic Acids Res*, *20*(6), 1425.
- Gill, J., & Parish, J. H. (1997). Minireview: Lipases—enzymes at an interface. *Biochem Educ*, *25*(1), 2-5. doi: 10.1016/S0307-4412(96)00125-2
- Goold, H., Beisson, F., Peltier, G., & Li-Beisson, Y. (2015). Microalgal lipid droplets: composition, diversity, biogenesis and functions. *Plant Cell Rep*, *34*(4), 545-555. doi: 10.1007/s00299-014-1711-7
- Gronke, S., Mildner, A., Fellert, S., Tennagels, N., Petry, S., Muller, G., Jackle, H., & Kuhnlein, R. P. (2005). Brummer lipase is an evolutionary conserved fat storage regulator in Drosophila. *Cell Metab*, *1*(5), 323-330. doi: 10.1016/j.cmet.2005.04.003
- Gross, D. A., & Silver, D. L. (2014). Cytosolic lipid droplets: from mechanisms of fat storage to disease. *Crit Rev Biochem Mol Biol*, *49*(4), 304-326. doi: 10.3109/10409238.2014.931337
- Haemmerle, G., Lass, A., Zimmermann, R., Gorkiewicz, G., Meyer, C., Rozman, J., Heldmaier, G., Maier, R., Theussl, C., Eder, S., Kratky, D., Wagner, E. F., Klingenspor, M., Hoefler, G., & Zechner, R. (2006). Defective lipolysis and altered energy metabolism in mice lacking adipose triglyceride lipase. *Science*, *312*(5774), 734-737. doi: 10.1126/science.1123965
- Harrison, S. J., Mott, E. K., Parsley, K., Aspinall, S., Gray, J. C., & Cottage, A. (2006). A rapid and robust method of identifying transformed Arabidopsis thaliana seedlings following floral dip transformation. *Plant Methods*, *2*, 19. doi: 10.1186/1746-4811-2-19
- Hemschemeier, A., Casero, D., Liu, B., Benning, C., Pellegrini, M., Happe, T., & Merchant, S. S. (2013). Copper response regulator1-dependent and -independent responses of the Chlamydomonas reinhardtii transcriptome to dark anoxia. *Plant Cell*, *25*(9), 3186-3211. doi: 10.1105/tpc.113.115741

- Iakoucheva, L. M., Radivojac, P., Brown, C. J., O'Connor, T. R., Sikes, J. G., Obradovic, Z., & Dunker, A. K. (2004). The importance of intrinsic disorder for protein phosphorylation. *Nucleic Acids Res*, *32*(3), 1037-1049. doi: 10.1093/nar/gkh253
- Jenkins, C. M., Mancuso, D. J., Yan, W., Sims, H. F., Gibson, B., & Gross, R. W. (2004). Identification, cloning, expression, and purification of three novel human calcium-independent phospholipase A2 family members possessing triacylglycerol lipase and acylglycerol transacylase activities. *J Biol Chem*, *279*(47), 48968-48975. doi: 10.1074/jbc.M407841200
- Kelly, A. A., Quettier, A. L., Shaw, E., & Eastmond, P. J. (2011). Seed storage oil mobilization is important but not essential for germination or seedling establishment in Arabidopsis. *Plant Physiol*, *157*(2), 866-875. doi: 10.1104/pp.111.181784
- Kim, K. K., Song, H. K., Shin, D. H., Hwang, K. Y., & Suh, S. W. (1997). The crystal structure of a triacylglycerol lipase from *Pseudomonas cepacia* reveals a highly open conformation in the absence of a bound inhibitor. *Structure*, *5*(2), 173-185.
- Kindle, K. L. (1990). High-frequency nuclear transformation of *Chlamydomonas reinhardtii*. *Proc Natl Acad Sci U S A*, *87*(3), 1228-1232.
- Krogh, A., Larsson, B., von Heijne, G., & Sonnhammer, E. L. (2001). Predicting transmembrane protein topology with a hidden Markov model: application to complete genomes. *J Mol Biol*, *305*(3), 567-580. doi: 10.1006/jmbi.2000.4315
- Kropat, J., Hong-Hermesdorf, A., Casero, D., Ent, P., Castruita, M., Pellegrini, M., Merchant, S. S., & Malasarn, D. (2011). A revised mineral nutrient supplement increases biomass and growth rate in *Chlamydomonas reinhardtii*. *Plant J*, *66*(5), 770-780. doi: 10.1111/j.1365-313X.2011.04537.x
- Kuo, M. H., Zhou, J., Jambeck, P., Churchill, M. E., & Allis, C. D. (1998). Histone acetyltransferase activity of yeast Gcn5p is required for the activation of target genes in vivo. *Genes Dev*, *12*(5), 627-639.
- Kurat, C. F., Natter, K., Petschnigg, J., Wolinski, H., Scheuringer, K., Scholz, H., Zimmermann, R., Leber, R., Zechner, R., & Kohlwein, S. D. (2006). Obese yeast: triglyceride lipolysis is functionally conserved from mammals to yeast. *J Biol Chem*, *281*(1), 491-500. doi: 10.1074/jbc.M508414200
- Li, X., Benning, C., & Kuo, M. H. (2012). Rapid triacylglycerol turnover in *Chlamydomonas reinhardtii* requires a lipase with broad substrate specificity. *Eukaryot Cell*, *11*(12), 1451-1462. doi: 10.1128/EC.00268-12
- Li-Beisson, Y., Beisson, F., & Riekhof, W. (2015). Metabolism of acyl-lipids in *Chlamydomonas reinhardtii*. *Plant J*, *82*(3), 504-522. doi: 10.1111/tpj.12787

- Livak, K. J., & Schmittgen, T. D. (2001). Analysis of relative gene expression data using real-time quantitative PCR and the 2(-Delta Delta C(T)) Method. *Methods*, 25(4), 402-408. doi: 10.1006/meth.2001.1262
- Luo, J., Xu, X., Hall, H., Hyland, E. M., Boeke, J. D., Hazbun, T., & Kuo, M. H. (2010). Histone h3 exerts a key function in mitotic checkpoint control. *Mol Cell Biol*, 30(2), 537-549. doi: 10.1128/MCB.00980-09
- Lv, H., Qu, G., Qi, X., Lu, L., Tian, C., & Ma, Y. (2013). Transcriptome analysis of *Chlamydomonas reinhardtii* during the process of lipid accumulation. *Genomics*, 101(4), 229-237. doi: 10.1016/j.ygeno.2013.01.004
- Ma, H., Kunes, S., Schatz, P. J., & Botstein, D. (1987). Plasmid construction by homologous recombination in yeast. *Gene*, 58(2-3), 201-216.
- Matthew, T., Zhou, W., Rupprecht, J., Lim, L., Thomas-Hall, S. R., Doebbe, A., Kruse, O., Hankamer, B., Marx, U. C., Smith, S. M., & Schenk, P. M. (2009). The metabolome of *Chlamydomonas reinhardtii* following induction of anaerobic H₂ production by sulfur depletion. *J Biol Chem*, 284(35), 23415-23425. doi: 10.1074/jbc.M109.003541
- Merchant, S. S., Prochnik, S. E., Vallon, O., Harris, E. H., Karpowicz, S. J., Witman, G. B., Terry, A., Salamov, A., Fritz-Laylin, L. K., Marechal-Drouard, L., Marshall, W. F., Qu, L. H., Nelson, D. R., Sanderfoot, A. A., Spalding, M. H., Kapitonov, V. V., Ren, Q., Ferris, P., Lindquist, E., Shapiro, H., Lucas, S. M., Grimwood, J., Schmutz, J., Cardol, P., Cerutti, H., Chanfreau, G., Chen, C. L., Cognat, V., Croft, M. T., Dent, R., Dutcher, S., Fernandez, E., Fukuzawa, H., Gonzalez-Ballester, D., Gonzalez-Halphen, D., Hallmann, A., Hanikenne, M., Hippler, M., Inwood, W., Jabbari, K., Kalanon, M., Kuras, R., Lefebvre, P. A., Lemaire, S. D., Lobanov, A. V., Lohr, M., Manuell, A., Meier, I., Mets, L., Mittag, M., Mittelmeier, T., Moroney, J. V., Moseley, J., Napoli, C., Nedelcu, A. M., Niyogi, K., Novoselov, S. V., Paulsen, I. T., Pazour, G., Purton, S., Ral, J. P., Riano-Pachon, D. M., Riekhof, W., Rymarquis, L., Schroda, M., Stern, D., Umen, J., Willows, R., Wilson, N., Zimmer, S. L., Allmer, J., Balk, J., Bisova, K., Chen, C. J., Elias, M., Gendler, K., Hauser, C., Lamb, M. R., Ledford, H., Long, J. C., Minagawa, J., Page, M. D., Pan, J., Pootakham, W., Roje, S., Rose, A., Stahlberg, E., Terauchi, A. M., Yang, P., Ball, S., Bowler, C., Dieckmann, C. L., Gladyshev, V. N., Green, P., Jorgensen, R., Mayfield, S., Mueller-Roeber, B., Rajamani, S., Sayre, R. T., Brokstein, P., Dubchak, I., Goodstein, D., Hornick, L., Huang, Y. W., Jhaveri, J., Luo, Y., Martinez, D., Ngau, W. C., Otiillar, B., Poliakov, A., Porter, A., Szajkowski, L., Werner, G., Zhou, K., Grigoriev, I. V., Rokhsar, D. S., & Grossman, A. R. (2007). The *Chlamydomonas* genome reveals the evolution of key animal and plant functions. *Science*, 318(5848), 245-250. doi: 10.1126/science.1143609
- Miller, R., Wu, G., Deshpande, R. R., Vieler, A., Gartner, K., Li, X., Moellering, E. R., Zauner, S., Cornish, A. J., Liu, B., Bullard, B., Sears, B. B., Kuo, M. H., Hegg, E. L., Shachar-Hill, Y., Shiu, S. H., & Benning, C. (2010). Changes in transcript abundance in

- Chlamydomonas reinhardtii* following nitrogen deprivation predict diversion of metabolism. *Plant Physiol*, 154(4), 1737-1752. doi: 10.1104/pp.110.165159
- Moellering, E. R., Muthan, B., & Benning, C. (2010). Freezing tolerance in plants requires lipid remodeling at the outer chloroplast membrane. *Science*, 330(6001), 226-228. doi: 10.1126/science.1191803
- Molnar, A., Bassett, A., Thuenemann, E., Schwach, F., Karkare, S., Ossowski, S., Weigel, D., & Baulcombe, D. (2009). Highly specific gene silencing by artificial microRNAs in the unicellular alga *Chlamydomonas reinhardtii*. *Plant J*, 58(1), 165-174. doi: 10.1111/j.1365-313X.2008.03767.x
- Musso, M., Bocciardi, R., Parodi, S., Ravazzolo, R., & Ceccherini, I. (2006). Betaine, dimethyl sulfoxide, and 7-deaza-dGTP, a powerful mixture for amplification of GC-rich DNA sequences. *J Mol Diagn*, 8(5), 544-550. doi: 10.2353/jmoldx.2006.060058
- Sakaki, T., Kondo, N., & Yamada, M. (1990a). Pathway for the synthesis of triacylglycerols from monogalactosyldiacylglycerols in ozone-fumigated spinach leaves. *Plant Physiol*, 94(2), 773-780.
- Sakaki, T., Saito, K., Kawaguchi, A., Kondo, N., & Yamada, M. (1990b). Conversion of monogalactosyldiacylglycerols to triacylglycerols in ozone-fumigated spinach leaves. *Plant Physiol*, 94(2), 766-772.
- Scherer, G. F., Ryu, S. B., Wang, X., Matos, A. R., & Heitz, T. (2010). Patatin-related phospholipase A: nomenclature, subfamilies and functions in plants. *Trends Plant Sci*, 15(12), 693-700. doi: 10.1016/j.tplants.2010.09.005
- Schønheyder, F., & Volqvartz, K. (1945). On the affinity of pig pancreas lipase for tricaproin in heterogeneous solution. *Acta Physiol Scand*, 9(1), 57-67. doi: 10.1111/j.1748-1716.1945.tb03084.x
- Sonnhammer, E. L., von Heijne, G., & Krogh, A. (1998). A hidden Markov model for predicting transmembrane helices in protein sequences. *Proc Int Conf Intell Syst Mol Biol*, 6, 175-182.
- Thiam, A. R., Farese, R. V., Jr., & Walther, T. C. (2013). The biophysics and cell biology of lipid droplets. *Nat Rev Mol Cell Biol*, 14(12), 775-786. doi: 10.1038/nrm3699
- Troncoso-Ponce, M. A., Cao, X., Yang, Z., & Ohlrogge, J. B. (2013). Lipid turnover during senescence. *Plant Sci*, 205-206, 13-19. doi: 10.1016/j.plantsci.2013.01.004
- Tsai, C. H., Warakanont, J., Takeuchi, T., Sears, B. B., Moellering, E. R., & Benning, C. (2014). The protein Compromised Hydrolysis of Triacylglycerols 7 (CHT7) acts as a repressor of cellular quiescence in *Chlamydomonas*. *Proc Natl Acad Sci U S A*, 111(44), 15833-15838. doi: 10.1073/pnas.1414567111

- Uversky, V. N. (2013a). A decade and a half of protein intrinsic disorder: biology still waits for physics. *Protein Sci*, 22(6), 693-724. doi: 10.1002/pro.2261
- Uversky, V. N. (2013b). Intrinsic disorder-based protein interactions and their modulators. *Curr Pharm Des*, 19(23), 4191-4213.
- Verger, R. (1976). Interfacial enzyme kinetics of lipolysis. *Annu Rev Biophys Bioeng*, 5, 77-117. doi: 10.1146/annurev.bb.05.060176.000453
- Villena, J. A., Roy, S., Sarkadi-Nagy, E., Kim, K. H., & Sul, H. S. (2004). Desnutrin, an adipocyte gene encoding a novel patatin domain-containing protein, is induced by fasting and glucocorticoids: ectopic expression of desnutrin increases triglyceride hydrolysis. *J Biol Chem*, 279(45), 47066-47075. doi: 10.1074/jbc.M403855200
- Yachdav, G., Kloppmann, E., Kajan, L., Hecht, M., Goldberg, T., Hamp, T., Honigschmid, P., Schafferhans, A., Roos, M., Bernhofer, M., Richter, L., Ashkenazy, H., Punta, M., Schlessinger, A., Bromberg, Y., Schneider, R., Vriend, G., Sander, C., Ben-Tal, N., & Rost, B. (2014). PredictProtein--an open resource for online prediction of protein structural and functional features. *Nucleic Acids Res*, 42(Web Server issue), W337-343. doi: 10.1093/nar/gku366
- Zechner, R., Kienesberger, P. C., Haemmerle, G., Zimmermann, R., & Lass, A. (2009). Adipose triglyceride lipase and the lipolytic catabolism of cellular fat stores. *J Lipid Res*, 50(1), 3-21. doi: 10.1194/jlr.R800031-JLR200
- Zimmermann, R., Strauss, J. G., Haemmerle, G., Schoiswohl, G., Birner-Gruenberger, R., Riederer, M., Lass, A., Neuberger, G., Eisenhaber, F., Hermetter, A., & Zechner, R. (2004). Fat mobilization in adipose tissue is promoted by adipose triglyceride lipase. *Science*, 306(5700), 1383-1386. doi: 10.1126/science.1100747

CHAPTER 4
Conclusion and Perspectives

Unicellular microalgae are important for the natural ecology of this planet; they are also a resource for the production of alternative energy, to help reduce the emission of greenhouse gases and provide a substitute for fossil fuel. These benefits accrue from the ability of microalgae to proficiently utilize energy from sunlight to produce high-energy molecules such as starch and oil. Among the microalgae, *Chlamydomonas* is currently the best characterized and, hence, it was chosen as the experimental organism. However, many aspects of lipid metabolism in *Chlamydomonas* have been deduced by analogy to pathways in *Arabidopsis*. These inferences should be viewed with caution because differences in fatty acids, lipid species, and lipid enzymes exist between these quite divergent photosynthetic organisms. In order to gain new insights into lipid metabolism in *Chlamydomonas*, this thesis research has focused on examining and explaining the differences between lipid metabolism of *Chlamydomonas* and *Arabidopsis*. In this study, two *Arabidopsis* orthologues were characterized in *Chlamydomonas*. The summaries, remaining questions and future directions for both projects are addressed below.

SUMMARY OF PHYSIOLOGICAL, GENETIC, AND BIOCHEMICAL FEATURES OF CHLAMYDOMONAS TGD2

Phenotype of the *tgd2* mutant. In this investigation, an orthologue of an *Arabidopsis* gene that functions in ER-to-chloroplast lipid trafficking was identified and characterized through a loss-of-function mutant named *tgd2*. This mutant was isolated from a forward genetic screen. The *tgd2* mutant has elevated levels of TAG at all stages of the life cycle (Figure 2.1A). Strikingly, the TAG that accumulates in the *tgd2* mutant contains unique fatty acids that are usually found in monogalactosyldiacylglycerol (MGDG) (Figure 2.1D). During conditions when N is plentiful (N+), the *tgd2* mutant also accumulates more phosphatidic acid (PtdOH) but no other lipids compared to the parental line (PL) (Figure 2.1B). In addition, during prolonged culture, the mutant has lower viability and it accumulates high concentrations of malondialdehyde, which is a product of lipid peroxidation (Figure 2.2).

Identification of the mutation in *tgd2*. Based on Southern blot and linkage analyses, the mutant was confirmed to contain one insertion/deletion event that segregates with the phenotype of the mutant. Through whole genome resequencing, the *tgd2* mutation in this mutant was localized to chromosome 16 which contains a ~31 kb deletion that either completely or partially deletes six genes. Complementation analysis was carried out for each gene by reintroducing

DNA subcloned from a BAC clone of the wild-type genomic region. Only the *Chlamydomonas TRIGALACTOSYLDIACYLGLYCEROL 2 (TGD2)* gene was able to complement the mutant phenotype. Subsequent characterization of the *Chlamydomonas tgd2* mutation was guided by our knowledge of the function of the TGD2 protein in ER-to-chloroplast lipid trafficking in *Arabidopsis*.

Characterization of changes in lipid trafficking in the *tgd2* mutant. The steady state amount of MGDG in the *tgd2* mutant did not change significantly compared to that of the parental line (PL). However, [¹⁴C]acetate pulse-chase labeling revealed that the mutant's MGDG labeling time course lacks a dip, which represents the phase when the [¹⁴C] flux from the chloroplast is depleted followed by [¹⁴C] flux coming back from the ER (Figure 2.4). This observation was similar to what had been observed in the *Arabidopsis tgd1* mutant (Xu *et al.*, 2003) and led to my conclusion that lipid trafficking between the ER and the chloroplast exists in *Chlamydomonas*.

Synthesis of galactoglycerolipid in *tgd2* is affected. Another major finding from the [¹⁴C]acetate labeling experiment in *tgd2* was the initially high [¹⁴C] incorporation into MGDG, which dropped greatly over time (Figure 2.4). This high rate of MGDG labeling did not transfer to its product, digalactosyldiacylglycerol (DGDG). These observations were confirmed by UDP-[¹⁴C]galactose labeling of isolated chloroplasts (Figure 2.5). These results suggested that in *tgd2*, MGDG is more actively synthesized than in the PL. However, this high MGDG synthesis did not result in increased DGDG synthesis. Instead, newly synthesized MGDG becomes mature MGDG by desaturation. The excess mature MGDG is then degraded to maintain the structure and function of the photosynthetic membrane.

Localization and lipid binding property of CrTGD2. Similarities between the TGD2 proteins of *Chlamydomonas* and *Arabidopsis* were that both proteins are located in the inner envelope membrane of the chloroplast (iEM) (Figure 2.6) and both bound to PtdOH *in vitro* (Figure 2.7).

Function of CrTGD2 and consequence of its absence. Based on the observations described above, I hypothesize that the *Chlamydomonas* TGD2 functions in transferring lipid precursors, presumably PtdOH, from the ER to the chloroplast (Figure 2.8). In the knockout mutant *tgd2*, extra PtdOH accumulates at the chloroplast outer envelope membrane (oEM). This high amount

of PtdOH stimulates MGDG synthesis but not DGDG synthesis. The excess MGDG is degraded and its fatty acids are either incorporated into TAG or further degraded. Degradation of polyunsaturated fatty acids from MGDG results in elevated levels of reactive oxygen species that can damage the cell and cause reduced viability.

New insights from this study

This study reveals contradictions in existing assumptions about *Chlamydomonas* lipid metabolism. In plants, ER-derived lipids from the eukaryotic pathway contain 18-carbon fatty acid (C18) at their *sn*-2 position, while chloroplast-derived lipids from the prokaryotic pathway contain C16 at their *sn*-2 position. The difference in lipid composition is due to difference in substrate specificity of the lysophosphatidic acid acyltransferases (LPAATs) in the ER and in the chloroplast. In *Chlamydomonas*, the chloroplast lipids predominantly contain C16 at their *sn*-2 position. This observation leads to two possibilities; (i) *Chlamydomonas* does not utilize the eukaryotic pathway, or (ii) both ER and chloroplast LPAATs prefer C16. My investigation suggests that the ER-to-chloroplast lipid trafficking exists in *Chlamydomonas*. The [¹⁴C]acetate pulse-chase labeling result suggests that CrTGD2 transfers lipid precursors (presumably PtdOH) from the ER to the chloroplast. This implies that the alga utilizes the eukaryotic pathway to synthesize galactoglycerolipids, and thus points to the conclusion that both ER and chloroplast LPAATs use C16. Thus, the origin of lipids cannot be distinguished based on their acyl chain at the *sn*-2 position. In order to verify this assumption, the substrate specificity of the different LPAAT isoforms in *Chlamydomonas* should be investigated directly.

In addition, my investigation also suggests that localization of MGDG synthase in *Chlamydomonas* is not the same as in *Arabidopsis*. In *Arabidopsis*, the main MGDG synthase (MGD1) is localized at the iEM. In *Chlamydomonas* only one MGDG synthase is present in the genome. The result from MGDG synthase activity assay with Thermolysin treated chloroplasts points to its presence in the oEM, where DGDG synthase is also localized. This result indirectly also leads to my conclusion that CrTGD2 is important for the ER-to-chloroplast lipid trafficking as follows: The [¹⁴C]acetate pulse-chase labeling showed an apparent disruption between MGDG and DGDG syntheses and one might assume that CrTGD2 transfers substrate MGDG from its previously presumed synthesis location at the iEM to the enzyme DGDG synthase at the oEM. However, MGDG and DGDG synthases are localized in the same membrane. Therefore, the

possibility that CrTGD2 transfers MGDG to the enzyme DGDG synthase seems unlikely as an alternative hypothesis for TGD2 function.

Remaining questions and future directions

From this study a number of issues remain elusive. Questions and proposed experiments to test the hypothesis are discussed below.

MGDG and DGDG syntheses. In the [¹⁴C]acetate pulse-chase labeling experiment, the flux of [¹⁴C] in MGDG of *tgd2* was not correlated with DGDG flux, in contrast to the PL (Figure 2.4). This observation was confirmed through the UDP-[¹⁴C]galactose labeling (Figure 2.5B). The lack of connection of radioactive flux from MGDG to DGDG cannot be explained by the spatial separation of the two enzymes (MGDG and DGDG synthases). Based on their sensitivity to Thermolysin treatment, both enzymes are associated with the oEM. To examine the apparent disconnect, metabolism of MGDG should be considered. In general, newly synthesized MGDG has three fates. (i) It can be used by DGDG synthase to make DGDG. (ii) Its fatty acids can undergo desaturation to become mature MGDG. (iii) During N-, MGDG can be degraded by a lipase called PLASTID GALACTOGLYCEROLIPID DEGRADATION1 (PGD1). In my investigation, the experiments were carried out in the N+ condition. Thus, the newly synthesized MGDG is likely to be used for (i) galactosylation by DGDG synthase or for (ii) desaturation by desaturases. Based on the disconnect of [¹⁴C] in MGDG to DGDG in the mutant it can be concluded that (ii) desaturation dominates (i) galactosylation. The reason for this remains unknown. Three possible explanations are given below.

Feedback inhibition of DGDG synthesis. It is possible that DGDG synthesis in the *tgd2* mutant is controlled by direct feedback inhibition of DGDG synthase. Product inhibition would keep cause DGDG levels to be constant, even when more MGDG substrate is available. The additional newly synthesized MGDG molecules in *tgd2* would then become substrates for desaturases. If this hypothesis is true, in the [¹⁴C]acetate pulse-chase labeling experiment, the absolute value of incorporation of radioactivity into DGDG in *tgd2* should remain unchanged from that of PL. However, the absolute value in the *tgd2* mutant was much lower than that of PL, similar to the relative value as plotted in Figure 2.4. Therefore, it is unlikely that the apparent disconnect between MGDG and DGDG synthesis in *tgd2* is the result of feedback inhibition.

Inaccuracy in the measurement of DGDG synthesis. It is possible that the measurements of DGDG synthesis through acetate or UDP-galactose labeling experiments do not reflect the actual rate in the algal cell. Both measurements were dependent on the labeling of MGDG from the precursor; conceivably, MGDG is also synthesized through another pathway. To overcome this problem, measuring DGDG synthesis directly from the [¹⁴C]MGDG substrate in the isolated chloroplasts of *tgd2* compared to the PL will eliminate the complication of how MGDG is labeled.

PtdOH inhibits DGDG synthase. Conceivably, accumulation of PtdOH inhibits DGDG synthase activity. This hypothesis can be tested by feeding [¹⁴C]MGDG substrate with or without exogenous PtdOH to isolated chloroplasts of the PL. Less radioactive incorporation into DGDG is expected when PtdOH is included in the experiment .

Labeling of other lipids. In addition to MGDG and DGDG synthesis, the synthesis of digalactosyl-*N,N,N*-trimethylhomoserine (DGTS) and phosphatidylglycerol (PtdGro) in the *tgd2* mutant differed from the PL. Explanations for these differences remain to be explored.

Metabolic flux analysis. To understand the [¹⁴C] labeling results, dynamic flux analysis should be applied to fit mathematical models to the labeling data. I would also suggest analysis of steady-state metabolic flux by labeling the *tgd2* culture (in parallel with the PL) with [¹³C]acetate or [¹³C] 16:0 fatty acid until an isotopic steady state is achieved. The signal of [¹³C] can be detected with nuclear magnetic resonance (NMR) or mass spectrometry (MS). The data obtained from this analysis would be used to compute the network flux from each individual molecule (lipids and their derivatives) based on the assumption that at the steady state, an influx is equal to an efflux. The results should be able to explain how each lipid is synthesized, which can then assist the interpretation of how TGD2 plays a role in lipid metabolism in *Chlamydomonas*. More information about this method and resources for analyzing the data are provided in Ratcliffe and Shachar-Hill (2006).

Does CrTGD2 form a complex with CrTGD1 and CrTGD3? Since AtTGD2 is part of a large protein complex in *Arabidopsis*, CrTGD2 is hypothesized to interact with the other TGD proteins and form a complex at the iEM. This question can be resolved through Blue-Native PAGE and Western-blotting or co-immunoprecipitation followed by mass spectrometry.

The absence of *TGD4* and *TGD5* in the *Chlamydomonas* genome. Homology searches have been unable to identify orthologues of Arabidopsis *TGD4* and *TGD5* in the *Chlamydomonas* genome. Although these two proteins are not part of the TGD1-2-3 complex in the chloroplast inner envelope membrane, they are hypothesized to transfer a lipid precursor from the ER to the oEM, then to the intermembrane space, where it becomes a substrate for the TGD1-2-3 complex in the iEM. Without the transport of precursors by TGD4 and TGD5, the TGD1-2-3 complex of *Chlamydomonas* cannot function in the same manner as in the Arabidopsis.

TGD4 and *TGD5* may be present in *Chlamydomonas* but may not be detectable. TGD4 is a β -barrel protein (Wang *et al.*, 2013). It is known that β -barrel proteins are divergent in amino sequence. Hidden Markov models (HMMs) based methods such as Pfam (Finn *et al.*, 2008) and SUPERFAMILY (Wilson *et al.*, 2007) have limitation to recognize a remote homologue of this type of proteins (Cowen *et al.*, 2002; Lifson & Sander, 1980; Olmea *et al.*, 1999; Steward & Thornton, 2002; Zhu & Braun, 1999). Different techniques, such as Markov random fields (MRFs) (Lathrop & Smith, 1996; Liu *et al.*, 2009; Menke *et al.*, 2010; Peng & Xu, 2011; Thomas *et al.*, 2008; Zhu & Braun, 1999), and SMURFLite (Daniels *et al.*, 2012), have been proposed to detect hydrogen bonds in beta sheets instead of the similarity in amino acid sequence. Thus, MRF or SMURFLite methods might be able to identify a protein that could function in *Chlamydomonas* as TGD4 does in Arabidopsis.

In Arabidopsis, TGD5 is a very small protein of 9.2 kDa (Fan *et al.*, 2015). The coding sequence of this gene is only 276 bp. It is possible that this protein was miss-annotated in the genome sequence of *Chlamydomonas*. For both TGD4 and TGD5, another possibility is that the genes could be located in a region of the chromosome that was intractable to sequencing (e.g. GC-rich or hairpin regions) (Blaby *et al.*, 2014). I consider this to be a likely possibility, due to the fact that *Chlamydomonas* has a GC-rich genome (64%) (Merchant *et al.*, 2007).

Other potential function(s) of CrTGD2. It is possible that CrTGD2 may not function in lipid trafficking between the ER and the chloroplast. Could CrTGD2 transport galactoglycerolipids from the oEM site of synthesis to the iEM? The galactoglycerolipids would then be transferred to the thylakoid for assembly. This possibility can be tested by labeling intact chloroplasts of the PL and *tgd2* mutant with UDP-[¹⁴C]galactose, [¹⁴C]MGDG or [¹⁴C]DGDG. If CrTGD2 functions in

transporting galactoglycerolipids to the iEM and the thylakoid membrane, radioactivity will be detected in these membrane fractions in the PL but not in the *tgd2* mutant.

Which galactolipase and/or lipoxygenase is responsible for degradation of MGDG? In order to test the hypothesis that the high turnover rate of MGDG in the *tgd2* mutant leads to the early senescence phenotype, it is crucial to identify gene(s) responsible for this process. The genome database can be searched for candidate galactolipase and lipoxygenase encoding genes. Quantitative reverse transcription can be used to analyze their transcript levels in the *tgd2* mutant compared to the PL.

Localization of MGDG and DGDG synthases. Although this study has shown that both MGDG and DGDG synthase in *Chlamydomonas* are localized in the oEM; I feel that more direct evidence is needed to confirm their location. A number of techniques could be employed. These include (i) a combination of subcellular fractionation and protease protection assay as was used in my localization of CrTGD2, (ii) immunogold labeling of the protein and detection by electron microscopy, and (iii) labeling the protein with a fluorescent-tag as in (Rasala *et al.*, 2013) and detection by confocal microscopy. In immunogold labeling, the quality of the antibodies is crucial since the reliability of the results depends on the purity of the antiserum. Any non-specific binding of the antiserum will lead to a false-positive result. A disadvantage of the fluorescent technique is that it may not be able to distinguish between the iEM and oEM; furthermore, the overexpressed protein could mislocalize, leading to incorrect conclusions. The first two approaches depend on producing clean antisera. My own preference would be to pursue the subcellular localization and protease protection assay.

CrLIP4: A PUTATIVE TAG LIPASE

Conclusion

CrLIP4 is a promising candidate as the primary TAG lipase in *Chlamydomonas*. Not only is it an orthologue of the *Arabidopsis* major seed TAG lipase, *SUGAR DEPENDENT 1 (SDPI)* (Eastmond, 2006), but additionally, its transcript decreases when the cells are in N-, when TAG accumulates (Miller *et al.*, 2010; Tsai *et al.*, 2014). Results from these transcriptomic studies were confirmed through quantitative reverse transcription PCR (Figure 3.1). Since none of the TAG lipases in *Chlamydomonas* have been characterized (Li-Beisson *et al.*, 2015), I aimed to investigate TAG lipase activity of CrLIP4. Down-regulation of the *CrLIP4* transcript through

artificial microRNA decreased the extent of degradation of TAG after N refeeding (NR) (Figure 3.5). The coding sequence of *CrLIP4* was cloned and used for *in vitro* and *in vivo* TAG lipase assays. Expression of CrLIP4 in *E. coli* led to altered neutral lipid composition in the bacteria (Figure 3.10). Recombinant CrLIP4 was able to digest TAG from Chlamydomonas and diolein based on the detection of TAG lipase products, diacylglycerol (DAG) and free fatty acids (FFAs) (Figure 3.11). From these results, I conclude that CrLIP4 is a TAG lipase.

Future directions

Although CrLIP4 seems to have a TAG lipase activity in Chlamydomonas and *in vitro*, it failed to complement yeast and Arabidopsis TAG lipase loss-of-function mutants. Many approaches are suggested below to verify its activity.

Heterologous expression in yeast and Arabidopsis experiments. As mentioned in Chapter 3, aspects of these two experiments can be improved as discussed below.

Heterologous expression of CrLIP4 in yeast double mutant. In order to confirm that CrLIP4 cannot rescue the *tgl3Δtgl4Δ* mutant, more biological replicates (at least three) are needed. In addition, codon optimization should be undertaken because the difference in codon usage between yeast and Chlamydomonas could result in suboptimal expression of *CrLIP4*. Additional and extended time points are needed to confirm the activity of the enzyme. Finally, due to the difference in cell size that can affect the amount of TAG accumulated in the cell, the measurement of TAG/cell number should be replaced by TAG/cell density (OD₆₀₀) to facilitate the interpretation of the results.

Heterologous expression of CrLIP4 in single mutants of yeast. In the yeast single mutant experiments, three points could be improved. First, since the size of CrLIP4 in the yeast single mutants through Western blot analysis appeared to be smaller than the expected size of CrLIP4 as detected in other experiments, the correct molecular size of the heterologously produced CrLIP4 protein should be confirmed prior to performing further analysis. Second, in order to directly compare the result with the double mutant experiment, the same analytical procedures should be followed. Finally, three biological replicates should be performed.

Heterologous expression of CrLIP4 in Arabidopsis mutant. In the Arabidopsis experiment, two points could be improved. First, to obtain expression, codon optimization should be undertaken since the Arabidopsis genome is low in GC content (38%), while the

Chlamydomonas genome is high (64%). Second, epitope tagging would assist the detection of expression of CrLIP4 in the Arabidopsis mutant. Alternatively, effort could be invested to obtain a CrLIP4-specific antibody.

Substrate specificity and kinetics study of CrLIP4. As shown in Chapter 3, recombinant CrLIP4 exhibited a TAG lipase activity toward diolein and TAG from Chlamydomonas. To further characterize this enzyme, examination of substrate specificity and kinetics should be undertaken. Various TAG substrates with different combinations of short chain, long chain, saturated, monounsaturated, and polyunsaturated fatty acids at different positions in the glycerol backbone can be tested with recombinant CrLIP4 by using the optimized condition shown in Chapter 3. In addition to the different species of TAG, other neutral and polar lipids can be tested with CrLIP4. A kinetic study would reveal whether or not the behavior of CrLIP4 is similar to that of a normal lipase that acts at a water-oil interface and needs a conformational change upon binding to its substrate.

Inhibitors of lipases. In order to verify the activity of recombinant CrLIP4, inhibitors of lipases can be incorporated into the *in vitro* assay experiment. These inhibitors include the classical serine esterase inhibitors; diethyl-*p*-nitrophenyl phosphate and diisopropyl fluorophosphates, and the iPLA2 inhibitor; [*E*]-6-[bromoethylene]-3-[1-naphthalenyl]-2*H*-tetrahydropyran-2-one. The addition of the lipase inhibitors to the assay also tests if CrLIP4 utilizes the same catalytic mechanism as SDP1 or patatin (Eastmond, 2006).

The function of the intrinsic disordered region (IDR) of CrLIP4. Research in other systems indicates that an IDR has the potential to act as a regulatory site through various mechanisms such as protein-protein interaction and phosphorylation (Uversky, 2013a, 2013b). The importance of the IDR in CrLIP4 can be tested by introducing a truncated CrLIP4, which lacks the IDR (CrLIP4^{ΔIDR}) into the artificial microRNA knockdown lines or a knockout mutant as discussed in the last section. I hypothesize that the CrLIP4^{ΔIDR} overexpression line in the knockdown background will not restore the normal TAG degradation phenotype. This is based on my hypothesis that IDR plays a role in controlling how CrLIP4 functions *in vivo*. However, recombinant CrLIP4^{ΔIDR} should be able to digest the TAG substrate *in vitro*. In addition, CrLIP4^{ΔIDR} with codon optimization may be able to rescue yeast and Arabidopsis mutants since it would lack the IDR, which results in better protein folding and thus affects catalytic activity.

Targeted mutation to obtain a *CrLIP4* loss-of-function mutant. My investigation of CrLIP4 function was limited by the lack of a knockout mutation. Knockdown Chlamydomonas mutants can be obtained through post-transcriptional gene silencing using antisense RNA, RNA silencing, or artificial microRNA (Jinkerson & Jonikas, 2015). However, knockdown mutants have some limitations. For example, the phenotype obtained from a knockdown mutant may be too subtle due to incomplete target gene suppression. In addition, modifiers and/or adaptation can lead to a loss of phenotype in culture. In the following section, techniques for knocking out *CrLIP4* are discussed.

Targeting Induced Local Lesions in Genomes (TILLING). TILLING is based on a forward genetic screen through a chemical mutagen (Comai & Henikoff, 2006; McCallum *et al.*, 2000). The mutation can be identified for a specific locus through gene specific primers. The products of amplification of the wild type and the mutant are denatured and then allowed to rehybridize. The mismatches between the wild type and mutant DNA strands form heteroduplex structures, which can be digested with the mismatch-specific celery nuclease CELI. The digestion products are then detected through gel electrophoresis. Since this technique relies on random mutagenesis, the mutation in *CrLIP4* might never be found. However, we can hope that the Chlamydomonas TILLING project may eventually produce such a mutant.

Homologous recombination. Homologous recombination is a useful tool to target gene modification by exploiting an endogenous mechanism of the cell to repair its genetic material. This technique has been widely used in many organisms such as mouse (Hall *et al.*, 2009) and *E. coli* (Sharan *et al.*, 2009). However, the rate of recombination events in plants is low (Puchta, 2002). The only plant that has been reported to be successfully mutated with this method is the moss *Physcomitrella patens* (Kamisugi *et al.*, 2006). In Chlamydomonas, this technique has been used, although it shows much lower frequencies of recombination (Gumpel *et al.*, 1994; Sodeinde & Kindle, 1993) and strong selection strategies were applied (Jinkerson & Jonikas, 2015). Several approaches have been employed to facilitate homologous recombination in Chlamydomonas as discussed in Jinkerson and Jonikas (2015), however, none of these modifications are very promising for knocking out a specific gene in Chlamydomonas.

Zinc-finger nucleases. Zinc-finger nucleases (ZFNs) are artificial nucleases that can be specifically designed to introduce a double strand break (DSB) in a specific DNA sequence (Kim

et al., 1996). DSBs can be repaired by homologous recombination or non-homologous end joining, both of which can introduce mutation at the repair site. ZFN technology has been a useful tool for editing the genome of *Drosophila melanogaster* (Bibikova *et al.*, 2002), Arabidopsis (Lloyd *et al.*, 2005), and mouse (Cui *et al.*, 2011). Sizova *et al.* (2013) reported a successful modification of a non-selectable gene in Chlamydomonas with this method. ZFNGenome was established to provide a database for ZFNs in many model organisms including Chlamydomonas (Reyon *et al.*, 2011). From this resource, *CrLIP4* can be scanned for ZFN recognition sites, which could subsequently be targeted. By co-introducing ZFNs and a construct with a selectable marker gene flanking the homologous sequence of *CrLIP4* into the Chlamydomonas genome, a knockout mutation may be obtained.

Transcription activator-like effector nucleases. Similar to ZFNs, transcription activator-like effector nucleases (TALENs) can be engineered to recognize and cut a specific DNA sequence in the genome (Li *et al.*, 2012). The advantage of this technique is, instead of recognizing a set of three nucleotides in ZFNs, transcription activator-like effector (TALE) can recognize a single nucleotide. This feature overcomes the limited availability of recognition sites in the DNA sequence. By attaching several TALEs to a nuclease module, one can design a specific cut site targeting a gene of interest. With more flexibility of the target sequence, a knockout mutant of *CrLIP4* could be generated.

CRISPR-Cas9. Another technique that can introduce DSB into DNA is CRISPR-Cas9 (Jinek *et al.*, 2012). Unlike ZFNs and TALENs that rely on protein recognition that is specific for each target gene, the CRISPR-Cas9 system utilizes a universal endonuclease (Cas9) and a guide RNA targeting a gene of interest. One can design RNA molecules to recognize only a specific target DNA sequence, without going through the complication of protein engineering. Therefore, CRISPR/Cas9 is simpler to apply than ZFNs and TALENs systems. This technique has been employed in human cells and in various organisms such as mouse, *D. melanogaster*, *C. elegans*, Arabidopsis, rice, etc. (Doudna & Charpentier, 2014). The first attempt to use CRISPR-Cas9 in Chlamydomonas was reported by Jiang *et al.* (2014). Although CRISPR-Cas9 activity was detected and a mutant was generated, the efficiency was far from satisfactory. If in the future this technique is optimized for Chlamydomonas, it will be the most promising and preferable method to knock out *CrLIP4*. Because this technique also allows mutation of multiple targets, *CrLIP4* and other putative TAG lipases could be knocked out at the same time. If these enzymes function

in the same pathway, I expect a more severe TAG degradation phenotype in the double or triple knockout lines than would be observed for the single mutants.

SUMMARY

In this thesis research two Arabidopsis orthologues were characterized in Chlamydomonas. Despite many remaining questions and future work discussed above, my investigation provides new insights into Chlamydomonas lipid metabolism. First, my research on CrTGD2 revealed that Chlamydomonas utilizes the eukaryotic pathway to synthesize their galactoglycerolipids. Second, this study also pointed out that Arabidopsis orthologues in Chlamydomonas function and locate differently in Chlamydomonas as seen in the LPAATs and MGDG synthase, respectively. Finally, characterization of CrLIP4 is the first report of TAG lipase activity characterized in this microalga. I hope that information from this thesis research will pave a way to the complete understanding of lipid metabolism in Chlamydomonas and can be applied in other microalgae in the future.

REFERENCES

REFERENCES

- Bibikova, M., Golic, M., Golic, K. G., & Carroll, D. (2002). Targeted chromosomal cleavage and mutagenesis in *Drosophila* using zinc-finger nucleases. *Genetics*, *161*(3), 1169-1175.
- Blaby, I. K., Blaby-Haas, C. E., Tourasse, N., Hom, E. F., Lopez, D., Aksoy, M., Grossman, A., Umen, J., Dutcher, S., Porter, M., King, S., Witman, G. B., Stanke, M., Harris, E. H., Goodstein, D., Grimwood, J., Schmutz, J., Vallon, O., Merchant, S. S., & Prochnik, S. (2014). The *Chlamydomonas* genome project: a decade on. *Trends Plant Sci*, *19*(10), 672-680. doi: 10.1016/j.tplants.2014.05.008
- Comai, L., & Henikoff, S. (2006). TILLING: practical single-nucleotide mutation discovery. *Plant J*, *45*(4), 684-694. doi: 10.1111/j.1365-313X.2006.02670.x
- Cowen, L., Bradley, P., Menke, M., King, J., & Berger, B. (2002). Predicting the beta-helix fold from protein sequence data. *J Comput Biol*, *9*(2), 261-276. doi: 10.1089/10665270252935458
- Cui, X., Ji, D., Fisher, D. A., Wu, Y., Briner, D. M., & Weinstein, E. J. (2011). Targeted integration in rat and mouse embryos with zinc-finger nucleases. *Nat Biotechnol*, *29*(1), 64-67. doi: 10.1038/nbt.1731
- Daniels, N. M., Hosur, R., Berger, B., & Cowen, L. J. (2012). SMURFLite: combining simplified Markov random fields with simulated evolution improves remote homology detection for beta-structural proteins into the twilight zone. *Bioinformatics*, *28*(9), 1216-1222. doi: 10.1093/bioinformatics/bts110
- Doudna, J. A., & Charpentier, E. (2014). The new frontier of genome engineering with CRISPR-Cas9. *Science*, *346*(6213), 1077-+. doi: ARTN 1258096
10.1126/science.1258096
- Eastmond, P. J. (2006). SUGAR-DEPENDENT1 encodes a patatin domain triacylglycerol lipase that initiates storage oil breakdown in germinating *Arabidopsis* seeds. *Plant Cell*, *18*(3), 665-675. doi: 10.1105/tpc.105.040543
- Fan, J., Zhai, Z., Yan, C., & Xu, C. (2015). *Arabidopsis* TRIGALACTOSYLDIACYLGLYCEROL5 Interacts with TGD1, TGD2, and TGD4 to Facilitate Lipid Transfer from the Endoplasmic Reticulum to Plastids. *Plant Cell*. doi: 10.1105/tpc.15.00394
- Finn, R. D., Tate, J., Mistry, J., Coghill, P. C., Sammut, S. J., Hotz, H. R., Ceric, G., Forslund, K., Eddy, S. R., Sonnhammer, E. L., & Bateman, A. (2008). The Pfam

- protein families database. *Nucleic Acids Res*, 36(Database issue), D281-288. doi: 10.1093/nar/gkm960
- Gumpel, N. J., Rochaix, J. D., & Purton, S. (1994). Studies on homologous recombination in the green alga *Chlamydomonas reinhardtii*. *Curr Genet*, 26(5-6), 438-442.
- Hall, B., Limaye, A., & Kulkarni, A. B. (2009). Overview: Generation of Gene Knockout Mice. In J. S. Bonifacino, J. B. Harford, J. Lippincott-Schwartz, & K. M. Yamada (Eds.), *Curr Protoc Cell Biol* (Vol. 44, pp. 19.12.01-19.12.17). Anglia, UK: John Wiley & Sons, Inc.
- Jiang, W., Brueggeman, A. J., Horken, K. M., Plucinak, T. M., & Weeks, D. P. (2014). Successful transient expression of Cas9 and single guide RNA genes in *Chlamydomonas reinhardtii*. *Eukaryot Cell*, 13(11), 1465-1469. doi: 10.1128/EC.00213-14
- Jinek, M., Chylinski, K., Fonfara, I., Hauer, M., Doudna, J. A., & Charpentier, E. (2012). A programmable dual-RNA-guided DNA endonuclease in adaptive bacterial immunity. *Science*, 337(6096), 816-821. doi: 10.1126/science.1225829
- Jinkerson, R. E., & Jonikas, M. C. (2015). Molecular techniques to interrogate and edit the *Chlamydomonas* nuclear genome. *Plant J*, 82(3), 393-412. doi: 10.1111/tpj.12801
- Kamisugi, Y., Schlink, K., Rensing, S. A., Schween, G., von Stackelberg, M., Cuming, A. C., Reski, R., & Cove, D. J. (2006). The mechanism of gene targeting in *Physcomitrella patens*: homologous recombination, concatenation and multiple integration. *Nucleic Acids Res*, 34(21), 6205-6214. doi: 10.1093/nar/gkl832
- Kim, Y. G., Cha, J., & Chandrasegaran, S. (1996). Hybrid restriction enzymes: zinc finger fusions to Fok I cleavage domain. *Proc Natl Acad Sci U S A*, 93(3), 1156-1160.
- Lathrop, R. H., & Smith, T. F. (1996). Global optimum protein threading with gapped alignment and empirical pair score functions. *J Mol Biol*, 255(4), 641-665. doi: 10.1006/jmbi.1996.0053
- Li, T., Liu, B., Spalding, M. H., Weeks, D. P., & Yang, B. (2012). High-efficiency TALEN-based gene editing produces disease-resistant rice. *Nat Biotechnol*, 30(5), 390-392. doi: 10.1038/nbt.2199
- Li-Beisson, Y., Beisson, F., & Riekhof, W. (2015). Metabolism of acyl-lipids in *Chlamydomonas reinhardtii*. *Plant J*, 82(3), 504-522. doi: 10.1111/tpj.12787

- Lifson, S., & Sander, C. (1980). Specific recognition in the tertiary structure of beta-sheets of proteins. *J Mol Biol*, *139*(4), 627-639.
- Liu, Y., Carbonell, J., Gopalakrishnan, V., & Weigele, P. (2009). Conditional graphical models for protein structural motif recognition. *J Comput Biol*, *16*(5), 639-657. doi: 10.1089/cmb.2008.0176
- Lloyd, A., Plaisier, C. L., Carroll, D., & Drews, G. N. (2005). Targeted mutagenesis using zinc-finger nucleases in Arabidopsis. *Proc Natl Acad Sci U S A*, *102*(6), 2232-2237. doi: 10.1073/pnas.0409339102
- McCallum, C. M., Comai, L., Greene, E. A., & Henikoff, S. (2000). Targeted screening for induced mutations. *Nat Biotechnol*, *18*(4), 455-457. doi: 10.1038/74542
- Menke, M., Berger, B., & Cowen, L. (2010). Markov random fields reveal an N-terminal double beta-propeller motif as part of a bacterial hybrid two-component sensor system. *Proc Natl Acad Sci U S A*, *107*(9), 4069-4074. doi: 10.1073/pnas.0909950107
- Merchant, S. S., Prochnik, S. E., Vallon, O., Harris, E. H., Karpowicz, S. J., Witman, G. B., Terry, A., Salamov, A., Fritz-Laylin, L. K., Marechal-Drouard, L., Marshall, W. F., Qu, L. H., Nelson, D. R., Sanderfoot, A. A., Spalding, M. H., Kapitonov, V. V., Ren, Q., Ferris, P., Lindquist, E., Shapiro, H., Lucas, S. M., Grimwood, J., Schmutz, J., Cardol, P., Cerutti, H., Chanfreau, G., Chen, C. L., Cognat, V., Croft, M. T., Dent, R., Dutcher, S., Fernandez, E., Fukuzawa, H., Gonzalez-Ballester, D., Gonzalez-Halphen, D., Hallmann, A., Hanikenne, M., Hippler, M., Inwood, W., Jabbari, K., Kalanon, M., Kuras, R., Lefebvre, P. A., Lemaire, S. D., Lobanov, A. V., Lohr, M., Manuell, A., Meier, I., Mets, L., Mittag, M., Mittelmeier, T., Moroney, J. V., Moseley, J., Napoli, C., Nedelcu, A. M., Niyogi, K., Novoselov, S. V., Paulsen, I. T., Pazour, G., Purton, S., Ral, J. P., Riano-Pachon, D. M., Riekhof, W., Rymarquis, L., Schroda, M., Stern, D., Umen, J., Willows, R., Wilson, N., Zimmer, S. L., Allmer, J., Balk, J., Bisova, K., Chen, C. J., Elias, M., Gendler, K., Hauser, C., Lamb, M. R., Ledford, H., Long, J. C., Minagawa, J., Page, M. D., Pan, J., Pootakham, W., Roje, S., Rose, A., Stahlberg, E., Terauchi, A. M., Yang, P., Ball, S., Bowler, C., Dieckmann, C. L., Gladyshev, V. N., Green, P., Jorgensen, R., Mayfield, S., Mueller-Roeber, B., Rajamani, S., Sayre, R. T., Brokstein, P., Dubchak, I., Goodstein, D., Hornick, L., Huang, Y. W., Jhaveri, J., Luo, Y., Martinez, D., Ngau, W. C., Otilar, B., Poliakov, A., Porter, A., Szajkowski, L., Werner, G., Zhou, K., Grigoriev, I. V., Rokhsar, D. S., & Grossman, A. R. (2007). The Chlamydomonas genome reveals the evolution of key animal and plant functions. *Science*, *318*(5848), 245-250. doi: 10.1126/science.1143609
- Miller, R., Wu, G., Deshpande, R. R., Vieler, A., Gartner, K., Li, X., Moellering, E. R., Zauner, S., Cornish, A. J., Liu, B., Bullard, B., Sears, B. B., Kuo, M. H., Hegg, E. L., Shachar-Hill, Y., Shiu, S. H., & Benning, C. (2010). Changes in transcript

- abundance in *Chlamydomonas reinhardtii* following nitrogen deprivation predict diversion of metabolism. *Plant Physiol*, 154(4), 1737-1752. doi: 10.1104/pp.110.165159
- Olmea, O., Rost, B., & Valencia, A. (1999). Effective use of sequence correlation and conservation in fold recognition. *J Mol Biol*, 293(5), 1221-1239. doi: 10.1006/jmbi.1999.3208
- Peng, J., & Xu, J. (2011). A multiple-template approach to protein threading. *Proteins*, 79(6), 1930-1939. doi: 10.1002/prot.23016
- Puchta, H. (2002). Gene replacement by homologous recombination in plants. *Plant Mol Biol*, 48(1-2), 173-182.
- Rasala, B. A., Barrera, D. J., Ng, J., Plucinak, T. M., Rosenberg, J. N., Weeks, D. P., Oyler, G. A., Peterson, T. C., Haerizadeh, F., & Mayfield, S. P. (2013). Expanding the spectral palette of fluorescent proteins for the green microalga *Chlamydomonas reinhardtii*. *Plant J*, 74(4), 545-556. doi: 10.1111/tpj.12165
- Ratcliffe, R. G., & Shachar-Hill, Y. (2006). Measuring multiple fluxes through plant metabolic networks. *Plant J*, 45(4), 490-511. doi: 10.1111/j.1365-313X.2005.02649.x
- Reyon, D., Kirkpatrick, J. R., Sander, J. D., Zhang, F., Voytas, D. F., Joung, J. K., Dobbs, D., & Coffman, C. R. (2011). ZFNGenome: a comprehensive resource for locating zinc finger nuclease target sites in model organisms. *BMC Genomics*, 12, 83. doi: 10.1186/1471-2164-12-83
- Sharan, S. K., Thomason, L. C., Kuznetsov, S. G., & Court, D. L. (2009). Recombineering: a homologous recombination-based method of genetic engineering. *Nat Protoc*, 4(2), 206-223. doi: 10.1038/nprot.2008.227
- Sizova, I., Greiner, A., Awasthi, M., Kateriya, S., & Hegemann, P. (2013). Nuclear gene targeting in *Chlamydomonas* using engineered zinc-finger nucleases. *Plant J*, 73(5), 873-882. doi: 10.1111/tpj.12066
- Sodeinde, O. A., & Kindle, K. L. (1993). Homologous recombination in the nuclear genome of *Chlamydomonas reinhardtii*. *Proc Natl Acad Sci U S A*, 90(19), 9199-9203.
- Steward, R. E., & Thornton, J. M. (2002). Prediction of strand pairing in antiparallel and parallel beta-sheets using information theory. *Proteins*, 48(2), 178-191. doi: 10.1002/prot.10152

- Thomas, J., Ramakrishnan, N., & Bailey-Kellogg, C. (2008). Graphical models of residue coupling in protein families. *IEEE/ACM Trans Comput Biol Bioinform*, 5(2), 183-197. doi: 10.1109/TCBB.2007.70225
- Tsai, C. H., Warakanont, J., Takeuchi, T., Sears, B. B., Moellering, E. R., & Benning, C. (2014). The protein Compromised Hydrolysis of Triacylglycerols 7 (CHT7) acts as a repressor of cellular quiescence in *Chlamydomonas*. *Proc Natl Acad Sci U S A*, 111(44), 15833-15838. doi: 10.1073/pnas.1414567111
- Uversky, V. N. (2013a). A decade and a half of protein intrinsic disorder: biology still waits for physics. *Protein Sci*, 22(6), 693-724. doi: 10.1002/pro.2261
- Uversky, V. N. (2013b). Intrinsic disorder-based protein interactions and their modulators. *Curr Pharm Des*, 19(23), 4191-4213.
- Wang, Z., Anderson, N. S., & Benning, C. (2013). The phosphatidic acid binding site of the Arabidopsis trigalactosyldiacylglycerol 4 (TGD4) protein required for lipid import into chloroplasts. *J Biol Chem*, 288(7), 4763-4771. doi: 10.1074/jbc.M112.438986
- Wilson, D., Madera, M., Vogel, C., Chothia, C., & Gough, J. (2007). The SUPERFAMILY database in 2007: families and functions. *Nucleic Acids Res*, 35(Database issue), D308-313. doi: 10.1093/nar/gkl910
- Xu, C., Fan, J., Riekhof, W., Froehlich, J. E., & Benning, C. (2003). A permease-like protein involved in ER to thylakoid lipid transfer in Arabidopsis. *EMBO J*, 22(10), 2370-2379. doi: 10.1093/emboj/cdg234
- Zhu, H., & Braun, W. (1999). Sequence specificity, statistical potentials, and three-dimensional structure prediction with self-correcting distance geometry calculations of beta-sheet formation in proteins. *Protein Sci*, 8(2), 326-342. doi: 10.1110/ps.8.2.326

SUPPORTING CHAPTER

Critical Role of *Chlamydomonas reinhardtii* Ferredoxin-5 in Maintaining Membrane Structure and Dark Metabolism[‡]

[‡] This work was carried out in collaboration with several laboratories and has been published at the Proceedings of the National Academy of Sciences of the United States of America in Wenqiang Yang, Tyler M. Wittkopp, Xiaobo Li, Jaruswan Warakanont, Alexandra Dubini, Claudia Catalanotti, Rick G. Kim, Eva C. M. Nowack, Luke Mackinder, Munevver Aksoy, Mark Dudley Page, Sarah D'Adamo, Shai Saroussi, Mark Heinnickel, Xenie Johnson, Pierre Richaud, Jean Alric, Marko Boehm, Martin C. Jonikas, Christoph Benning, Sabeeha S. Merchant, Matthew C. Posewitz, Arthur R. Grossman (2015) Critical Role of *Chlamydomonas reinhardtii* Ferredoxin-5 in Maintaining Membrane Structure and Dark Metabolism. Proc Natl Acad Sci U S A 112: 14978-14983, doi:10.1073/pnas.1515240112
I contributed to Figure A.2E-F, A.3A, A.S9, and A.S10.

ABSTRACT

Photosynthetic microorganisms typically have multiple isoforms of the electron transfer protein ferredoxin, although we know little about their exact functions. Surprisingly, a *Chlamydomonas reinhardtii* mutant null for the ferredoxin-5 gene (*FDX5*) completely ceased growth in the dark, with both photosynthetic and respiratory functions severely compromised; growth in the light was unaffected. Thylakoid membranes in dark-maintained *fdx5* mutant cells became severely disorganized concomitant with a marked decrease in the ratio of monogalactosyldiacylglycerol (MGDG) to digalactosyldiacylglycerol (DGDG), major lipids in photosynthetic membranes, and the accumulation of triacylglycerol (TAG). Furthermore, FDX5 was shown to physically interact with the fatty acid desaturases Cr Δ 4FAD and CrFAD6, likely donating electrons for the formation of the desaturated fatty acids that stabilize MGDG. Our results strongly suggest that in photosynthetic organisms, specific electron mediators sustain dark metabolism, with little impact on daytime growth, likely reflecting the tailoring of electron carriers to unique intracellular metabolic circuits under these two very distinct redox conditions.

SIGNIFICANCE STATEMENT

Our results strongly suggest that particular ferredoxins in photosynthetic organisms are tailored to serve as electron carriers that sustain day-time and night-time metabolism, and that chloroplast-localized FDX5 appears to function in the desaturation of fatty acids required for maintaining the correct ratio of the dominant lipids in the thylakoid membranes and the integration of chloroplast and mitochondrial metabolism, which is absolutely required for growth in the dark. The most important messages from this work are that redox components associated with critical activities in photosynthetic organisms must be tuned to the redox conditions of the cells and the overall carbon budget of photosynthetic cells requires an understanding of metabolic features that accompany the movement of cells between light and dark conditions.

INTRODUCTION

Ferredoxins (FDXs) are soluble, non-heme iron-sulfur proteins that mediate electron transfer in a variety of essential metabolic reactions (G. Hanke & Mulo, 2013; G. T. Hanke *et al.*, 2004; Valentine, 1964) (Figure A.S1). The *Chlamydomonas* genome encodes 13 ferredoxins (Table A.S1) with localization and redox properties that suggest involvement in specific redox reactions

(Terauchi *et al.*, 2009). Using a yeast two hybrid approach, a global FDX interaction network was established for *Chlamydomonas*, suggesting putative roles for FDX1 (originally designated Fd) in redox metabolism, carbohydrate modification and fatty acid biosynthesis (Peden *et al.*, 2013); this FDX was already known to function in both linear and cyclic photosynthetic electron flow (Schmitter *et al.*, 1988; Terauchi *et al.*, 2009). FDX1 also accepts electrons from ferredoxin-NADP oxidoreductase (FNR)(van Lis *et al.*, 2013) and donates electrons to HYDA hydrogenases (Noth *et al.*, 2013; Peden *et al.*, 2013; Winkler *et al.*, 2010). Other FDXs may be involved in state transitions, nitrogen metabolism, cellular responses to reactive oxygen species (ROS) and dark anoxia (Hemschemeier *et al.*, 2013; Jacobs *et al.*, 2009; Lambertz *et al.*, 2010; Mus *et al.*, 2007; Peden *et al.*, 2013; Terauchi *et al.*, 2009).

The major lipids in thylakoid membranes are monogalactosyldiacylglycerol (MGDG), digalactosyldiacylglycerol (DGDG), phosphatidylglycerol (PtdGro) and sulfoquinovosyldiacylglycerol (SQDG) (Dörmann & Benning, 2002; Dörmann *et al.*, 1995; Kelly & Dormann, 2004; Liu & Benning, 2013), with MGDG being the most abundant, followed by DGDG (Dörmann & Benning, 2002; Dörmann *et al.*, 1995). In *Arabidopsis*, three enzyme systems are involved in MGDG and DGDG synthesis (Benning & Ohta, 2005). In contrast, there is only a single copy each of an MGDG and DGDG synthase gene in *Chlamydomonas* (Riekhof *et al.*, 2005). *Chlamydomonas* uses the prokaryotic pathway for thylakoid lipid synthesis (Giroud *et al.*, 1988) in which the MGDG species synthesized in chloroplasts contain predominantly C18:3^{Δ9,12,15}-*sn-1* with the unusual hexadeca-4, 7, 10, 13-tetraenoic acid, C16:4^{Δ4,7,10,13} at the *sn-2* position (Giroud *et al.*, 1988). Desaturation of the *sn-2* acyl group of *Chlamydomonas* MGDG requires the CrΔ4FAD desaturase, which is not present in *Arabidopsis*²¹, and MGDG accumulation in *Chlamydomonas* is reduced in strains that make less CrΔ4FAD (Zäuner *et al.*, 2012). Under conditions of nutrient deprivation, there are small amounts of C16:4^{Δ4,7,10,13} and C18:3^{Δ9,12,15} that are integrated into triacylglycerol (TAG) (Fan *et al.*, 2011; Moellering & Benning, 2010), indicating that fatty acids within TAG can be at least partly recycled from membrane lipids such as MGDG.

In this study, we show that a *fdx5* mutant (*i*) cannot grow in the dark despite having a growth rate similar to that of wild-type (WT) cells in the light, (*ii*) has altered photosynthetic properties, membrane structure and lipid composition relative to WT cells, and (*iii*) accumulates higher levels of TAG. In addition, FDX5 appears to interact with the CrΔ4FAD and CrFAD6

desaturases. Together, these results suggest a critical role for FDX5 in fatty acid desaturation and maintaining thylakoid membrane composition and functionality specifically during growth in the dark.

RESULTS

***fdx5* is a null mutant.** The *Chlamydomonas FDX5* gene (Figure A.S2A) encodes a protein of 130 amino acids with residues 35-107 forming the 2Fe-2S cluster binding domain (Figure A.S2B). We used random insertional mutagenesis (Gonzalez-Ballester *et al.*, 2011; Pootakham *et al.*, 2010) and a PCR-based screen to isolate a mutant disrupted for *FDX5* (*FDX5* specific primers shown in Table A.S2). Southern blot hybridizations indicated that the *FDX5* gene was disrupted by the *AphVIII* cassette (Figure A.S2C, D). Characterization of the site of insertion in *FDX5* was performed by PCR and sequencing (Figure A.S2E). The cassette insertion resulted in a 46 bp deletion in the second exon that caused a shift in the open reading frame and a truncation of the C-terminal sequence (Figure A.S2B, F). The truncated protein no longer contains the conserved cysteine residues that bind the 2Fe-2S cluster required for protein activity. Using immunological analyses we were unable to detect FDX5 in the mutant (Figure A.S2G, left), while the FDX5 protein was restored in the rescued strains (Figure A.S2G, left and right).

FDX5 localizes to chloroplasts. Amino acids 1-18 of FDX5 are predicted to encode an N-terminal chloroplast transit peptide (Tardif *et al.*, 2012) (Figure A.S2B). Previous biochemical (Jacobs *et al.*, 2009) and proteomic (Terashima *et al.*, 2010) studies demonstrated chloroplast localization of FDX5, which was confirmed in this study (Figure A.S3); the various mutant strains and constructs used for this and other analyses presented below are given in Tables A.S3 and A.S4.

Disruption of FDX5 causes a dark growth deficiency. As shown in Figure A.1A, B, the *fdx5* mutant grows normally on TAP (tris-acetate-phosphate) agar and liquid medium in the light, but is unable to grow on the same medium in the dark. Very low light intensities (2 and 5 $\mu\text{mol photons m}^{-2} \text{s}^{-1}$) were sufficient for *fdx5* to grow, albeit at a slower rate than WT and the complemented cells (Figure A.S4A, B). With slight increases in light intensity (10 and 40 $\mu\text{mol photons m}^{-2} \text{s}^{-1}$), the rate of *fdx5* growth became the same as that of WT and the complemented strains (Figure A.S4C, D). Tetrad analyses demonstrated that the dark growth phenotype cosegregated with the insertion conferring paromomycin resistance (Figure A.S5). To confirm

that disruption of *FDX5* was the cause of the phenotype, we introduced WT *FDX5* cDNA and gDNA into *fdx5* cells, which grew under both light and dark conditions on solid and in liquid medium, as shown for *fdx5(FDX5)*-1 and *fdx5(FDX5)*-2 rescued strains (Figure A.1A, B); *fdx5(FDX5)*-1 was used for the remaining studies and is hereafter designated *fdx5(FDX5)*. The growth-rescued transformants also regained their ability to accumulate FDX5 protein (Figure A.S2G). Overall, these results conclusively demonstrate that a strain unable to synthesize FDX5 cannot grow in the dark, but readily resumes growth in the light.

Photosynthesis and respiration decrease in dark-maintained *fdx5*. The inability of *fdx5* to grow in the dark suggested a loss of respiratory activity. As shown in Figure A.1C, respiratory O₂ consumption is comparable in WT and mutant cells in the light and after transfer to the dark for up to 6 h. However, after 24 and 48 h in the dark there was ~2 fold more respiratory O₂ consumption in WT and the complemented strain than in *fdx5*. A similar trend was observed for light-mediated net photosynthetic O₂ evolution, indicating a rapid decline in the ability of *fdx5* to perform photosynthetic electron transport after dark-acclimation (Figure A.1D). Hence, both respiratory and photosynthetic processes were seriously compromised in the dark-maintained *fdx5* mutant.

To determine the extent of absolute O₂ consumption after dark grown cells were placed in the light, we performed membrane inlet mass spectrometry (MIMS) with added gaseous ¹⁸O₂ to distinguish between absolute O₂ consumption and evolution (from H₂¹⁶O). As shown in Figure A.S6, the decline in net light-dependent O₂ evolution in *fdx5* is partly reflected by an increased rate of light-dependent O₂ consumption, which is substantially higher in *fdx5* than in WT cells.

Photosynthetic electron flow is altered in dark-maintained *fdx5*. To examine photosynthetic electron transport rates (ETR), we monitored the induction of Chl fluorescence. Induction curves of cultures transferred to the dark for 24 h showed that illumination caused an increase in steady-state fluorescence (F_s) for *fdx5* relative to WT or complemented cells (Figure A.S7A), indicating that the plastoquinone (PQ) pool in the mutant was more reduced. Following the addition of the PSII inhibitor DCMU to the cultures (Figure A.S7A), Chl fluorescence was the same for all dark-grown strains, indicating normal functioning of PSII reaction centers. These results indicate that when maintained in the dark, *fdx5* develops a partial block in photosynthetic electron flow.

To assess the effect of different actinic light intensities on light- or dark-grown cultures, Chl fluorescence induction curves were assayed. For all growth conditions, F_v/F_m values were similar

among the strains (Figure A.S7B; Φ PSII at time 0), suggesting that PSII is active and not responsible for the block in electron flow. The light curves also confirmed a reduction in ETR after the *fdx5* mutant had been maintained in the dark (Figure A.S7B, middle panel). Furthermore, as shown in Figure A.S7C (bottom right panel), the addition of MV, which accepts electrons from PSI, to dark-grown cultures relieved elevated PQ pool reduction in *fdx5* relative to WT cells, strongly suggesting that the block in electron transport was the result of a defect downstream of PSI, potentially caused by a lack of a suitable electron acceptor. Surprisingly, the rate of cyclic electron flow (CEF) was drastically reduced for *fdx5* grown in the dark (Figure A.S7D, right panel), but not in the light (Figure A.S7D, left panel). The addition of MV, which competes with CEF for PSI electrons, had a similar effect for all strains (Figure A.S7D). Overall, *fdx5* appears to be defective for both photosynthetic and respiratory processes after dark acclimation.

Photosynthetic polypeptides are not altered in *fdx5*. The decrease in ETR and CEF in *fdx5* grown in the dark could result from altered thylakoid membrane structure and/or aberrant accumulation of photosynthetic polypeptides or complexes. To explore the latter, we examined representative subunits of each photosynthetic complex by immunoblots. As shown in Figure A.S8, we immunologically detected the proteins of all of the major photosynthetic complexes; these include PsbA, OEE2, Cyt *f*, PSAD, both CF1- β and F1- β , LS, NDA2, and PGRL1 (full names provided in Figure A.S8). These proteins accumulated in *fdx5* to approximately WT levels in both the light and dark (mitochondrial F1- β was somewhat lower in the ‘Back to Light’ samples), suggesting no major alteration in the composition of membrane proteins associated with photosynthetic function in the mutant. These results oriented our further analyses toward examining membrane structure and lipid composition in dark-maintained *fdx5*.

Dark-maintained *fdx5* has altered membrane ultrastructure. A potential explanation for the phenotypes described above is that the membrane structure/lipid composition is aberrant in dark-maintained *fdx5*, which in turn could retard efficient electron transport or other membrane-associated processes (e.g. ion transport). To evaluate this possibility, we performed TEM of sectioned *Chlamydomonas* cells. In WT cells, thylakoid membranes are arranged as layers within chloroplasts, with some of the membranes appressed. Features in the light and dark were similar, although the membranes appeared to be more regularly arranged in light-grown cells (compare Figure A.2A, C). While the layered arrangement of thylakoids is observed in light-grown *fdx5*

(Figure A.2B), transfer of the mutant to the dark (Figure A.2D) caused the membrane structure to become highly aberrant. Dark-grown mutant membranes appear wavier, have more convoluted configurations and seem to be more fragmented than membranes of WT cells. The cytoplasm and the chloroplast stroma in *fdx5* had reduced granularity and did not accumulate large thylakoid-associated starch granules compared to WT (Figure A.2D).

Membrane lipids are altered in dark-maintained *fdx5*. The phenotypes described above raised the possibility that *fdx5* is defective in generating normal membranes in the dark, which may explain the aberrant membrane structures and disrupted activities that require specific lipid environments. Therefore, we analyzed classes of lipids and their acyl groups in membranes of *fdx5* and WT cells. The relative levels of MGDG and DGDG in light-grown *fdx5* and WT cells exhibited minor differences (Figure A.2E, F, Light). However, after 24, 48 and 72 h in the dark (Figure A.2E, F, Dark), the ratio of MGDG to DGDG in *fdx5* strongly declined in comparison with WT cells. By 48 and 72 h in the dark, the mutant had a ~2:1 ratio of MGDG to DGDG while the ratio in WT cells was ~5:1 (Figure A.2E, F, Dark).

We also examined total fatty acid profiles under the same experimental conditions (Figure A.3A). The fraction of specific fatty acids that contain four double bonds (C16:4^{Δ4,7,10,13}) was decreased in *fdx5* maintained in the dark for 48 h, but not in the light. This difference could be a consequence of a decrease in the synthesis of C16:4^{Δ4,7,10,13} (in accord with this finding, more C16:3^{Δ7,10,13} accumulated in *fdx5* than in WT cells), an increase in degradation of MGDG containing C16:0 to C16:4^{Δ4,7,10,13} on the *sn*-2 position of MGDG, an increase in conversion of MGDG to DGDG (prior to desaturation of C16 on *sn*-2 of MGDG), or a combination of these events. We note that the change in the level of C16:4^{Δ4,7,10,13} in *fdx5* in the dark was not as extensive as the change in the relative MGDG levels, which is consistent with previous results²¹ and suggests: *i*) a decline in synthesis of C16:4^{Δ4,7,10,13} is also accompanied by conversion of MGDG containing C16:4^{Δ4,7,10,13} to DGDG; and *ii*) a proportion of the MGDG is degraded and the C16:4^{Δ4,7,10,13} is converted into TAG and potentially other lipids. The latter possibility is consistent with additional findings. The MGDG fatty acid composition showed no major difference in the fraction of C16:4^{Δ4,7,10,13} (relative to total fatty acids) in *fdx5* in the dark relative to WT cells (Figure A.S9), with only a small change in the level of C16:4^{Δ4,7,10,13} in DGDG (Figure A.S10). There were also changes in the levels of C16:0, C16:1^{Δ7}, 18:1^{Δ9} and 18:3^{Δ9,12,15} in DGDG (Figure A.S10) of *fdx5*, but these changes are independent of light/dark conditions and

do not appear to impact the MGDG:DGDG ratio (in the light the ratio of these lipids in *fdx5* is similar to that of WT cells). Overall, aberrations in lipid composition (most notably the MGDG:DGDG ratio) and an altered ability to maintain the proper desaturation state of the fatty acids in dark-maintained *fdx5* could explain the defects in photosynthesis, distorted membrane structure and the overall appearance of mutant chloroplasts (membranes and stroma), which could also impact other cellular processes including respiration. Therefore, we sought to obtain mechanistic insights into the ways in which the *fdx5* mutation impacts membrane lipid and fatty acid composition.

FDX5 interacts with CrΔ4FAD and CrFAD6 desaturases. Previous yeast two hybrid experiments demonstrated that FDX5 might associate with two fatty acid desaturases (Peden *et al.*, 2013); CrFAD6 (Cre13.g590500), which is involved in desaturation of C18:1 in plastidic lipids (MGDG, DGDG, PG, SQDG) to C18:2, and CrΔ4FAD (Cre01.g037700), which is specific to *Chlamydomonas* MGDG and is involved in desaturation of C16:3^{Δ7,10,13} to C16:4^{Δ4,7,10,13}. Venus-tagged CrΔ4FAD and CrFAD6 desaturases, like FDX5 (Figure A.S3), localized to chloroplasts (Figure A.S11).

As shown in Figure A.3B (central panel), the mating-based split ubiquitin system (Grefen *et al.*, 2009) clearly demonstrated an interaction between FDX5 and both CrΔ4FAD and CrFAD6. No interaction was detected between NubG and Cub or NubG and the FDX5-Cub fusion protein (negative controls), while NubWT and NubI interacted with the fused protein FDX5-Cub (Figure A.3B) (positive control). These studies show that FDX1 also interacts with CrΔ4FAD and CrFAD6 (Figure A.3B, central panel).

Increased TAG in *fdx5* mutant in the dark. Mature MGDG synthesis in chloroplasts requires specific desaturation of fatty acids. The inability to properly desaturate fatty acids (e.g. generate C16:4^{Δ4,7,10,13} in dark) may destabilize newly synthesized MGDG, causing it to be recycled and its fatty acids to be stored as TAG. This possibility was supported by the finding that *fdx5* accumulates TAG in the dark (Figure A.4B, C, and A.S12). Sustained TAG accumulation was observed by thin-layer chromatography (TLC) in the mutant for up to 72 h in the dark and much of the TAG was retained even 24 h after *fdx5* was transferred back to the light (Figure A.S12). It was previously shown that the lipase PGD1 could cleave C18:1^{Δ9} from nascent MGDG and transfer it to TAG during nitrogen deprivation (Li *et al.*, 2012). To determine if TAG accumulation was mediated by PGD1, *fdx5pgd1* double mutants were generated by crossing *fdx5*

with *pgd1* (Figure A.4A); progeny with both lesions were identified by PCR (Figure A.S13). To visualize TAG production in *fdx5*, Nile-Red was used to stain lipid droplets (LDs). Fluorescence from stained LDs was observed in dark-maintained *fdx5* cells, with LD content significantly lower in WT and the other strains (Figure A.4B). TLC (Figure A.4C) analysis also demonstrated TAG accumulation in *fdx5* but not in any of the *fdx5pgd1* double mutants, suggesting that PGD1 mediates the transfer of fatty acids from membrane lipids such as MGDG to TAG in the *fdx5* mutant. The analysis of TAG in *fdx5* and *fdx5#13* (segregant from a cross between *fdx5* and *pgd1*) showed that the TAG that accumulated in the mutant contained C16:0, C16:4^{Δ4,7,10,13} and C18:3^{Δ9,12,15} (Figure A.S14), suggesting that fatty acids of membrane-associated MGDG were transferred to TAG. These results suggest that fatty acid reshuffling and TAG accumulation in the dark depend on PGD1.

DISCUSSION

For photosynthetic organisms, metabolism under dark anoxic conditions is impacted by a different cellular redox environment than metabolism in the light. Unlike WT cells, the *fdx5* mutant is unable to grow in the dark. Dark-maintained *fdx5* has low MGDG and high DGDG content (Figure A.2E, F), less C16:4^{Δ4,7,10,13} relative to total fatty acids (Figure A.3A) and accumulates TAG, which may at least in part be a consequence of a decrease in C16 desaturation by CrΔ4FAD to generate C16:4^{Δ4,7,10,13}, as depicted in Figure A.S15 and A.S16. FDX5 also interacts with and may donate electrons to CrFAD6. However, CrFAD6 acts on fatty acids of both MGDG and DGDG (Hugly *et al.*, 1989; Riekhof *et al.*, 2005) and although the *fdx5* mutant exhibits alterations in the ratio of the various C18 fatty acids (different desaturation states), the changes observed occur in both the light and dark; in the light, the mutant shows no defect in growth or in its MGDG:DGDG ratio. The donation of electrons from FDX5 (in the dark) and potentially FDX1 (in the light) to CrFAD6 (Cre13.g590500) (Figure A.3B) may be responsible for conversion of C18:1^{Δ9} on the *sn-1* position to C18:2^{Δ9,12}, and C16:1^{Δ7} on the *sn-2* position to C16:2^{Δ7,10} in MGDG, and also for conversion of C18:1^{Δ9} on the *sn-1* position to C18:2^{Δ9,12} in DGDG (Riekhof *et al.*, 2005). In the dark maintained *fdx5* mutant, the C18:3^{Δ9,12,15} level was considerably elevated in both total fatty acids and fatty acids in DGDG, while C18:2^{Δ9,12} showed only a modest increase (Figure A.3A, A.S10). Plausible explanations for this finding are that another desaturase can function in place of CrFAD6 (Cre13.g590500) and/or that the CrFAD6 desaturase can accept electrons from another ferredoxin or a cytochrome *b*₅ (*b*-type cytochromes

can also donate electrons to desaturases) that is reduced in the dark. Indeed, while most *Arabidopsis* desaturases have a single homolog, the *Chlamydomonas* genome encodes two plastidic forms of ω -6 desaturases (Riekhof *et al.*, 2005), Cre06.g288650 and Cre13.g590500. Therefore, it is reasonable to suggest that Cre06.g288650 may function in the *fdx5* mutant to synthesize C18:2^{Δ9,12} in the dark.

C18:3^{Δ9,12,15} is typically synthesized through the activity of an ω -3 desaturase which uses C18:2^{Δ9,12} as its substrate. CrFAD7 (Cre01.g038600), likely localized to chloroplasts, was shown to be the only ω -3 desaturase in *Chlamydomonas*, and is responsible for ω -3 desaturation of plastid- and ER-synthesized lipids (Nguyen *et al.*, 2013). Since CrFAD7 does not appear to interact with FDX5 (Peden *et al.* 2013), it likely requires a different electron donor (e.g. another ferredoxin isoform). The presence of multiple CrFAD6 desaturases and a chloroplast CrFAD7 enzyme may explain why there is no reduction of DGDG C18:3^{Δ9,12,15} in the *fdx5* mutant in the dark. It is also likely that fatty acids from other lipids serve as substrates that are used in the synthesis of DGDG. This possibility is supported by the finding that there are over 100 mostly uncharacterized lipases encoded on the *Chlamydomonas* genome and that some of these lipases function in conjunction with acyl-transferases to modify or edit the acyl chains on membrane glycerolipids (Li *et al.*, 2012). Thus, certain lipases may release C18:2^{Δ9,12} and C18:3^{Δ9,12,15} from diacylglyceryl trimethyl homoserine (DGTS) and phosphatidylethanolamine (PtdEtn) in the ER or phosphatidylglycerol (PtdGro) and sulfoquinovosyl diacylglycerol (SQDG) in the chloroplast, promoting the recycling of these fatty acids.

In *Chlamydomonas*, ‘immature’ MGDG (C18:1^{Δ9}/C16:0) is known to be utilized in three ways (Figure A.S15): (i) desaturation to mature MGDG (C18:3^{Δ9,12,15}/C16:4^{Δ4,7,10,13}) by multiple fatty acid desaturases; (ii) galactosylation of MGDG to synthesize DGDG by the enzyme DGD1; (iii) hydrolysis of the fatty acids from the glycerol backbone by PGD1, with the export of C18:1^{Δ9} and its incorporation into TAG (Dörmann *et al.*, 1999; Giroud *et al.*, 1988; Li *et al.*, 2012; Riekhof *et al.*, 2005; Zäuner *et al.*, 2012). This last fate of MGDG may in part explain the reduced levels of C18:1^{Δ9} in DGDG, although this is observed in both the light and dark. Some MGDG would also be converted to DGDG (Figure A.2E, F).

Finally, an inability to generate C16:4^{Δ4,7,10,13} at the *sn*-2 position of newly synthesized MGDG in dark-maintained *fdx5* would prevent the maturation of MGDG, resulting in its destabilization and decreased accumulation of both MGDG and total C18:3^{Δ9,12,15} in MGDG. The C18:1^{Δ9} fatty

acid present at the *sn-1* position of immature MGDG could then be further desaturated (or remain C18:1^{Δ9}) and become a constituent of DGDG (through conversion of MGDG to DGDG) or be released from MGDG through a PGD1-dependent cleavage (Li *et al.*, 2012) and used for the production of TAG. Mature MGDG present in *fdx5* after growth in the light also contributes to TAG production through its turnover and recycling of its fatty acids; a similar MGDG recycling process is observed in *Chlamydomonas* cells deprived of nitrogen (Li *et al.*, 2012; Moellering & Benning, 2010).

In the *fdx5* mutant, desaturation of the C16 fatty acid to C16:4^{Δ4,7,10,13} may be decreased in the dark, as evidenced by the lower MGDG:DGDG ratio and a reduced fraction of C16:4^{Δ4,7,10,13} among all fatty acids relative to WT cells (the level of C16:4^{Δ4,7,10,13} remains the same in MGDG relative to WT cells, as expected), probably due to the lack of FDX5 protein as an electron donor for the CrΔ4FAD desaturase. Generation of C16:4^{Δ4,7,10,13} through the activity of CrΔ4FAD was shown to be a crucial limiting factor in the conversion of immature MGDG into mature MGDG, which would limit the overall MGDG content²¹. Consequently, we observed an elevated level of DGDG and accumulation of TAG (probably caused by greater conversion of immature MGDG into these products) as well as a lower overall amount of MGDG in dark-maintained *fdx5* (Figure A.2E-F, A.S15, and A.S16).

Together, our results suggest that FDX5 is a redox carrier that donates electrons to at least two fatty acid desaturases (CrΔ4FAD, CrFAD6) involved in converting C16:3^{Δ7,10,13} to C16:4^{Δ4,7,10,13} and C18:1^{Δ9} to C18:2^{Δ9,12}. We confirmed physical interactions of FDX5 with these desaturases (Figure A.3B). Since the mutant is unable to synthesize the proper fatty acids in the dark, there is an increase in DGDG production relative to MGDG as well as an increase in TAG synthesis; elevated TAG accumulation can be prevented if the *pgd1* lesion is introduced into the *fdx5* strain (Figure A.4, and A.S12). The altered ratio of MGDG to DGDG (Figure A.2) in *fdx5* causes aberrant membrane structure (Figure A.2), which impacts the activity of many cellular processes including photosynthetic electron flow, and causes other abnormalities potentially associated with altered membrane composition. These results raised several questions about TAG production in *fdx5*: *i*) How are the enzymes involved in TAG production regulated in the dark? *ii*) How does PGD1 affect TAG production in *fdx5* in the dark? *iii*) What is the contribution of other lipases to the accumulation of TAG? TAG production is low in WT cells and the *pgd1* mutant, and these two strains have a similar complement of MGDG, DGDG and

TAG in the dark (Figure A.S16A, B). However, TAG accumulation in *fdx5* in the dark (Figure A.S16C) is blocked in the *fdx5pgd1* double mutant (Figure A.S16D). The incompletely processed MGDG in this double mutant cannot provide fatty acids for TAG biosynthesis, although it can still be converted to DGDG (Figure A.S16D).

The dramatic dark-specific defect in lipid biosynthesis in *fdx5* may limit its growth in the dark, although we cannot eliminate the possibility that the growth phenotype may be the consequence of an inability to perform other FDX5-mediated reactions in the dark (Yang *et al.*, 2015). Preliminary pull-down assays have revealed several potential FDX5 interacting proteins (Table A.S5). Furthermore, rescue of the *fdx5* growth phenotype occurs in very low light, suggesting that the rescue may require only low-level production of reductant by the photosynthetic apparatus, but may also involve light-associated regulatory processes. What seems most apparent from these studies is that some redox carriers have light- or dark-specific activities and play a major role in the diel metabolism of photosynthetic organisms.

MATERIALS AND METHODS

Strains, mutant isolation and growth conditions. Parental, WT Chlamydomonas strains used were CC-124 (*nit2⁻, mt⁻*) and CC-125 (*nit2⁻, mt⁺*) (Table A.S3). The *fdx5* mutant was generated in the *D66* (CC-4425; *nit2⁻, cw15, mt⁺*) genetic background (Pollock *et al.*, 2003) and identified using a PCR-based screen (Gonzalez-Ballester *et al.*, 2011; Pootakham *et al.*, 2010) while the *pgd1* strain (*nit1⁻, cw15, mt⁺*) was previously characterized (Li *et al.*, 2012). Strain cMJ030 (CC-4533, *nit2⁻, cw15, mt⁻*) was used for protein localization. Primers used for the mutant screen and genotyping are listed in Table A.S2. The *fdx5* mutant was backcrossed 5 times to CC-124 or CC-125, and *fdx5pgd1* double mutants were generated by crossing *fdx5* and *pgd1* single mutants. Cells were grown on TAP agar and liquid medium, minimal medium (MM) or high salt medium (HS) at various light intensities (as indicated in text). For TEM, cells were grown in HEPES-Acetate-Phosphate buffered medium.

Complementation and transformation. Complementation was performed with either FDX5 cDNA or gDNA under the control of the *PSAD* promoter in the pGEM T-easy vector (Promega, Sunnyvale, CA). Transformation was performed by introducing 1 μ g DNA of plasmids pJM43Ble-FDX5cDNA and pJM43Ble-FDX5gDNA (both linearized with *NotI*) into *fdx5* (in *CC-124* background) by electroporation (0.8 kv, 25 uF) using a BioRad GenePulser II Electroporator (Bio-Rad, Hercules, CA) as previously described (Yang *et al.*, 2014).

Transformants were selected on solid TAP medium containing 100 µg/ml ampicillin, 5 µg/ml paromomycin (for original *fdx5* mutation) and 6 µg/ml Zeocin (for introduced *FDX5* gene) and then selected for growth in the dark. Transformants that grew in the dark were assayed by PCR for insertion of the different drug resistance cassettes.

Phenotyping and growth rates. Growth was analyzed in liquid and solid medium, with or without various antibiotics. Samples from liquid cultures were collected and cells counted and/or quantified based on chlorophyll (Chl) levels (Aksoy *et al.*, 2014; Heinnickel *et al.*, 2013).

Photosynthetic O₂ evolution and respiratory O₂ consumption. The evolution and consumption of O₂ were measured using a Clark electrode (CBID; Hansatech). Respiratory O₂ consumption was measured in the dark, while photosynthetic O₂ evolution was measured using white actinic light (~500 µmol photons m⁻² s⁻¹).

Transmission electron microscopy (TEM). For TEM, cells were grown in modified TAP medium (Tris replaced by 20 mM HEPES), fixed in growth medium containing glutaraldehyde and OsO₄, negatively stained with uranyl acetate, dehydrated in ethanol and embedded in LR White. Ultrathin sections (~60 nm) were mounted onto Formvar-coated copper grids, contrasted with lead citrate (Reynolds, 1963) and micrographs obtained using a Jeol JEM-1400 transmission electron microscope.

Analysis of total and membrane lipids. Total lipids were extracted from samples frozen in liquid nitrogen (Bligh & Dyer, 1959), dried under a N₂ stream and stored at -80°C. Dried lipids were dissolved in 55 µl of chloroform, separated by thin layer chromatography (TLC) using a mixture of chloroform:methanol:acetic acid:water (75:13:9:3 v/v, respectively). After separation, the MGDG and DGDG bands and a spot containing total lipid (derived from 20 µl of the extract), were scraped from the TLC plate, converted into fatty acid methyl esters (FAMES) (Benning & Somerville, 1992), and the amount of each of the FAMES quantified by gas chromatography (GC) on an HP6890 system as described previously (Zäuner *et al.*, 2012).

TAG analysis and staining of lipid droplets. Lipid extraction and TAG analysis by TLC were conducted as described previously (Li *et al.*, 2012). To visualize lipid droplets, cells were suspended in PBS-0.011% Triton X-100, stained with 1 µg/ml Nile-Red, immobilized on a 0.5% TAP-agarose pad and imaged by spinning disk confocal microscopy; excitation was at 512 nm and emission at 570-590 nm.

Mating-Based Split Ubiquitin assay. *FDX1*, *FDX5*, *CrΔ4FAD* and *CrFAD6* genes were amplified from cDNAs using primers listed in Table A.S2, and cloned into pENTR/D_TOPO (Invitrogen). The *FDX1* and *FDX5* genes from pENTR/D-TOPO_*FD* and pENTR/D-TOPO_*FDX5* were introduced into pNX22-DEST by LR cloning, while *CrΔ4FAD* and *CrFAD6* genes from pENTR/D-TOPO_*CrΔ4FAD* and pENTR/D-TOPO_*CrFAD6* were introduced into pMetYC-DEST by LR cloning (Table A.S4). Interactions between *FDX1*, *FDX5* and *CrΔ4FAD* and *CrFAD6* were assessed by the mating based split ubiquitin system (Grefen *et al.*, 2009) (<https://associomics.dpb.carnegiescience.edu/Associomics/Protocols.html>).

ACKNOWLEDGEMENTS

This work was supported by the Office of Biological and Environmental Research, GTL Program, Office of Science, US Department of Energy Grants DE-FG02-07ER64427, DE-FG02-12ER16338 (to A.R.G.), DE-FG02-12ER16339 (to M.C.P), NSF Grant IOS-1359682 (to M.C.J.), NSF Grant MCB 1157231 (to C.B.), NIH Grant GM42143 (to S.S.M.), MSU AgBioResearch (C.B.), as well as funds from the Carnegie Institution for Science (A.R.G. and M.C.J.). J. W. is supported by the Royal Thai Government Scholarship. Publication costs were defrayed in part by the payment of page charges. This article must therefore be hereby marked ‘advertisement’ in accordance with 18 U.S.C. Section 1734, solely to indicate this fact. We thank Dr. Gilles Peltier for PGRL1 antibodies, Dr. Fabrice Franck for Nda2 antibodies, and MIMS experiments (JA, XJ and PR) were supported by Héliobiotec, an EU Grant 1944-32670, PACA DEB 09-621 and CEA. The plasmids of pMetYC-DEST and pNX22-DEST and the yeast strains THY.AP4 and THY.AP5 were kindly provided by Dr. Wolf Frommer. We acknowledge the NIH grant *1s10RR02678001* for the Jeol TEM 1400.

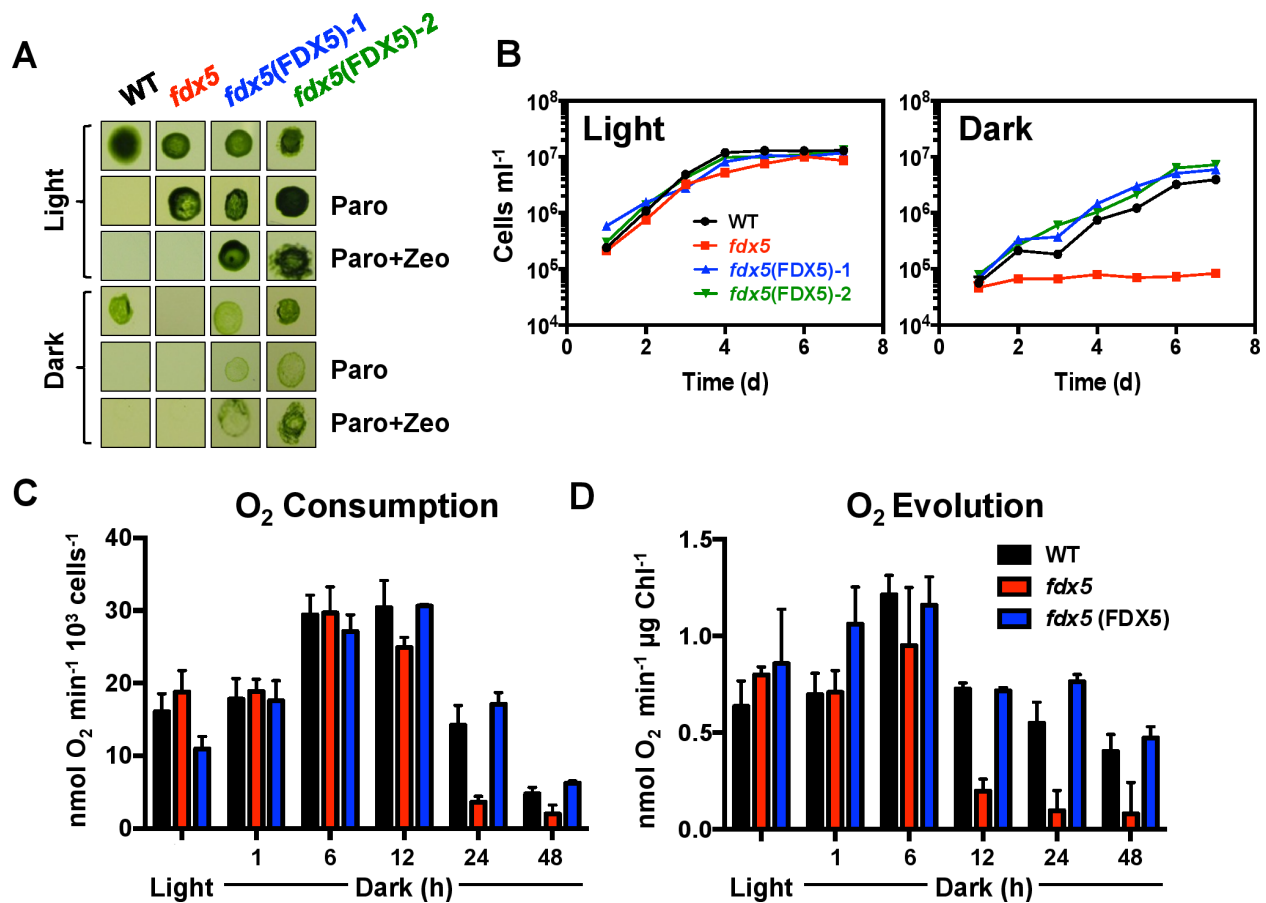


Figure A.1. The *fdx5* mutant is unable to grow and has attenuated respiration and photosynthesis rates in the dark.

(A) Colonies of WT, *fdx5* and two rescued strains [*fdx5(FDX5)-1* and *fdx5(FDX5)-2*] after 9 d of growth on solid TAP medium in the light and dark. The medium was unsupplemented, supplemented with paromomycin (Paro) or supplemented with paromomycin and Zeocin (Paro + Zeo). (B) Growth of WT, *fdx5* and two rescued strains in liquid TAP medium over 7 d in the light and dark. (C) Respiratory O₂ consumption after transferring WT cells, *fdx5* and the *fdx5(FDX5)* complemented strain from the light to the dark for various times (1-48 h). (D) Photosynthetic O₂ evolution in saturating actinic light after transferring WT cells, *fdx5* and the *fdx5(FDX5)* complemented strain from the light to the dark for various times (1-48 h). The results for the various strains are given in different colors, as indicated. Error bars for B, C and D represent standard deviation (n=3); experiments were performed in triplicate.

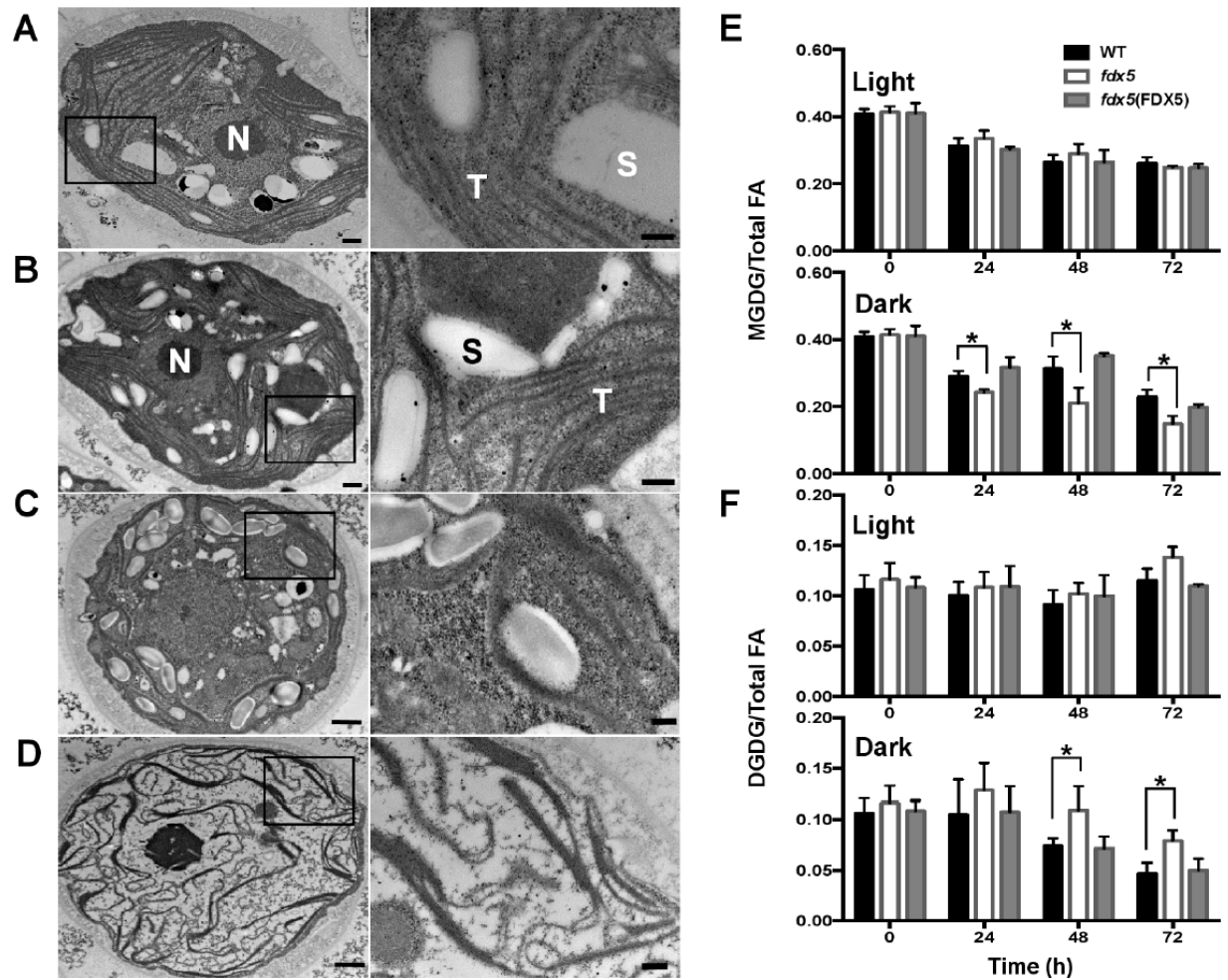


Figure A.2. Altered membrane morphologies and lipid compositions in dark-maintained *fdx5*.

TEM of sectioned *Chlamydomonas* WT cells (A) and the *fdx5* mutant (B) grown in the light. WT cells (C) and the *fdx5* mutant (D) maintained in the dark for 48 h. Areas delineated by the rectangles are enlarged (right) to reveal structural features of the membranes. N, nucleus; S, starch granules; T, thylakoid membranes; these structures are only noted for (A) and (B). Scale bars for the original images are 500 nm for (A) and (B), and 1000 nm for (C) and (D), and 200 nm for all enlargements (at right). Relative levels of MGDG (E) and DGDG (F) in WT cells, *fdx5* and the *fdx5*(FDX5) complemented strain in the light and following transfer to the dark for the indicated times. Error bars represent S.D. (n=3); experiments were performed three times. 0 was the time just prior to transferring cells to the light or dark. * $P < 0.05$, by two-tailed Student's t tests.

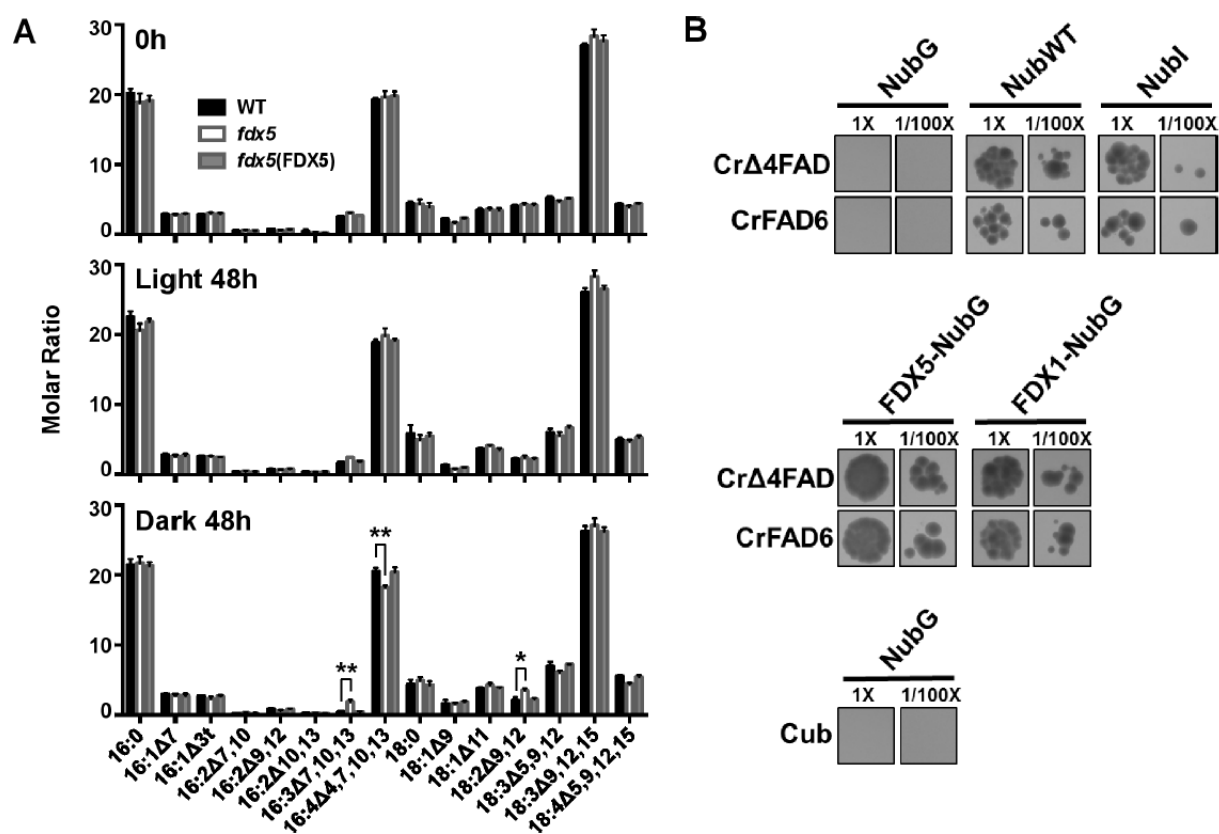


Figure A.3. C16:4^{Δ4,7,10,13} fatty acid is decreased in dark-grown *fdx5* and FDX5 interacts with fatty acid desaturases.

(A) Fatty acid profiles in WT, *fdx5* and the *fdx5*(FDX5) complemented strain in the light and dark at 0 and 48 h. Error bars represent standard deviation (n=3). Experiments were performed three times. * $P < 0.05$, ** $P < 0.01$, by two-tailed Student's t tests. (B) Mating based split-ubiquitin system showing interactions of FDX5 and FDX1 (Fd) with CrΔ4FAD and CrFAD6 in the presence of 500 μM methionine (Met500). The NubG (empty) vector combined with Cub or vectors containing the desaturase genes served as negative controls, while NubWT and Nubl vectors served as positive controls. The assay was performed on 8 separate occasions, yielding similar results.

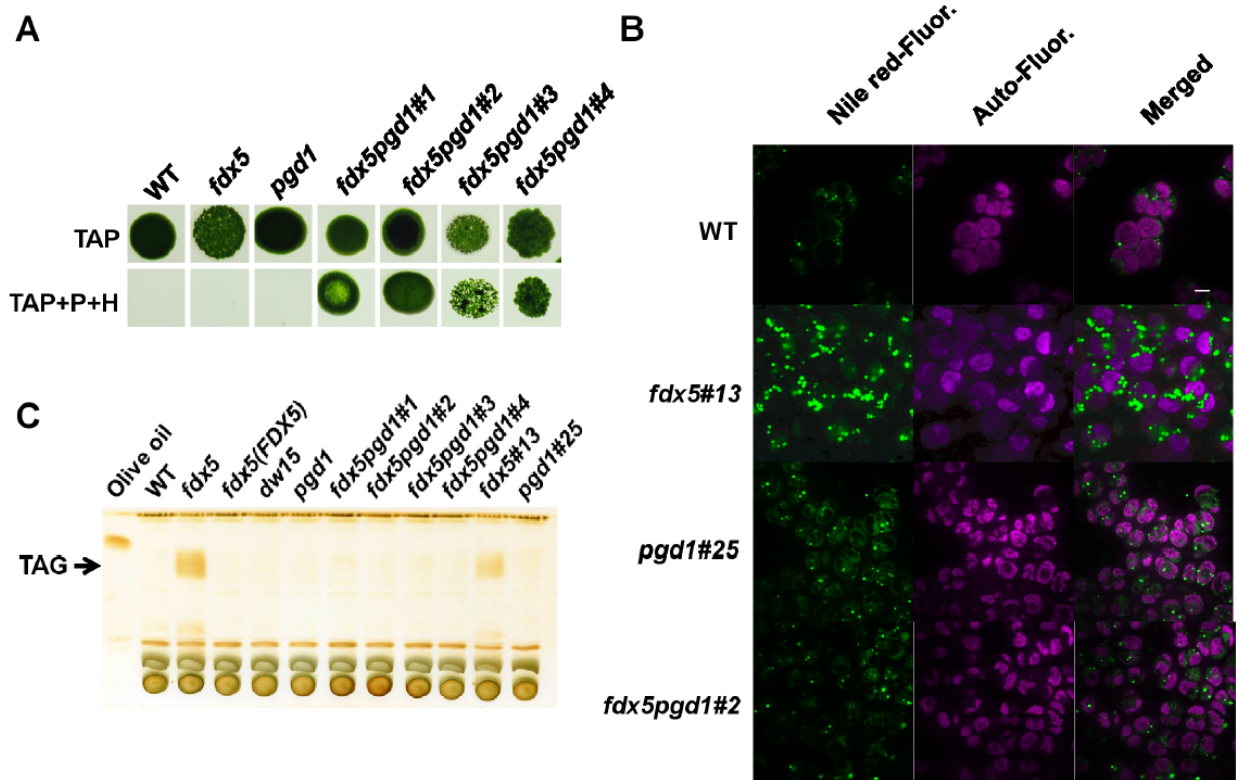


Figure A.4. PGD1-mediated TAG accumulation in *fdx5* in the dark.

(A) Growth of WT, *fdx5* and *pgd1* single mutants, and 4 *fdx5pgd1* double mutants for 9 d on solid TAP medium in the light. The medium was unsupplemented or supplemented with both paromomycin (P) and hygromycin (H), as indicated. (B) Imaging of lipid droplets in WT, *fdx5*#13 and *pgd1*#25 single mutants and the *fdx5pgd1*#2 double mutant. (C) TLC analysis of TAG in various strains grown in the dark. *dw15* was the parental strain of the *pgd1* mutant. Different isolates of the *fdx5pgd1* double mutants, noted as ‘#’, are also shown.

APPENDICES

APPENDIX A. SUPPORTING FIGURES

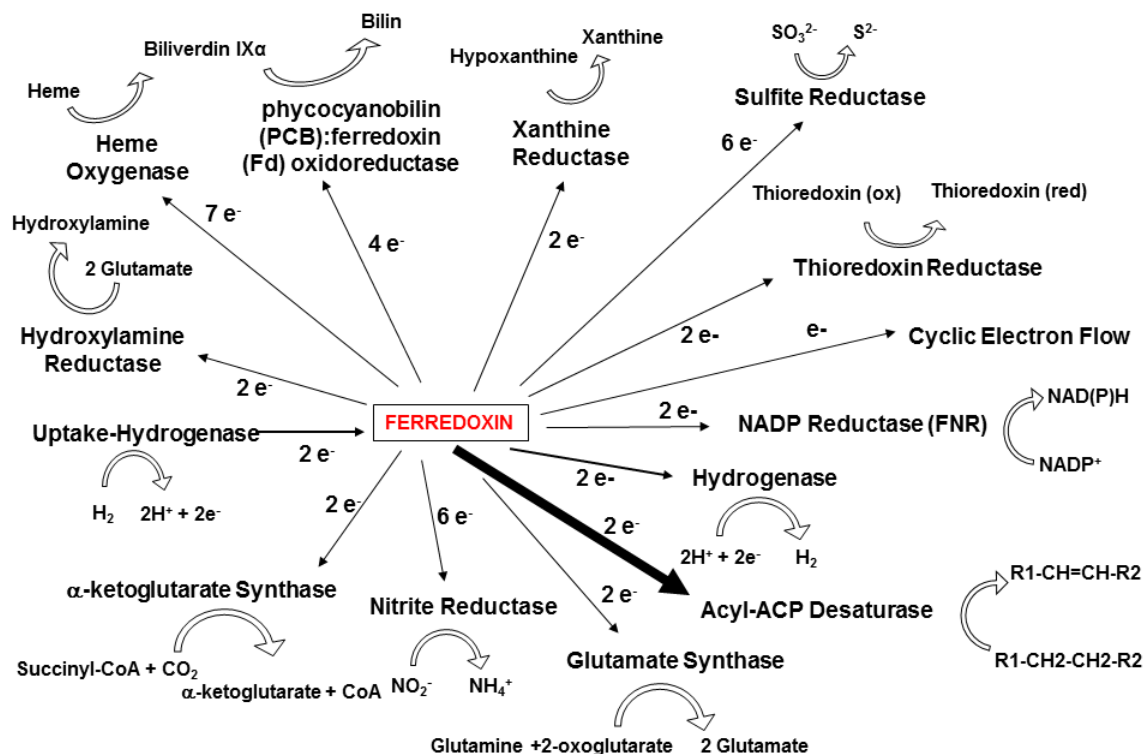


Figure A.S1. Ferredoxin-mediated electron transfer reactions.

Ferredoxins participate in a variety of electron transfer reactions, including those depicted; these reactions require donation of between 1 (CEF) and 7 (heme oxygenase) electrons. The transfer of electrons from ferredoxins to desaturases is highlighted by a thicker arrow since it pertains to the research presented.

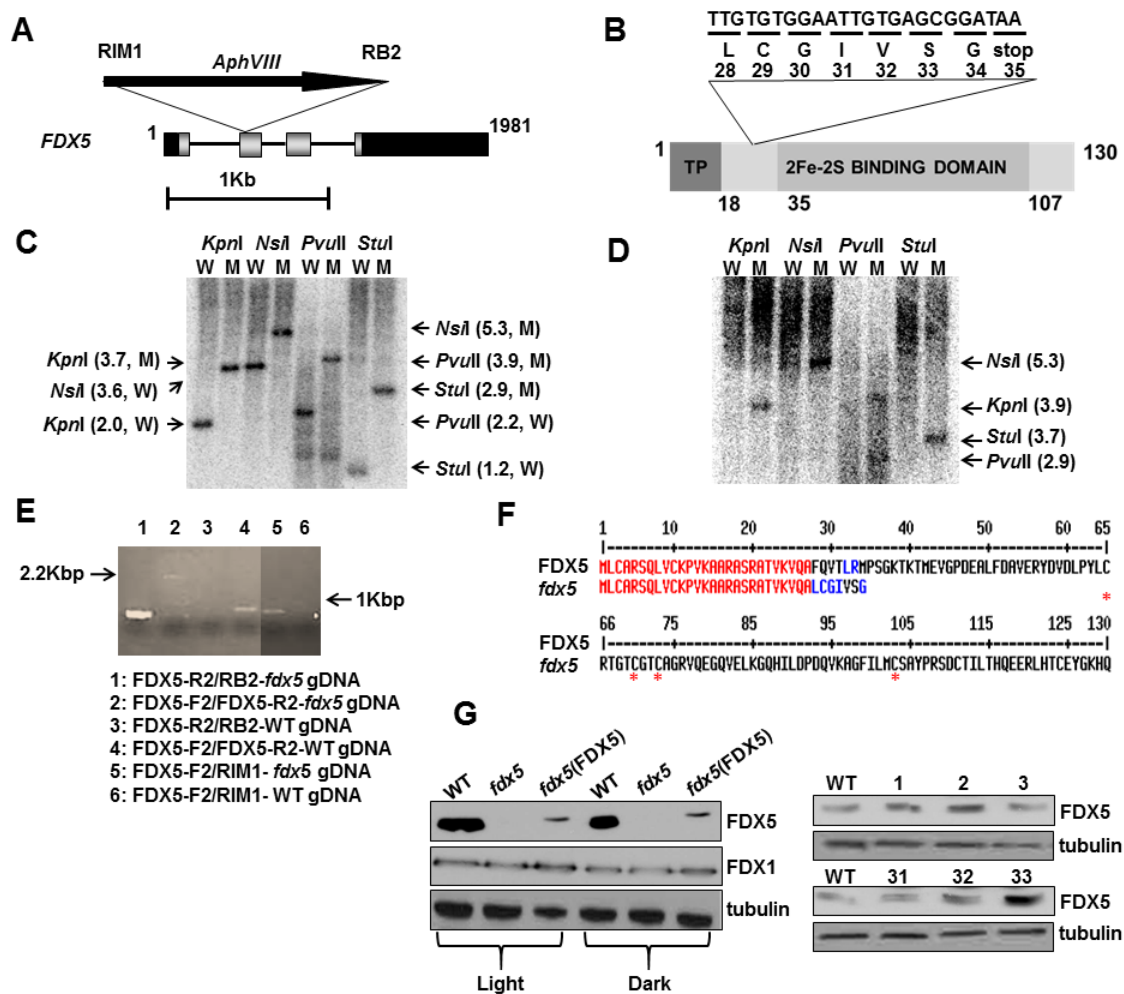


Figure A.S2. Generation and molecular analyses of *fdx5* mutant.

(A) Representation of the site of insertion of the *AphVIII* gene in the *fdx5* mutant. Black boxes represent 5' and 3'UTRs, grey boxes and black lines represent exons and introns, respectively. The arrow indicates the orientation of the insertion while the sites of primer annealing used to sequence from the cassette into the *Chlamydomonas* genome are designated RIM1 and RB2. (B) Diagram showing structure of FDX5 protein and the predicted amino acid sequence that precedes the site of translation termination of the protein in the *fdx5* mutant. TP is the chloroplast targeting transit peptide while the light grey box represents the domain that binds the 2Fe-2S cluster. The site of insertion, at amino acid 28, is indicated along with the amino acids introduced by the insertion, ending with a stop codon. (C) Southern blot hybridization analysis of genomic DNA from the *fdx5* mutant. The membrane with the transferred DNA was incubated with a radiolabeled probe containing the entire *FDX5* nucleotide sequence. Sizes of the hybridizing

Figure A.S2. (cont'd) fragments are given on both sides of the blot (in Kbp). W and M represent WT and *fdx5* mutant strains, respectively. **(D)** Southern blot hybridization of genomic DNA from *fdx5* mutant using an *AphVIII* gene probe. The sizes of the hybridizing fragments are given to the right of the blot (in Kbp). **(E)** PCR with specific primers and genomic DNA (gDNA) as template was used to identify the *AphVIII* insertion site. The products generated using gDNA from WT and *fdx5* are shown. The primer pairs and templates used were: 1. FDX5-R2/RB2-*fdx5*gDNA. 2. FDX5-F2/FDX5-R2-*fdx5*gDNA. 3. FDX5-R2/RB2-WTgDNA. 4. FDX5-F2/FDX5-R2-WTgDNA. 5. FDX5-F2/RIM1-*fdx5*gDNA. 6. FDX5-F2/RIM1-WTgDNA. The fragments amplified from the gDNA were sequenced to localize the exact insertion site. **(F)** Alignment of full-length FDX5 and the truncated FDX5 synthesized in the mutant. Note that the sequences diverge at amino acid 27 and the mutant protein is terminated at amino acid 35. The asterisks in red highlight the 4 cysteine residues involved in 2Fe-2S binding. Red represents identical amino acids between mutant and WT while the blue and black represent amino acids predicted as a consequence of the insertion. **(G)** Left panel: Western blot showing the absence of the FDX5 protein in the *fdx5* mutant [but restored in the *fdx5*(FDX5) rescued strain]. Upper panel shows abundance of FDX5, the middle panel shows the abundance of FDX1 (Fd) protein, and the lower panel shows abundance of tubulin, which was used as a loading control. Right panel: Western blot showing accumulation of FDX5 in additional *fdx5*(FDX5) rescued strains. 1, 2 and 3 represent the *fdx5*(FDX5) rescued strains from *FDX5* coding sequence (CDS), while 31, 32, 33 represent the *fdx5*(FDX5) rescued strains from *FDX5* genomic DNA. Tubulin accumulation is shown as loading controls.

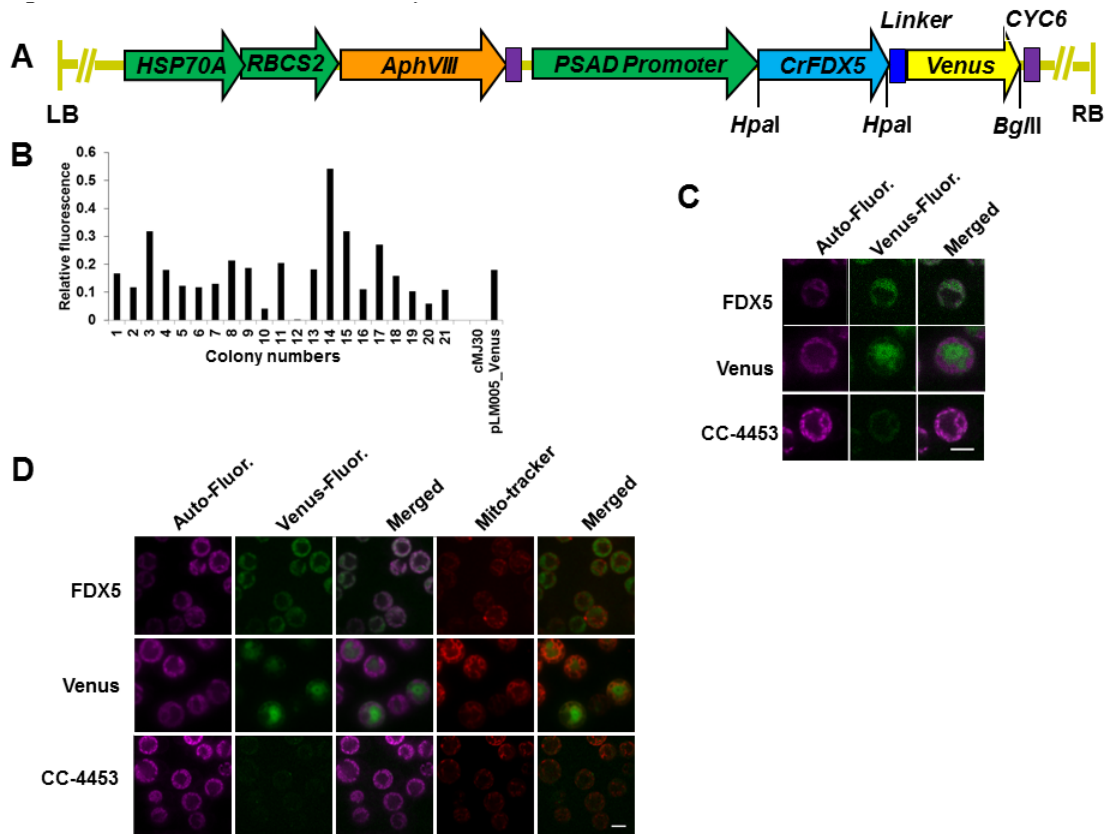


Figure A.S3. Localization of FDX5.

Figure A.S3. (cont'd)

(A) Schematic representation of pLM005_Venus construct containing the fusion between the *FDX5* and Venus genes. Dark green arrows represent promoters, which include the dual *HSP70* and *RBCS2* promoter driving the *AphVIII* gene (orange) and the *PSAD* (constitutive, green) promoter driving the gene encoding the FDX5-Venus fusion proteins. The *CrFDX5* gene is in blue and *Venus* in yellow. LB and RB stand for left and right border, respectively. Venus is fused to FDX5 through the linker (35) (dark blue) and the terminator is from *CYC6* (purple). (B) Fluorescence was measured from the Venus-tagged *Chlamydomonas* transformants using a TECAN plate reader before confocal imaging of the sample was performed. Untransformed cMJ030 (CC-4533) and cMJ030 transformed with pLM005_Venus vectors (without the fusion) were used as negative and positive controls, respectively. The y-axis gives the relative fluorescence compared to the positive control (pLM005_Venus), and the x-axis represents various strains, with the rescued strains given as numbers 1-21. Fluorescence was measured 3 separate times; all replicates showed similar results. (C) Localization of FDX5 protein in a single *Chlamydomonas* cell. The cells either contained the introduced vector with neither the *Venus* nor *FDX5* sequence (CC-4533), the vector expressing *Venus* (Venus), or the vector expressing *FDX5* fused to *Venus* (FDX5-Venus). Column 1 shows Venus fluorescence (green), column 2 shows Chl autofluorescence (magenta) and column 3 shows the merged image of column 1 and column 2. The scale bar represents 5 μm . (D) Intracellular localization of FDX5 in *Chlamydomonas*. Column 1 shows Chl auto-fluorescence (magenta), column 2 shows Venus fluorescence (green), column 3 shows the merged image of column 1 and column 2, column 4 shows fluorescence of the Mito-tracker (red), and column 5 shows the merged image of column 4 and column 2. The scale bar (bottom right) represents 5 μm .

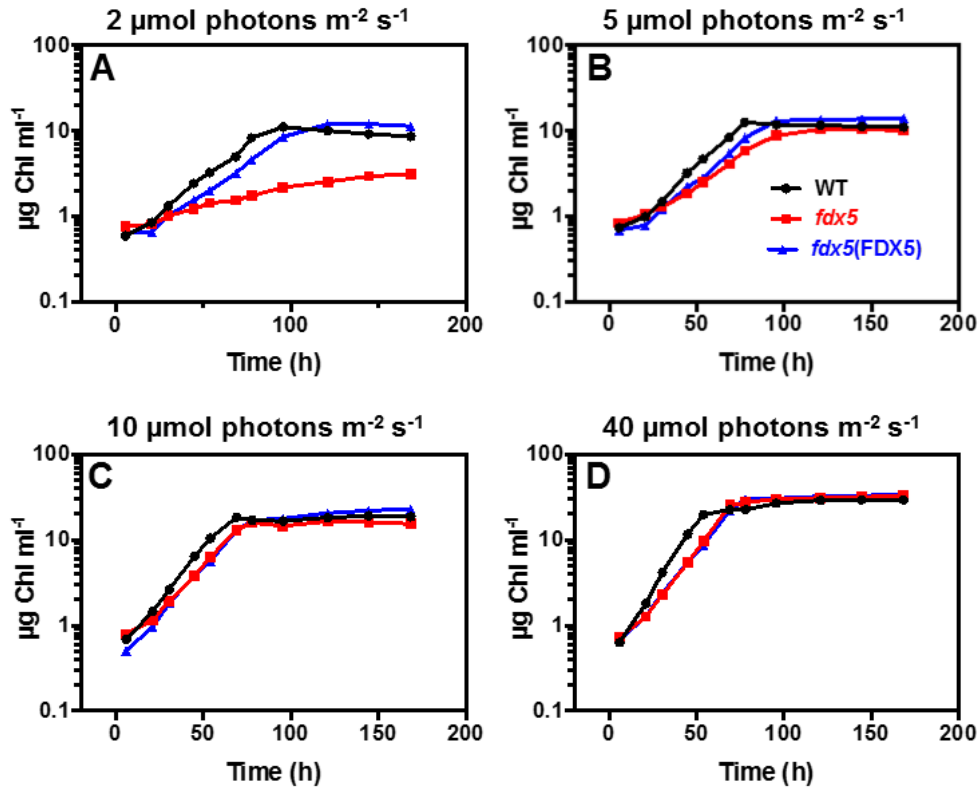


Figure A.S4. *fdx5* growth at different light intensities.

Growth of WT, *fdx5* and a complemented strain [*fdx5*(FDX5)] in liquid TAP medium for 7 d at 2 $\mu\text{mol photons m}^{-2} \text{s}^{-1}$ (A), 5 $\mu\text{mol photons m}^{-2} \text{s}^{-1}$ (B), 10 $\mu\text{mol photons m}^{-2} \text{s}^{-1}$ (C) and 40 $\mu\text{mol photons m}^{-2} \text{s}^{-1}$ (D). Growth was determined by measurements of Chl concentration ($\mu\text{g ml}^{-1}$), as indicated on the y-axes.

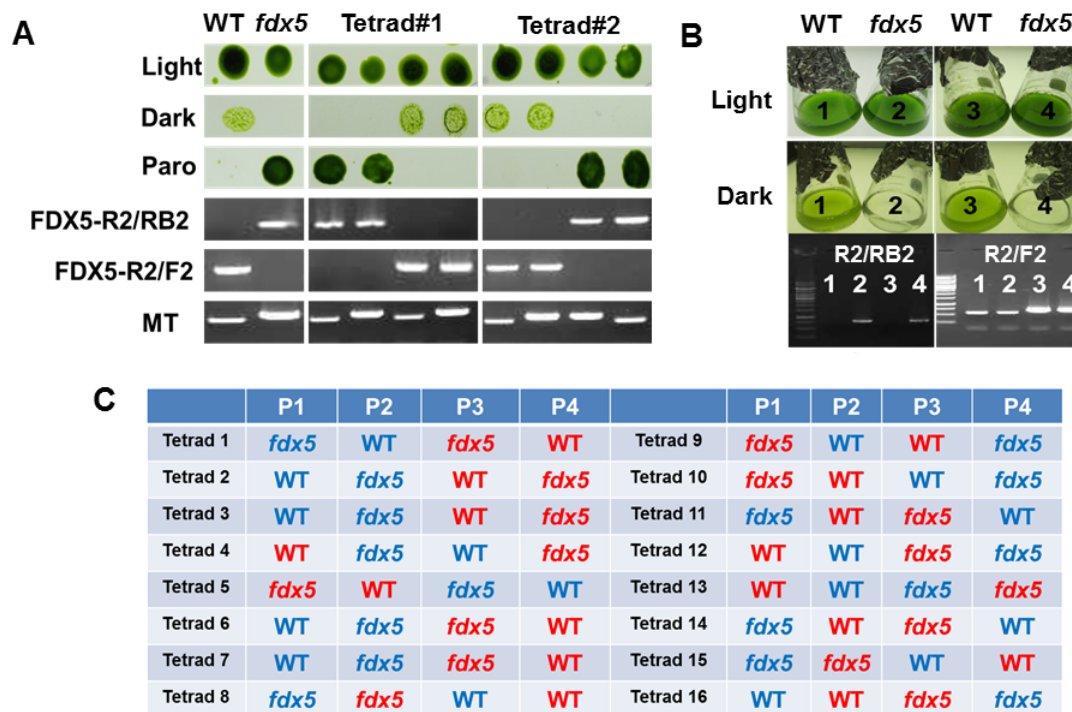


Figure A.S5. The *fdx5* dark growth deficiency is linked to paromomycin resistance.

(A) Tetrad analyses: Progeny from tetrads #8 and #16 were spotted onto TAP agar (and supplemented with paromomycin), grown in the light and dark, and also inoculated into TAP liquid medium with 10 μ g/ml paromomycin (Paro) and grown in the light. Liquid cultures were used for PCR to determine segregation of the *fdx5* mutation (2:2) using the FDX5-R2/RB2 primer pair (a band is amplified in the mutant but not WT progeny) or the FDX5-R2/F2 primer pair (a band is amplified in WT but not mutant progeny). PCR for mating type (MT) also exhibited 2:2 segregation. WT and the *fdx5* mutant (two leftmost columns) were used as controls. (B) Growth phenotype of progeny from tetrad #2; each of the progeny were grown in liquid TAP medium. 1-4 are the four daughter cells from tetrad #2, which were grown in the light or dark. PCR was performed to confirm the genotype of the progeny; the DNA from progeny 2 and 4 (the progeny unable to grow in the dark) was amplified with the FDX5-R2/RB2 primers, which only amplifies mutant DNA. (C) Summary of the tetrad analyses. The tetrads from 16 zygotes were analyzed by PCR. The blue and red lettering of WT and *fdx5* represent mating type + and -, respectively. P1-P4 are the four progeny of a selected tetrad.

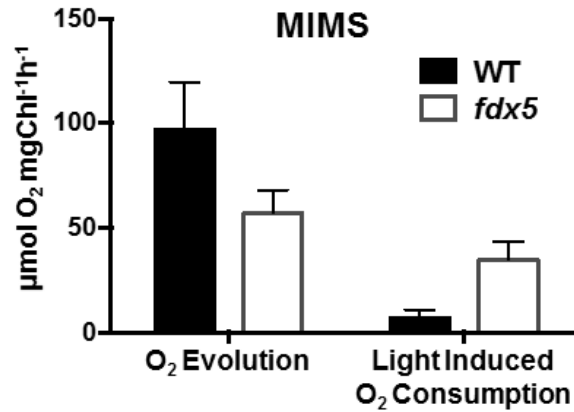


Figure A.S6. Elevated light-induced O₂ consumption occurs in *fdx5* maintained in the dark. Membrane Inlet Mass Spectrometry (MIMS analysis) was used to quantify light-induced O₂ evolution and consumption in the *fdx5* mutant and WT after 24 h in the dark. The cells used for the experiments were in mid-logarithmic phase. Error bars represent standard deviation (n=3), and the experiments were performed in triplicate.

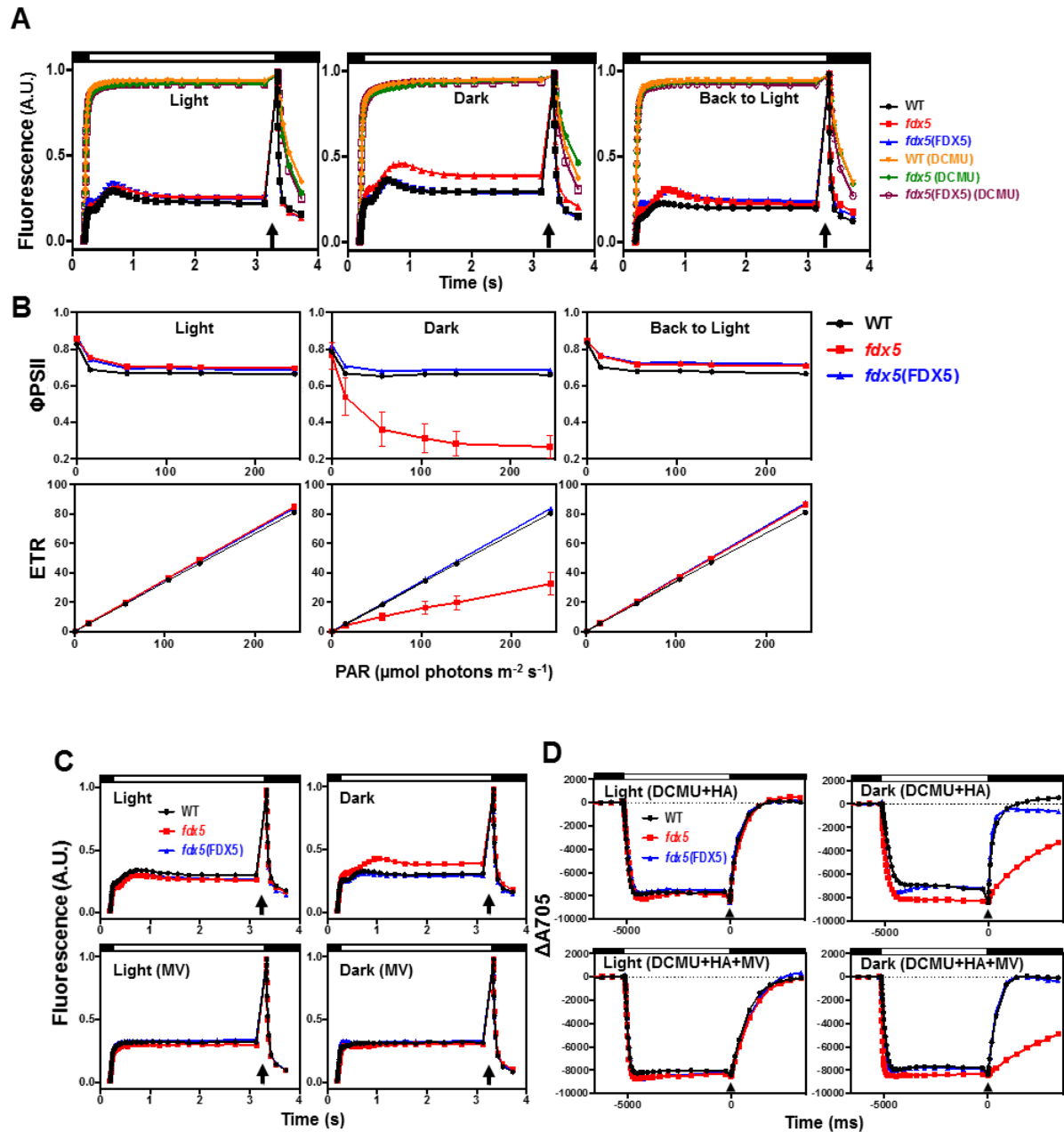


Figure A.S7. Fluorescence and spectroscopic analyses show impairment of photosynthetic electron transport.

(A) Relative Chl fluorescence induction kinetics for cells [*fdx5* mutant, WT and the *fdx5*(FDX5) complemented strain] maintained in light or dark for 24 h, as indicated. All cells were dark-adapted for 20 min prior to the measurements. Fluorescence was measured either in the presence or absence of 3-(3,4-dichlorophenyl)-1-1-dimethylurea (10 μM) (DCMU), as indicated.

Figure A.S7. (cont'd) The left curves show fluorescence induction for the various strains after growth in the light (**Light**); the middle curves show fluorescence induction for the various strains after maintenance in the dark for 24 h (**Dark**); the right curves show fluorescence induction after returning the dark-maintained strains to the light for 24 h (**Back to Light**). The light intensity used for the fluorescence induction curves was 156 $\mu\text{mol photons m}^{-2} \text{ s}^{-1}$. (**B**) Measurement of quantum efficiency of PSII (ΦPSII) and electron transport rates (ETR) for WT, *fdx5* and the *fdx5*(FDX5) complemented strain after growth in the light (**Light**, left), maintenance in the dark for 24 h (**Dark**, middle), and maintenance in the dark for 24 h and then the dark-maintained cells transferred back to the light for 24 h (**Back to Light**, right). Cultures were grown in TAP medium and concentrated in the same medium to 10 $\mu\text{g/mL}$ Chl. All measurements were made using a DUAL-PAM 100 fluorometer. Photosynthetically Active Radiation (PAR) is given as $\mu\text{mol photons m}^{-2} \text{ s}^{-1}$. Error bars represent standard deviation. (**C**) Relative Chl fluorescence measurements (using JTS-10 spectrophotometer) for WT, *fdx5* and *fdx5*(FDX5) cells grown in the light or maintained in the dark in the presence or absence of 1 mM methyl viologen (MV) as an electron acceptor, as indicated. Actinic light was on for 3 s at an intensity of 156 $\mu\text{mol photons m}^{-2} \text{ s}^{-1}$. Resuspended cells were dark-adapted for 20 min prior to the measurements. (**D**) P700 oxidation-reduction kinetics on WT, *fdx5* and *fdx5*(FDX5) cells grown in the light or maintained in the dark (using JTS-10 spectrophotometer) in the presence and absence of MV. To assess the pool of electron donors to PSI, cells were resuspended in HEPES-KOH (pH 7.5, 10% Ficoll) to 30 $\mu\text{g/ml}$ Chl and incubated with 3-(3,4-dichloroprenyl)-1- β -dimethylurea (10 μM DCMU) and hydroxylamine (1 mM HA) to completely block PSII activity. Actinic light was 165 $\mu\text{mol photons m}^{-2} \text{ s}^{-1}$ for 5 s followed by a flash of saturating light, and then complete darkness. Changes in the redox state of P700 were measured based on optical changes at 705 nm. In panels (**C**) and (**D**), bottom, 1 mM MV was added to the reaction as an electron acceptor for PSI and to inhibit FDX-dependent and NADPH-dependent CEF. Upward arrows present in (**A**), (**C**) and (**D**) represent saturating pulses of light.

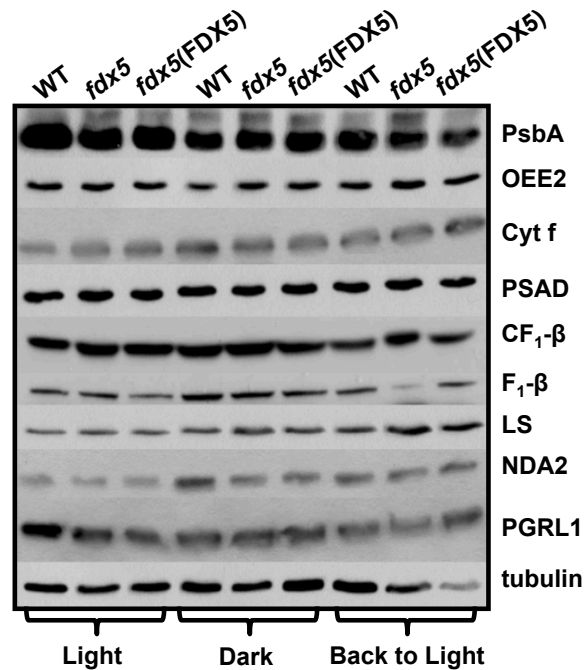


Figure A.S8. Immunoblot of representative photosynthetic proteins.

Immunoblot shows similar expression levels of representative photosynthetic proteins in different strains under distinct light conditions. Proteins were resolved by SDS-PAGE (12% polyacrylamide) with 2.5 μg Chl (whole cell) applied per lane. Tubulin was used as a loading control. Samples were collected at 0, 24 h in the dark, and back to light for 24 h (after a 24 h dark period). The proteins examined were PsbA (reaction center protein of PSII), OEE2 (oxygen evolving enhancer complex of PSII), Cyt f (PetA) (subunit of Cyt *b₆f* complex), PSAD (subunit of PSI), CF₁- β (chloroplast catalytic subunit of ATP synthetase), F₁- β (mitochondria catalytic subunit of ATP synthetase), LS (RuBisco large subunit of), NDA2 (NADPH dehydrogenase complex involved in chlororespiration and NADPH-dependent CEF), PGRL1 (FDX-plastoquinone reductase, which is involved in ferredoxin-dependent CEF), tubulin. The strains used were WT, *fdx5* and *fdx5(FDX5)* rescued strain.

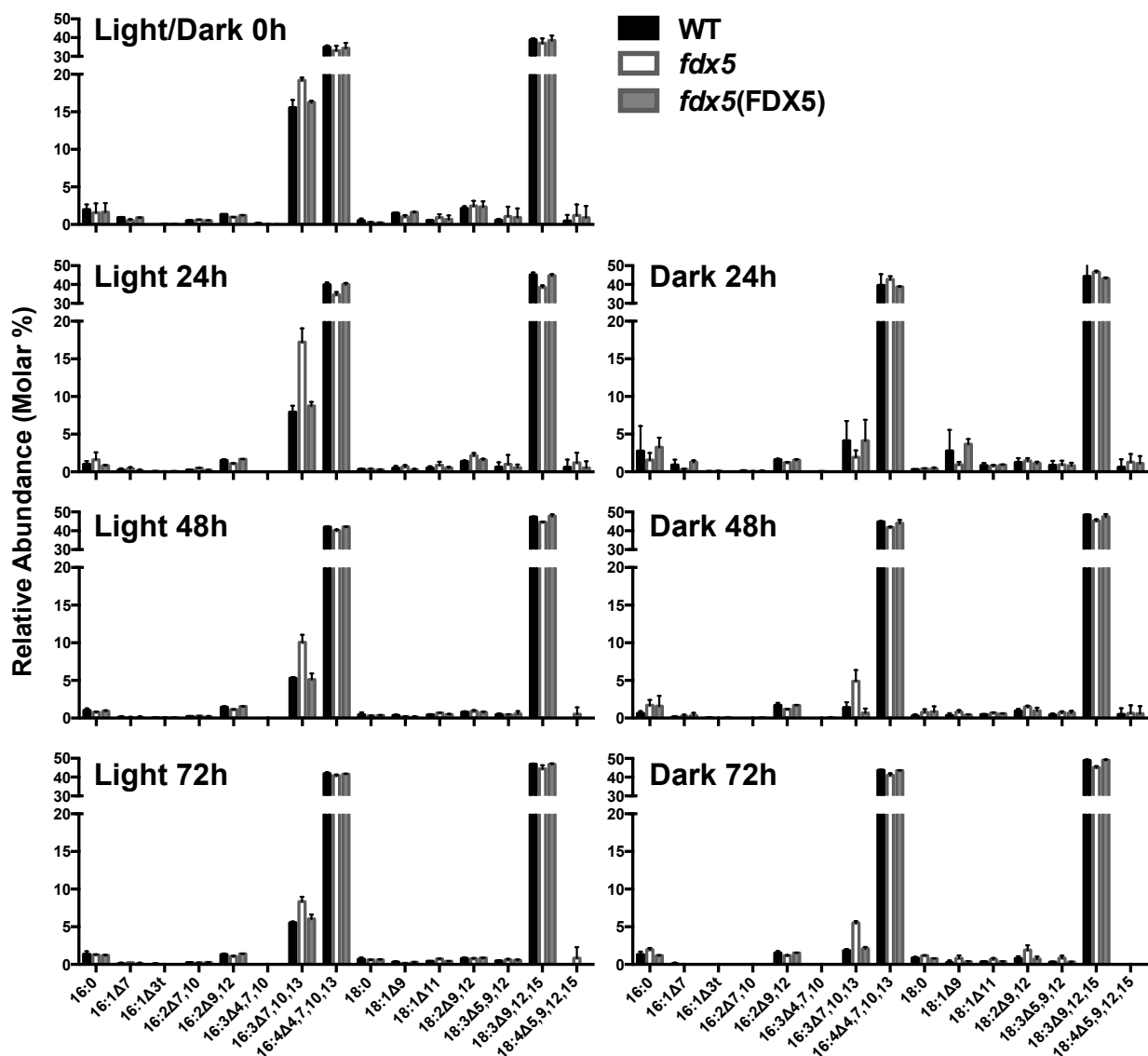


Figure A.S9. Profiles of fatty acids in MGDG after growth in the light and dark.

Levels of MGDG associated fatty acids after growth of the cells in the light or dark for 48 and 72 h. Fatty acids are C16 and C18 with the predominant C16 species having 4 double bonds (C16:4 $\Delta^{4,7,10,13}$), while the predominant C18 species has 3 double bonds (C18:3 $\Delta^{9,12,15}$). Error bars, which are barely visible, represent standard deviations. The strains used were WT, *fdx5* and *fdx5*(FDX5) rescued strain.

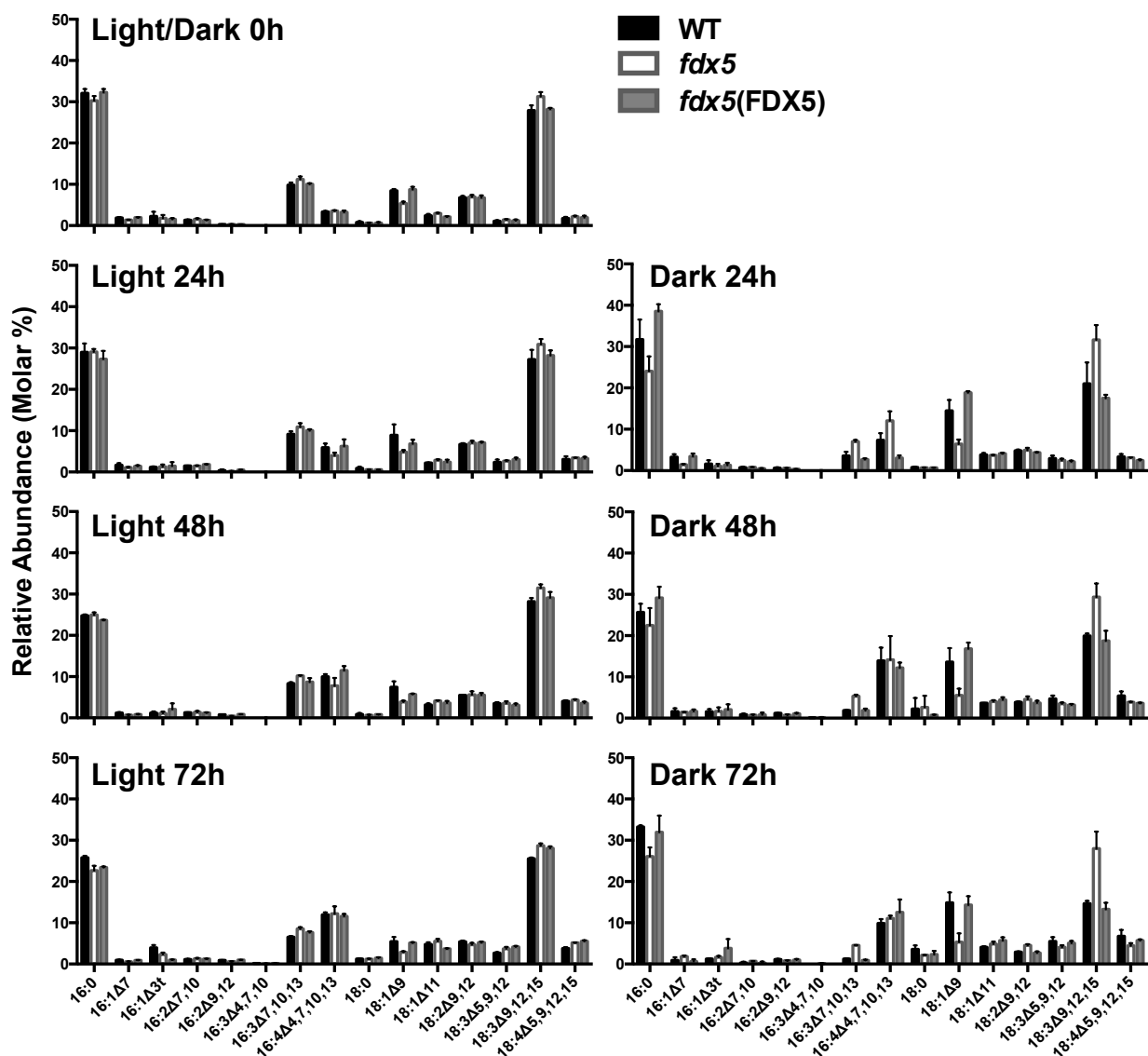


Figure A.S10. Profiles of fatty acids in DGDG after growth in the light and dark.

Levels of DGDG associated fatty acids after growth of the cells in the light or dark for 48 and 72 h. Fatty acids are C16 and C18 with the predominant C16 species having 0 (C16:0) and 4 (C16:4^{Δ4,7,10,13}) double bonds, while the predominant C18 species have 1 (C18:1^{Δ9} and C18:1^{Δ11}), 2 (C18:2^{Δ9,12}) and 3 (C18:3^{Δ5,9,12}, and C18:3^{Δ9,12,15}) double bonds. Error bars represent standard deviation. The strains used were WT, *fdx5* and *fdx5*(FDX5) rescued strain.

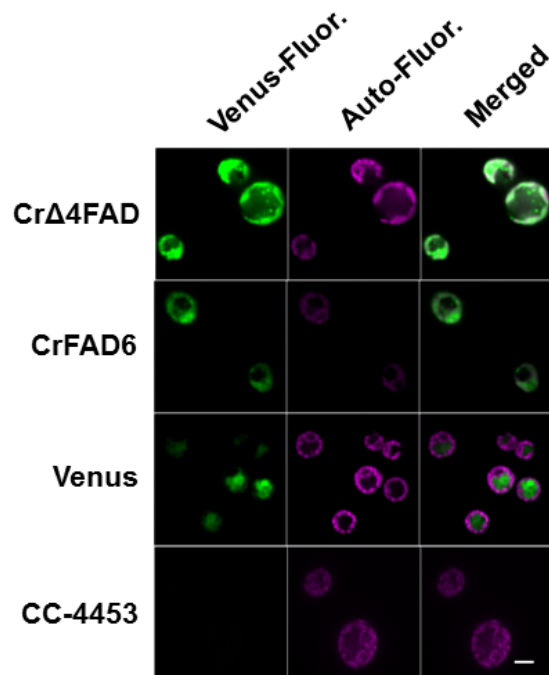


Figure A.S11. Localization of Cr Δ 4FAD and CrFAD6.

Cr Δ 4FAD and CrFAD6 are localized to chloroplasts in *Chlamydomonas*. The cells either contained the introduced vector with neither *Venus* nor the *FDX5* sequence (CC-4533), with *Venus* (*Venus*) or with *Cr Δ 4FAD* or *CrFAD6* fused to *Venus* (indicated as Cr Δ 4FAD and CrFAD6). Column 1 shows *Venus* fluorescence (*Venus-Fluor.*; green fluorescence), column 2 shows Chl auto-fluorescence (*Auto-Fluor.*; magenta fluorescence), column 3 shows the merged image of column 1 and column 2 (green-blue indicates co-localization). The scale bar represents 5 μ m.

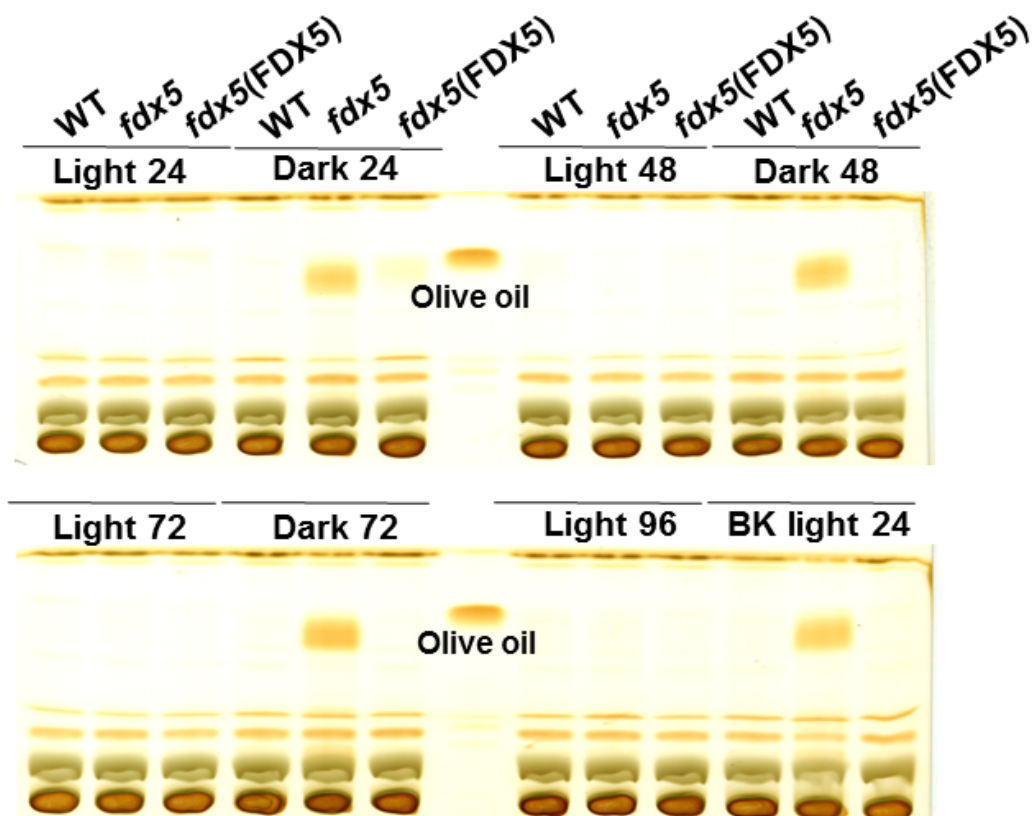


Figure A.S12. Separation of neutral lipids in different cell types under different light conditions.

TAG accumulates in *fdx5* in the dark. Total TAG was separated by thin layer chromatography at 24, 48, 72 h after growth of the cells in the light and dark, and from the dark (72 h) back to light for 24 h (BK light 24). Analyses were performed for WT, the *fdx5* mutant and the *fdx5*(FDX5) complemented strain. 20 μ g olive oil was used as the standard.

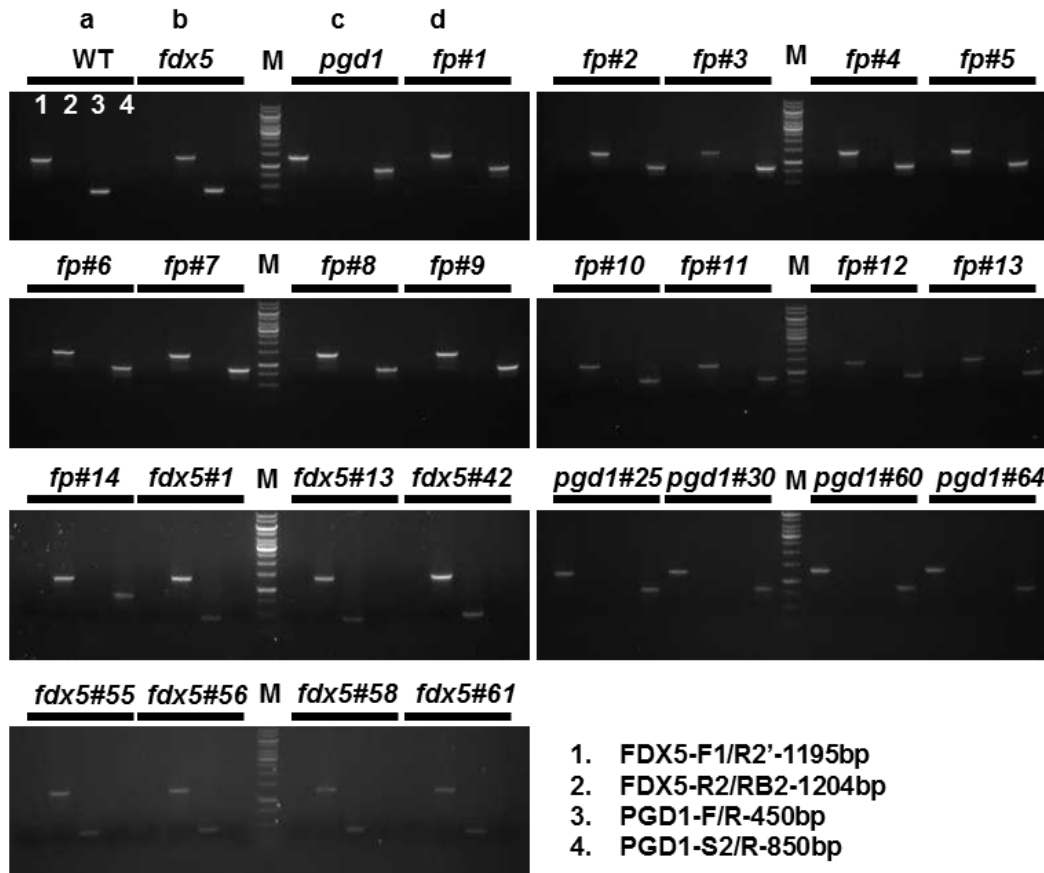


Figure A.S13. Genotyping of the *fdx5pgd1* double mutants.

fp represents the *fdx5pgd1* double mutants. *fdx5* and *pgd1* were used as the parental strains, *fdx5#1*, *fdx5#13*, *fdx5#42*, *fdx5#55*, *fdx5#56*, *fdx5#58*, *fdx5#61* are *fdx5* mutants that segregated in the cross, while the *pgd1#25*, *pgd1#30*, *pgd1#60*, *pgd1#64* were *pgd1* mutants that segregated in the cross. The primers and sizes of the amplification products are listed at the bottom. M represents DNA ladder. The primer pairs (1) FDX5-F1/R2 (for *FDX5*), (2) FDX5-R2/RB2 (for insertion into *FDX5*), (3) PGD1-F/R (for *PGD1*), and (4) PGD1-S2/R (for insertion into *PGD1*) were used to genotype the progeny (determine whether or not the strains had an insertion in *FDX5*, *PGD1* or both genes): progeny *a* has intact *FDX5* and *PGD1* genes (WT); progeny *b* has a disrupted *FDX5* and intact *PGD1* gene (*fdx5*); progeny *c* has an intact *FDX5* gene and a disrupted *PGD1* gene (*pgd1*); progeny *d* has a disrupted *FDX5* gene and a disrupted *PGD1* gene (*fdx5pgd1#1*). M represents DNA ladder.

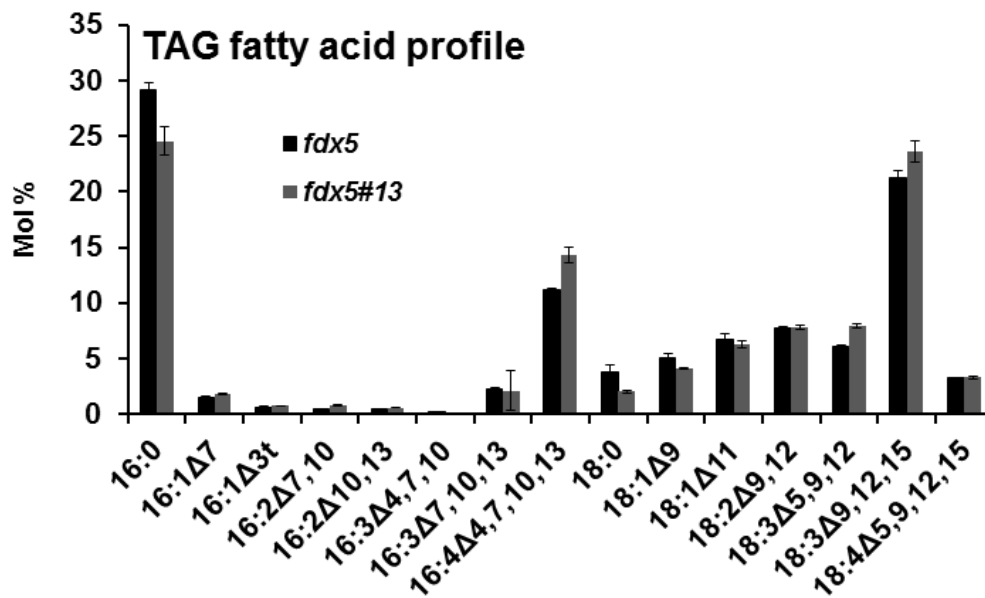


Figure A.S14. Fatty acid profiles in *fdx5* and the *fdx5#13* strains in the dark at 48 h.

Error bars represent standard deviation (n=3). The molar percentage of the various fatty acids is given on the y-axis.

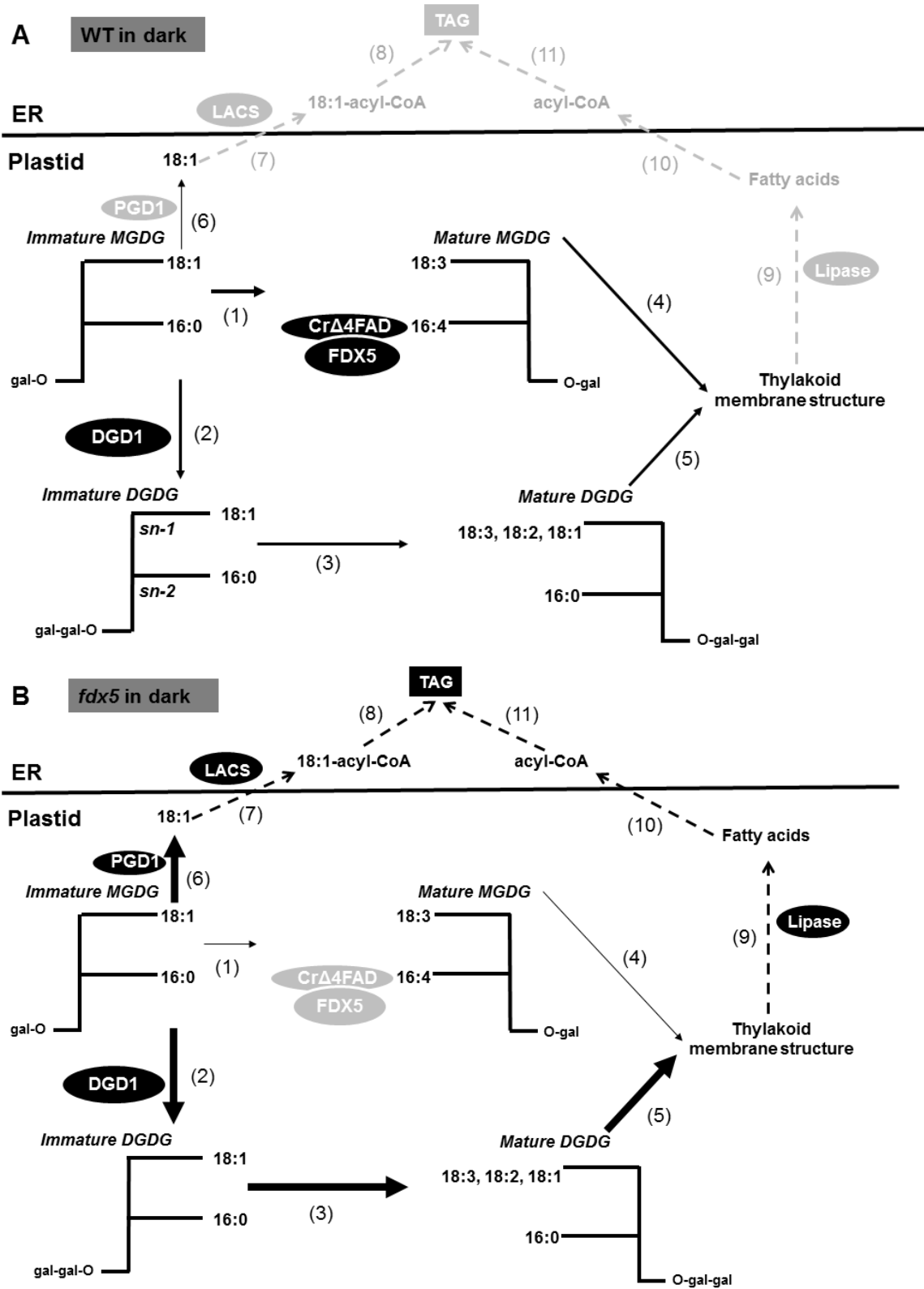


Figure A.S15. Model for FDX5-mediated regulation of thylakoid membrane structure in the dark.

Figure A.S15. (cont'd)

The filled shapes and arrows represent proteins/enzymes and reactions, respectively. The black and grey colors represent the active and inactive status of the enzymes or reactions, respectively; and the thickness of the arrows represents the extent of the biosynthetic reactions. (A) Model for WT cells. (B) Model for the *fdx5* mutant. In the dark, the immature MGDG can be converted to a number of different products: (1) conversion of immature to mature MGDG by desaturation of C18:1 at *sn-1* and C16:0 at *sn-2* to C18:3 and C16:4 through CrFAD6 and CrΔ4FAD, respectively, with electron donation potentially from FDX5; (2) conversion from immature MGDG to immature DGDG through addition of a second galactose head group to the MGDG, which is catalyzed by DGD1 (digalactosyldiacylglycerol synthase); (3) conversion of immature DGDG to mature DGDG by desaturation of the C18:1 at *sn-1* position to C18:3 through the activity of CrFAD6 and electron donation potentially from FDX5; (4 and 5) integration of mature MGDG and DGDG into thylakoid membranes; (6) conversion of immature MGDG to lyso-immature MGDG by PGD1-dependent cleaving of C18:1 from the *sn-1* position; (7) conversion of cleaved C18:1 from plastid to C18:1-acyl-CoA by LACS (long chain acyl-CoA synthetase) in the ER; (8) recruitment of C18:1-acyl-CoA for TAG synthesis; (9) degradation of thylakoid membrane by lipases to release free fatty acids in plastid; (10) movement of free fatty acids from plastid to ER to generate acyl-CoA; (11) recruitment of the free acyl-CoA for TAG synthesis in the ER. The inability to perform (1) would promote (2) and (6). Fatty acids in addition to C18 can also be recruited for TAG formation.

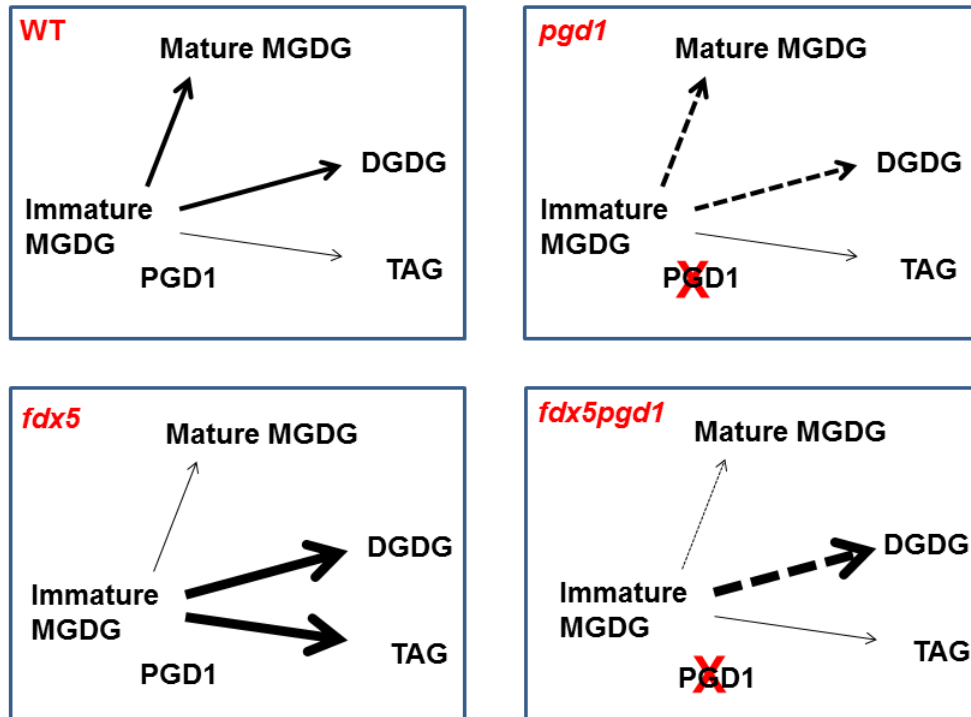


Figure A.S16. The impact of PGD1 on lipid production in the various strains in the dark.
 The arrows are of different thicknesses, indicating a relative level of immature MGDG that is converted to various products. The dashed lines represent possible metabolic fates in *pgd1*.

APPENDIX B. SUPPORTING TABLES

Table A.S1. Genes encoding ferredoxins in the *Chlamydomonas* genome.

PredAlgo software (<https://giavap-genomes.ibpc.fr/cgi-bin/predalgotdb.perl?page=main>) (Tardif *et al.*, 2012) was used to predict the subcellular localization of Ferredoxins. Names, protein IDs, NCBI accession numbers, and predicted localizations are indicated.

Gene	JGI v4.0	Phytozome v10.0.4	NCBI	Localization
FDX1(Fd)	147787	g15094	XP_001692808.1	Chloroplast
FDX2	159161	Cre16.g658400	XP_001697912.1	Chloroplast
FDX3	196707	Cre06.g306350	XP_001691381.1	Chloroplast
FDX4	196705	Cre07.g334800	XP_001700106.1	Chloroplast
FDX5	156833	Cre17.g700950	XP_001691603.1	Chloroplast
FDX6	196703	Cre03.g183850	XP_001702961.1	Chloroplast
FDX7	160049	Cre01.g006100	XP_001702098.1	Chloroplast
FDX8	179658	Cre01.g005600	XP_001702123.1	Chloroplast
FDX9	188740	Cre12.g487900	XP_001690910.1	Chloroplast
FDX10	189455	Cre04.g225450	XP_001692319.1	Chloroplast
FDX11	174881	Cre06.g291650	XP_001695531.1	Chloroplast
FDX12	205989	Cre08.g374550	-	?
MFDX	154720	Cre12.g559950	XP_001703155.1	Mitochondria

Table A.S2. Primers used in this study.

Primer names	Use of primers	Orientation	Sequence	Tm
FDX5-F1	Mutant screen	forward	5'- GCATTGCCTAACAGCCTTACCTCCA -3'	60.0°C
FDX5-R1	Mutant screen	reverse	5'- CCCAACAACCGTGTGTGCCACGCTTC -3'	60.0°C
FDX5-F2	Mutant screen	forward	5'- GAAGCGTGGCACACACGGTTGTTGGG -3'	60.0°C
FDX5-R2	Mutant screen	reverse	5'- TACTGGTGCTTGCCGTACTC -3'	60.0°C
FDX5-F3	Mutant screen	forward	5'- GAGTACGGCAAGCACCAGTA -3'	60.0°C
FDX5-R3	Mutant screen	reverse	5'- ATCAGTCCCATCCTCAACCAATCCTCA CG -3'	60.0°C
FDX5-COM-F	Complementation	forward	5'- GAATTCATTACACAGCAGTTTCAGGCAT T -3'	59.7°C
FDX5-COM-R	Complementation	reverse	5'- TAGGATCCCCATAGTTGGGGTTACATG AA-3'	58.8°C
RB1	Insert localization	forward	5'- ATGGGGCGGTATCGGAGGAAAAG -3'	60.0°C
RB2	Insert localization	forward	5'- TACCGCTGTTGGACGAGTTCTTCTG -3'	60.0°C
RIM1	Insert localization	reverse	5'- GCTGGCACGAGTACGGGTTG -3'	58.0°C
Mid-up	Mating type	forward	5'- ATGGCCTGTTTCTTAGC -3'	52.0°C
Mid-low	Mating type	reverse	5'- CTACATGTGTTTCTTGACG -3'	52.0°C
Fus-up	Mating type	forward	5'- ATGCCTATCTTTCTCATTCT -3'	52.0°C
Fus-low	Mating type	reverse	5'- GCAAAATACACGTCTGGAAG -3'	52.0°C
FDX5Loc	Localization	forward	5'-GGTTAACATGCTGTGCGCGCTCCC-3'	60.0°C
FDX5Loc	Localization	reverse	5'-GGTTAACCTGGTGCTTGCCGTACTCG-3'	60.0°C
APHVIII-F1	Southern blot probe	forward	5'-ATGGACGATGCGTTGCGT-3'	66.0°C
APHVIII-R1	Southern blot probe	reverse	5'-CTCAGAAGAACTCGTCCAACA-3'	62.0°C
FDX5-F4	Southern blot probe	forward	5'-TACTCCCTCCGACCCACATCCTGA-3'	72.0°C
FDX5-R4	Southern blot probe	reverse	5'-GACCCACCTTACCCACATCAG-3'	70.0°C
PGD1-F	Genotyping	forward	5'- ACATCGTGAATGGCAAAACA -3'	60.0°C
PGD1-R	Genotyping	reverse	5'- ATTGCGCGGTTTAGAACTT -3'	60.0°C
PGD1-S2-1	Genotyping	forward	5'- ATAGGGGTTCCGCGCACAT -3'	70.0°C
FDX5-Y2H-F	Y2H	forward	5'- CACCATGCTGTGCGCGCTCCCAGC -3'	60.0°C
FDX5-Y2H-R	Y2H	reverse	5'- TTACTGGTGCTTGCCGTACT -3'	60.0°C
FD-Y2H-F	Y2H	forward	5'- CACCATGGCCATGGCTATGCGCTC -3'	60.0°C
FD-Y2H-R	Y2H	reverse	5'- GTACAGGGCCTCCTCCTGGTG -3'	60.0°C
CrΔ4FAD-Y2H-F	Y2H	forward	5'- CACCATGAACGCCACGATGCAGCG -3'	60.0°C
CrΔ4FAD-Y2H-R	Y2H	reverse	5'- TTAGAACTTGAGAGCATCAGCATCTCG C -3'	60.0°C
CrFAD6-Y2H-F	Y2H	forward	5'- CACCATGGCGTTTCGCTCTGCGCTC -3'	60.0°C
CrFAD6-Y2H-R	Y2H	reverse	5'- TTAGAAGCGCGGAGTCGG -3'	60.0°C
FDX5_Venus -F	Gibson Cloning	forward	5'- GCTACTCACAACAAGCCCAGTTATGCTG TGCGCGCGCTCCCAGC -3'	60.0°C

Table A.S2. (cont'd)

Primer names	Use of primers	Orientation	Sequence	Tm
FDX5_Venus -R	Gibson Cloning	reverse	5'- GAGCCACCCAGATCTCCGTTCTGGTGCTT GCCGTACT -3'	60.0°C
CrΔ4FAD_Venus -F	Gibson Cloning	forward	5'-GCTACTCACAACAAGCCCAGTTATGAAC GCCACGATGCAGCG -3'	60.0°C
CrΔ4FAD_Venus -R	Gibson Cloning	reverse	5'- GAGCCACCCAGATCTCCGTTGAACTTGG AGAGCATCAGCATCTCGC -3'	60.0°C
CrFAD6_Venus -F	Gibson Cloning	forward	5'- GCTACTCACAACAAGCCCAGTTATGGCG TTCGCTCTGCGCTC -3'	60.0°C
CrFAD6_Venus -R	Gibson Cloning	reverse	5'- GAGCCACCCAGATCTCCGTTGAAGGCGG CGGAGTCGG -3'	60.0°C
oMJ237	Gibson sequencing	forward	5'- GGAGGTACGACCGAGATGGCT-3'	60.0°C
oMJ555	Venus sequencing	reverse	5'-CACGTCGCCGTCCAGCTC -3'	60.0°C
oMJ556	mCherry sequencing	reverse	5'- CTCCTTGATGATGGCCATG-3'	60.0°C

Table A.S3. Strains used in this study.

Name	Note	Background
CC124/5	Wild-type - mating type pair	<i>nit1nit2</i>
D66	Wild-type - CC-4425	<i>nit2, cw15, mt⁺</i>
21gr(+/-)	Wild-type - mating type pair	<i>NIT1, NIT2</i>
cMJ030	Wild-type - from 4A x D66 cross, CC-4533	<i>nit1nit2cw15</i>
<i>fdx5</i> in D66	The mutant was generated in D66	<i>nit1nit2cw15, Paro⁺</i>
<i>fdx5</i> in CC124/5	Backcross of <i>fdx5</i> into CC124/5	<i>nit1nit2, Paro⁺</i>
<i>fdx5</i> in 21gr	Backcross of <i>fdx5</i> into 21gr(+/-)	<i>NIT1, NIT2, Paro⁺</i>
dw15	CC-4619	<i>nit1nit2cw15</i>
<i>pgd1</i> in dw15	CC-4593	<i>nit1nit2cw15, Hyg⁺</i>
<i>fdx5</i> #	Segregated from cross of <i>fdx5pgd1</i>	<i>nit1nit2, Paro⁺</i>
<i>pgd1</i> #	Segregated from cross of <i>fdx5pgd1</i>	<i>nit1nit2, Hyg⁺</i>
<i>fdx5pgd1</i>	Segregated from cross of <i>fdx5pgd1</i>	<i>nit1nit2, Paro⁺, Hyg⁺</i>
<i>pLM005FDX5</i>	Transformed to cMJ030, for localization	<i>nit1nit2, Paro⁺</i>
<i>pLM005CrΔ4FAD</i>	Transformed to cMJ030, for localization	<i>nit1nit2, Paro⁺</i>
<i>pLM005CrFAD6</i>	Transformed to cMJ030, for localization	<i>nit1nit2, Paro⁺</i>
<i>fdx5</i> (FDX5) -1	By <i>FDX5</i> -cDNA	<i>nit1nit2, Paro⁺, Zeo⁺</i>
<i>fdx5</i> (FDX5) -2	By <i>FDX5</i> -gDNA	<i>nit1nit2, Paro⁺, Zeo⁺</i>

Table A.S4. Constructs used in this study.

Use	Construct	Plasmid name	Insert or PCR product	Primers	Plasmid backbone	Cloning method
Localization	Venus	pLM005_Venus	-	-	pUC19	-
	Venus:FDX5	pLM005FDX5_Venus	FDX5 CDS	FDX5_Venus -F/ FDX5_Venus -R	pUC19	Gibson Cloning
	Venus:CrΔ4FAD	pLM005 CrΔ4FAD_Venus	CrΔ4FAD CDS	CrΔ4FAD_Venus -F/ CrΔ4FAD_Venus -R	pUC19	Gibson Cloning
	Venus:CrFAD6	pLM005 CrFAD6_Venus	CrFAD6 CDS	CrFAD6_Venus -F/ CrFAD6_Venus -R	pUC19	Gibson Cloning
Mating-based split ubiquitin system (mbSUS)	D-TOPO:FD	pENTR/D-TOPO_FD	FD CDS	FD-Y2H -F/ FD-Y2H -R	pENTR	D-TOPO Cloning
	D-TOPO:FDX5	pENTR/D-TOPO_FDX5	FDX5 CDS	FDX5-Y2H -F/ FDX5-Y2H -R	pENTR	D-TOPO Cloning
	D-TOPO:CrΔ4FAD	pENTR/D-TOPO_CrΔ4FAD	CrΔ4FAD CDS	CrΔ4FAD-Y2H-F/ CrΔ4FAD-Y2H-R	pENTR	D-TOPO Cloning
	D-TOPO:CrFAD6	pENTR/D-TOPO_CrFAD6	CrFAD6 CDS	CrFAD6-Y2H-F/ CrFAD6-Y2H-R	pENTR	D-TOPO Cloning
	NubG	pXN22	-	-	pUC	-
	FD:NubG	pXN22_FDX1	FD CDS	FD-Y2H -F/ FD-Y2H -R	pUC	LR Cloning
	FDX5:NubG	pXN22_FDX5	FDX5 CDS	FDX5-Y2H -F/ FDX5-Y2H -R	pUC	LR Cloning
	Cub	pMet-YC	-	-	pUC	-
	Cub:CrΔ4FAD	pMet-YC_CrΔ4FAD	CrΔ4FAD CDS	CrΔ4FAD-Y2H-F/ CrΔ4FAD-Y2H-R	pUC	LR Cloning
	Cub:CrFAD6	pMet-YC_CrFAD6	CrFAD6 CDS	CrFAD6-Y2H-F/ CrFAD6-Y2H-R	pUC	LR Cloning
Complementation	PSAD:FDX5 cDNA	pJM43Ble_FDX cDNA	FDX5 cDNA	FDX5-COM-F1/ FDX5-COM-R1	pSP124	EcoRI/BamHI
	PSAD:FDX5 gDNA	pJM43Ble_FDX gDNA	FDX5 gDNA	FDX5-COM-F1/ FDX5-COM-R1	pSP124	EcoRI/BamHI

Table A.S5. Pull down assay using FDX5 to establish interacting proteins.

Name	ID Number	Annotation	Accession ID	MW ¹	Hits ²
FDX5	Cre17.g700950	apoferrredoxin	gi 159466834	14 kDa	8
chlorophyll a/b binding protein					
LHCBM6	Cre06.g285250	chlorophyll a/b binding protein of LHCII	gi 159474480	27 kDa	7
LHCA5	Cre10.g425900	chlorophyll a/b binding protein of LHCI	gi 159489490	28 kDa	6
LHCBM1	Cre01.g066917	chlorophyll a/b binding protein of LHCII	gi 20269804	28 kDa	4
LHCB5	Cre16.g673650	chlorophyll a/b binding protein of LHCII	gi 159475641	31 kDa	4
LHCBM2	Cre12.g548400	chlorophyll l a/b binding protein of LHCII	gi 159471686	27 kDa	4
LHCB4	Cre17.g720250	chlorophyll a/b binding protein of LHCII	gi 159478202	30 kDa	4
LHCA7	Cre16.g687900	chlorophyll a/b binding protein of LHCI	gi 40714521	26 kDa	4
LHCA4	Cre10.g452050	chlorophyll a/b binding protein of LHCI	gi 40714509	29 kDa	4
LHCA3	Cre11.g467573	chlorophyll a/b binding protein of LHCI	gi 40714511	29 kDa	4
LHCA9	Cre07.g344950	chlorophyll a/b binding protein of LHCI	gi 159468772	23 kDa	3
LHCA8	Cre06.g272650	chlorophyll a/b binding protein of LHCI	gi 159476206	26 kDa	3
LHCBM5	Cre03.g156900	chlorophyll a/b binding protein of LHCII	gi 159478875	29 kDa	3
LHCA6	Cre06.g278213	chlorophyll a/b binding protein of LHCI	gi 159479992	28 kDa	3
LHCA2	Cre12.g508750	chlorophyll a/b binding protein of LHCI	gi 159465641	27 kDa	3
LHCBM3	Cre04.g232104	chlorophyll a/b binding protein of LHCII	gi 159491492	27 kDa	2
Ribosomal protein					
PRL4	Cre09.g397697	ribosomal protein L4	gi 159473354	45 kDa	8
PRL6	Cre01.g011000	ribosomal protein L6	gi 159463286	24 kDa	7
PRPL7	Cre13.g581650	plastid ribosomal protein L7/L12	gi 159470865	14 kDa	6
RPS7	Cre12.g498900	ribosomal protein S7	gi 159488703	22 kDa	6
RPL13	Cre14.g630100	ribosomal protein L13	gi 159469029	24 kDa	5
RPS3	Cre11.g467702	ribosomal protein S3	gi 213517427	82 kDa	5
RPL18A	Cre01.g047750	ribosomal protein L18a	gi 159463026	21 kDa	5
RPS3	Cre02.g102250	ribosomal protein S3	gi 159483497	26 kDa	4
PRPL4	Cre11.g479500	plastid ribosomal protein L4	gi 159478579	26 kDa	4
RPP0	Cre12.g520500	acidic ribosomal protein P0	gi 159477927	35 kDa	4
RPL7A	Cre12.g529651	ribosomal protein L7a	gi 159477735	29 kDa	4
PRPL1	Cre02.g088900	plastid ribosomal protein L1	gi 159487501	32 kDa	4
RPL21	Cre06.g278135	ribosomal protein L21	gi 159479900	18 kDa	4
PRPL31	Cre48.g761197	plastid ribosomal protein L3	gi 159485314	28 kDa	4
RPS13	Cre07.g331900	ribosomal protein S13	gi 159464389	17 kDa	4
PSRP3	Cre02.g083950	plastid-specific ribosomal protein 3	gi 159487801	33 kDa	4
PRPL9	Cre12.g556050	plastid ribosomal protein L9	gi 159472060	22 kDa	3
RPL19	Cre02.g075700	ribosomal protein L19	gi 159487227	23 kDa	3
RPS3a	Cre13.g568650	ribosomal protein S3a	gi 159471131	29 kDa	3
RPL10	Cre09.g388200	ribosomal protein L10	gi 159472591	26 kDa	3
RPL14	Cre17.g701200	ribosomal protein L14	gi 159466828	15 kDa	3

Table A.S5. (cont'd)

Name	ID Number	Annotation	Accession ID	MW¹	Hits²
RPL11	Cre01.g027000	ribosomal protein L11	gi 159463566	20 kDa	3
RPL12	Cre12.g528750	ribosomal protein L12	gi 159477751	18 kDa	3
RPS5	Cre06.g290950	ribosomal protein S5	gi 159474574	22 kDa	3
RPL11	Cre01.g027000	ribosomal protein L5	gi 126165895	20 kDa	3
RPS14	Cre11.g480150	ribosomal protein S14	gi 159478595	16 kDa	3
PRPS5	Cre16.g659950	plastid ribosomal protein S5	gi 159479560	72 kDa	3
RPS24	Cre10.g456200	ribosomal protein S24	gi 159480596	15 kDa	3
RPS16	Cre13.g573351	ribosomal protein S16	gi 159470701	16 kDa	3
RPS4	Cre06.g308250	ribosomal protein S4	gi 159466042	29 kDa	3
RPS6	Cre09.g400650	ribosomal protein S6	gi 159473970	28 kDa	2
RPS28	Cre12.g510450	ribosomal protein S28	gi 159465687	7 kDa	2
RPS8	Cre06.g272800	ribosomal protein S8	gi 159476204	24 kDa	2
RPL13A	Cre12.g532550	ribosomal protein L13a	gi 159469516	21 kDa	2
PRPL6	Cre09.g415950	plastid ribosomal protein L6	gi 159477461	22 kDa	2
PRPL31	Cre08.g365400	plastid ribosomal protein L31	gi 159476036	15 kDa	2
RPL9	Cre12.g494050	ribosomal protein L9	gi 159484990	22 kDa	2
RPL7	Cre12.g537800	ribosomal protein L7	gi 159469644	30 kDa	2
RPS15	Cre08.g360900	ribosomal protein S15	gi 159475964	17 kDa	2
PRPL19	Cre17.g734450	plastid ribosomal protein L19	gi 159469822	17 kDa	2
Translation factor					
EEF1A3	Cre06.g263450	eukaryotic translation elongation factor 1 alpha 1	gi 159476938	51 kDa	17
EFG8	Cre06.g259150	elongation factor Tu	gi 41179007	46 kDa	6
EIF3G	Cre06.g269450	eukaryotic translation initiation factor	gi 159476822	31 kDa	3
EFG2	Cre12.g516200	elongation factor 2	gi 159490505	94 kDa	2
HEL30	Cre06.g298650	eukaryotic initiation factor 4A-like protein	gi 159466510	47 kDa	4
Cytoskeleton					
TUB1	Cre12.g542250	beta tubulin 2	gi 159471706	50 kDa	11
TUA2	Cre04.g216850	alpha tubulin 1	gi 159467393	50 kDa	9
ACT1	Cre13.g603700	actin	gi 159482014	42 kDa	3
ATP synthase					
mATP2	Cre17.g698000	ATP synthase subunit beta, chloroplastic	gi 226698718	52 kDa	9
ATP2	Cre17.g698000	beta subunit of mitochondrial ATP synthase	gi 159466892	62 kDa	9
ATP1A	Cre02.g116750	ATP synthase CF1 alpha subunit	gi 213517431	55 kDa	7
ATPG	Cre11.g481450	CF0 ATP synthase subunit II precursor	gi 159478483	22 kDa	2
ASA1	Cre07.g340350	mitochondrial F1F0 ATP synthase associated protein	gi 159468466	63 kDa	3
ATP1A	Cre02.g116750	mitochondrial F1F0 ATP synthase, alpha subunit	gi 159483185	62 kDa	2
ASA2	Cre09.g415550	mitochondrial F1F0 ATP synthase associated protein	gi 159477287	48 kDa	4

Table A.S5. (cont'd)

Name	ID Number	Annotation	Accession ID	MW ¹	Hits ²
Photosynthes					
is related					
protein					
PSBP1	Cre12.g550850	Oxygen-evolving enhancer protein 2	gi 131389	26 kDa	9
PsbB	Cre09.g416200	photosystem II 47 kDa protein	gi 213517415	56 kDa	8
PSBQ	Cre08.g372450	oxygen evolving enhancer protein 3	gi 159486609	22 kDa	8
PSBO	Cre09.g396213	oxygen-evolving enhancer protein 1	gi 159473144	31 kDa	8
PsbC	Cre09.g388356	photosystem II 44 kDa protein	gi 41179065	51 kDa	5
PSAF	Cre09.g412100	photosystem I reaction center subunit III	gi 159477399	24 kDa	4
PsaB	Cre17.g702500	photosystem I subunit PsaB	gi 41179048	82 kDa	3
PETO	Cre12.g558900	cytochrome b6f complex subunit V	gi 159489663	20 kDa	2
D2	Cre07.g317201	photosystem II protein D2	gi 225115	41 kDa	3
PSAD	Cre05.g238332	photosystem I reaction center subunit II	gi 159479282	21 kDa	2
CGLD37	Cre09.g392350	glycine-rich RNA-binding protein	gi 159472653	16 kDa	5
CPLD20	Cre01.g000900	predicted protein	gi 159484580	46 kDa	3
ASC1	Cre01.g013700	predicted protein	gi 159462440	28 kDa	2
RCA1	Cre04.g229300	rubisco activase	gi 159468147	45 kDa	4
PHT1	Cre03.g199000	phototropin	gi 159470479	81 kDa	2
Lipid metabolism					
FAB2	Cre17.g701700	plastid acyl-ACP desaturase	gi 159466822	45 kDa	7
ACX2	Cre12.g519100	acetyl-CoA carboxylase	gi 159477697	54 kDa	3
Chaperon					
HSP70A	Cre08.g372100	heat shock protein 70A	gi 159486599	71 kDa	2
HSP70B	Cre06.g250100	heat shock protein 70B	gi 1225970	72 kDa	6
CPN60B2	Cre07.g339150	chaperonin 60B2	gi 159468684	62 kDa	2
RUBA	Cre04.g231222	chaperonin 60A	gi 159491478	62 kDa	4
Nucleotide metabolism					
PNBP	Cre06.g269050	pyridine nucleotide binding protein	gi 159476278	75 kDa	4
ANT1	Cre09.g386650	adenine nucleotide translocator	gi 159474120	34 kDa	4
AAA1	Cre08.g358526	plastidic ADP/ATP translocase	gi 159491564	62 kDa	3
Starch					
metabolism					
AGP1	Cre13.g567950	ADP-glucose pyrophosphorylase large subunit	gi 159470605	55 kDa	4
GAD1	Cre03.g169400	UDP-D-glucuronic acid decarboxylase	gi 159491066	37 kDa	3
SBP1	Cre03.g185550	sedoheptulose-1,7-bisphosphatase	gi 159467635	42 kDa	3
PRK1	Cre12.g554800	phosphoribulokinase	gi 159471788	42 kDa	3

Table A.S5. (cont'd)

Name	ID Number	Annotation	Accession ID	MW ¹	Hits ²
Anoxia					
PFL1	Cre01.g044800	pyruvate-formate lyase	gi 159462978	91 kDa	4
ADH1	Cre17.g746997	aldehyde-alcohol dehydrogenase	gi 92084840	102 kDa	4
ATO1	Cre17.g723650	acetyl-CoA acyltransferase	gi 159478266	47 kDa	3
FUM1	Cre06.g254400	fumarate hydratase	gi 159477070	63 kDa	5
GAP1	Cre12.g485150	Glyceraldehyde-3-phosphate dehydrogenase	gi 1346064	37 kDa	3
ALS2	Cre01.g055453	acetolactate synthase	gi 159484278	52 kDa	3
Histone					
HFO11	Cre06.g266600	histone H4	gi 159464880	11 kDa	3
HTA17	Cre12.g505550	histone H2A	gi 159464886	14 kDa	2
Mitochondria metabolism					
QCR2	Cre12.g509750	mitochondrial processing peptidase alpha subunit	gi 159465665	50 kDa	3
COX90	Cre16.g691850	cytochrome c oxidase subunit	gi 159482474	12 kDa	2
QCR7	Cre06.g262700	ubiquinol:cytochrome c oxidoreductase 14 kDa subunit	gi 159476418	14 kDa	2
Various metabolism					
GAP3	Cre01.g010900	glyceraldehyde-3-phosphate dehydrogenase	gi 159463282	40 kDa	5
CIS2	Cre03.g149100	citrate synthase	gi 159474920	55 kDa	5
AST1	Cre09.g387726	aspartate aminotransferase	gi 159473837	47 kDa	6
MES1	Cre03.g180750	cobalamin-independent methionine synthase	gi 159489910	87 kDa	12
PRX2	Cre02.g114600	2-cys peroxiredoxin	gi 159483223	22 kDa	4
APR1	Cre12.g517150	adenylylphosphosulfate reductase	gi 159477975	46 kDa	3
IDH2	Cre02.g143250	NAD-dependent isocitrate dehydrogenase	gi 159473471	39 kDa	2
MAS1	Cre03.g144807	malate synthase	gi 159475042	61 kDa	2
ACH1	Cre01.g042750	aconitate hydratase	gi 159462944	86 kDa	2
MAP	Cre06.g254917	minus agglutinin protein	gi 159477066	255 kDa	2
SHMT1	Cre16.g664550	serine hydroxymethyltransferase	gi 159486853	57 kDa	2
Signal transduction					
TEF2	Cre12.g497300	calcium sensing receptor	gi 46093489	39 kDa	5
NOP58	Cre10.g441400	nucleolar protein, component of C/D snoRNPs	gi 159464245	55 kDa	2
MAPK6	Cre12.g508900	mitogen-activated protein kinase 6	gi 159465279	43 kDa	2
CDPK1	Cre17.g705000	calcium-dependent protein kinase 1	gi 159466768	67 kDa	2
CAV8	Cre12.g532350	voltage-gated Ca ²⁺ channel, alpha subunit	gi 159469522	471 kDa	2
Unknown protein					
Unknown	Cre03.g145507	hypothetical protein	gi 159475228	28 kDa	5
FAP24	Cre02.g081050	flagellar associated protein	gi 159487357	57 kDa	5
Unknown	no ID	Chain A, N153q Mutant Of Cytochrome F	gi 10121062	27 kDa	4
HEL47	Cre10.g427700	predicted protein	gi 159489124	63 kDa	3
TEF10a	Cre03.g146167	hypothetical protein	gi 159474984	25 kDa	3

Table A.S5. (cont'd)

Name	ID Number	Annotation	Accession ID	MW¹	Hits²
Unknown	Cre02.g112150	hypothetical protein	gi 159483731	35 kDa	3
Unknown	Cre03.g197450	predicted protein	gi 159469995	132 kDa	2
Unknown	Cre06.g263250	predicted protein	gi 159476406	65 kDa	2

Note: ¹ represents protein molecular weight; ² represents the numbers of hits from the pull-down assay.

APPENDIX C. APPENDIX C.

Genomic DNA sequence of the *fdx5* mutant. The italic uppercase letters represent UTR regions, the underlined uppercase letters represent exons, and the black uppercase letters represents intron. The lowercase letters represent the insertion cassette.

ATTACACAGCAGTTTCAGGCATTGCCTAACAGCCTTACCTCCAAACCTTGCCCCGACCTGTCCGTCGCGACT
CTTCCGAAAGAATGCTGTGCGCGCTCCAGCTGGTCTGCAAGCCTGTGAAGGCTGCTCGCGCCTCTC
GCGCTACCGTCAAGGTGCGCACCGACCGGTATCGCGTTCAGGTTGAGCAATCAAGTCGCCGCAAGCCA
GGTTTTTCGCTTTGGTCGCTGTGAGGCTCCGGGGCTATTTGCTGGTATCCACTATGATGTCTCGATGT
GCAATTGATTGGGCGCGGTCTGTGAGGGCTCTTAGTGGAAGCTGCCAAACCATGCAAGCATAAAGCG
GCGCCGGTCGCCTTTTTACGTGCAGTAAAAGCGCGCAGTGAGCGCTGTGACGCGTTCAGCTTGCATCA
*ATTCCTGACATAATCCTTCGCCTATCGCGTCCCGCCCTGCCGTGCAGGTGCAGGCCT**tggtggaattgtgagc*
ggataacaatttcacacaggaaacagctatgacctgattacccaagcgcgaattaacctcactaaaggaacaaaagctgggtaccgggccccccctc
gagcacacacctgtcagaaacagctctcccaacgctctccctctcaegggcagccccgagccctttgccccttctagccaccgacaggaccaggcgt
ctcagcatgctcaacaacccgtaactgctgccagcgggtcccttctgctggtgatcgttgaagcgcgatgcaagacgaagggggcggagcaggcggcctgg
ctgttcgaagggctcggccagttcgggtgcttctccacgcgcctccacacctaccgatgcgtgaaggcaggcaaatgctcatgtttgccgaactcgg
agtccttaaaaagcgccttctgtcgtctccgagacatgtagcagatcgcagtgccaccttctgacgcgctcggcccatattcgagcgaattgtcattg
tagcacaattggagcaaatctggcgaggcagtaggctttaaagttgcaaggcgagagcaaaagtgaggcgcggcgtgattattggtatttacgcgacggccc
ggcgcgttagcggccctccccaggccaggacgattatgtatcaatattgttgcgttcgggcactcgtgcgagggctcctcgggctggggaggggatctg
ggaattggaggtacgaccgagatggcttgcctggggggagggttctcgcgcgagcaagccagggttaggtgttgcgctcttactcgttgcattctaggacc
ccactgtaactcaacaagcccatatggacgatcgttgcgtgcaactcggggctcggtatcccgttgcgtgagtggttgcgtgaggatggggcctcggggg
ctgggtttatcggcttcggggtgggtggggagggttcttcaaggtggcagctctggggcgggggtgggcttgggtgaggtgagcggctggtgtgtgt
tggcggaggtggggattcccgtaactcgttgcgtgagggtgggtggggacgagagggtcgctggttgcacccaagcgggttcggggcgtcggccagtc
gcggtggccgggagcagcggctggacgtggcggtggcgtcgcggggctcgtcgttcgctgcacgcgctggactgggagcgggtccggttcgatcgcag
tctcgggtgacggtgccgagcggcccgctgctgctgctgaagggagcgtcgactggaggatctggacgaggagcgaaggggtggtcgggggagcggc
ttctcggcagctggagcggactcggcctcgggacgaggatctggcggtttgccaggtcacctgtgcccgacaactgctgctgcacctcgtactcgcag
gtgaccgggtgatcagctggggcgggtcggcgtcgggaccggcactccgatctcgcgctgggtgctgcgcgagctggcccacaggaggaccctgggtc
ggcccggaggttccgcccgtctcgcgggagtagggcggggtgggatggggcggtatcggaggaaaagctggcgttttaccggctgttgacgagttct
*tctgagatatcgaattctcaggtcgggacatccccgaccagggggcgggggatgttctggggccgatgaaag**GGTCGGCCCCGACGAGGC*
GCTGTTTCGACGCCGTGGAGCGCTACGATGTGGACCTGCCCTACCTGTGCCGCACTGGTGAGAGTTCGT
GTGTTTCGGCACACATACGCAGAAGCGTGGCACACACGGTGTGTTGGGCAGCCCCGCTGCAAGTGCACCA
GTGCCCTTACTCCCTTCCGACCCACATCCTGACCCTCCCCGCCCTCCTCTCCTCCCCAACCCCCAGGC
ACCTGCGGCACGTGCGCGGGCCGTGTGCAGGAGGGCCAGGTGGAGCTCAAGGGTCAGCACATCCTGG
ACCCGATCAGGTCAAGGCCGGCTTCATCCTCATGTGCTCCGCCTACCCCGCTCCGACTGCACCATCC
TCACGCACCAGGTGAGGAGAGGGAAACAGGGATTGAAAAGAGATACGGCGCATCCGTGTGTGCGGCT
TGTGCGTGTGACCAGTGGTGCGGTGGCTGATGTGGGGTAAGGTGGGGTTCGCGAAAGATGGATGCGAT
GGCCAGGGGTGCTGCTGGGCTGCTGCTCGAACGGCCTGCAACCGCACGTGCGTGTCTTCGGAGCC
GCACCTGGCCGCGCCACACGTGCCTGTTTACTCCCAAGTCATTGACGCCTCCGCCCCCCTGTGCTCCC

CGCCCCTCCCTCCCCCTCAGGAGGAGCGCCTGCACACCTGCGAGTACGGCAAGCACCAGTAAGCGG
CACACACACGCCGCACGTACCATTCTGTGTCAGCGTCCGCTGCCTGGCGCCTGCTTGGAGCTAGAGGCGGGC
GATGGCGCAGTGGCACCAACATGACTCTGACTCATAGGACAACATTGTTACTTTATCACGCAACGGAGGGG
CATAGCTACGCTGGACAGGCTAGGCACGCACGACTCCTGCGCTGATTTGACTCCGTAGGTAGATGAATGACT
TCCACACAGTACCGGTATTGAACACCTTGACTCGCGCCTTGACGCATTGTTTTGCCCGCACATATACGGGGCA
GGAGTGGGTGGTGGTGCAAGCCGCCGCTCCGTGATTTTTGACGTTTTGACACGCGGCTTGAAGAGTCAA
GAGTGGCTGCAGCAGGATGCGAAGCATGTATGGCGGGGGTACTGAGGTAGGGCCGTAGAGGCAGGTTGA
CCGTTAGGCCTTAGGACGTCATGCATTGCCAATGCCATACATGAGTGGGGCACGTGAGGATTGGTTGAGGA
TGGGACTGATTGAGGCACACATACCGTAGGCAGGTGATTATAATAACGGAGCGACTGCTCCTGGGTAGCGTG
TGTGTGTGGCAAGGACACGGGTATGTATGGCTCTGGTGTGGCTGAGTGCGGCGCCCCGCTAGCAAGCGGG
GCTGCTGGAGGCGACTGGGTACCCGCGTGTCTACTGCCGCAGAGAAGATTAATCAAGCGATGAATTGGGTC
ACGGCTAGCTGCAATGCAGCAGCTTCATGTAACCCCCAACTATGG

CDS sequence of *fdx5* mutant. The red uppercase letters represent the exons, and the lowercase letters represent the insertion cassette.

ATGCTGTGCGCGCGCTCCCAGCTGGTCTGCAAGCCTGTGAAGGCTGCTCGCGCCTCTCGCGCTACCGTC
AAGGTGCAGGCCTtggtggaattgtgagcggataacaatttcacacaggaacagctatgacatgattacgccaagecgcgaattaaccctact
aaaggaacaaaagetgggtaccgggccccctcgagcacacactgtcagaaacagctcctccgacgctcctctcagggcgacccccgagccctt
tgccttcttagccaccgacaggaccaggcctctcagatgectcaacaacctactcgtccagcgggtcccttctgctggtgatccttggaaagcgc
atgcaagacgaagggggcggagcaggcggcctggctgttcgaagggctcggccagctcgggtgcttctccacgcgcctccacactaccgatgctg
aaggcaggcaaatgctcatgttgccegaactcggagtcttaaaaagccttctgtcgtcgttcagacatgtagcagatcgcagtgccaccttctga
cgcctcggccccatattcgagcgaattgtcattgtagcacaattggagcaaatctggcaggcagtaggctttaagttgcaaggcgagagagcaaatg
ggacgcggcgtgattattggtatttacgcagcggccccggcgttagcggccctccccaggccaggacgattatgtatcaatattgttgcgttgggca
gtgcgagggctcctcgggctggggaggggatctgggaattggaggtacgaccagatggcttgcctcggggggaggttctcgcgagcaagccagggt
agggttgcgctcttgcactgtgtgctatttaggacccccactgctactcaacaagccatattggacgatgcgttgcgtgactcggggctcggtatccgggt
gtgagtgggtgtgtgaggatggggcctcggggctgggtttatcgctcgggggtggggcgggagttgtttgcaaggtggcagctcggggcggg
gtggccttgtgggtgagcgtgagcggctgggtgggtggcggaggtgggattcccgtaactcgtgtgtggaggggtggggacgagagggctcctggt
ggtcaccgaagcgggtcggggcgtcggccagtgccgggtggccgaggcagcggctggacgtggcgggtggcgtcggggctcgtcgttgcctgca
cgcctggactgggagcgggtgctcgttcgatcagctcgcggtagcgtgcccagcggcggcctgctgctgtaagggagcgtcactggaggatcgt
gacgaggagcggaaaggggtggtcggggagcggcttctcgcgagctggagcggactcggcctcggacgaggatctggcggttgccacggtcactgtg
cccggacaacgtgctcgcacctgtaactcgcaggtgaccggcgtgatcagctggggcgggtcggcgtcggacggcactccgatctcgcgctgggt
ctgcgcgagctggcccacgaggaggaccctgggtcgggcccaggttcccgggcgttctcgggagtagggcgcgggtgggatggggcgggtatcgga
ggaaaagctggcgttttaccggctgttggacgagttctctgagatcgaattctcaggtcgggacatccccgaccagggggcggggatgttctggggccg
atgaaagGTCGGCCCCGACGAGGCGCTGTTCGACGCCGTGGAGCGCTACGATGTGGACCTGCCCTACC
TGTGCCGCACTGGCACCTGCGGCACGTGCGCGGGCCGTGTGCAGGAGGGCCAGGTGGAGCTCAAGGG
TCAGCACATCCTGGACCCCGATCAGGTCAAGGCCGGCTTCATCCTCATGTGCTCCGCCTACCCCGCTC
CGACTGCACCATCCTCACGCACCAGGAGGAGCGCCTGCACACCTGCGAGTACGGCAAGCACCAGTAA

APPENDIX D. SUPPORTING METHODS

Southern Blot analysis. Genomic DNA (gDNA) was isolated and purified using a standard phenol-chloroform extraction from 50 ml liquid cultures, digested with various restriction enzymes and the DNA fragments resolved by agarose (0.8%) gel electrophoresis, and then blotted for 20 h in SSC onto nylon membranes (Bio-Rad, Hercules, CA). Transferred DNA was cross-linked, with hybridizations performed as previously described (Xie & Merchant, 1996). The *AphVIII* ORF (805 bp) and *FDX5*-specific DNA fragments (315 bp) were amplified with primers APHVIII-F1/APHVIII-R1 and FDX5-F4/ FDX5-R4 (Table A.S2) and used as hybridization probes. To visualize hybridizing bands, blots were exposed to a phosphor screen (Molecular Dynamics) and imaged using a Pharos FX Plus scanner with Quantity One software (Bio-Rad).

pLM005_Venus constructs and transformation. The *FDX5*, *CrΔ4FAD* and *CrFAD6* genes were amplified from cDNAs and cloned into pLM005_Venus by Gibson assembly cloning (Gibson *et al.*, 2009; Yang *et al.*, 2014) to generate pLM005FDX5_Venus, pLM005CrΔ4FAD_Venus, and pLM005CrFAD6_Venus with various regulatory regions, as noted in the text. The constructs were transformed into cMJ030 (CC-4533) and transformants identified based on fluorescence outputs of individual colonies, and localized as previously described (Rasala *et al.*, 2013; Yang *et al.*, 2014).

Thylakoid membrane purification. Cells were grown in the light and dark to exponential phase and thylakoids purified according to (Takahashi *et al.*, 2006).

Membrane inlet mass spectrometry (MIMS). MIMS was used to differentiate between O₂ consumption and evolution in the light (Radmer & Kok, 1976). WT and mutant cell suspensions were equilibrated with equimolar concentrations of ¹⁸O₂ and ¹⁶O₂. Dark respiration was measured for 1-2 min prior to illuminating samples with white actinic light (~500 μmol photons m⁻² s⁻¹); O₂ evolution and consumption were calculated as previously described (Radmer & Kok, 1976).

***In vivo* photosynthetic measurements.** The quantum yield of PSII (Φ_{PSII} ; F_v/F_m) and electron transport rates (ETR) were determined using a Walz DUAL-PAM 100 fluorometer, as described by the manufacturer.

Chlorophyll fluorescence measurements. Whole cell Chl fluorescence measurements were performed using a Bio-Logic JTS-10 spectrophotometer with and without the addition of inhibitors [10 μ M 3-(3,4-dichloroprenyl)-1-1-dimethylurea (DCMU)] and electron acceptors [1 mM methyl viologen (MV)].

P700 determination. PSI was measured by monitoring absorption changes at 705 nm in the presence of PSII inhibitors [10 μ M DCMU and 1 mM hydroxylamine (HA)] during a brief period of illumination at 165 μ mol photons $m^{-2} s^{-1}$. A saturating pulse was provided after 5 sec of illumination to completely oxidize all P700. In some cases, 1 mM MV was added as an electron acceptor from PSI.

Protein isolation, SDS-PAGE and immunoblot analysis. Cells were stored at $-80^{\circ}C$, prior to resolution of proteins by SDS-PAGE (Heinzel *et al.*, 2013). The resolved proteins were immunoblotted, probed with specific antibodies and detected using the secondary antibody horseradish peroxidase-conjugated anti-rabbit IgG (Promega, Madison, WI); peroxidase activity was detected by an enhanced chemiluminescence assay (ECL) (Amersham Biosciences, GE Healthcare, Piscataway, NJ).

Pull-Down assay. FDX5 was coupled to cyanogen bromide (CnBr)-activated sepharose beads (GE Healthcare, USA; 5 mg of protein per ml resin) and prepared according to the manufacturer's instruction. The pull-down assay was performed like described previously (Peden *et al.*, 2013).

Mass-Spectrometry analysis. The protein samples (25 μ g) were pretreated to get the peptides, and the resulting peptide mixtures were analyzed by reversed-phase chromatography using a Waters nanoAcquity UPLC pump coupled online to an LTQ/Orbitrap mass spectrometer described as previously (Peden *et al.*, 2013). The interacting proteins were analyzed and blasted in *Chlamydomonas* genome (Merchant *et al.*, 2007).

REFERENCES

REFERENCES

- Aksoy, M., Pootakham, W., & Grossman, A. R. (2014). Critical function of a *Chlamydomonas reinhardtii* putative polyphosphate polymerase subunit during nutrient deprivation. *Plant Cell*, 26(10), 4214-4229. doi: 10.1105/tpc.114.129270
- Benning, C., & Ohta, H. (2005). Three enzyme systems for galactoglycerolipid biosynthesis are coordinately regulated in plants. *J Biol Chem*, 280(4), 2397-2400. doi: 10.1074/jbc.R400032200
- Benning, C., & Somerville, C. R. (1992). Isolation and genetic complementation of a sulfolipid-deficient mutant of *Rhodobacter sphaeroides*. *J Bacteriol*, 174(7), 2352-2360.
- Bligh, E. G., & Dyer, W. J. (1959). A rapid method of total lipid extraction and purification. *Can J Biochem Physiol*, 37(8), 911-917.
- Dörmann, P., Balbo, I., & Benning, C. (1999). Arabidopsis galactolipid biosynthesis and lipid trafficking mediated by DGD1. *Science*, 284(5423), 2181-2184.
- Dörmann, P., & Benning, C. (2002). Galactolipids rule in seed plants. *Trends Plant Sci*, 7(3), 112-118.
- Dörmann, P., Hoffmann-Benning, S., Balbo, I., & Benning, C. (1995). Isolation and characterization of an Arabidopsis mutant deficient in the thylakoid lipid digalactosyl diacylglycerol. *Plant Cell*, 7(11), 1801-1810. doi: 10.1105/tpc.7.11.1801
- Fan, J., Andre, C., & Xu, C. (2011). A chloroplast pathway for the de novo biosynthesis of triacylglycerol in *Chlamydomonas reinhardtii*. *FEBS Lett*, 585(12), 1985-1991. doi: 10.1016/j.febslet.2011.05.018
- Gibson, D. G., Young, L., Chuang, R. Y., Venter, J. C., Hutchison, C. A., 3rd, & Smith, H. O. (2009). Enzymatic assembly of DNA molecules up to several hundred kilobases. *Nat Methods*, 6(5), 343-345. doi: 10.1038/nmeth.1318
- Giroud, C., Gerber, A., & Eichenberger, W. (1988). Lipids of *Chlamydomonas reinhardtii*. Analysis of Molecular Species and Intracellular Site(s) of Biosynthesis. *Plant Cell Physiol*, 29(4), 587-595.
- Gonzalez-Ballester, D., Pootakham, W., Mus, F., Yang, W., Catalanotti, C., Magneschi, L., de Montaigu, A., Higuera, J. J., Prior, M., Galvan, A., Fernandez, E., & Grossman, A. R. (2011). Reverse genetics in *Chlamydomonas*: a platform for isolating insertional mutants. *Plant Methods*, 7, 24. doi: 10.1186/1746-4811-7-24

- Grefen, C., Obrdlik, P., & Harter, K. (2009). The determination of protein-protein interactions by the mating-based split-ubiquitin system (mbSUS). *Methods Mol Biol*, 479, 217-233. doi: 10.1007/978-1-59745-289-2_14
- Hanke, G., & Mulo, P. (2013). Plant type ferredoxins and ferredoxin-dependent metabolism. *Plant Cell Environ*, 36(6), 1071-1084. doi: 10.1111/pce.12046
- Hanke, G. T., Kimata-Arigo, Y., Taniguchi, I., & Hase, T. (2004). A post genomic characterization of Arabidopsis ferredoxins. *Plant Physiol*, 134(1), 255-264. doi: 10.1104/pp.103.032755
- Heinrich, M. L., Alric, J., Wittkopp, T., Yang, W., Catalanotti, C., Dent, R., Niyogi, K. K., Wollman, F. A., & Grossman, A. R. (2013). Novel thylakoid membrane GreenCut protein CPLD38 impacts accumulation of the cytochrome b6f complex and associated regulatory processes. *J Biol Chem*, 288(10), 7024-7036. doi: 10.1074/jbc.M112.427476
- Hemschemeier, A., Casero, D., Liu, B., Benning, C., Pellegrini, M., Happe, T., & Merchant, S. S. (2013). Copper response regulator1-dependent and -independent responses of the Chlamydomonas reinhardtii transcriptome to dark anoxia. *Plant Cell*, 25(9), 3186-3211. doi: 10.1105/tpc.113.115741
- Hugly, S., Kunst, L., Browse, J., & Somerville, C. (1989). Enhanced thermal tolerance of photosynthesis and altered chloroplast ultrastructure in a mutant of Arabidopsis deficient in lipid desaturation. *Plant Physiol*, 90(3), 1134-1142.
- Jacobs, J., Pudollek, S., Hemschemeier, A., & Happe, T. (2009). A novel, anaerobically induced ferredoxin in Chlamydomonas reinhardtii. *FEBS Lett*, 583(2), 325-329. doi: 10.1016/j.febslet.2008.12.018
- Kelly, A. A., & Dormann, P. (2004). Green light for galactolipid trafficking. *Curr Opin Plant Biol*, 7(3), 262-269. doi: 10.1016/j.pbi.2004.03.009
- Lambertz, C., Hemschemeier, A., & Happe, T. (2010). Anaerobic expression of the ferredoxin-encoding FDX5 gene of Chlamydomonas reinhardtii is regulated by the Crr1 transcription factor. *Eukaryot Cell*, 9(11), 1747-1754. doi: 10.1128/EC.00127-10
- Li, X., Moellering, E. R., Liu, B., Johnny, C., Fedewa, M., Sears, B. B., Kuo, M. H., & Benning, C. (2012). A galactoglycerolipid lipase is required for triacylglycerol accumulation and survival following nitrogen deprivation in Chlamydomonas reinhardtii. *Plant Cell*, 24(11), 4670-4686. doi: 10.1105/tpc.112.105106
- Liu, B., & Benning, C. (2013). Lipid metabolism in microalgae distinguishes itself. *Curr Opin Biotechnol*, 24(2), 300-309. doi: 10.1016/j.copbio.2012.08.008
- Merchant, S. S., Prochnik, S. E., Vallon, O., Harris, E. H., Karpowicz, S. J., Witman, G. B., Terry, A., Salamov, A., Fritz-Laylin, L. K., Marechal-Drouard, L., Marshall, W. F., Qu,

- L. H., Nelson, D. R., Sanderfoot, A. A., Spalding, M. H., Kapitonov, V. V., Ren, Q., Ferris, P., Lindquist, E., Shapiro, H., Lucas, S. M., Grimwood, J., Schmutz, J., Cardol, P., Cerutti, H., Chanfreau, G., Chen, C. L., Cognat, V., Croft, M. T., Dent, R., Dutcher, S., Fernandez, E., Fukuzawa, H., Gonzalez-Ballester, D., Gonzalez-Halphen, D., Hallmann, A., Hanikenne, M., Hippler, M., Inwood, W., Jabbari, K., Kalanon, M., Kuras, R., Lefebvre, P. A., Lemaire, S. D., Lobanov, A. V., Lohr, M., Manuell, A., Meier, I., Mets, L., Mittag, M., Mittelmeier, T., Moroney, J. V., Moseley, J., Napoli, C., Nedelcu, A. M., Niyogi, K., Novoselov, S. V., Paulsen, I. T., Pazour, G., Purton, S., Ral, J. P., Riano-Pachon, D. M., Riekhof, W., Rymarquis, L., Schroda, M., Stern, D., Umen, J., Willows, R., Wilson, N., Zimmer, S. L., Allmer, J., Balk, J., Bisova, K., Chen, C. J., Elias, M., Gendler, K., Hauser, C., Lamb, M. R., Ledford, H., Long, J. C., Minagawa, J., Page, M. D., Pan, J., Pootakham, W., Roje, S., Rose, A., Stahlberg, E., Terauchi, A. M., Yang, P., Ball, S., Bowler, C., Dieckmann, C. L., Gladyshev, V. N., Green, P., Jorgensen, R., Mayfield, S., Mueller-Roeber, B., Rajamani, S., Sayre, R. T., Brokstein, P., Dubchak, I., Goodstein, D., Hornick, L., Huang, Y. W., Jhaveri, J., Luo, Y., Martinez, D., Ngau, W. C., Otiillar, B., Poliakov, A., Porter, A., Szajkowski, L., Werner, G., Zhou, K., Grigoriev, I. V., Rokhsar, D. S., & Grossman, A. R. (2007). The Chlamydomonas genome reveals the evolution of key animal and plant functions. *Science*, *318*(5848), 245-250. doi: 10.1126/science.1143609
- Moellering, E. R., & Benning, C. (2010). RNA interference silencing of a major lipid droplet protein affects lipid droplet size in *Chlamydomonas reinhardtii*. *Eukaryot Cell*, *9*(1), 97-106. doi: 10.1128/EC.00203-09
- Mus, F., Dubini, A., Seibert, M., Posewitz, M. C., & Grossman, A. R. (2007). Anaerobic acclimation in *Chlamydomonas reinhardtii*: anoxic gene expression, hydrogenase induction, and metabolic pathways. *J Biol Chem*, *282*(35), 25475-25486. doi: 10.1074/jbc.M701415200
- Nguyen, H. M., Cuine, S., Beyly-Adriano, A., Legeret, B., Billon, E., Auroy, P., Beisson, F., Peltier, G., & Li-Beisson, Y. (2013). The green microalga *Chlamydomonas reinhardtii* has a single omega-3 fatty acid desaturase that localizes to the chloroplast and impacts both plastidic and extraplastidic membrane lipids. *Plant Physiol*, *163*(2), 914-928. doi: 10.1104/pp.113.223941
- Noth, J., Krawietz, D., Hemschemeier, A., & Happe, T. (2013). Pyruvate:ferredoxin oxidoreductase is coupled to light-independent hydrogen production in *Chlamydomonas reinhardtii*. *J Biol Chem*, *288*(6), 4368-4377. doi: 10.1074/jbc.M112.429985
- Peden, E. A., Boehm, M., Mulder, D. W., Davis, R., Old, W. M., King, P. W., Ghirardi, M. L., & Dubini, A. (2013). Identification of global ferredoxin interaction networks in *Chlamydomonas reinhardtii*. *J Biol Chem*, *288*(49), 35192-35209. doi: 10.1074/jbc.M113.483727
- Pollock, S. V., Colombo, S. L., Prout, D. L., Jr., Godfrey, A. C., & Moroney, J. V. (2003). Rubisco activase is required for optimal photosynthesis in the green alga

- Chlamydomonas reinhardtii in a low-CO₂ atmosphere. *Plant Physiol*, 133(4), 1854-1861. doi: 10.1104/pp.103.032078
- Pootakham, W., Gonzalez-Ballester, D., & Grossman, A. R. (2010). Identification and regulation of plasma membrane sulfate transporters in Chlamydomonas. *Plant Physiol*, 153(4), 1653-1668. doi: 10.1104/pp.110.157875
- Radmer, R. J., & Kok, B. (1976). Photoreduction of O₂ Primes and Replaces CO₂ Assimilation. *Plant Physiol*, 58(3), 336-340.
- Rasala, B. A., Barrera, D. J., Ng, J., Plucinak, T. M., Rosenberg, J. N., Weeks, D. P., Oyler, G. A., Peterson, T. C., Haerizadeh, F., & Mayfield, S. P. (2013). Expanding the spectral palette of fluorescent proteins for the green microalga Chlamydomonas reinhardtii. *Plant J*, 74(4), 545-556. doi: 10.1111/tpj.12165
- Reynolds, E. S. (1963). The use of lead citrate at high pH as an electron-opaque stain in electron microscopy. *J Cell Biol*, 17, 208-212.
- Riekhof, W. R., Sears, B. B., & Benning, C. (2005). Annotation of genes involved in glycerolipid biosynthesis in Chlamydomonas reinhardtii: discovery of the betaine lipid synthase BTA1Cr. *Eukaryot Cell*, 4(2), 242-252. doi: 10.1128/EC.4.2.242-252.2005
- Schmitter, J. M., Jacquot, J. P., de Lamotte-Guery, F., Beauvallet, C., Dutka, S., Gadal, P., & Decottignies, P. (1988). Purification, properties and complete amino acid sequence of the ferredoxin from a green alga, Chlamydomonas reinhardtii. *Eur J Biochem*, 172(2), 405-412.
- Takahashi, H., Iwai, M., Takahashi, Y., & Minagawa, J. (2006). Identification of the mobile light-harvesting complex II polypeptides for state transitions in Chlamydomonas reinhardtii. *Proc Natl Acad Sci U S A*, 103(2), 477-482. doi: 10.1073/pnas.0509952103
- Tardif, M., Atteia, A., Specht, M., Cogne, G., Rolland, N., Brugiere, S., Hippler, M., Ferro, M., Bruley, C., Peltier, G., Vallon, O., & Cournac, L. (2012). PredAlgo: a new subcellular localization prediction tool dedicated to green algae. *Mol Biol Evol*, 29(12), 3625-3639. doi: 10.1093/molbev/mss178
- Terashima, M., Specht, M., Naumann, B., & Hippler, M. (2010). Characterizing the anaerobic response of Chlamydomonas reinhardtii by quantitative proteomics. *Mol Cell Proteomics*, 9(7), 1514-1532. doi: 10.1074/mcp.M900421-MCP200
- Terauchi, A. M., Lu, S. F., Zaffagnini, M., Tappa, S., Hirasawa, M., Tripathy, J. N., Knaff, D. B., Farmer, P. J., Lemaire, S. D., Hase, T., & Merchant, S. S. (2009). Pattern of expression and substrate specificity of chloroplast ferredoxins from Chlamydomonas reinhardtii. *J Biol Chem*, 284(38), 25867-25878. doi: 10.1074/jbc.M109.023622
- Valentine, R. C. (1964). Bacterial Ferredoxin. *Bacteriol Rev*, 28, 497-517.

- van Lis, R., Baffert, C., Coute, Y., Nitschke, W., & Atteia, A. (2013). Chlamydomonas reinhardtii chloroplasts contain a homodimeric pyruvate:ferredoxin oxidoreductase that functions with FDX1. *Plant Physiol*, 161(1), 57-71. doi: 10.1104/pp.112.208181
- Winkler, M., Hemschemeier, A., Jacobs, J., Stripp, S., & Happe, T. (2010). Multiple ferredoxin isoforms in Chlamydomonas reinhardtii - their role under stress conditions and biotechnological implications. *Eur J Cell Biol*, 89(12), 998-1004. doi: 10.1016/j.ejcb.2010.06.018
- Xie, Z., & Merchant, S. (1996). The plastid-encoded ccsA gene is required for heme attachment to chloroplast c-type cytochromes. *J Biol Chem*, 271(9), 4632-4639.
- Yang, W., Catalanotti, C., D'Adamo, S., Wittkopp, T. M., Ingram-Smith, C. J., Mackinder, L., Miller, T. E., Heuberger, A. L., Peers, G., Smith, K. S., Jonikas, M. C., Grossman, A. R., & Posewitz, M. C. (2014). Alternative acetate production pathways in Chlamydomonas reinhardtii during dark anoxia and the dominant role of chloroplasts in fermentative acetate production. *Plant Cell*, 26(11), 4499-4518. doi: 10.1105/tpc.114.129965
- Yang, W., Catalanotti, C., Wittkopp, T. M., Posewitz, M. C., & Grossman, A. R. (2015). Algae after dark: mechanisms to cope with anoxic/hypoxic conditions. *Plant J*, 82(3), 481-503. doi: 10.1111/tpj.12823
- Zäuner, S., Jochum, W., Bigorowski, T., & Benning, C. (2012). A cytochrome b5-containing plastid-located fatty acid desaturase from Chlamydomonas reinhardtii. *Eukaryot Cell*, 11(7), 856-863. doi: 10.1128/EC.00079-12